POLITEHNICA UNIVERSITY TIMIŞOARA
Civil Engineering Faculty
Department of Steel Structures and Structural Mechanics

DAMAGE CHARACTERIZATION IN BUILDING STRUCTURES DUE TO BLAST ACTIONS

Author: Bulbul Ahmed, SUSCOS_M Student

Supervisor: Professor Florea DINU, Ph.D.

Co-Supervisor: Assistant Professor Ioan Marginean, Ph.D.

Universitatea Politehnica Timişoara, Romania

Study Program: SUSCOS_M

Academic year: 2017/ 2018

DAMAGE CHARACTERIZATION IN BUILDING STRUCTURES DUE TO BLAST ACTIONS

Bulbul Ahmed

February 2018

DAMAGE CHARACTERIZATION IN BUILDING STRUCTURES DUE TO BLAST ACTIONS

This thesis report is submitted to the Faculty of Civil Engineering, Department of Steel Structures and Structural Mechanics, Politehnica University Timişoara, for partial fulfilment of the requirements, for the degree of

MASTERS OF SCIENCE

ON

SUSTAINABLE CONSTRUCTIONS UNDER NATURAL

HAZARDS AND CATASTROPHIC EVENTS

SUPERVISED BY

FLOREA DINU, Ph.D.
Professor
Department of Steel Structures and Structural Mechanics; Politehnica University Timişoara

SUBMITTED BY

BULBUL AHMED
SUSCOS_M Student
Department of Steel Structures and Structural Mechanics; Politehnica University Timişoara

Members of the Jury

PRESIDENT:

Acad. Professor dr. ing. Dan DUBINA, Ph.D.
C. M. of the Romanian Academy
Politehnica University Timişoara
Str. Ion Curea, Nr. 1
300224, Timisoara, Timiş, Romania

THESIS SUPERVISOR:

Professor dr. ing. Florea DINU, Ph.D.
Politehnica University Timişoara
Str. Ion Curea, Nr. 1
300224, Timisoara, Timiş, Romania.

MEMBERS:

Professor dr. ing. Adrian CIUTINA, Ph.D.
Politehnica University Timişoara
Str. Ion Curea, Nr. 1
300224, Timişoara, Timiş, Romania.

Professor dr. ing. Viorel UNGUREANU, Ph.D.
Politehnica University Timişoara
Str. Ion Curea, Nr. 1
300224, Timişoara, Timiş, Romania.

Conf. dr. ing. Adrian DOGARIU, Ph.D.
Politehnica University Timişoara
Str. Ion Curea, Nr. 1
300224, Timişoara, Timiş, Romania.

SECRETARY:

Dr. ing. Ioan MARGINEAN, Ph.D.
Politehnica University Timişoara
Str. Ion Curea, Nr. 1
300224, Timişoara, Timiş, Romania.

ACKNOWLEDGMENT

This dissertation work is a partial fulfilment of my master course of SUSCOS (2016-2018) within the department of Steel Structures and Structural Mechanics (http://www.ct.upt.ro/cmmc) under the Research Center for Mechanics of Materials and Structural Safety, from Politehnica University Timisoara in Romania.

I would like to express deepest gratitude to my supervisor, Dr. Florea DINU, PhD for guidance and help throughout my research activity in Politehnica University Timisoara. Without his help and guidance, it would not have been possible to finish this research work. His devotion in helping young researchers is truly appreciable and I wish him all the very best in his future endeavors. Such professors are hard to find and must be truly appreciated.

I would also like to thank my co-supervisor, Dr. Ioan MARGINEAN, PhD for his continuous support and guidance in performing experimental test and developing finite element models and being available all the time for clarifying my doubts in numerical modeling.

I would like to thank the laboratory staff, Ovidiu Abrudan, Dan Scarlat, and Miloico Ung, for their help, technical advice, and support for the experimental program.

I am thankful to Professor Dan DUBINA for giving me this opportunity to write my thesis with FRAMEBLAST (2017-2018); CNCS/CCCDI-UEFISCDI Research Program (https://www.ct.upt.ro/centre/cemsig/frameblast.htm).

Furthermore, I would like to thank Professor Adrian CIUTINA for bearing with us and taking good care of us during our tenure in Romania. I am also thankful to Professor Viorel UNGUREANU for his positive feedbacks.

Moreover, I am really thankful to the professors that are coordinating this SUSCOS master program and making it possible: Professor František WALD, Professor Dan DUBINA, Professor Raffaele Landolfo, Professor Milan Veljkovic, Professor Luís Simões da Silva, and Professor Jean-Pierre JASPART and all the other professors involved in our course. I feel deeply honored for meeting you and to have been able to participate in the lectures held by such great people. Last but not the least, I also feel thankful personally to hidden helper, Barbora Skálová for her supporting during studying period.

Moreover, I am deeply thankful to my parents for moral support and encouragement in every aspect of my life. I would like to thank my brothers and my sister to support me morally. I feel proud to be a part of such a supporting family.

I am deeply in debt of all the people who helped me in completing my course of SUSCOS (2016-2018) and being part of my life and specially in finalizing this research work.

Finally, I am thankful to Creator Almighty ALLAH for everything I have in my life.

ABSTRACT

Structural identification is a technique that can be used to assess/characterize the damage state through the variation in eigenfrequencies, damping ratios and modal shapes in a structure or element. It has recently received more attention for the practical implementation in several fields, including damage assessment for structures following blast or explosion events. At present, large infrastructure components, like civil engineering structures, are the most turning point for the consideration for structural identification. Structures can be moderately or severely deteriorated due to accidental or intentional blasts or explosions. The structural engineers but also other stakeholders, like rescue and emergency agencies, are more concerned about the design of structures, design life span, proper maintenance, repair and residual capacity of structural systems in many countries.

This dissertation work focuses on the experimental and analytical modal analysis of a full-scale steel frame structure building aiming to develop coherent scenarios that combine the probability of the hazard event with the structural vulnerability in case of a close in detonation. The field tests were carried out by forced vibration testing under hammer excitations. First series of tests were done for the undamaged structure using classical experimental modal analysis. Then, in order to model a structural damage, a secondary beam was dismantled (thus a damage was created artificially) and the measurements were repeated.

The change in structural behaviour was observed by identifying the changes in the stiffness and natural frequencies of the structure. The modal parameters measured from field test were used then to validate finite element models using SAP2000 program. They were corrected so that the numerical natural frequencies and mode shapes match the experimental data. Good agreement was obtained in identifying the frequencies for the three-dimensional finite element models for both damaged and undamaged structure. Then, using the calibrated numerical model, several blast induced damages were used in a numerical study. For the internal damage or non-visible crack, four different damage scenarios were made by the FE model for internal and external blast actions. The modal parameters changed significantly for higher modes for higher reduction of stiffness at the column-beam and base connections. The results (experimental data, calibrated numerical model) will be used as reference values of the undamaged structure for further investigations after blast tests will be performed.

This research is a part of FRAMEBLAST project supported by a grant of the Romanian National Authority for Scientific Research and Innovation, CNCS/CCCDI-UEFISCDI, project number PN-III-P2-2.1-PED-2016-0962, within PNCDI III. “Experimental validation of the response of a full-scale frame building subjected to blast load”-FRAMEBLAST (2017-2018)”.

Table of Contents **Page No.**

List of Figures **Page No.**

List of Tables **Page No.**

ACRONYMS

EMA	Experimental Modal Analysis
St-Id	Structural Identification
SHM	Structural Health Monitoring
SSI	Stochastic Subspace Identification
OMA	Operational Modal Analysis
ODS	Operating Deflection Shapes
FVT	Forced Vibration Testing
FEM	Finite Element Model
SSI-COV	Covariance-drive Stochastic Subspace Identification
LSCF	Least Squares Complex Frequency
NExT/ERA	Eigensystem Realisation Algorithm
EFDD	Enhanced Frequency Domain Decomposition
FDD	Frequency Domain Decomposition
CFDD	Curve-fit Frequency Domain Decomposition
MAC	Modal Assurance Criteria
FRF	Frequency Response Function
IRF	Impulse Response Functions
PP	Peak Picking
SISO	Single Input Single Output
SIMO	Single Input Multiple Output
MIMO	Multiple Input Multiple Output
MISO	Multiple Input Single Output
FFT	Fast Fourier Transformation
STFT	Short-Time Fourier Transform
MRP	Multi Rigid Polygons
ARMA	Autoregressive Moving Average
VARMA	Vector Autoregressive Moving-Average
MDL	Minimum Description Length
LTI	Linear Time Invariant
LTV	Linear Time Variant
EMD	Empirical Mode Decomposition
MTC	Modal Test Consultant

1. INTRODUCTION

1.1. Motivation

Structural identification is a technique that can be used to assess/characterize the damage state through the variation in eigenfrequencies, damping ratios and modal shapes in a structure or element. It has recently received more attention for the practical implementation in several fields, including damage assessment for structures following blast or explosion events. At present, large infrastructure components, like civil engineering structures, are the most turning point for the consideration for structural identification. Structures can be moderately or severely deteriorated due to accidental or intentional blasts or explosions. The structural engineers but also other stakeholders, like rescue and emergency agencies, are more concerned about the design of structures, design life span, proper maintenance, repair and residual capacity of structural systems in many countries.

There are several examples of such events that attracted the attention of the large public due to the dramatic consequences:

- On April 19, 1995, nine-story ordinary concrete moment frame office building, Murrah Federal Office Building, in Oklahoma City, Oklahoma,167 people were killed and injured 782. The resulting explosion caused the disproportionate (progressive) collapse [Andres R. Perez, 2009].
- On August 7, 1998, United States embassy were attacked by simultaneous truck bomb explosions in Nairobi, Kenya, 224 people were killed and 4,000 were wounded. [https://en.wikipedia.org/wiki/1998_United_States_embassy_bombings].
- On September 4-16, 1999, Russian apartment bombings, eight-story apartment buildings, Buynaksk, Moscow and Volgodonsk, 293 people were killed, 1000 were injured [https://en.wikipedia.org/wiki/Russian_apartment_bombings#Overview].
- On September 11, 2001, World Trade Center buildings in New York City collapsed because of terrorist attacks and subsequent fires. The whole structure suffered disproportionate collapse because of the buckling of columns which in turn is due to the sagging of bridge-like floor systems because of fire [https://en.wikipedia.org/wiki/September_11_attacks].

- On November 1, 1966, the 7-story steel-frame building, University of Aberdeen Zoology Department building in Aberdeen, Scotland. Five people were killed and three others injured and the building collapsed due to fatigue and progressive collapse [https://en.wikipedia.org/wiki/Progressive_collapse#cite_note-3].
- On February 12, 2005, the 28-story composite steel-frame and steel-reinforced concrete Windsor Tower in Madrid, Spain failed for progressive collapse of the upper 11 floors of the building [https://en.wikipedia.org/wiki/Windsor Tower_(Madrid)].
- On 24 April 2013, the 8 story Rana Plaza commercial office complex in Savar, Bangladesh, 1129 people died in the building and approximately 2,515 people were injured. The building collapsed completely all on a sudden due to oscillation of garment machinery and weight of the workers. It was the deadliest accidental structural failure in modern human history [http://www.bbc.co.uk/news/world-asia-22394094].

1.2. Scope and objectives of the thesis

Experimental validation is the most reliable way to demonstrate the performance of a building structural system. However, there are still some uncertainties about the expected performance of the building system when subjected to blast load because of the many variables included in the process. The application of structural identification for full scale laboratory testing of a steel frame building subjected to blast allows a better understanding of blast effects, including the post-blast condition and residual capacity of building structure. The research mainly focused on the assessment of dynamic properties of a full-scale steel frame building model and some preliminary evaluations regarding the structural vulnerability in case of a close-in detonation.

1.3. Research framework

This research developed in the thesis has been supported by a grant of the Romanian National Authority for Scientific Research and Innovation FRAMEBLAST,CNCS/CCCDI- UEFISCDI, project number PN-III-P2-2.1-PED-2016-0962, within PNCDI III [Dinu et al. 2017-2018].

The main objective of the project is to develop specific/comprehensive design guidelines for robustness of the building structures. Experimental testing for data extracting and overcoming the complexity. Also, to provide the validation of a full-scale building structural frame system under internal and external blast loading in laboratory environment and structural identification

will be applied to assess the performance of the building (damage level, residual capacity). For this aim, the other technical supporting information comes from CODEC project (PCCA 55/2012), where individual components and scaled sub-assemblies were tested under different loading conditions associated with blast or column removal. Within this phase, the behavior of structural components were tested experimentally and validated numerically [Dinu et al. 2017-2018]. The research project was divided into three main phases. The detail information about the phases of the project is presented in Table 1.

The dissertation is prepared for the partial fulfilment of Masters program on Sustainable Constructions under natural hazards and catastrophic events. This course is funded by European commission for European Erasmus Mundus Master, 520121-2011-1-CZ-ERA MUNDUS-EMMC project. The main objectives of this master course SUSCOS_M is to provide attendees the engineering ability and know-how to design and construct structures in a balanced approach between economic, environmental and social aspects, enhancing the sustainability and competitiveness of the steel industry. The course is organized in three modules covering buildings; bridges and energy-related infra-structures from concrete, steel, timber, and composite structures and equipments with a practice-oriented approach. A strong emphasis is given to the reduction of carbon footprint, the energy efficiency of buildings considering a life-cycle approach and the integration in the structural systems of renewable energies and innovative technologies [http://steel.fsv.cvut.cz/suscos/index.htm].

The Master course had duration of three semesters during the academic years 2016-2018. The program involved six European Universities. The first and second semester consist of 60 ECTS course work in the university of Liege and University of Politehnica Timisoara. For the third semester 30 ECTS of dissertation work in the University of Politehnica Timisoara [http://steel.fsv.cvut.cz/suscos/index.htm].

Table 1: FRAMEBLAST research framework phases.

Phase	Phase Title
Phase 1	Preliminary analyses and design of experimental program.
Phase 2	Experimental program.
Phase 3	Validation of a full scale building structural frame system under blast loading in laboratory environment.

Followings are the important summary of different complete phases regarding the project:

Phase 1: Preliminary analyses and design of experimental program

Preliminary analyses and design of experimental program involved the following sub-divisions:

- Preliminary analysis of external blast load on the building envelope.
- Preliminary analysis of internal blast on the structural/non-structural building elements.
- Design of experimental full-scale building model.
- Design of small scale tests for materials and components.
- Fabrication of full scale test specimen and material samples and components.

Phase 2: Experimental program

Phase 2 involved the experimental test of the building based on the loading. Experimental tests are conducted on materials and components; erection of full scale building at the testing facility; full scale building model under internal blast and full-scale building model under external blast.

Phase 3: Validation of a full scale building structural frame system under blast loading in laboratory environment

Phase 3 involved on validation and qualification of full scale testing due to internal and external blast load in laboratory environment. Structural identification and damage characterization of building components with damages due to internal and external blast.

2. LITERATURE REVIEW

2.1. Principles of structural identification

Structural identification is getting more importance through finite element model updating and experimental modal analysis technique to assess the dynamic properties and structural health and performance monitoring [Timothy Kernicky et al. 2017]. Structural identification basically uses performance-based civil engineering modeling that is performed by field/experimental measurements and the validation is done by using numerical models. In the study, SAP2000 program was used for calibration of the experimental data obtained using Bruel & Kjaer vibration measurement technology and equipment. Structural design validation, practical

quality control of construction, performance for retrofitting and rehabilitation effectiveness, damage detection and lifecycle analysis for long-term performance and structural health and performance monitoring [Çatbaş et al. 2013] is a promising issue for structural identification and characterization [Timothy Kernicky et al. 2017]. Structural identification studies for large civil engineering structures, like long span bridges, high rise buildings, wind turbines, offshore structure, towers, subjected to the undesired and/or unexpected hazards. In case of blast action, structural deterioration of the frame building, structural responses for pre-blast and post-blast conditions are conducted by blast overpressure transducers and shock accelerometers. Performance-based [Aktan. A et al. 2013] analysis for civil engineering structure and health monitoring has some key challenges for structural identification because of uncertainties of parameter estimation and finding the alternative better solutions for physical properties of the structures. The main goal of model updating is to find the solution to get best possible match of stiffness and mass matrices of an analytical model of the structure to the experimentally measured values [Timothy Kernicky et al. 2017]. Two important methods are: deterministic and probabilistic are used for finite element model updating. The uncertainties parameters of the model can be assessed by deterministic methods for structural identification of several full-scale structures [Bakir et al. 2008; Deng L et al. 2009; Marwala T. 2010]. Modal parameters estimation through system identification using both deterministic and Stochastic Subspace Identification (SSI) system algorithm. Structural identification for the existing structures is auspicious solution for decision making to minimize the unnecessary cost for repairing, retrofitting and replacement [Romain Pasquier et al. 2016]. Unexpected errors of the modeling can be minimized for the existing civil engineering structures by structural identification process based on residual minimization approaches [Yarnold et al. 2015; Fontan et al. 2014; Baroth et al. 2010; Schlune et al. 2009]. Physical properties and structural conditions from the identification results is observed by the diagnostics process. Higher number of sensor required for computing structural identification for diagnosis and prognosis of existing structures.

The response of the structures under reacting forces define the structural behavior that is urging to analyze. External forces can introduce in different ways and characterize the dynamic properties (modes and natural resonant frequencies). Modal parameters are important because they describe the inherent dynamic properties of a structure. The set of modal parameters constitutes a unique set of numbers that can be used for model correlation and updating, design verification, benchmarking, troubleshooting, quality control or structural health monitoring. The structure by exciting with a hammer or shaker and measuring its response with

accelerometers. Techniques like operational modal analysis (OMA) and operating deflection shapes analysis (ODS) work while the structure is in operation, allow to get a realistic picture without having to artificially excite the structure [Bruel & Kjaer module: Type 7765, 7765-A, 7765-B and 8761].

2.2. Application of St-Id in structural engineering applications

The development of the society and the needs for more advanced, more economical and longer lifetime of buildings and infrastructures, like tall buildings, dams, large cable stayed or suspension bridges, towers, wind turbines, aircrafts structures, or other special structures, require adequate methods and tools to allow for accurate structural identification of the most relevant static and dynamic properties. Numerical modelling, even it is a powerful tool that seen important developments in the last decades, require the validation of the results through analytical and/or experimental means.

A lot of research work had been done in the past to identify the dynamic characteristics of civil engineering structures. Some applications of Bruel & Kjaer experimental modal analysis (EMA) for estimation of modal parameters for different structures are presented in the Figure 1-5. Many researchers have done the experimental modal analysis and analytical modal analysis for the long span bridges, tall buildings, traffic roads, towers, wind turbines and so on. A list of research related to structural identification and structural health monitoring has done by different researchers based on and experimental modal analysis for civil engineering structures.

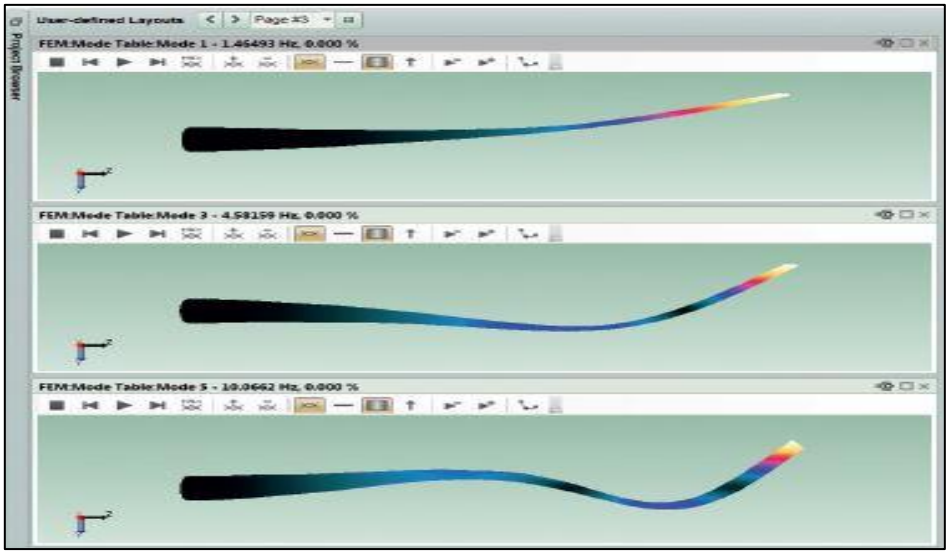

Figure 1: Modal parameters estimation for wind turbine [Bruel & Kjaer manual: Type 8760].

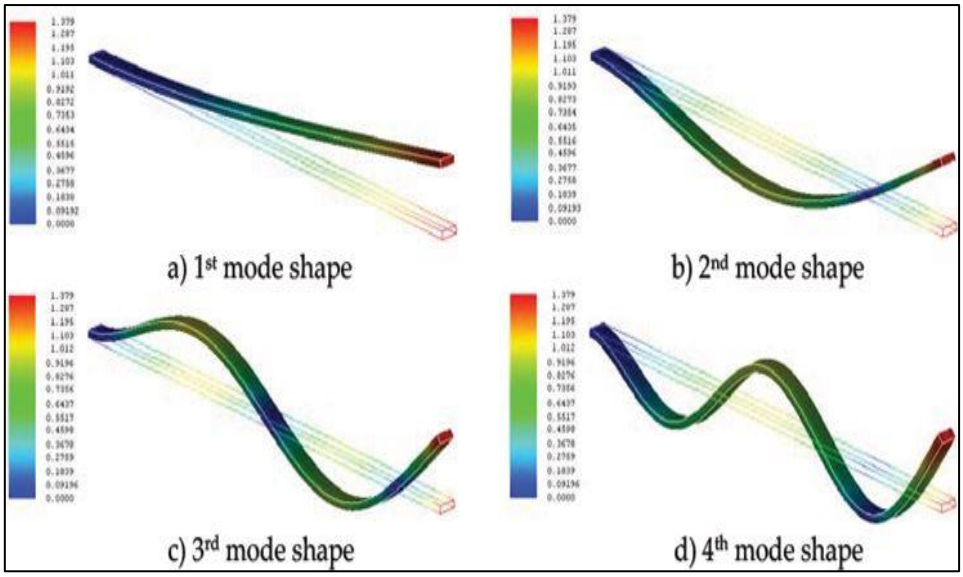

Figure 2: Modal parameters estimation for bridge [Abdurrahman Sahin et al. 2016].

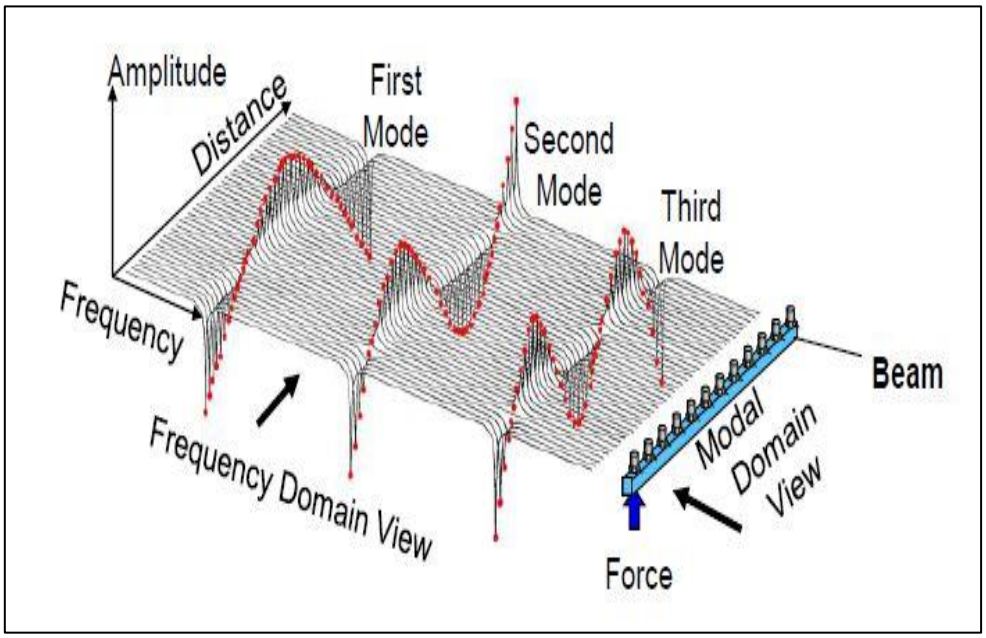

Figure 3: Modal parameters estimation for a beam structure [Bruel & Kjaer manual:

Access code: 636 832 431, 2017].

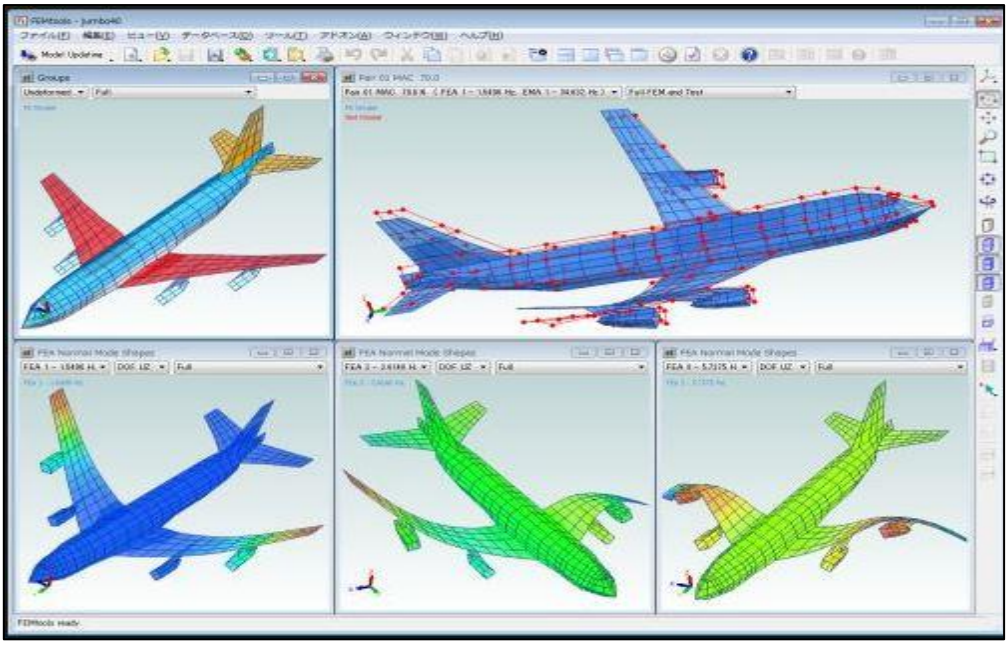

Figure 4: Modal parameters estimation for air craft [Bruel & Kjaer manual: Type 8761].

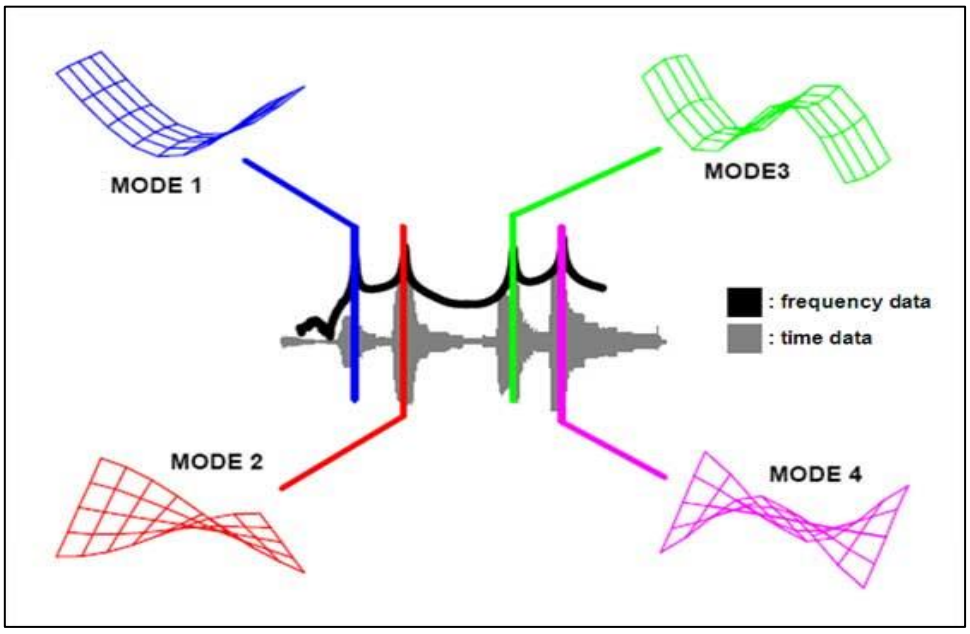

Figure 5: Different physical mode shape by experimental modal analysis [Peter. 2017].

2.2.1. Damage detection by experimental modal analysis

The structural health monitoring after long term operation is the key source to detect damage. Time to time health monitoring indicates the physical changes of the structures that helps to identify the damage occurrence, location of damage, severity of damage. Mainly the damage indicators are the key parameters as input and unify them to a single control value with a corresponding statistical based threshold. This threshold acts as a control chart for identifying

damage automatically when the threshold is being passed after an analysis. As for example, a bridge is taken (Figure 6) for detecting damage after long term service of that bridge by eight reference measurements representing the undamaged state were performed. Eight measurements recorded for undamaged bridge and other 14 measurements were taken after introducing damage. The first six measurements of eight measurements used as a baseline (reference) model is determined by the module. The threshold is automatically estimated based on the statistical evaluation of the damage indices of the six reference measurements. The last two reference measurements remain below the reference threshold (green bars). It means that the bridge is still serviceable or undamaged. The last 14 measurements that were recorded after damage introduced all pass the threshold significantly and indicate a permanent damage (red bars). Mode tracking was done as well. The lower left display indicates that the first two modes are basically unaffected by the damage, whereas the natural frequency for the highest mode changes and disappears completely during the first set of damage measurements and reappears again later. Tracking of the third mode is impossible after damage is introduced [Bruel & Kjaer product document: OMA Pro BZ-8553].

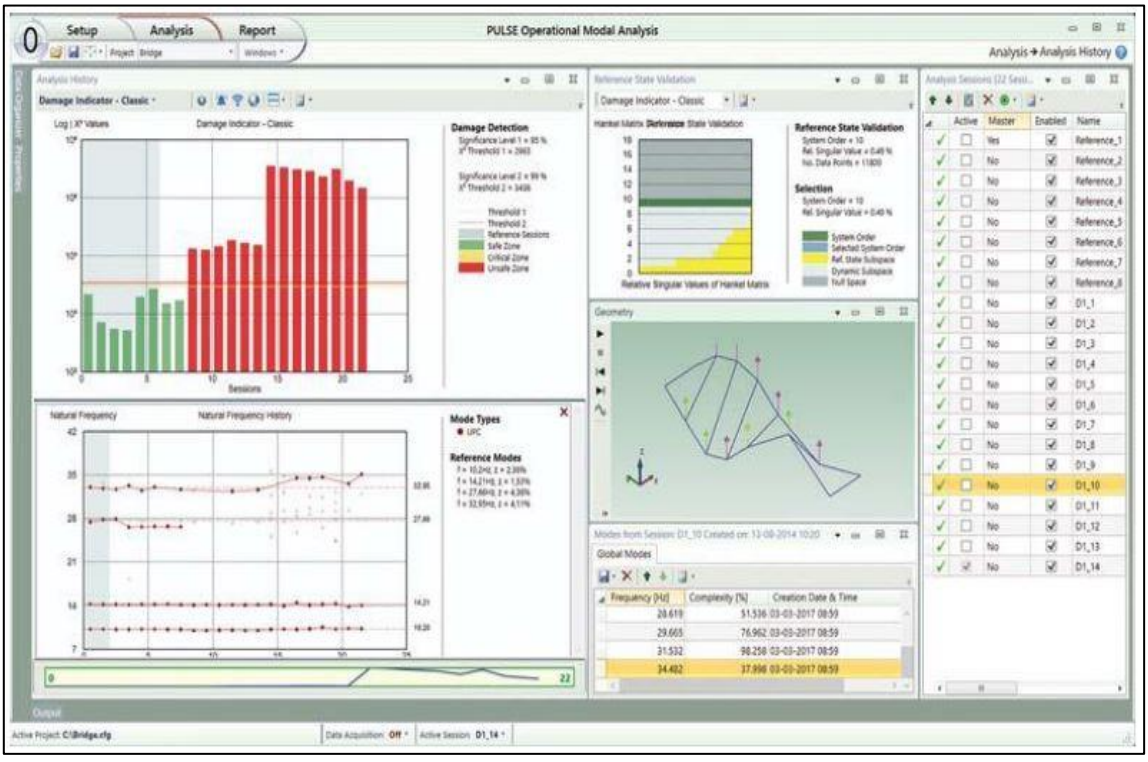

Figure 6: Damage detection of bridge by operational modal analysis [Bruel & Kjaer manual: Type 8760-8762; OMA Pro BZ: 8553].

2.3. Literature review of the previous studies

Vibrations are global phenomena in everyday life [Gaetan Kerschen et al. 2010]. They have undesirable effects such as noise disturbances [Gaetan Kerschen et al. 2010] or may even cause the collapse of a structure. Vibration is the dynamic properties of the structures. Dynamic forces are the seismic action, wind, blasting, fire and structure operational forces [M. Hassan Haeri et al. 2017]. All of the structures are excited for the action of dynamic forces. The three important modal parameters are the natural frequencies, damping ratios and mode shapes, has become a major concern for representing of structural dynamic.

R. Cantieni (2004) did a very valuable research on experimental methods used in system identification of civil engineering structures like buildings, bridges, dams, wind turbines, towers, road networks that are vibrated due to the dynamic forces. Forced vibration testing, some mechanical devices and ambient vibration testing for some civil engineering structures had been done for structural identification. A short span 72m bridge was taken for the experiment is shown in Figure 7.

Figure 7: Bridge on the Aare River at Aarburg (short span bridge) [R. Cantieni. 2004].

Experimental modal parameters estimated by the forced vibration testing validated by the finite element model software shown in Figure 8.

Brownjohn et el. (2010) examined the dynamic behavior of Humber bridge based on operational modal analysis in ambient conditions.

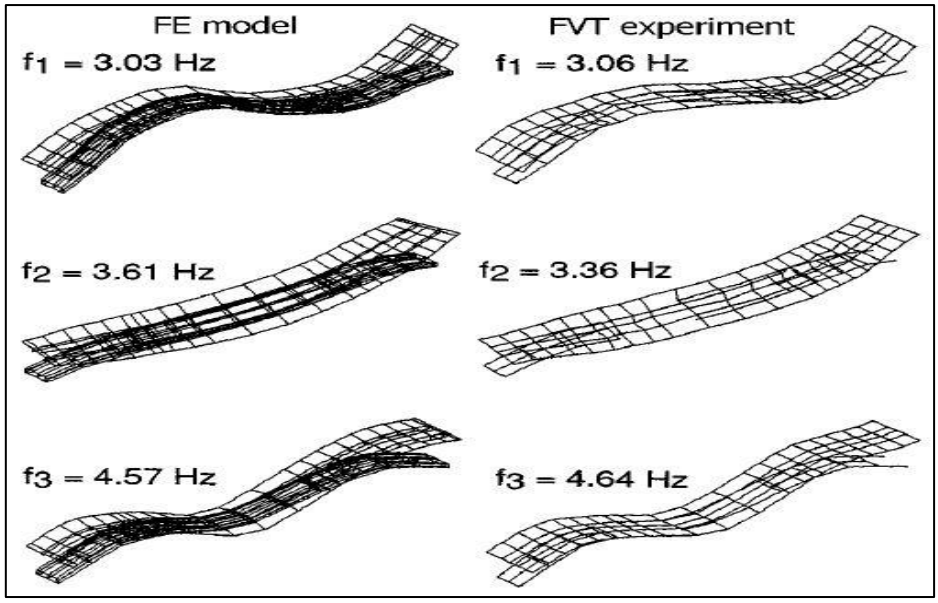

Figure 8: Frequency and shape of the first three bridge modes; FVT results to the right, updated FE model to the left [R. Cantieni. 2004].

NExT/ERA, SSI-COV and p-LSCF techniques were applied for the modal parameters and compared mode shape and frequency for vertical, lateral, torsional modes up to 1 Hz. Among three methods SSI-COV was the best technique to measure the practical modes. The vertical and lateral modes measured by the SSI-COV methods in Figure 9-10.

The experimental modal analysis is the extraction of modal parameters; natural frequencies, damping ratios, and mode shapes of the structures from measurements of dynamic responses [Wei-Xin Ren et al. 2005]. For the structural damage detection (Figure 11) and structural identification for decision making; structural safety evaluation; assessment of the structural integrity and reliability; and structural health monitoring; the modal parameters are the main basic [M. Hassan Haeri et al. 2017 and C. Kr. AAmer et al. 1999].

Ahmet Can Altunışık et el. (2017) experimented the structural identification of a cantilever beam with multiple cracks by three different operational methods (EFDD, CFDD & SSI) and the modal parameters were verified by finite element tool ANSYS. The modal parameters measured experimentally were verified by the modal assurance criteria (MAC) and Auto MAC. Automated model updating method was also used to minimize the gap/difference between experimental and numerical analysis by the FEMtools. Six different damage scenarios were made for the cantilever beam, see Figure 12. Damage is much effective to decrease stiffness and strength of structural components and it changes dynamic behaviour and damping

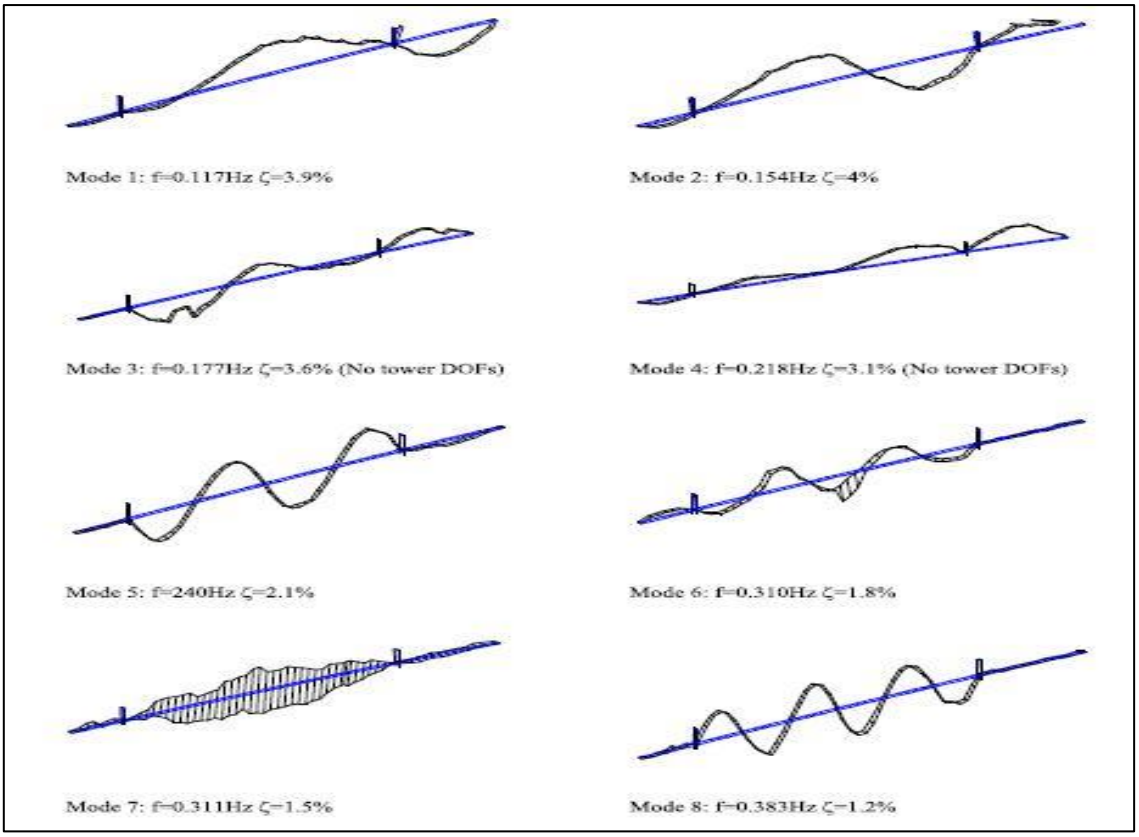

Figure 9: Modes in SSI-COV applied to all vertical response DOFs [Brownjohn et al. 2010].

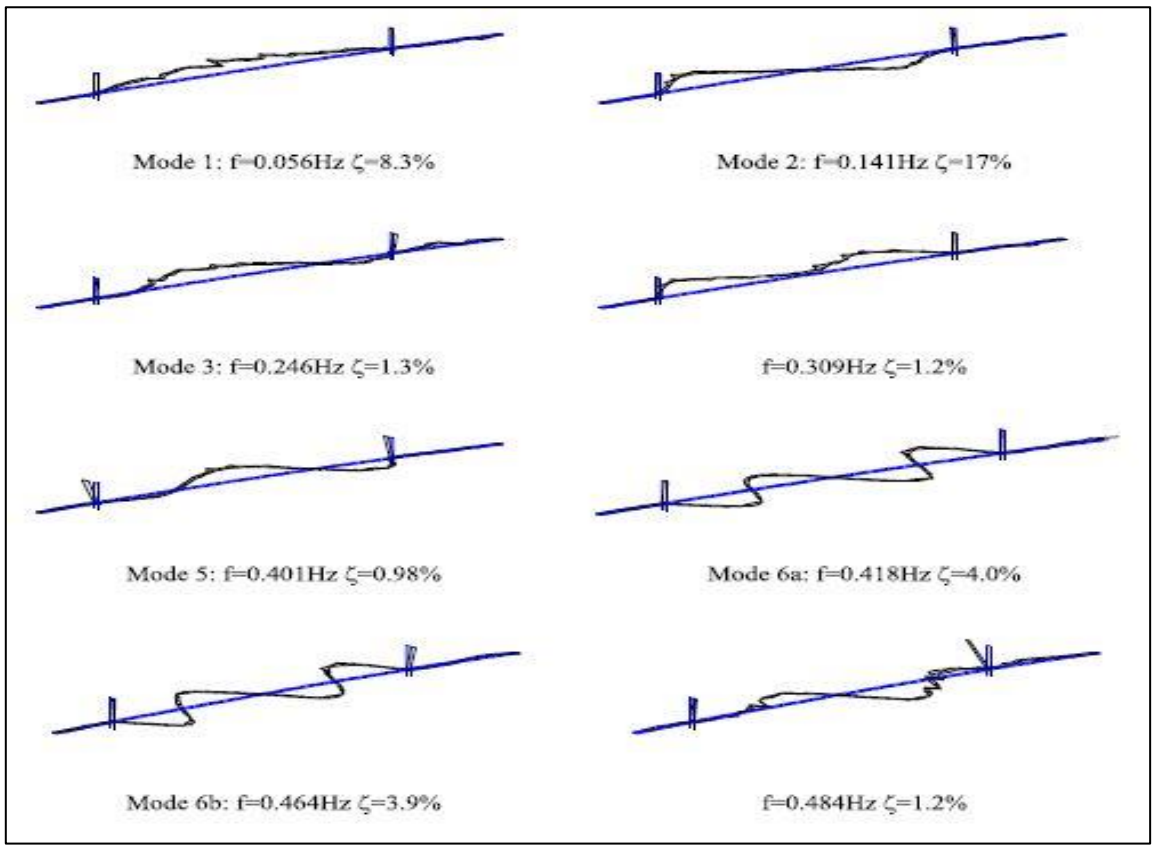

Figure 10: Lateral deck and tower modes from SSI-COV [Brownjohn et al. 2010].

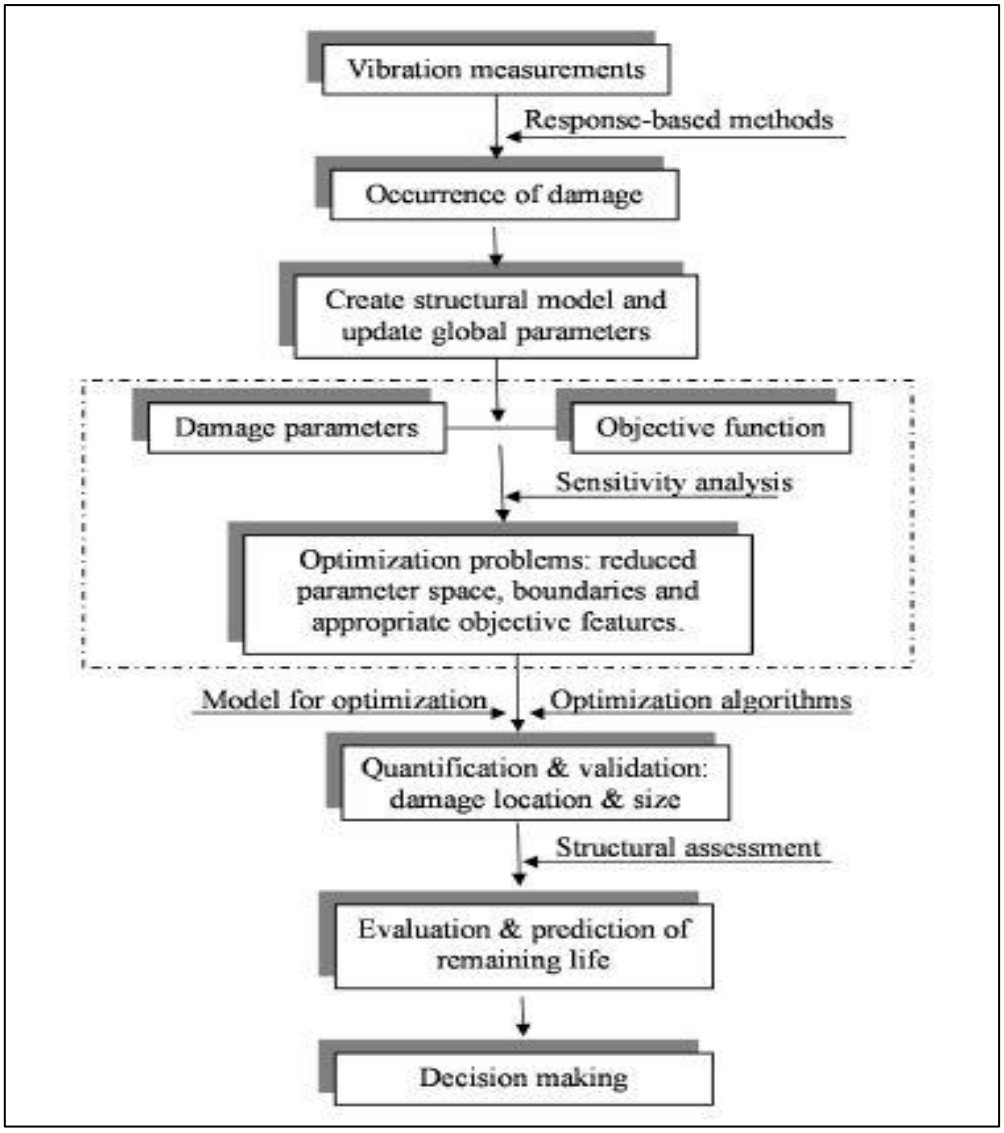

Figure 11: Flowchart for damage identification [Xuan Kong et el. 2017].

ratio of whole structures. The modal parameters in the experimental and numerical method are strongly affected by the presence of cracks and severity of the cracks of the beam. The stability, stiffness and flexural rigidity of the beam decrease with the increase of the depth of cracks, see Figure 13.

J. B. Hansen et el. (2017) represented on "A new scenario-based approach to damage detection using operational modal parameter estimates". He did vibration-based damage introduction and identification by the modal parameters. The modal parameters were extracted by experimentally OMA and numerically FEM method. Structural health monitoring (SHM) of the structures were measured by the damage detection techniques of four important factors such as: detection; localization; quantification and prognosis [A. Rytter. 1993]. Damage

assessment methodology was modified for updating the experimental and numerical model and demonstrating the limitations by modal driven techniques. Five scenarios were created by adding some masses at different points for simulation by finite element model (Figure 14-15).

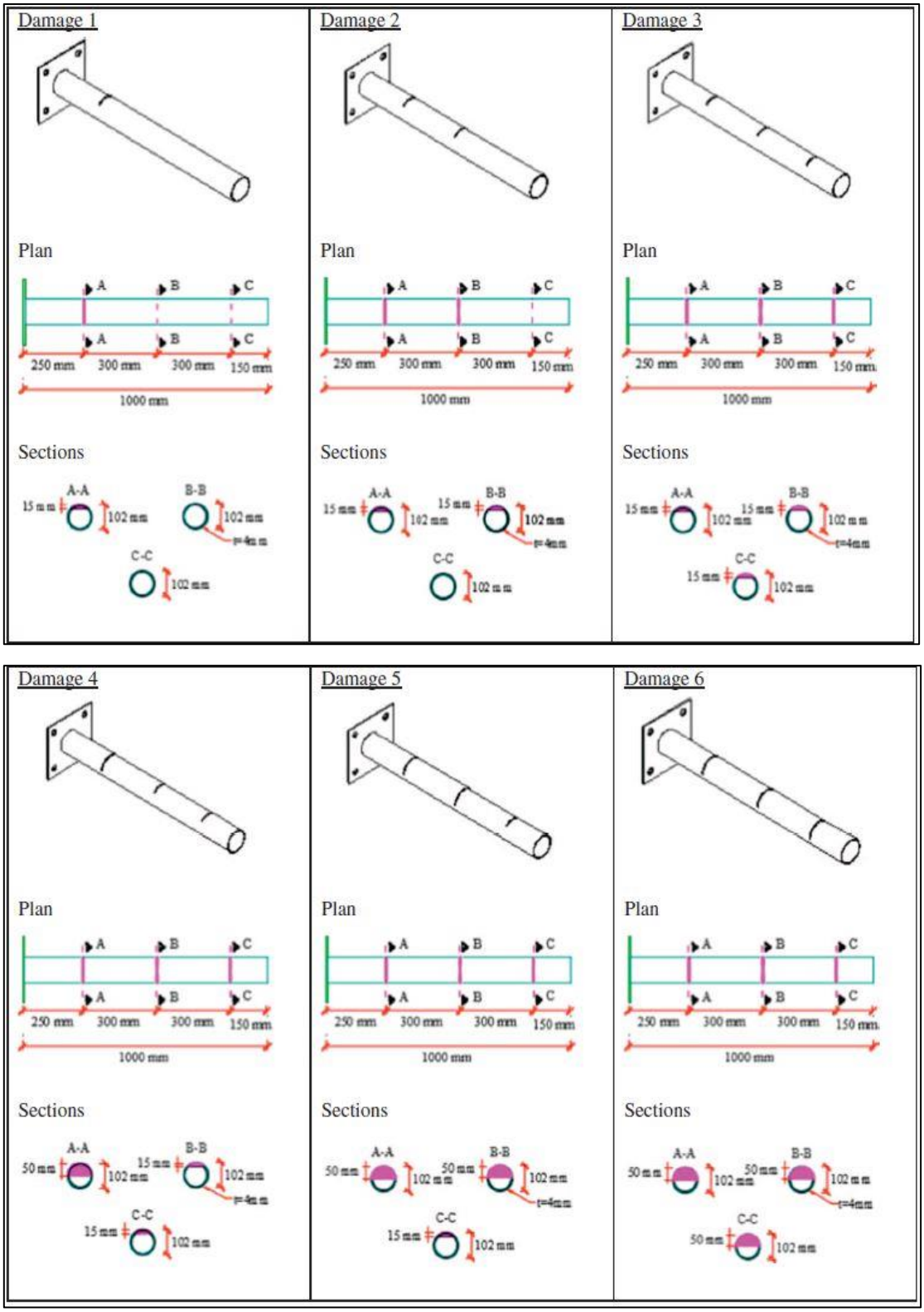

Figure 12: Damage scenarios in plan and section views [Ahmet Can Altunışık et al. 2017].

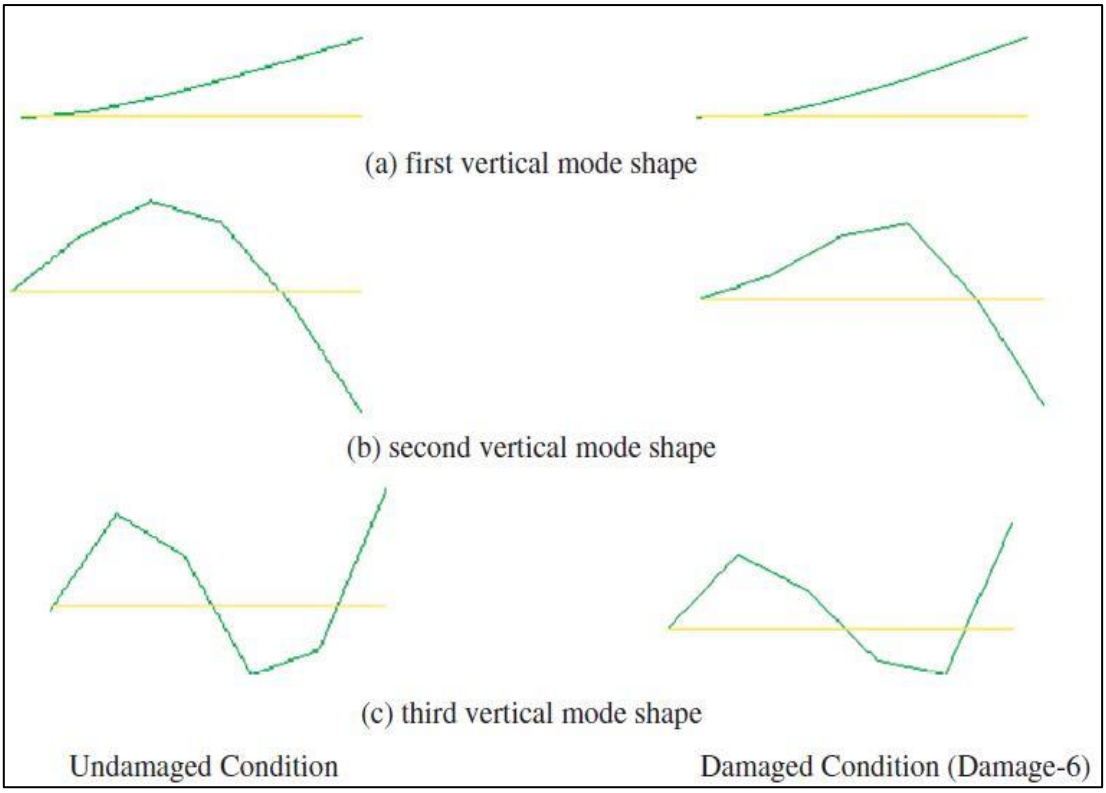

Figure 13: The experimentally determined first mode shapes for intact and damaged condition [Ahmet Can Altunışık et al. 2017].

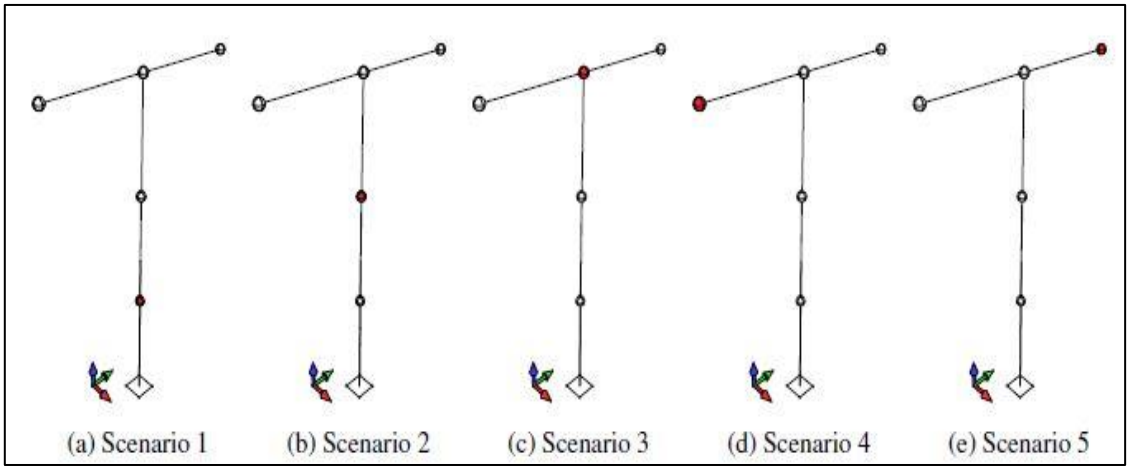

Figure 14: Scenario 1–5 – the red dot marks the added mass [J. B. Hansen et al. 2017].

Mustapha Dahak et el. (2017) measured the physical properties in cantilever beam and made it flexible to reduce the natural frequencies. Damages introduced in the different zones on the cantilever beam and experimental investigation was done for measuring the modal parameters and ANSYS software were used for the verification of the experimental results. MAC value can correlate the modal shapes of the damaged and undamaged structure [W. M. West. 1984].

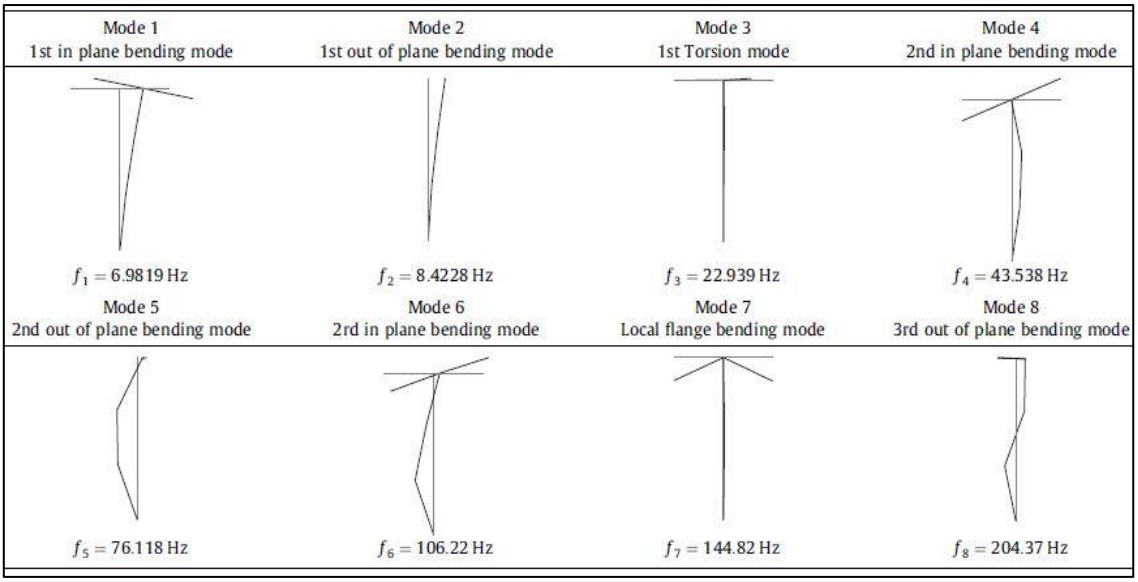

Figure 15: The experimental mode shapes and the corresponding natural frequencies of the structure in the reference state [J. B. Hansen et al. 2017].

The first and second damage location is detected by experimentally and numerically. The normalized frequencies are important to detect the damage location. The damage location is slightly differing from the created real location but it is very close to the introduced crack.

J. Zhang et el. (2013) presented the structural identification for the long span bridge by three separate post processing experimental methods including Peak Picking, PolyMAX, and Complex mode indicator function. Finite element software ADINA 8.7 was used for modelling the structural component of the bridge. The main five steps were followed for estimating the modal parameters. The mode shapes and modal parameters were validated by the finite element model. The experimental arrangement in the Figure 16 and the detail procedure for ambient vibration test shown in Figure 17. The comparison of modal parameters is shown in Figure 18.

Aktan, A. E et el. (1997) identified structural parameters by experimental analysis and calibrated by numerical models. The measured response of the physical system is shown in Figure 19.

Kijewski-Correa et el. (2007) measured the dynamic parameters experimentally and validated by finite element tools, see Figure 20-21.

Conte J. P et el. (2008) identified normalized vibration mode shapes using MNExT-ERA based on ambient vibration data (S = Symmetric; AS: = Anti-Symmetric; H, V, T = Horizontal, Vertical, and Torsional mode, respectively), see Figure 22-23.

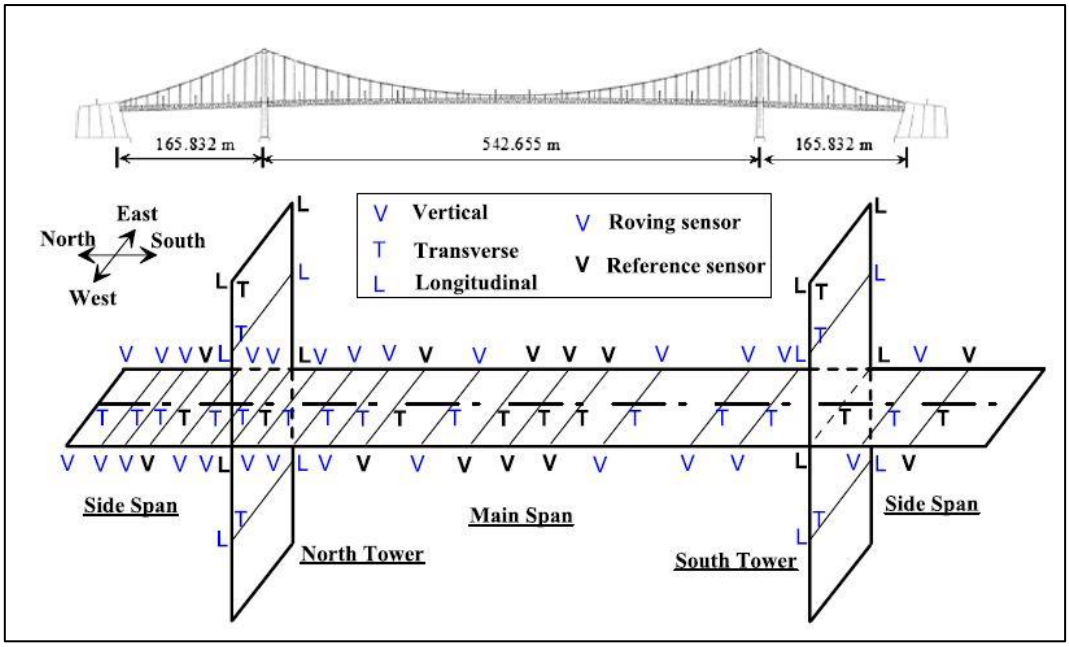

Figure 16: Accelerometer layout for stiffening trusses and tower [J. Zhang et al. 2013].

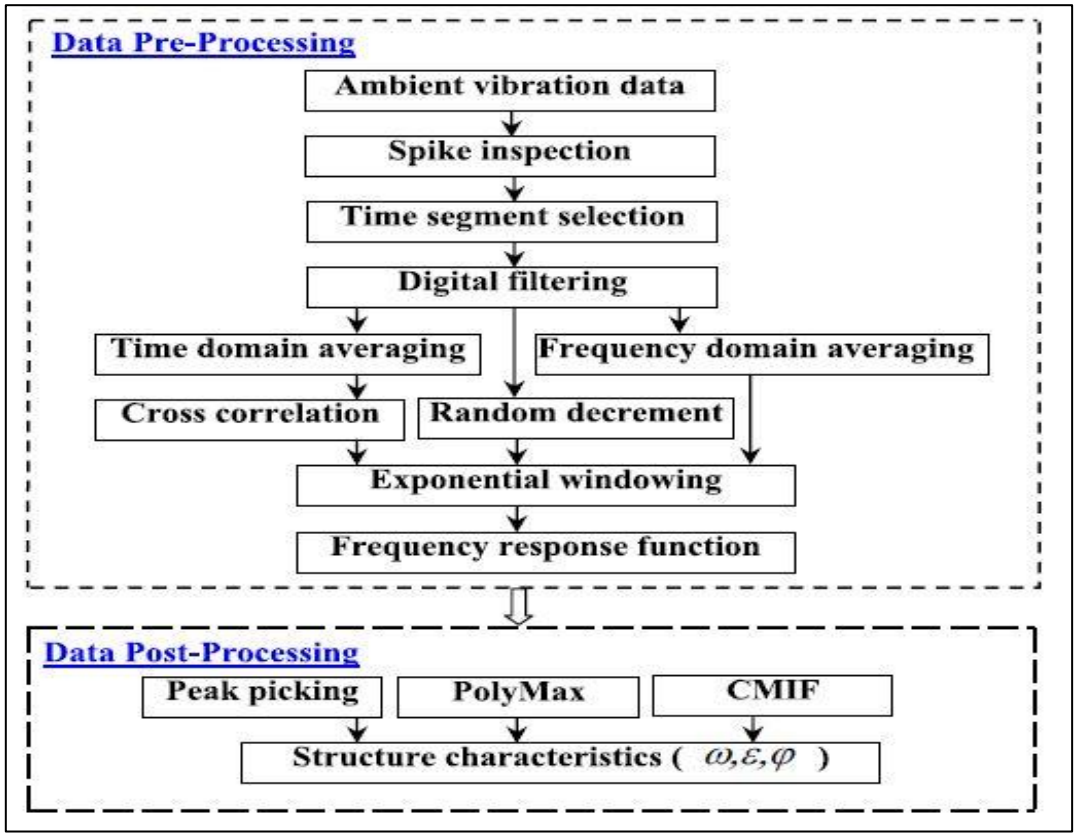

Figure 17: Flowchart of the data processing procedure [J. Zhang et al. 2013].

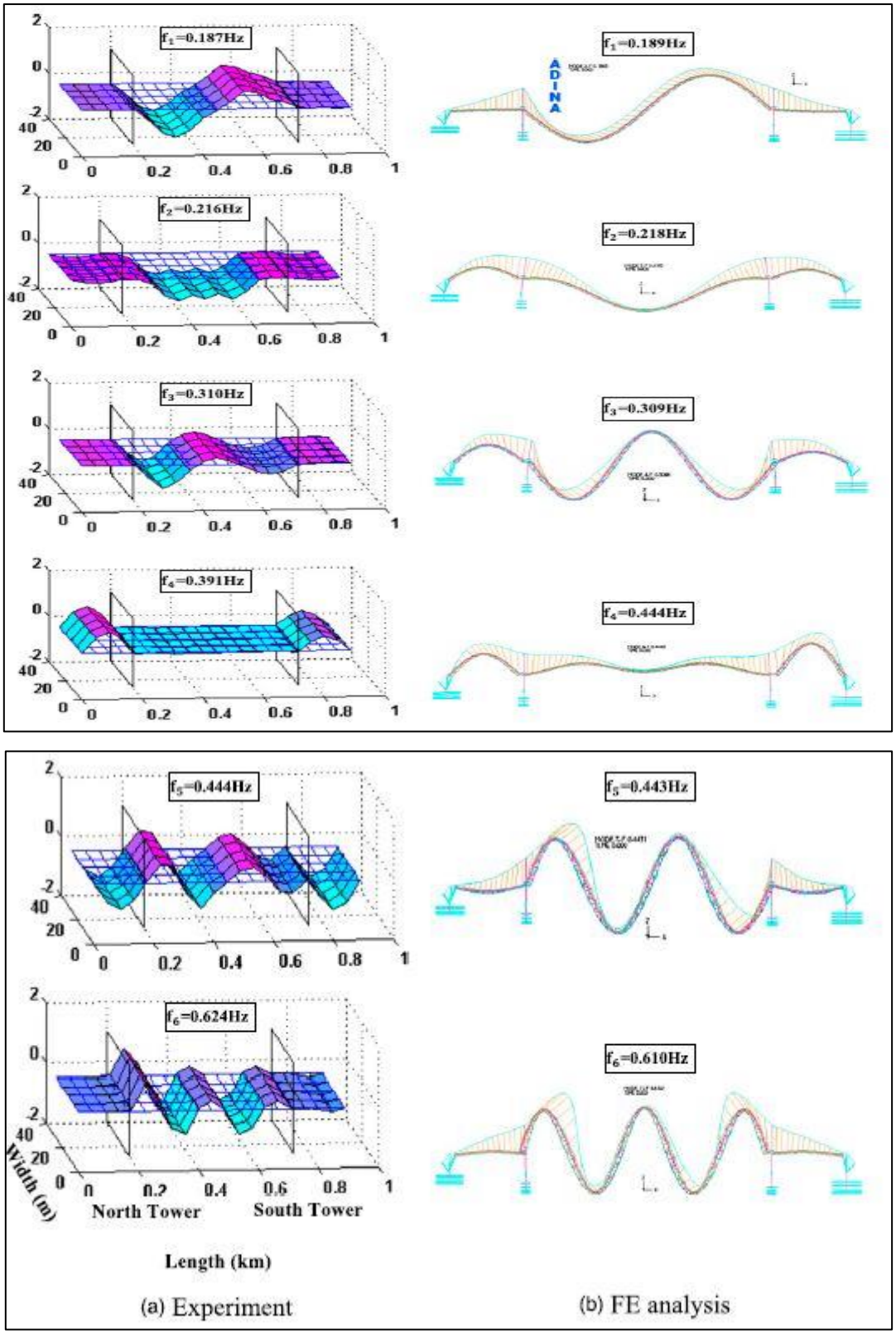

Figure 18: Experimental and numerical mode shape correlation [J. Zhang et al. 2013].

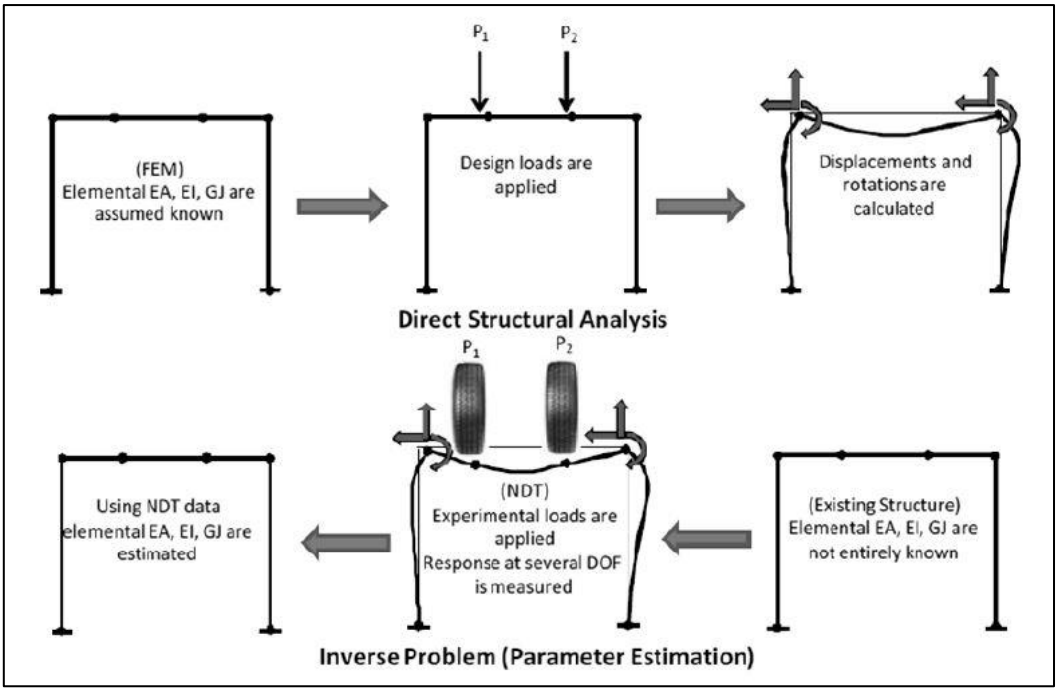

Figure 19: Structural identification and inverse analysis [Aktan, A. E et el. 1997].

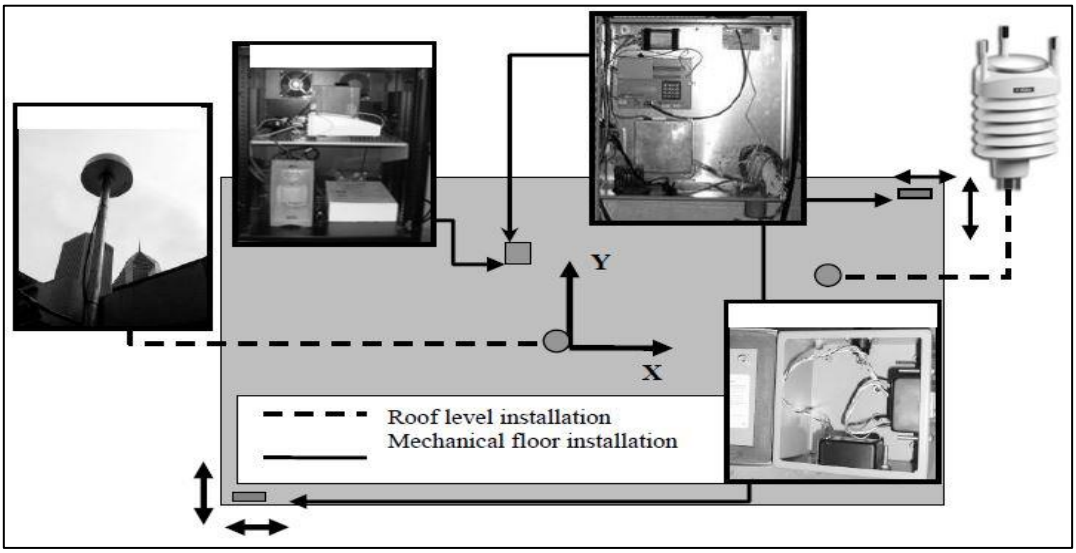

Figure 20: Schematic representation of sensors used in the Chicago full-scale monitoring program [Kijewski-Correa et el. 2007].

Wei-Xin Ren et el. (2004) conducted laboratory experimental testing to measure the modal parameters of a steel arch bridge in operating conditions. The experimental modal analysis procedure is carried out according to both input and output measurement data through the frequency response functions (FRF) in the frequency domain, or impulse response functions (IRF) in the time domain testing. Experimental testing in ambient conditions by both the peak picking method (frequency domain) and the stochastic subspace identification method (time

domain) and found very good agreement of the measured parameters. The three-dimensional finite element tools SAP2000 was used to validate and calibrate the measured parameters form PP and SSI methods.

Álvaro Cunha et el. (2004) applied output only modal identification methods to perform the modal parameters extraction for different types of civil engineering structures.

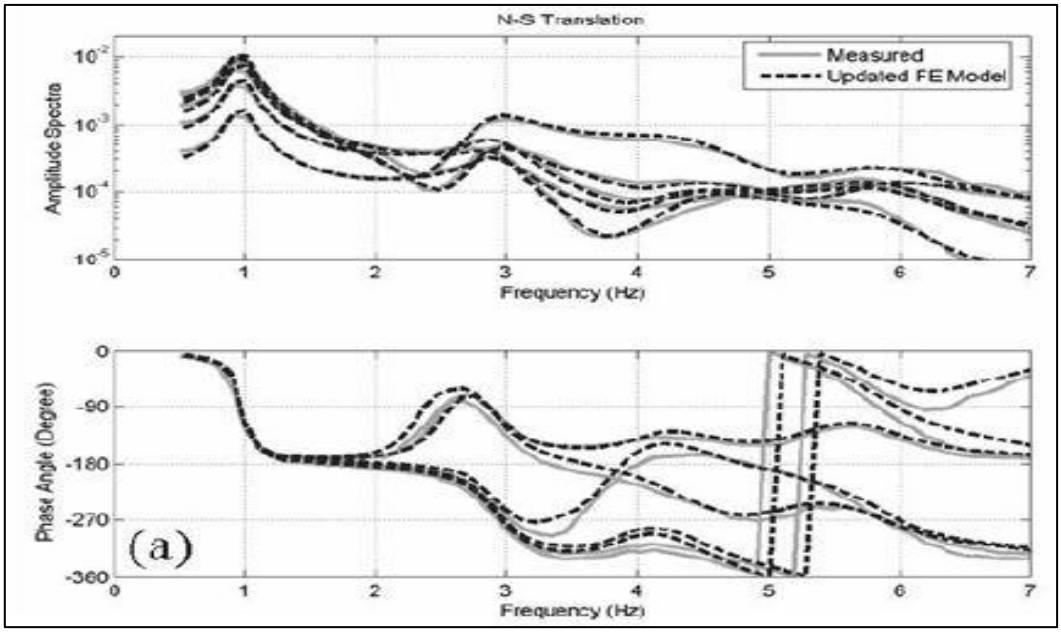

Figure 21: Comparison of measured and predicted functions [Kijewski-Correa et el. 2007].

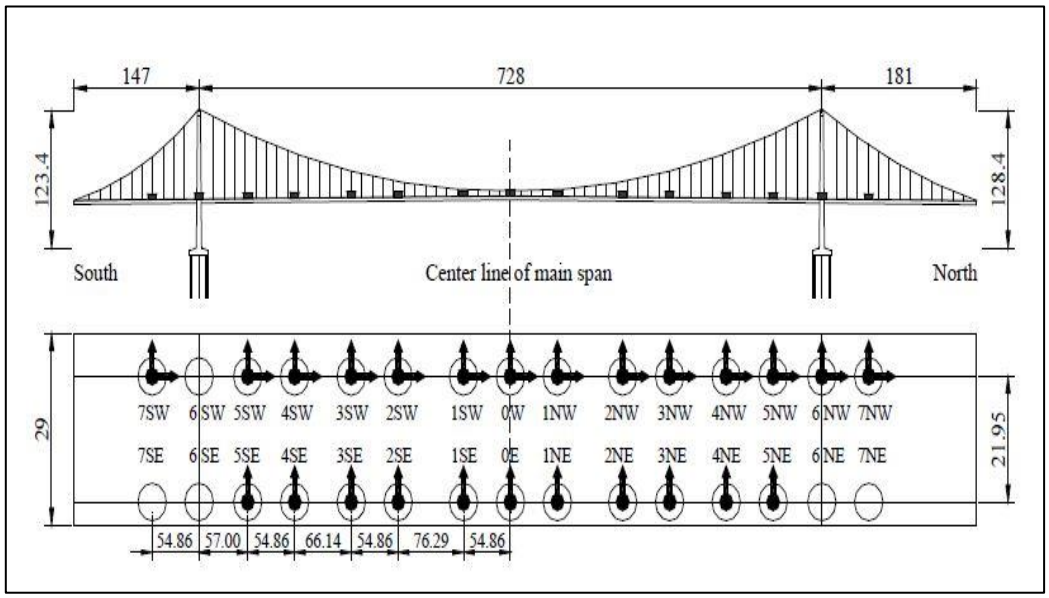

Figure 22: Overall dimensions of the AZMB and instrumentation layout [Conte J. P et el. 2008].

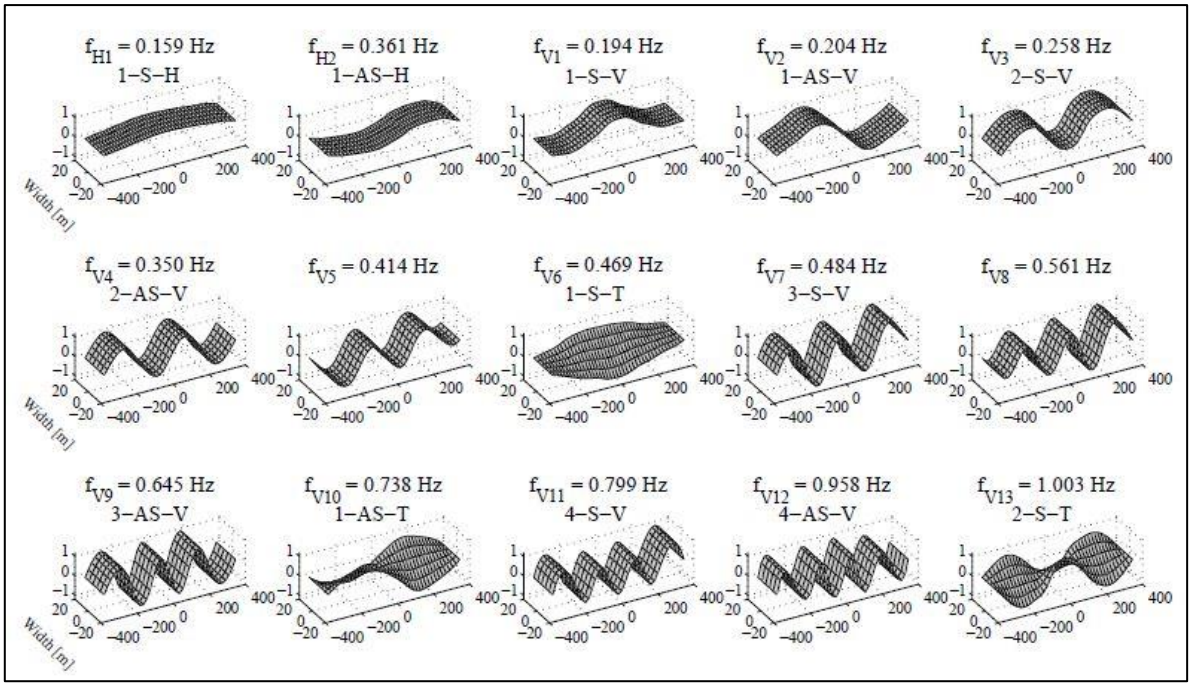

Figure 23: Normalized vibration mode shapes identified using MNExT-ERA based on ambient vibration [Conte J. P et el. 2008].

Output only modal identification techniques are classified according to the following criteria: (i) Domain of application (Time or Frequency); (ii) Type of formulation (Indirect or Modal and Direct); (iii) Number of modes analyzed (SDOF or MDOF); (iv) Number of inputs and type of estimates (SISO, SIMO, MIMO, MISO). The modal parameters are correlated by the finite element models for updating and validation.

Brian J. Schwarz et al. (1999) represented on “Experimental modal analysis” that the research study was done for measuring the FRF (modal parameters) by using the FFT analyzer and a set of FFT curve fitting. Modal excitation techniques also observed for the civil engineering structures. Digital FFT analyzer, and has grown steadily in popularity.

Ibsen et al. (2006) represented on “Experimental modal analysis” that the research study was done for wind turbine and estimation of modal parameters by using ambient response testing and modal identification (ARTeMIS). He had identified the modal parameters by frequency domain decomposition (FDD) and stochastic subspace iteration (SSI).

Dongming Feng et el. (2017) introduced advanced technique to monitor the structural health in a cost-effective way. Advanced noncontact vision-based systems offer a promising alternative of conventional experimental methods. Vision sensor for measuring the actual natural frequencies and mode shapes. Vision sensor is useful where it is difficult or expensive

to obtain the measurement using conventional sensors for important civil engineering structures.

Wei-Xin Ren et al. (2005) evaluated the dynamic characteristics of a large span cable-stayed bridge by an analytical modal analysis and experimental modal analysis. The output-only modal parameter identification was then carried out by using the peak picking of the average normalized power spectral densities in the frequency-domain and stochastic subspace identification in the time-domain. A good correlation is achieved between the finite element and ambient vibration test results.

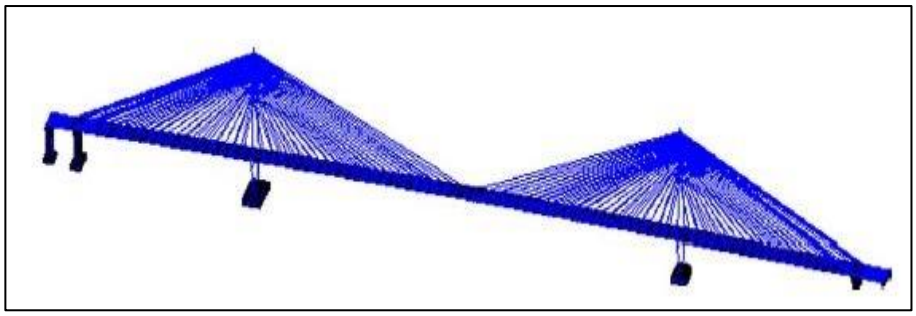

Figure 24: Three-dimensional finite element model of the bridge [Wei-Xin Ren et al. 2005].

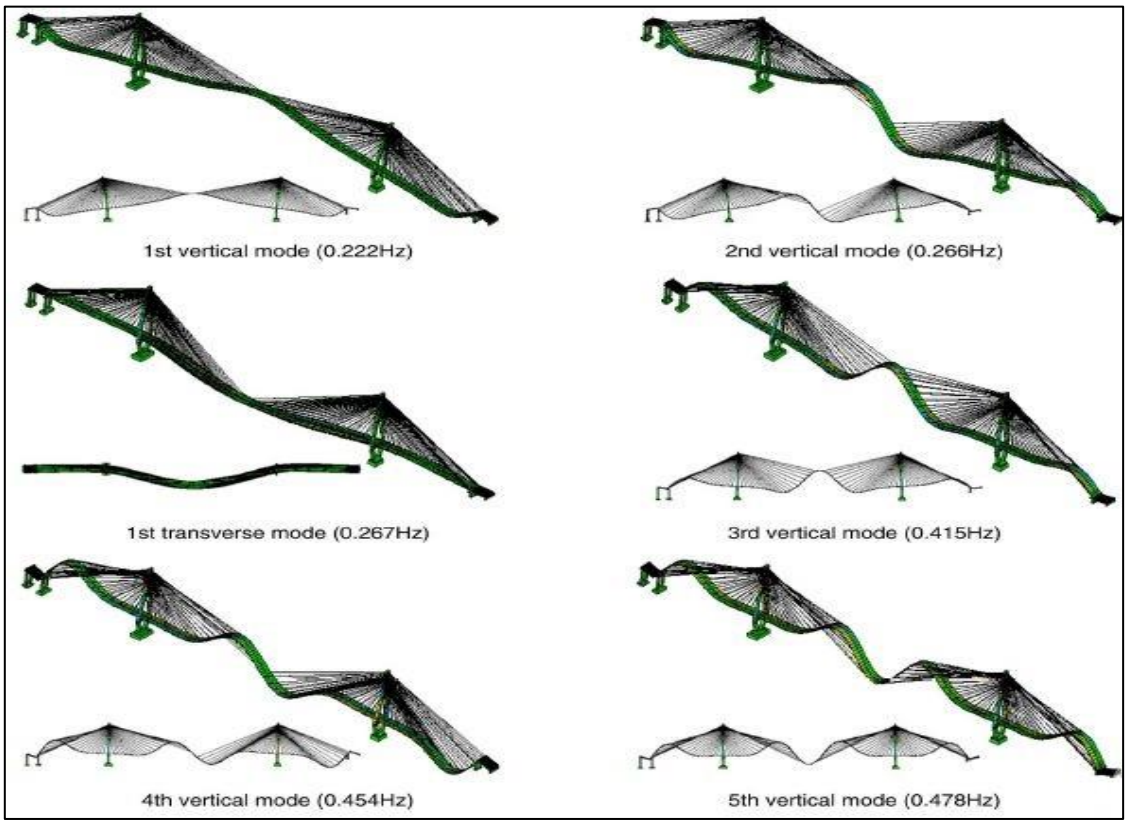

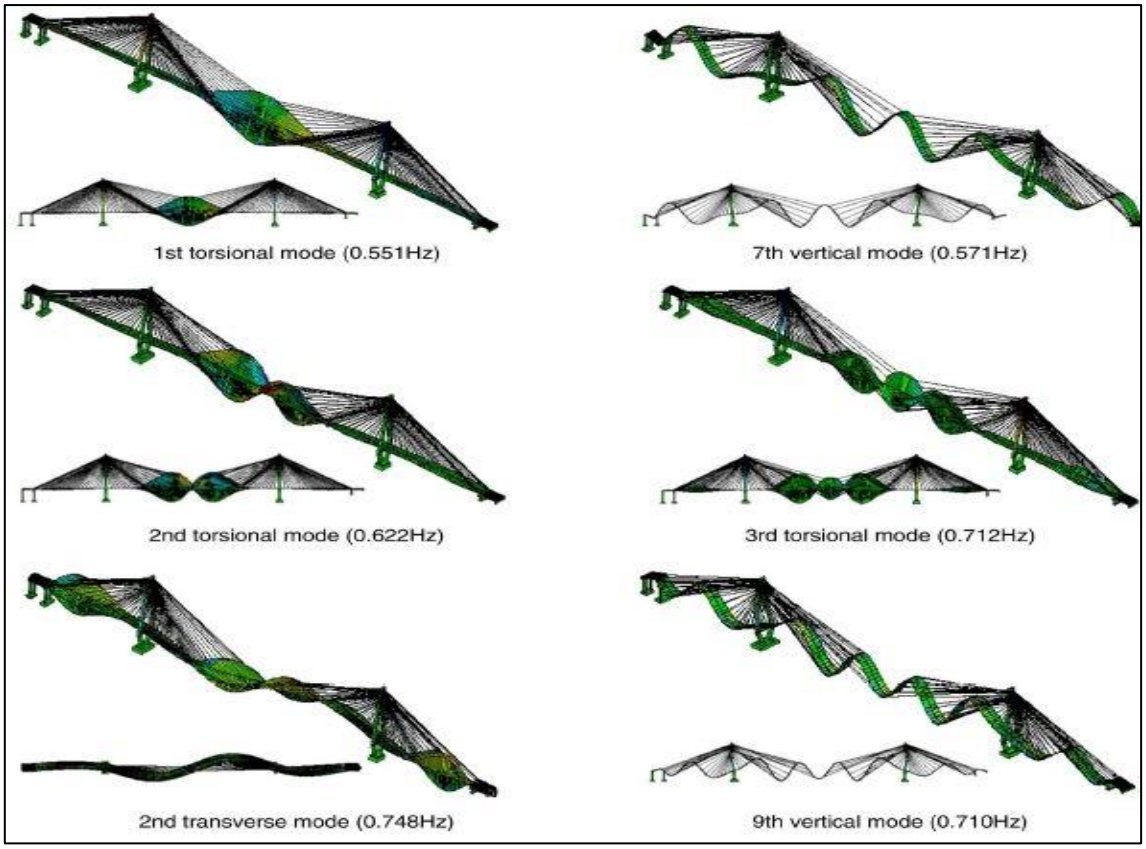

Figure 25: Mode shapes obtained from finite element analysis [Wei-Xin Ren et al. 2005].

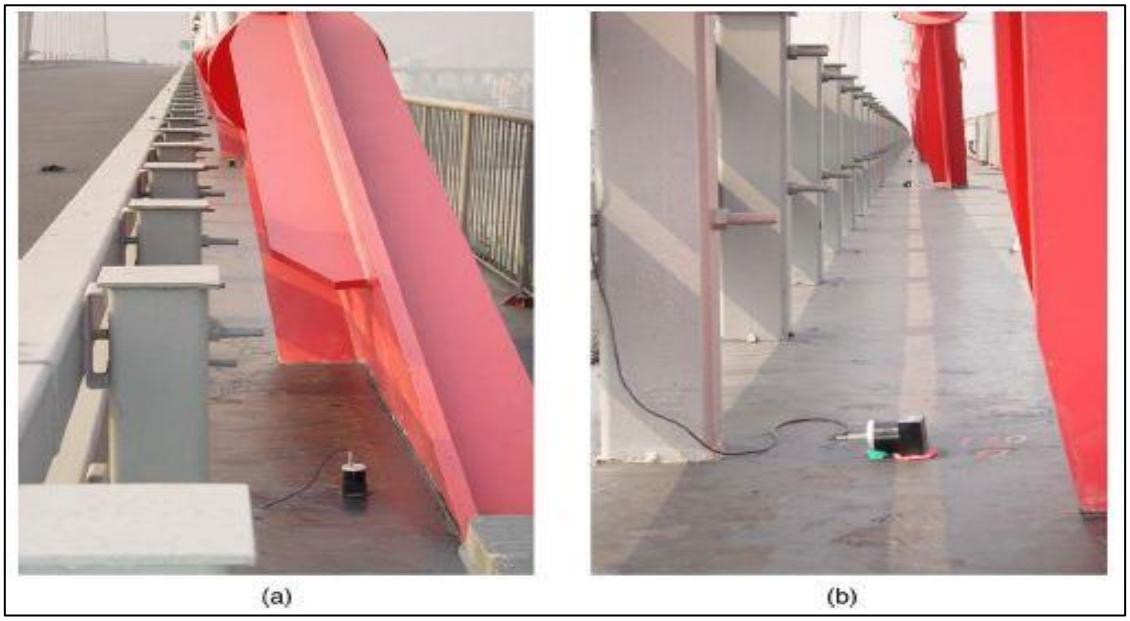

Figure 26: Accelerometers mounted on the deck. a) vertical accelerometer; b) transverse accelerometer [Wei-Xin Ren et al. 2005].

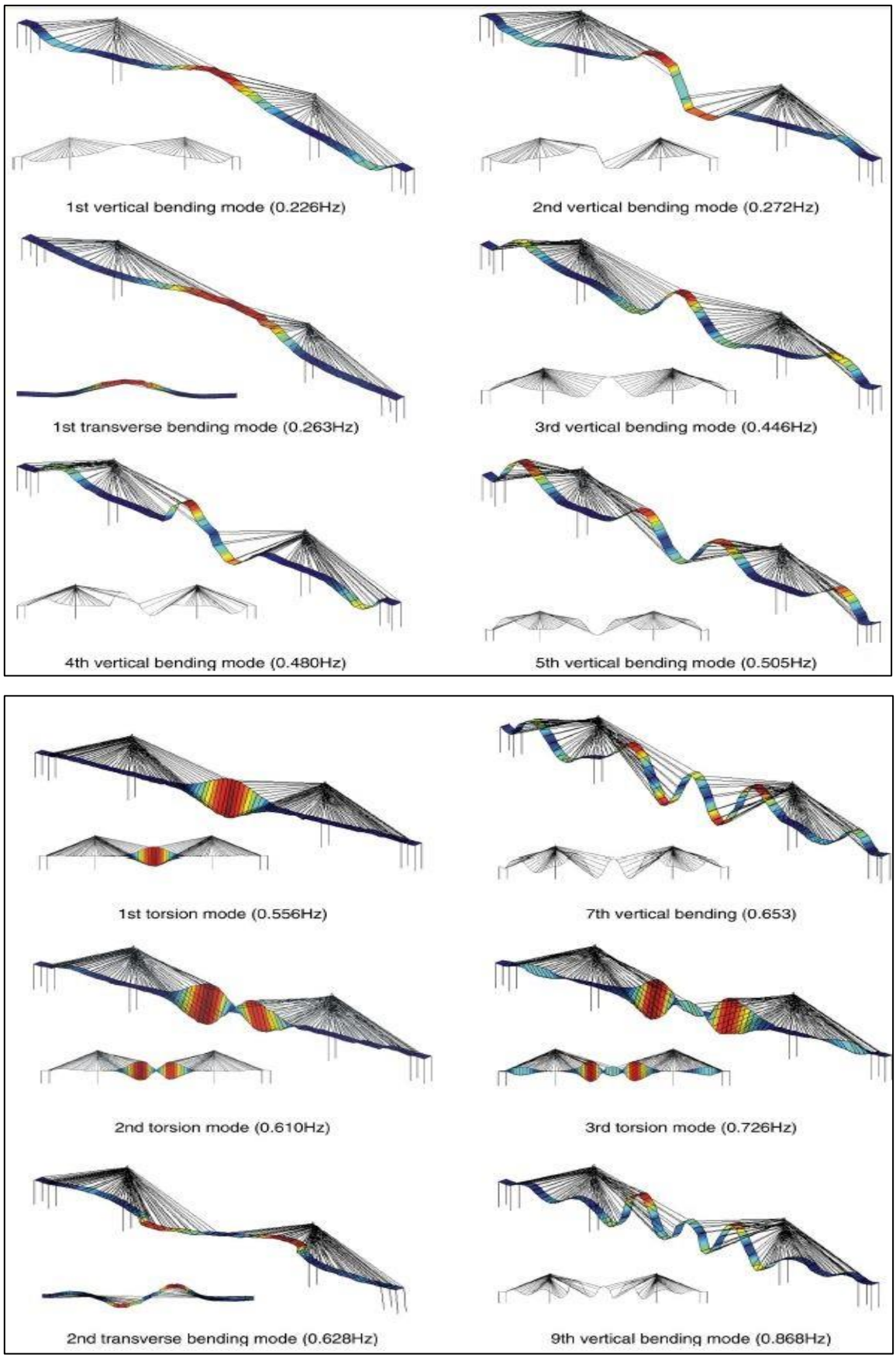

Figure 27: Typical mode shapes obtained from field tests by stochastic subspace identification [Wei-Xin Ren et al. 2005].

M. Molinari et al. (2009) represented on "Damage identification of a 3D full scale steel–concrete composite structure with partial-strength joints at different pseudo-dynamic load levels" that highlighted system identification methods for damage detection, localization and quantification by measuring actual modal parameters of a structure. The resistance and stiffness of semi-rigid and partial strength beam-to-column joints undergoing severe inelastic damage of composite structure. The modal parameters of the joints were resulted experimentally and updated in three different phases. After introducing small damage in the joint, the same way followed for modal parameters. Modal parameter estimation procedure was updated by Standard Monte Carlo simulations. The structure severely damaged after phase II and III.

Ruqiang Yan et el. (2015) discussed about the structural health monitoring of spindle by stochastic subspace identification (SSI) [Peeters B et al. 1999] experimental methods in operating conditions.

Emilio Di Lorenzo et el. (2017) evaluated mode shape curvature for wind turbine blade by two identical methods; whirling mode as damage detectors and mode shape curvature as damaged indicators. He compared the mode shapes obtained from these two methods for structural health monitoring. For cantilever beam structures like wind turbine, second method is better than the first one for indicating damage of the blade of wind turbine. Finite elements methods are done for the validation of experimental methods.

M. Hassan Haeri et el. (2017) introduced innovative methods namely inverse vibration technique for offshore jacket platforms. The offshore structures are affected by the sea current and wave and excited by wave loads, boat impacts, sea typhoons and seawater corrosive properties. New techniques are developed for measuring the crack presence, crack location, damage severity and prediction of the remaining service life of the structure. SHM was investigated by the damage localization step of offshore platforms. 2D shear reference model, 2D flexural reference model and 3D shear building reference model was used to find the level of damage, flexural behavior of structure after damage and translational stiffness variation to detect the defected level.

Jia. He et el. (2017) applied two set of investigation: MR dampers were employed for vibration control and the EKF-based approach was used for damage detection for Kobe earthquake and Northridge earthquake. MR dampers were used for 5 storey shear building vibration with an additional column and without an additional column. Without vibration control the structural

responses were significantly reduced with control in terms of peak displacement and acceleration.

Alberto Barontini et el. (2017) used nature-inspired optimization algorithms to keep the value of heritage, cultural identity, environmental and economic benefits for the historic buildings.

G. Acunzo et el. (2017) proposed new method, Multi Rigid Polygons (MRP) model for the building modal estimations. In this method, modal mass ratio was considered based on an ideal subdivision of each floor in one or more rigid polygons. The classical experimental modal analysis (EMA) [D. Ewins. 1984], is based on the measurement of the dynamic response and of the applied excitation, from which FRFs or IRFs of the system are built. Two types of building: first one is geometrical imperfect and second one is complex historical building were considered for evaluating modal mass in ambient situations. Different uncertainties such as eccentricity, complex in shape and irregularity of mass distribution had been validated numerical simulation.

E. Peter Carden et el. (2008) examined structural health monitoring (SHM) for the civil engineering structure was done by Autoregressive Moving Average (ARMA) models to detect and locate damage. The experimental data was measured by the IASC–ASCE benchmark [S.J. Dyke et al. 2003] for four-story frame structure. The sensitivity of ARMA models proved the typical infrastructural damage of static response data.

T. H. Ooijevaar et el. (2010) developed damage detection methods applied experimentally for a carbon fiber PEKK reinforced composite T-beam. Accelerometers and laser vibrometer were fixed according to the setup manual. Mode shapes due to bending and torsion verified by the Modal Strain Energy Damage Index. The location and severity of damage depends on the vibrational parameters. The point of measurement and location of measurement affects the sensitivity to identify damage at a certain distance from the measured points. Integrated sensors are very good solution for mode shape measurements and damage identification based on structural health monitoring and proposed numerical model [Loendersloot R et al. 2009] will be perfect to optimally place the different sensors.

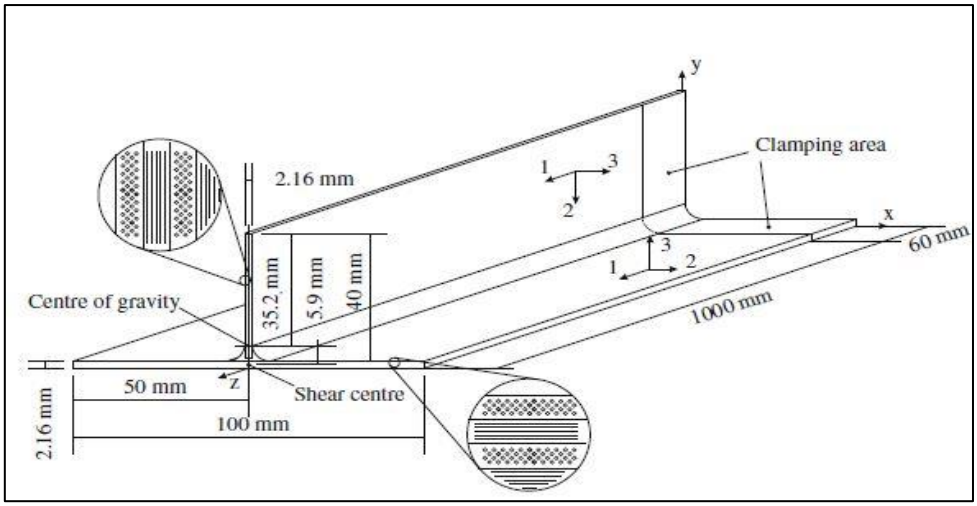

Figure 28: Laminate lay-up and dimensions [T. H. Ooijevaar et al. 2010].

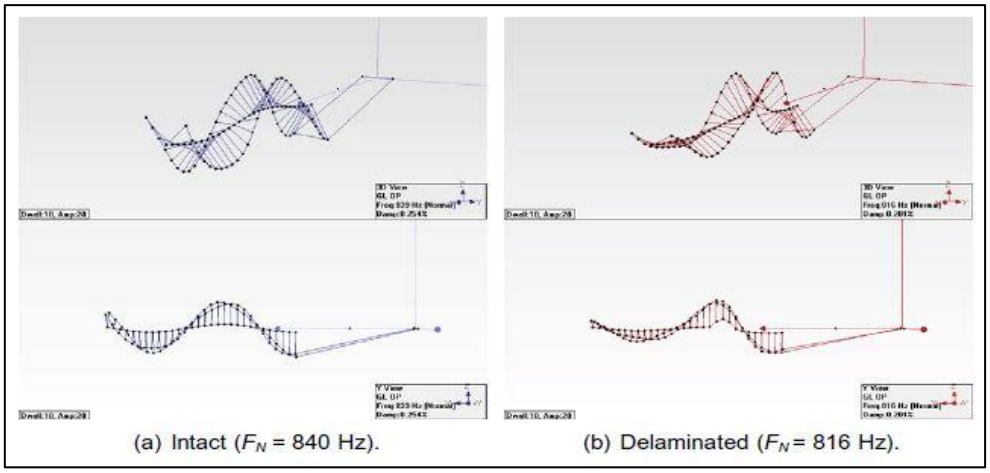

Figure 29: Experimentally obtained 7th bending mode shape (MAC = 0.8328)

[T. H. Ooijevaar et al. 2010].

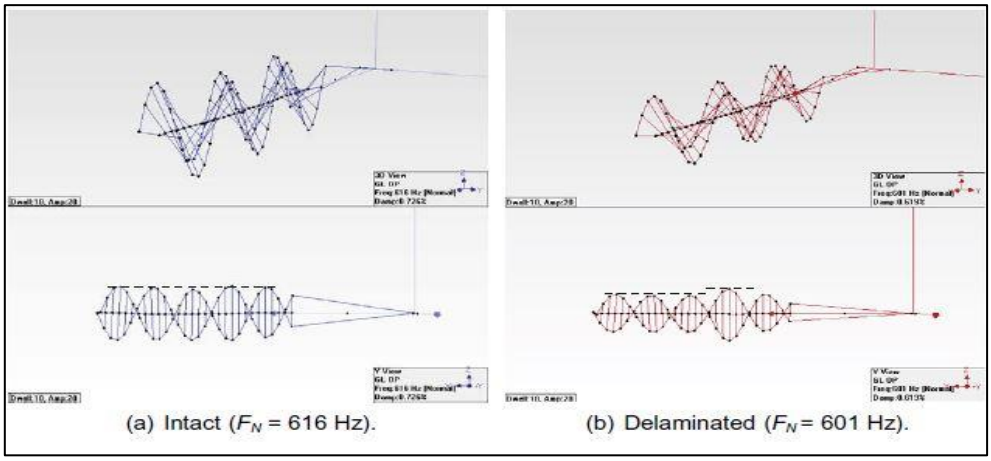

Figure 30: Experimentally obtained 9th torsion mode shape (MAC = 0.9707)

[T. H. Ooijevaar et al. 2010].

N. Larbi et al. (2000) represented on "Experimental modal analysis of a structure excited by a random force" that the study had done for estimation of modal parameters by multivariate procedure. The vibrating system was excited by a random force and only output sensors were used to estimate the natural frequencies and damping factors of the system. The method works in time domain and a vector autoregressive moving-average (VARMA) process was used. The information about modal parameters was contained in the multivariate AR part, which was estimated using an iterative maximum likelihood algorithm. This algorithm used as a score technique and output data only. The order of the AR part is obtained via the minimum description length associated with an instrumental variable procedure. Experimental results showed the effectiveness of the method for model order selection and modal parameters estimation. The critical problem of order estimation has been resolved using the minimum description length (MDL) criterion associated with an instrumental variable matrix. The method is currently being generalized to be applied to large industrial structures at work.

Timothy. M et al. (2008) examined the effect of damages on mode shape due to higher order derivatives. Higher order mode shape derivatives depend on the presence of damage, location of the damage and damage radius. Mass loss, stiffness loss for the local damage and damage radius has great influence on the mode shape derivatives. Experimental investigations were verified by the numerical investigations for better understanding the effect of sensitivity to various damage related parameters.

S. Nagarajaiah et al. (2009) introduced a new technique for modal parameters estimation. He applied output only modal identification modal for structural damage detection. Output modal identification technique consists of linear time invariant (LTI), linear time variant (LTV), Time-frequency, short-time Fourier transform (STFT), empirical mode decomposition (EMD), and wavelets. The experimental modal parameters were determined by free vibration response test and white noise vibration test for both damaged and undamaged member. The significant change in the frequency for both test after 10 seconds. Damage detection and frequency changes after damage can be measured very effectively by the wavelet technique.

2.4. Building frames under blast actions

Blast loading is an explosion in a rapid release of stored energy characterized by bright flash and an audible blast. Part of the energy released as thermal radiation (flash) and part is coupled into the air as air blast and into the soil as ground shock both as rapidly expanding shock waves. Blast loads on structures can be classified into two followings main groups on the basis of

confinement of the explosive charge. Unconfined explosion which include free air burst, air burst and surface burst explosion having un-reflected and reflected loads respectively. Confined explosion includes fully vented explosions, partially confined explosions, fully confined explosions.

Blast loading effects on structural members may produce both local and global responses associated with different failure modes. The type of structural response depends mainly on: the loading rates; the orientation of the target with respect to the direction of the blast wave propagation and boundary conditions. Failure modes accompanying with global response: flexure, direct shear or punching shear. Failure modes associated with local response (close-in effects): localized breaching and spalling.

2.4.1. Global structural behavior

The global response of structural elements is generally a consequence of transverse (out-of-plane) loads with long exposure time (quasi-static loading) [Woodson et al. 1993]:

- global membrane (bending)
- shear responses-diagonal tension; diagonal compression; punching shear; direct (dynamic) shear

2.4.2. Local structural behavior

The close-in effect of explosion may cause localized shear (localized punching-or breaching and spalling) or flexural failure in the closest structural elements [Clarence W. de Silva. 2005]. Breaching failures are typically accompanied by spalling and scabbing of concrete covers as well as fragments and debris.

Figure 31: Column responses subject to near-contact blast charges [T. Brewer et al. 2016].

2.4.3. Pressure-impulse (P-I) diagrams (ISO-damage curves)

The pressure-impulse (P-I) diagram is an easy way to mathematically relate a specific damage level to a combination of blast pressures and impulses impose on a particular structural element [Clarence W. de Silva. 2005]. There are P-I diagrams that concern with human response to blast as well, in which three categories of blast-induced injury are identified as primary, secondary, and tertiary injury [Baker et al. 1983].

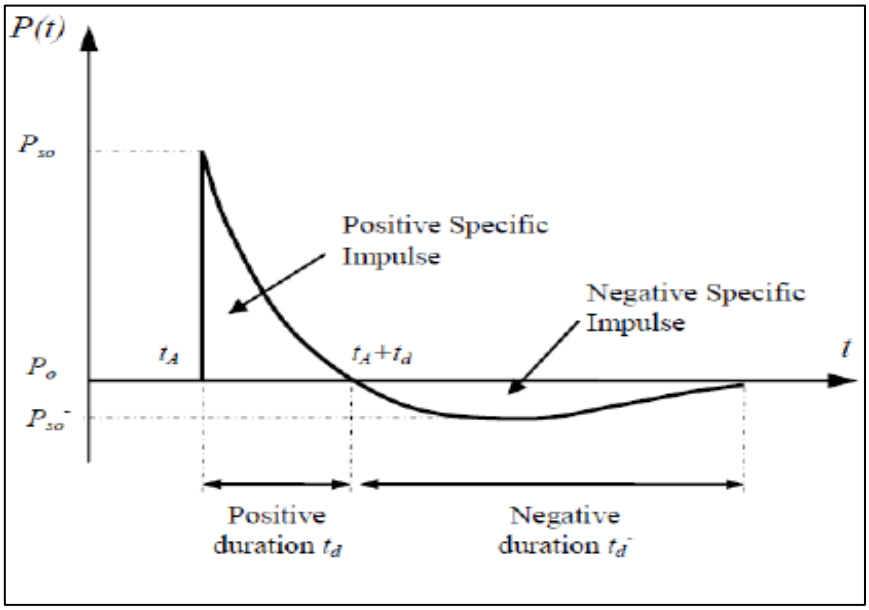

Figure 32: Time history function of blast wave pressure on building [Islam. 2016].

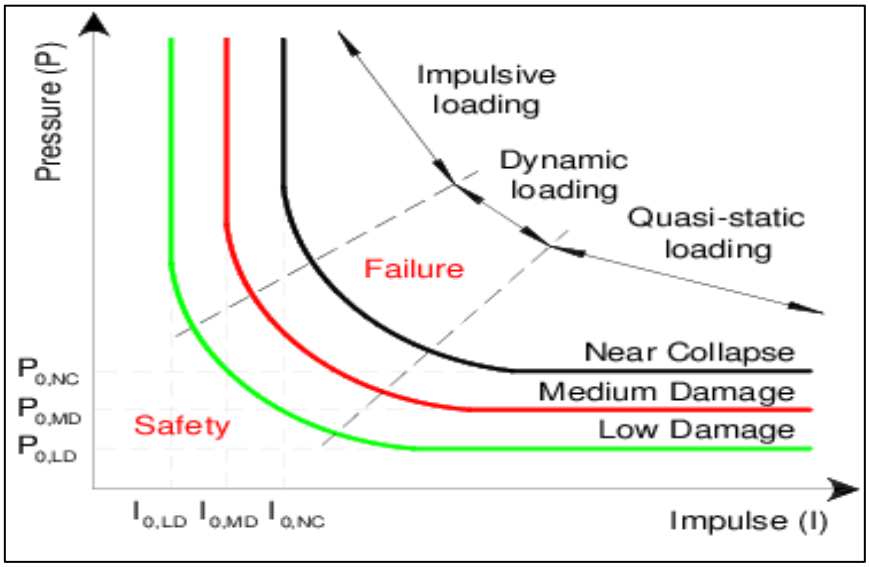

Figure 33: Typical pressure-impulse diagrams associated with increasing levels of damage [Fulvio Parisi et al. 2016].

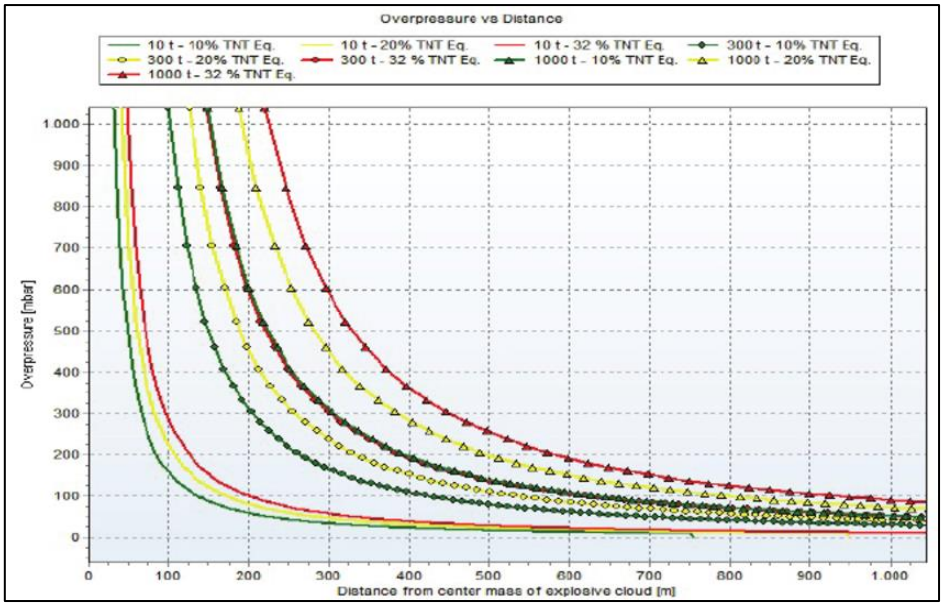

Figure 34: Overpressure-distance diagram to buildings [Török et al. 2015 and FEMA-IS156].

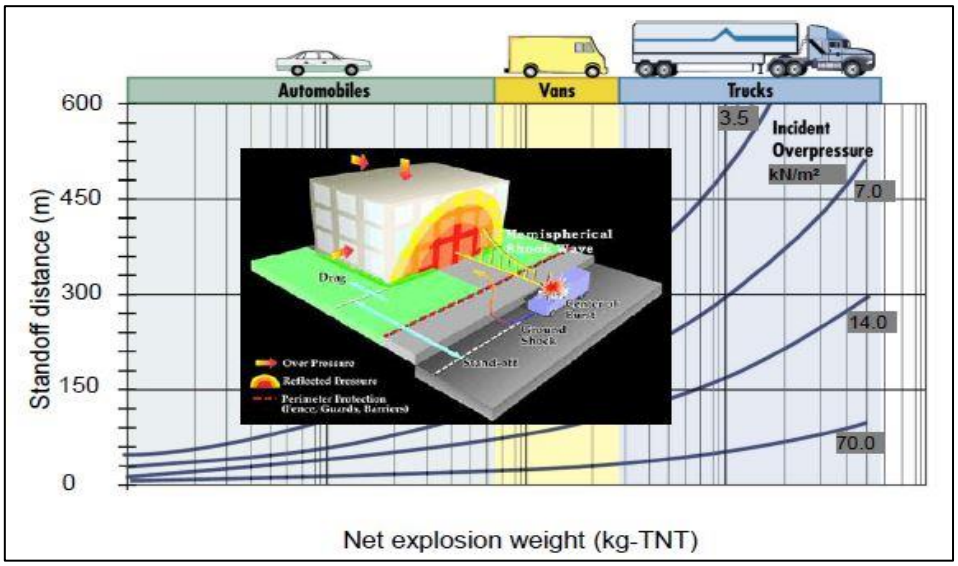

Figure 35: Standoff distance-explosion weight diagram to buildings [Török et al. 2015].

2.5. Concluding remarks, needs for new developments

Structural identification (St-Id) is a transformation and application of system identification to civil (constructed) engineering structural systems. Important civil engineering structures such as tall buildings, long span bridge, wind turbine, tower and road transportation network highways are very prone to the dynamic actions like explosion, earthquakes, impacts, and blast. Newly constructed structures and existing reinforced concrete structures, masonry structures, steel structures and composite steel-concrete structures are subjected to the dynamic actions has great scope to innovate for the researchers. Structural deterioration, stability losses,

stiffness wounded of joints, crack initiation and propagation settlement of the foundations and damage detection and/or other types of performance under the blast actions for newly constructed structures is a crucial issue. Designing structural modification, retrofit or hardening due to changes in use-modes, codes, aging, actions and/or for increasing system-reliability for existing structures. The structural response and damage initiation for both newly constructed and existing structures subjected to blast loads is unique from that of most operational and extreme loads due to the wide bandwidth, highly impulsive nature of blast overpressures. In addition, unlike most natural hazards, the manufactured design of this artificial threat means that the nature of the blast hazard is often unpredictable and likely to remain ever-changing [ASCE. 2011].

Recently, blast resistant design considerations have received great attention in the commercial sector. Government trying to establish the development of research fund and encourage engineers, professional and researchers to get complete perception about the behavior of important structures under unexpected loadings. Many researchers have done many research works for identifying the dynamic characteristics of civil engineering structures for the structural health and performance monitoring before and after damaged of the structures. Most of them highlighted on the long span bridges under the ambient loadings and a few of them considered the vibrations for the seismic and accidental actions. They have done by other technology for experimental and finite element analysis. Research on buildings is so limited for dynamic actions. Very few research had been conducted on condition assessment and residual performance evaluation of structures subject to blast actions. Some of them had done for the masonry building under blast actions for measuring the residual performance after blast actions. But the ductility problem is great extent for the masonry building subjected to blast actions. Not much research is available to study the structural identification for the moment resisting steel structural frame building under blast actions. There is a need to study the structural identification by Bruel & Kjaer experimental modal analysis for measuring the modal parameters for undamaged and damaged conditions. Bruel & Kjaer experimental modal analysis is very promising and latest technology to invention the dynamic modal parameters. In this research, complete data sets measured from field testing of full-scale structures under dynamic loading condition, and validate to the finite element analysis for simulating the actual performance.

3. SYSTEM IDENTIFICATION OF SIMPLE STEEL FRAME

3.1. Forced vibration experimental modal parameter calibration in laboratory

3.1.1. Description of frame in laboratory-step 1

The steel frame in the laboratory (test structure) is a simple frame made by HEA 180 section for the beams, columns and diagonal bracing. The spacing of columns is 0.83m and the height of column is 3.0m. Spacing of beams is 1.0m; 0.70m and 1.30 m respectively. The design steel material in profiles was S275. The detail of the frame is shown in the Figure 36.a-b.

a) b)

Figure 36: Simple steel frame in the laboratory (test structure): a) intact frame (Case A); b) frame after dismantling lower beam (Case B).

3.1.2. Modeling main structural components-step 2

This steel frame was modelled using the numerical commercial FEM software SAP2000. The structural system is made of braced frames. Beam-to-column connections are designed as pinned. Columns are also pinned at the base. The modal mass is distributed on the length of the column in several points shown in Figure 37.a-b.

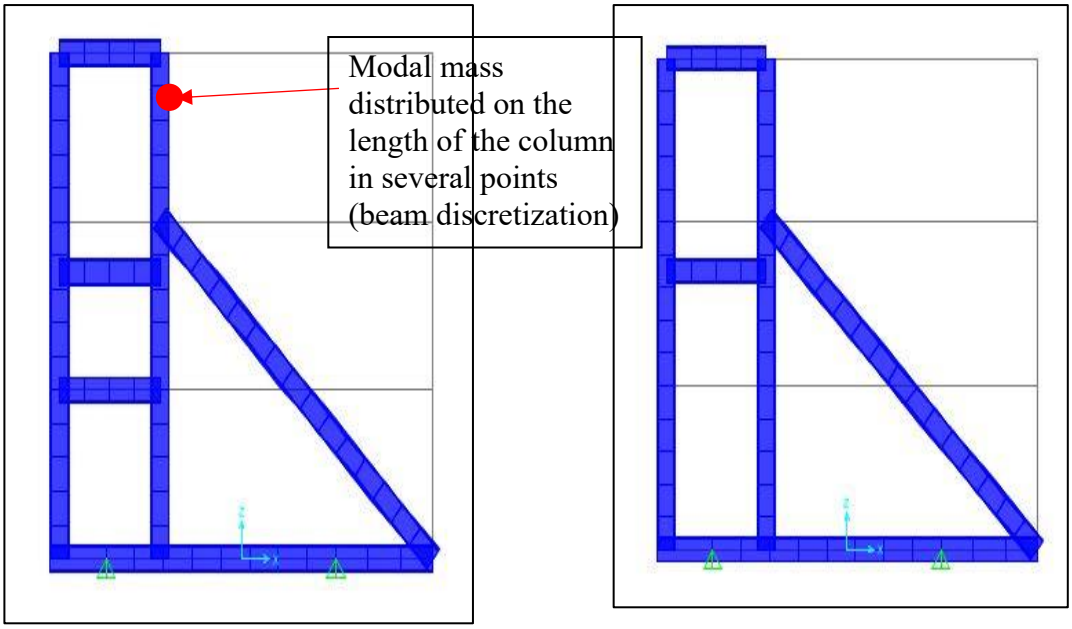

a) b)

Figure 37: Simple steel frame modelling by SAP2000: a) intact frame (Case A); b) frame after dismantling lower beam (Case B).

3.1.3. Forced vibration testing-step 3

The geometry is directly drawn in MTC hammer measurement software. For both intact frame and frame after dismantling lower beam, 7 accelerometers were fixed at a distance of 0.0m, 0.50m, 0.70m, 0.43m, 0.43m, and 0.43m respectively from the bottom is shown in Figure 38. The accelerometers are numbered to make proper connection according to the serial in the proper channel of transducer. To make sure that the channel and accelerometers is fixed properly in the frame was checked. A 3.20lb black and hard hammer was positioned at 1.0m height from the bottom in the frame carefully. The other end of the accelerometers and hammer is connected to the signal processing device LAN-XI and this device is connected to the laptop by cable connector.

3.1.4. Field test and data collection

The on-site portion of the vibration-testing program included both the installation and verification of the operation of the accelerometers, positioning of accelerometers and exciting hammer, cabling, and data acquisition components. The hardware is setup by reconfiguring of accelerometers and hammer location in the channel of transducer. Selection of the position of

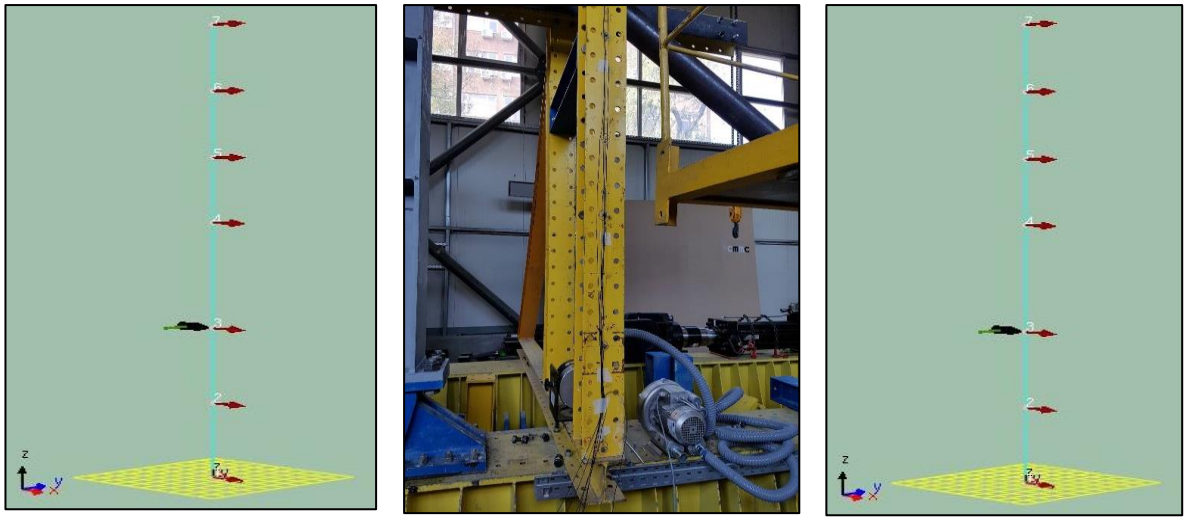

Figure 38: Positioning of accelerometers and impact hammer.

accelerometer and force and also identify the code of accelerometer and hammer was done accurately. Second phase is to measure the vibration of the frame for excitation by hammer. Before starting measurement, analysis set up is important to check the frequency is sufficient or not for proper hit detection. The measuring time was 6.4 second and the span of frequency for FFT was fixed as 1000 Hz. The average number of measurement 5 for getting better signal response from the excitation. Hammer weighting can be uniform/exponential or transient. I took it uniform for measurement of vibration for getting better result. This phase is most important to measure the response. Excite the exact position that is considered in the frame and measurement is recorded for five hitting and taking the average value. After measurement the initial mode shape can see from MTC hammer test FRF validation task. MTC hammer test data is exported for interpretation of data, getting modal parameters by pulse reflex experimental modal analysis. Universal file format is supported for the pulse reflex analysis and data is exported in terms of frequency response H_1.

3.1.5. Data processing-step 4

Step 4 of the St-Id process involves the processing and interpretation of data collected during Step 3. For modal identification of the columns, forced vibration data from 7 accelerometers fixed in plane (Figure 38) is processed.

The response weighting, computed from a single data set that is processed with the two different averaging methods, are shown in Figure 39 and Figure 42 for both case respectively. Frequency response function measured from the MTC hammer excitation is plotted in Figure

40 and Figure 43 for both case respectively. The measurement was validated by the FRF validation by computing frequency vs acceleration curve is shown in Figure 41 and Figure 44 for both case respectively.

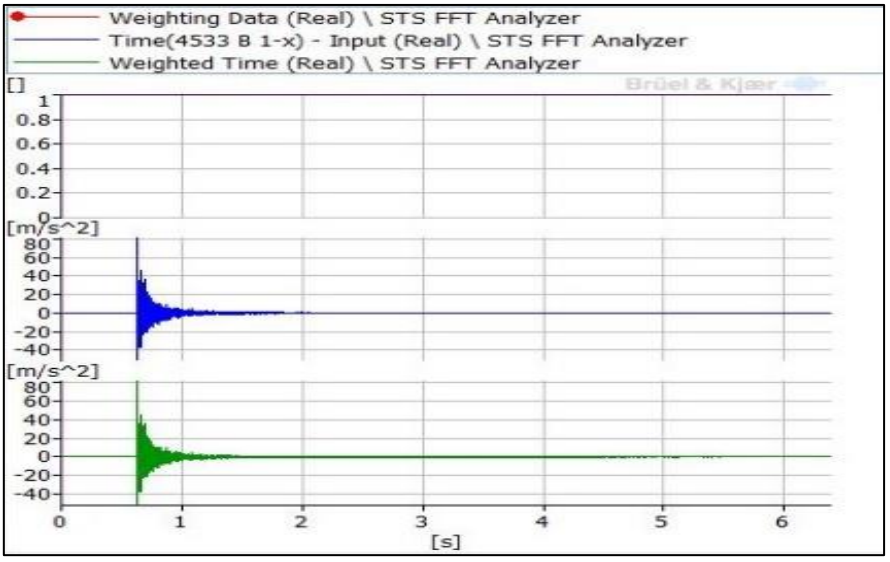

Figure 39: Response weighting function for case A.

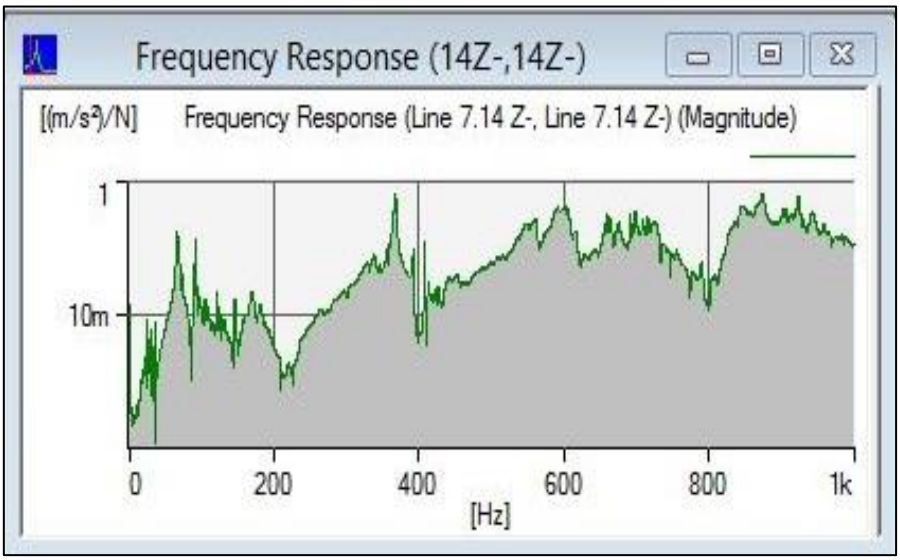

Figure 40: Frequency response function for case A.

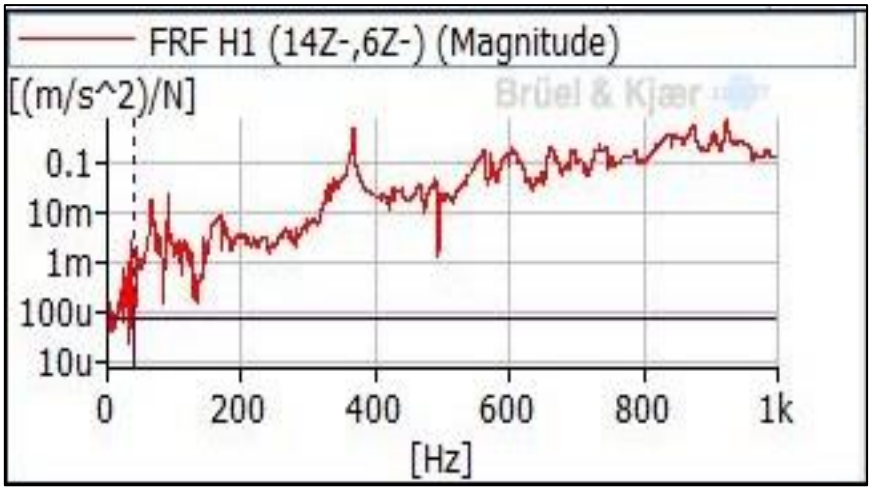

Figure 41: Frequency vs acceleration curve for case A.

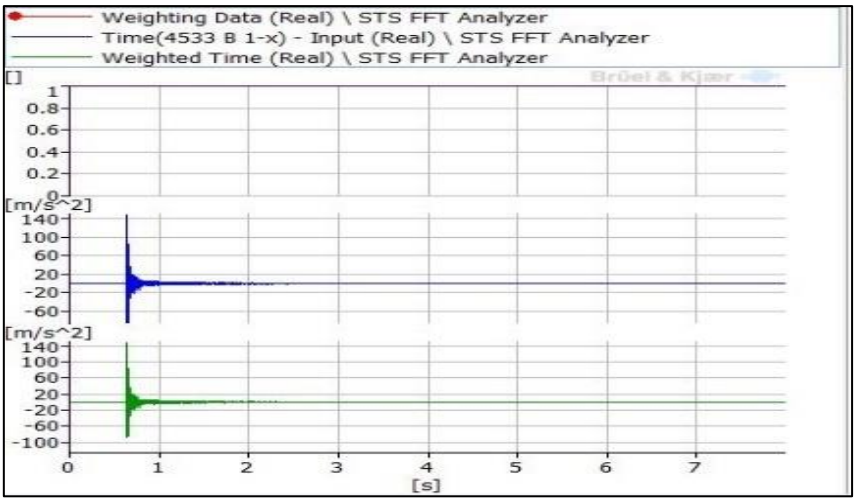

Figure 42: Response weighting function for case B.

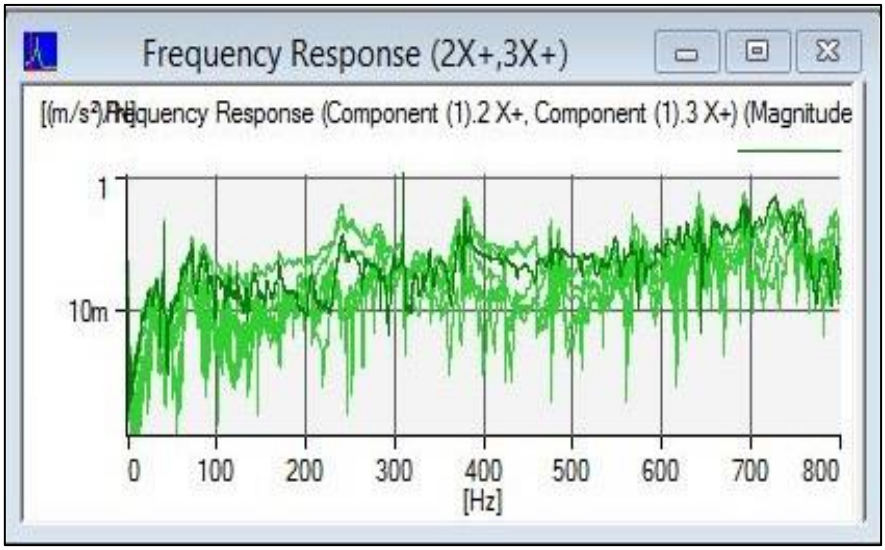

Figure 43: Frequency response function for case B.

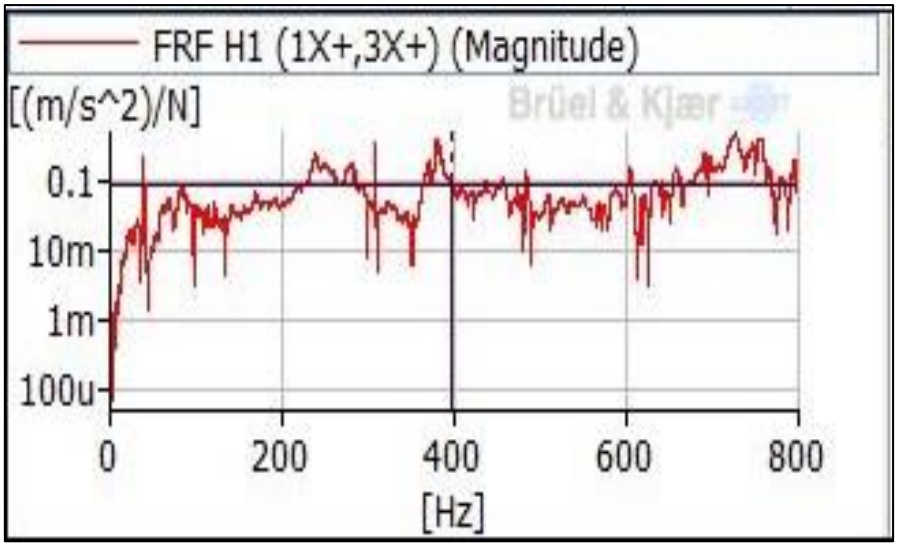

Figure 44: Frequency vs acceleration curve for case B.

3.1.6. Data post processing for modal parameter identification

Bruel & Kjaer experimental modal analysis is the specific modal identification method that are applied for identifying the vibration data. In this method, very sensitive accelerometers are used for recording very low signal-to-noise ratios, and for the damping ratio estimates. To evaluate and validate the experimental modal identification results, finite element software SAP2000 was used. Experimental modal analysis is one of the most basic approaches that can be used to identify structural modal properties from the output-only measurements. The main drawback of this method is to measure the response signal from field that hampers by the noise or errors, harmonics and uncertainties that may be present in the unmeasured excitation spectrum.

The span of the frequency where the modes are available for cumulative modal identification factor is selected manually by the user is shown in Figure 45 and Figure 49 for case A and case B respectively. The stable mode is indicated by the redline for 150 number of iteration in rational function polynomial method.

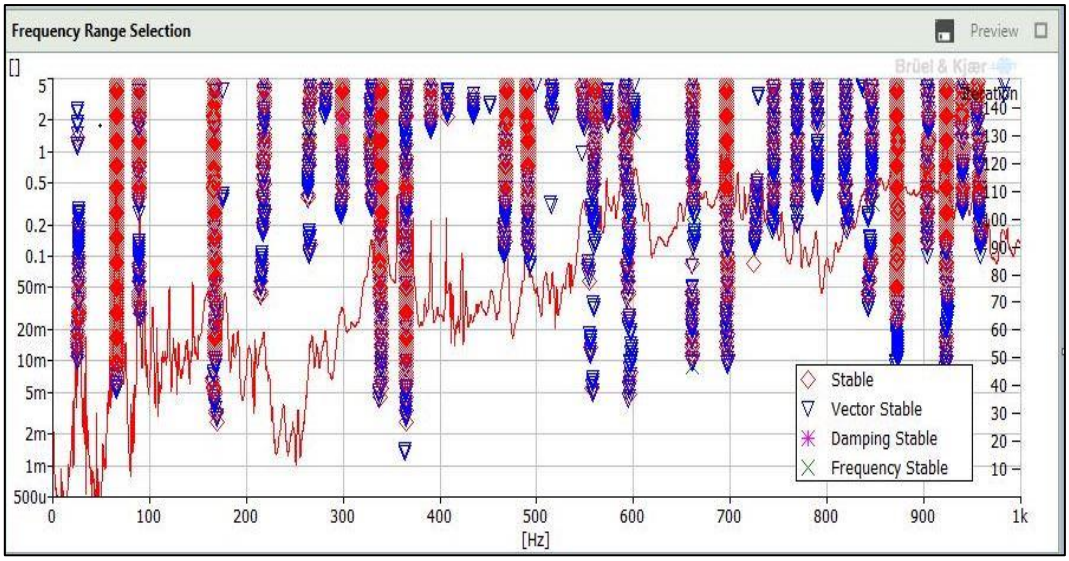

Figure 45: Frequency span for experimental modal analysis (Case A).

The synthesis curve after iteration indicates the data interpretation. The red line indicates the actual response from MTC processing and pink colour means the synthesis curve. The error is minimized after trial and error based on the iteration number and interpretation method. The minimum error shows the better result for modal parameters and accuracy of the measurement during experimental testing. Synthesis curve for case A and case B is shown in the Figure 46 and Figure 50 respectively.

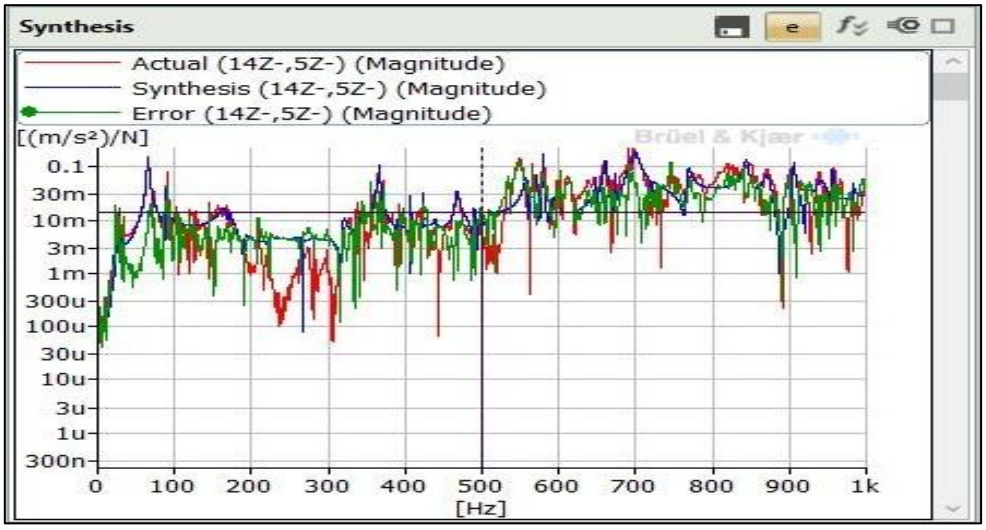

Figure 46: Synthesis curve after iteration for EMA (Case A).

The number of modes is selected only from the stable mode in the singular value stability diagram by auto selection. The modes can be selected by manually but these modes are not

reliable for the better performance of the modal parameters. Figure 47 and Figure 51 show the stability diagram for EMA.

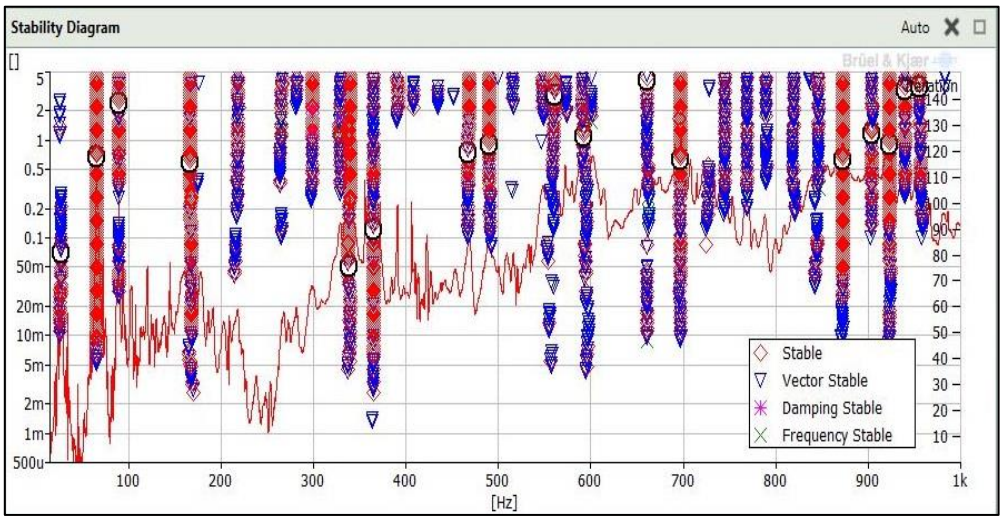

Figure 47: Singular value stability diagram for EMA (Case A).

The mode shape and modal parameters conducted from the EMA is need to validate for better performance. This is done by the modal assurance criteria (MAC). The limiting value of MAC is 0.0 to 1.0. The maximum value 1.0 shows along the diagonal (red line), it means the best curve fitting is performed in EMA (Figure 48 and Figure 52).

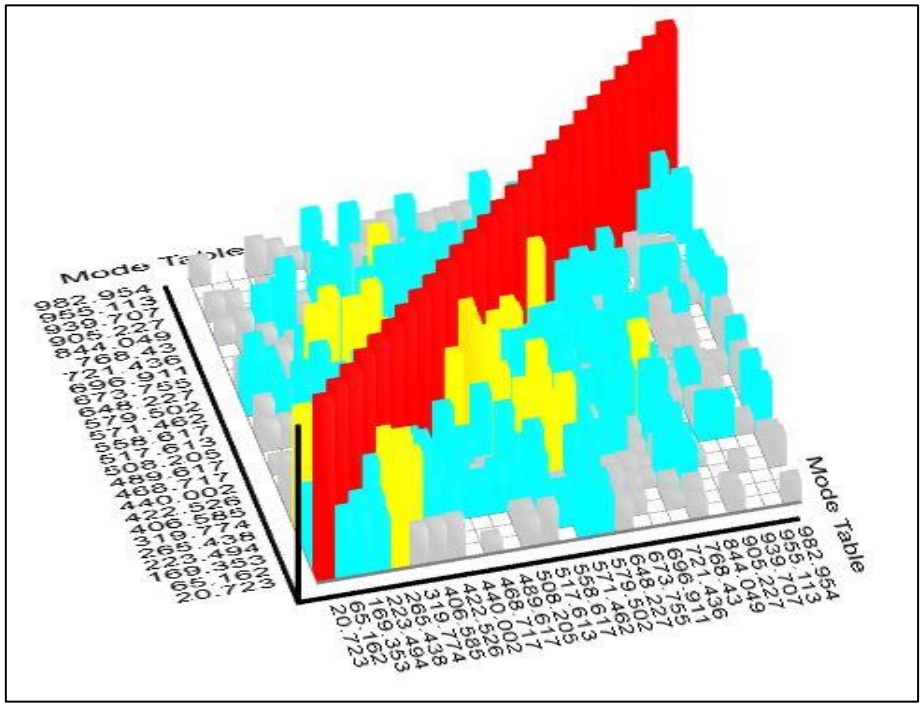

Figure 48: Modal assurance criteria for modal parameters (Case A).

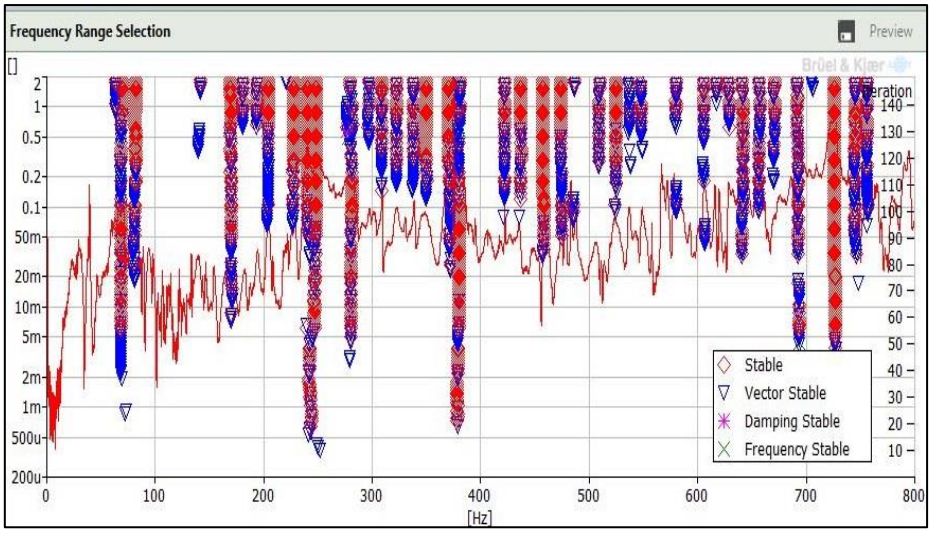

Figure 49: Frequency span for experimental modal analysis (Case B).

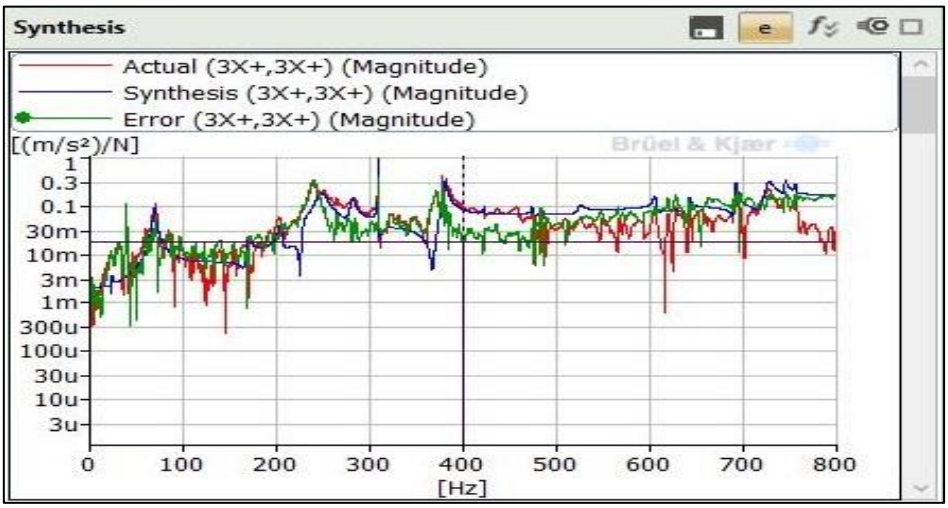

Figure 50: Synthesis curve after iteration for EMA (Case B).

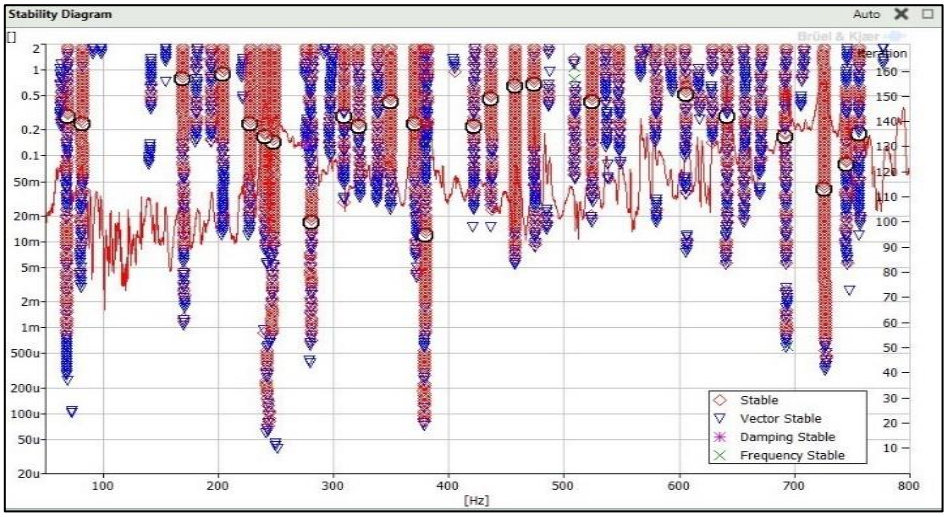

Figure 51: Singular value stability diagram for EMA (Case B).

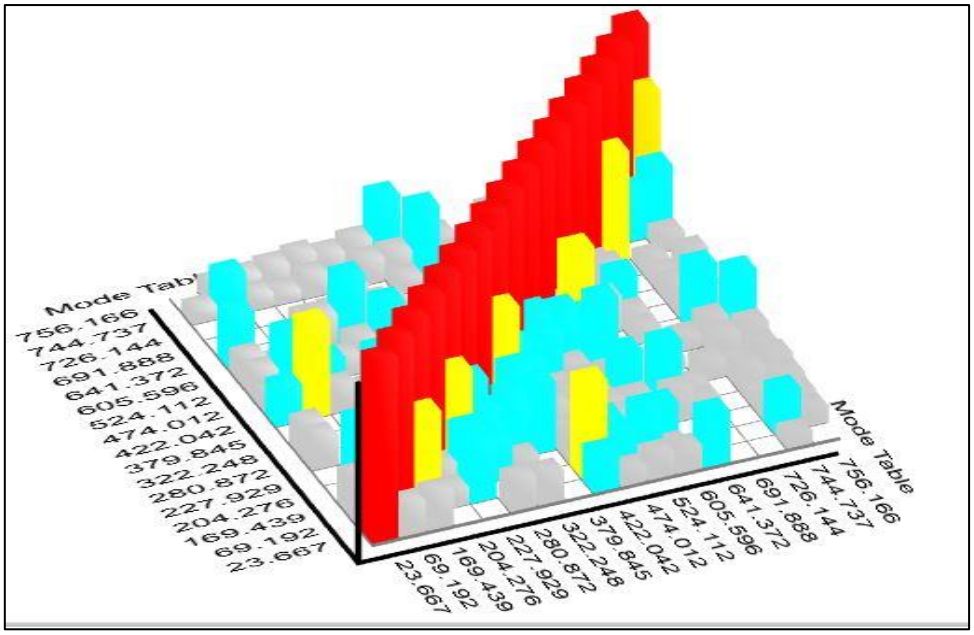

Figure 52: Modal assurance criteria for modal parameters (Case B).

3.2. Experimental results and discussions

The St-Id process involves the comparison of experimental results with the numerical model results. The correlation of the analytical model with the experimental results for required additional calibration and updating. Finite element software SAP2000 was used for correlations and updating the experimental results. The natural frequencies determined from EMA post processing method is presented in Table 2. The first 9 mode shapes of the column obtained from the FEM analysis and the forced vibration test data are compared in Figure 55 for case A and in Figure 56 for case B shows very good relation with each other. The reasonable agreement obtained between the experimental and numerical results indicates that the St-Id results from the FEM have not much errors in modeling and test results.

Table 2: Modal parameters computed by EMA and FEM tool.

CASE A				CASE B			
EMA [f_n (Hz)]	SAP [f_n (Hz)]	(%) Error	Damping (%)	EMA [f_n (Hz)]	SAP [f_n (Hz)]	(%) Error	Damping (%)
20.72	20.72	0.00	1.10	23.66	20.92	11.58	0.75
65.16	65.96	-1.23	1.17	69.19	68.67	0.75	2.05
169.35	165.17	2.47	1.88	169.4	167.01	1.41	1.29
--	--	--	--	204.30	198.24	2.97	0.84
223.49	221.14	1.05	0.26	227.90	225.60	1.01	1.42
265.43	264.51	0.35	0.36	280.87	272.00	3.16	0.83
319.77	319.83	-0.02	0.56	322.25	322.59	-0.11	0.45
406.59	400.90	1.40	0.06	379.80	402.25	-5.91	0.51
422.53	420.71	0.43	0.00	422.00	419.35	0.63	0.10

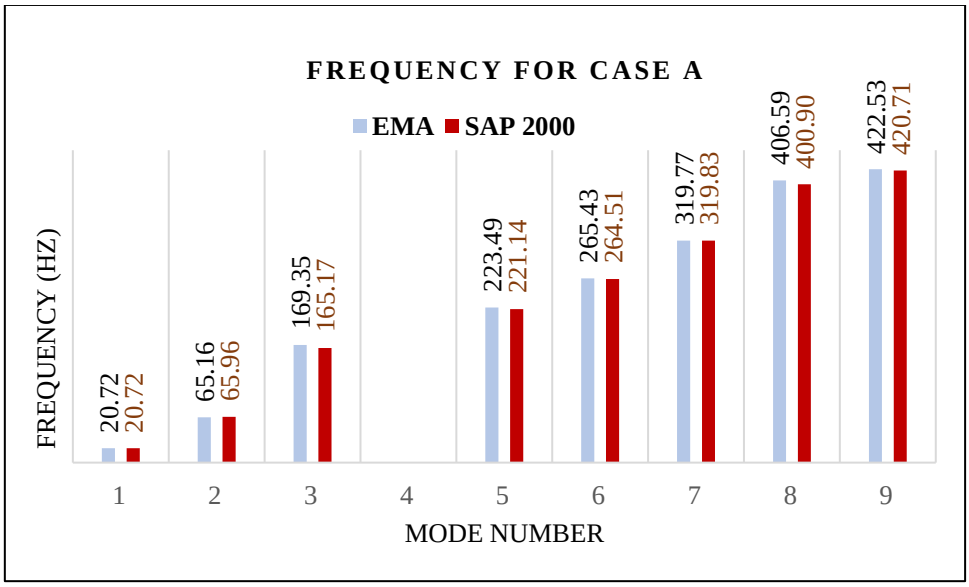

Figure 53: Frequency measured by EMA and FEM Software for case A.

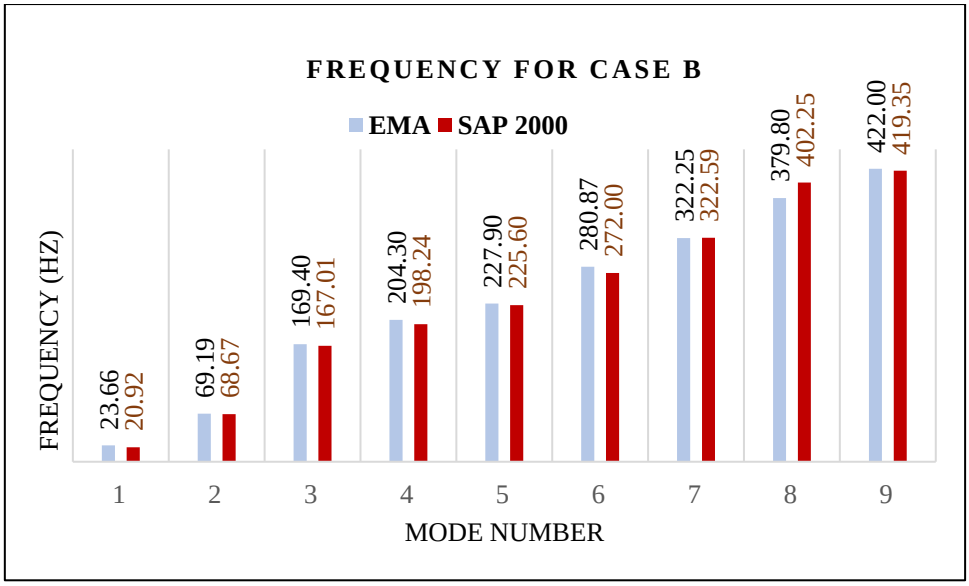

Figure 54: Frequency measured by EMA and FEM Software for case B.

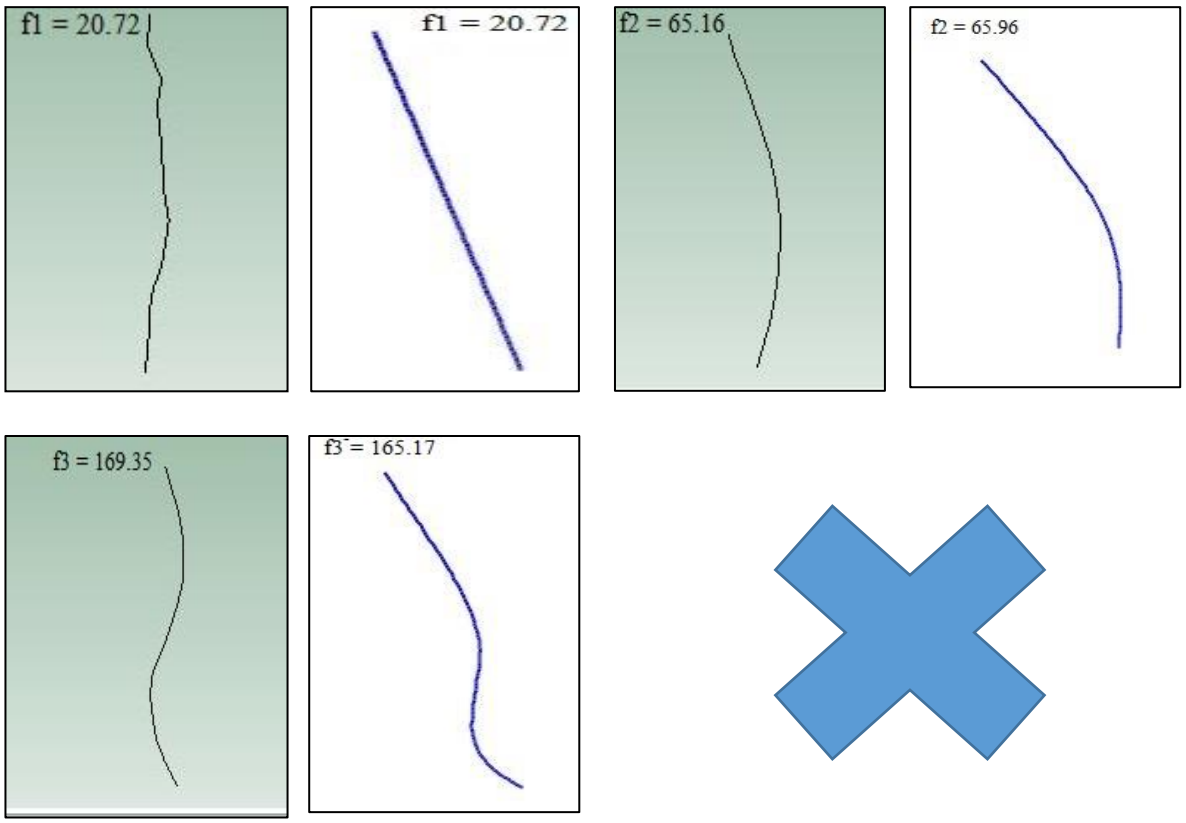

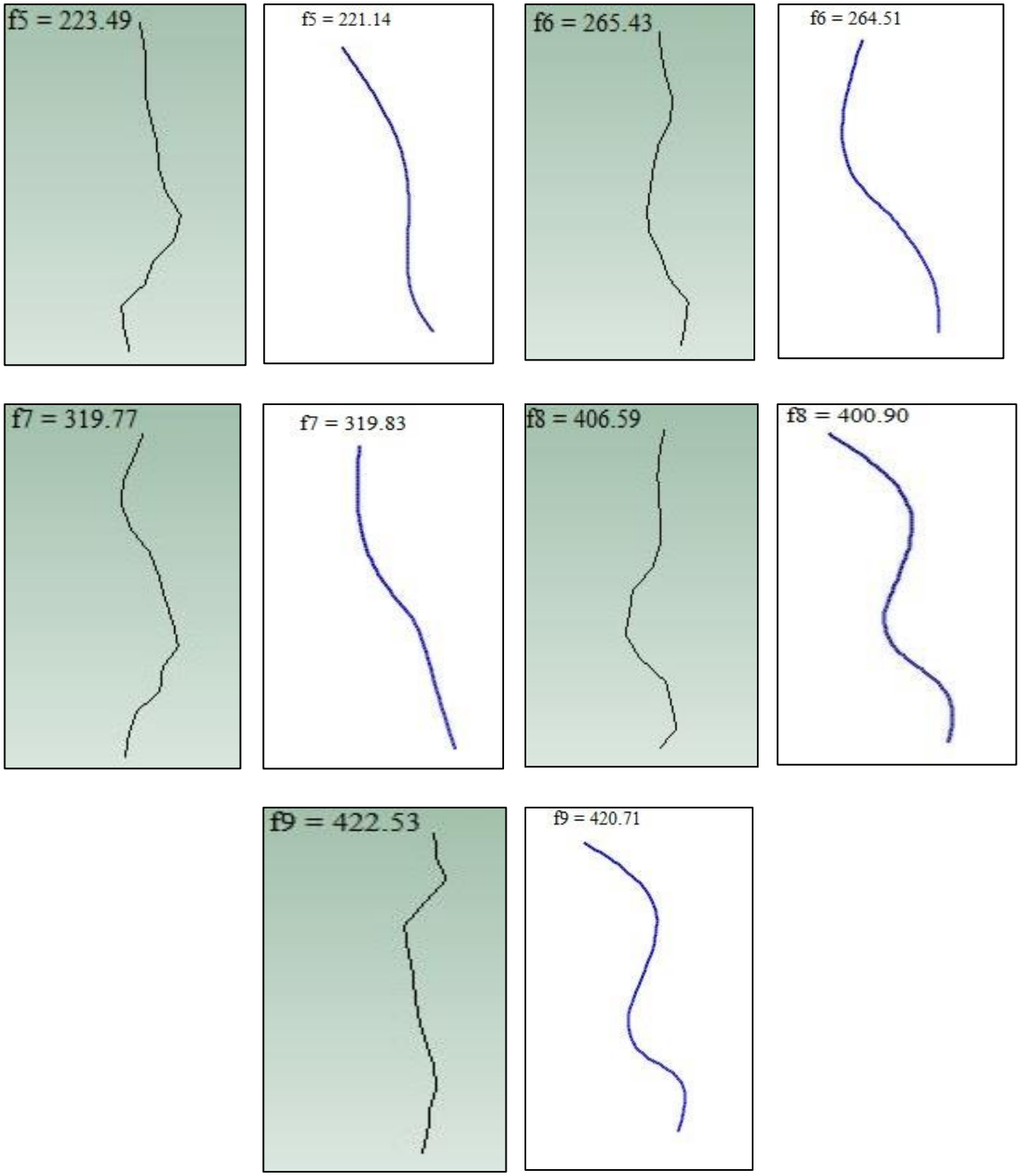

Figure 55: Comparison of modal parameters by EMA and SAP2000 for Case A.

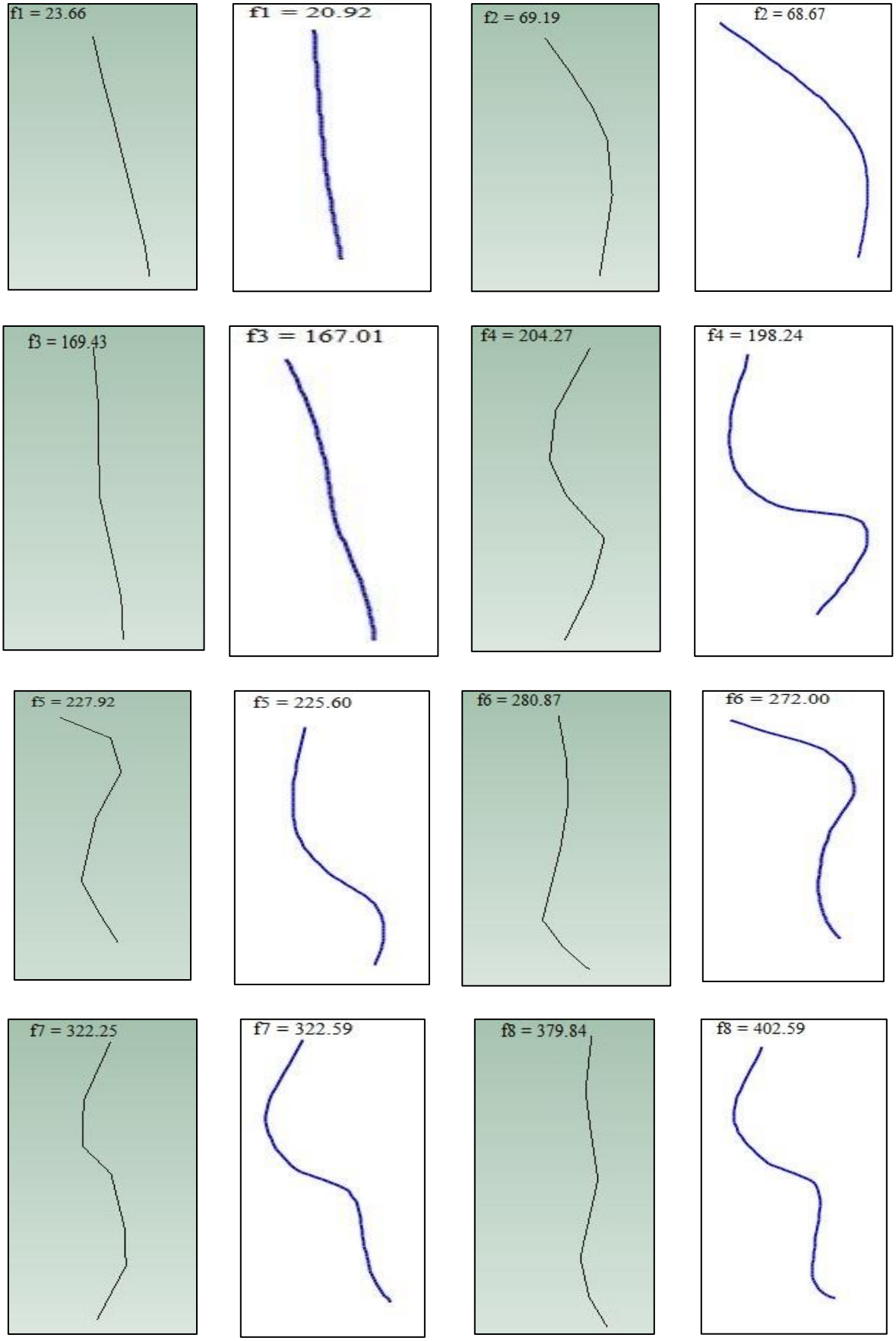
f1 = 23.66
f1 = 20.92
f2 = 69.19
f2 = 68.67
f3 = 169.43
f3 = 167.01
f4 = 204.27
f4 = 198.24
f5 = 227.92
f5 = 225.60
f6 = 280.87
f6 = 272.00
f7 = 322.25
f7 = 322.59
f8 = 379.84
f8 = 402.59

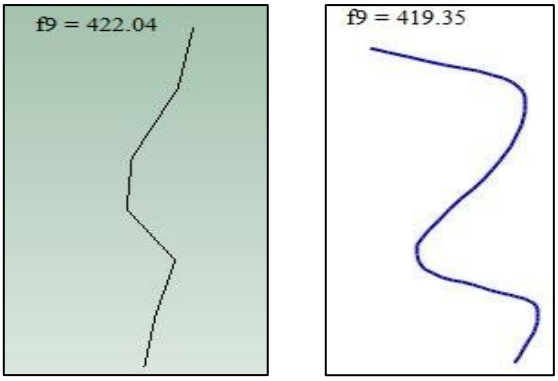

Figure 56: Comparison of modal parameters by EMA and SAP2000 for Case B.

Experimental modal analysis was performed by Bruel & Kjaer technique for the frame and the first 9 natural frequencies are obtained between 20.72 and 422.53 Hz for the intact frame (Case A) and 23.66 and 422.00Hz for case B. The maximum differences are calculated for both case as 14.19% for first mode. The first mode shapes are obtained as bending modes for each condition. Comparison of the experimentally identified natural frequencies is given in Table 3.

Three-dimensional (3D) finite element models shown in Figure 37(a) and Figure 37(b) are constituted with solid elements in SAP2000. The first 9 natural frequencies are obtained between 20.72 and 420.71 Hz for the intact frame (Case A) and 20.92 and 419.35 for case B. The maximum differences are calculated for both case as 4.11% for second mode. The first mode shapes are obtained as bending modes for each condition. Comparison of the numerically identified natural frequencies is given in Table 4.

Table 3: Comparison of the experimentally identified natural frequencies (Hz).

Mode number	Case A [f_n (Hz)]	Case B [f_n (Hz)]	Max. differences (%)
1	20.72	23.66	14.19
2	65.16	69.19	6.18
3	169.35	169.4	0.03
4	---	204.30	---
5	223.49	227.90	1.97
6	265.43	280.87	5.82
7	319.77	322.25	0.78
8	406.59	379.80	-6.59
9	422.53	422.00	-0.13

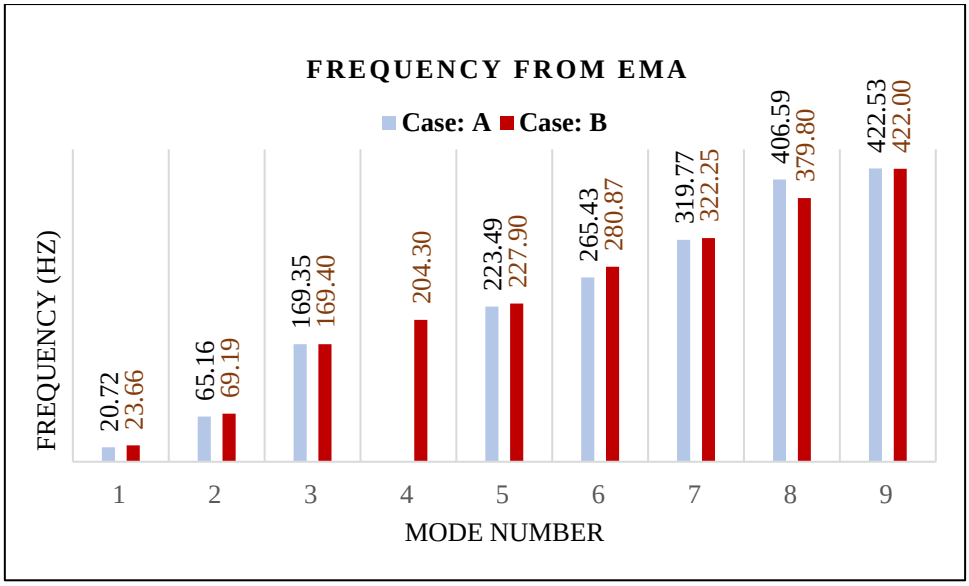

Figure 57: Frequency measured by EMA for case A and case B.

Table 4: Comparison of the numerically identified natural frequencies (Hz).

Mode number	Case A [f_n (Hz)]	Case B [f_n (Hz)]	Max. differences (%)
1	20.72	20.92	0.97
2	65.96	68.67	4.11
3	165.17	167.01	1.11
4	---	198.24	---
5	221.14	225.60	2.02
6	264.51	272.00	2.83
7	319.83	322.59	0.86
8	400.90	402.25	0.34
9	420.71	419.35	-0.32

For the numerical and experimental analysis there are no significant changes between the frequency and the mode shapes. For better understanding Figure 55 and Figure 56 show comparison of the mode shapes for case A and case B.

3.3. Conclusions

The mode shapes and frequencies have good relation for both case for experimental modal analysis and numerical modal analysis. The physical properties (stiffness, modal mass and stability) of the frame change due to removal of lower beam. The maximum difference 14.19%

of frequency in first mode from EMA for both case and numerically estimated frequency difference 6.18% for second mode. The 4th mode is completely missing for intact frame (case A) because of physical property changes of structural frame. The presence of lower beam restrains this specific mode shape in case of intact frame. Frame is comparatively flexible after removing the lower beam.

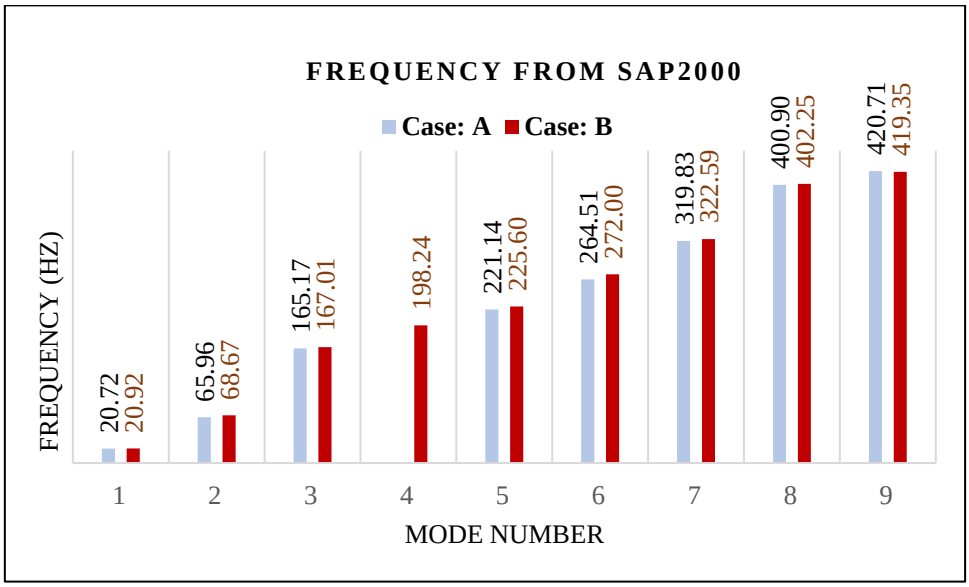

Figure 58: Frequency measured by SAP2000 for case A and case B.

4. STRUCTURAL IDENTIFICATION FOR FULL-SCALE STEEL BUILDING

4.1. Description of frame building model

The full-scale building model is a two-span, two-bay, and two-story steel structure (Figure 59.a. The bays and spans measure 4.50 m and 3.0 m, respectively, while each story is 2.5 m high, see Figure 59.b-d. The structural system is made of moment resisting frames on the transversal direction, while on the longitudinal direction it is made of concentrically braced frames placed on perimeter frames. The extended end-plate bolted beam-to-column connections in the moment resisting frames are designed as fully rigid and fully restrained connections, see Figure 59.e. Secondary beam-to-column connections and secondary beam-to primary beam connections are pinned connections, see Figure 59.f-g. Columns are rigid at the base (Figure 59.h). Frame joint detailing is shown in Figure 59.i. The design of the structure for permanent and seismic (low seismicity, 0.10 g horizontal acceleration) design conditions resulted in an IPE 270 section for main beams; IPE 200 for main secondary beams, and secondary beams between frame is IPE 160 sections, while columns were HEB 260. Note that structural steel S275 (yield strength of 275 N/mm^2) was used for beams and columns [Dinu et al. 2017-2018].

a)

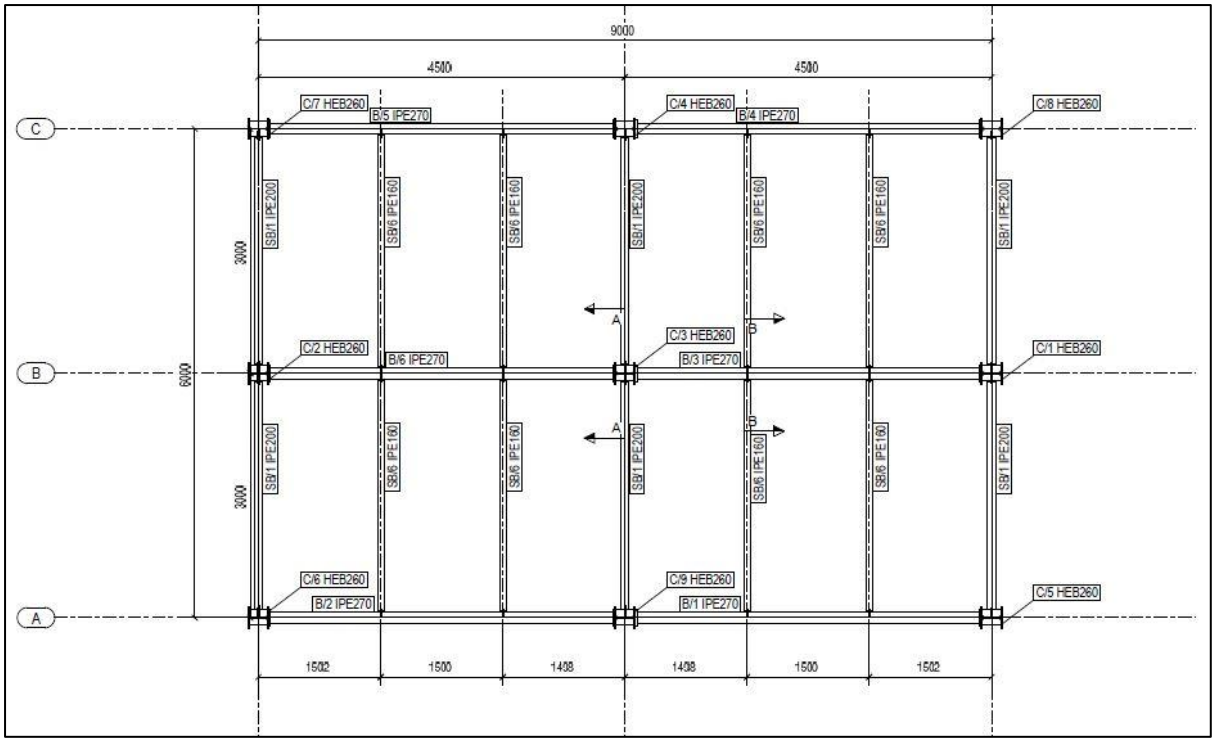
9000
4500
4500
C/7 HEB260
B/5 IPE270
C/4 HEB260
B/4 IPE270
C/8 HEB260
SB/1 IPE200
SB/6 IPE160
3000
C/2 HEB260
B/6 IPE270
C/3 HEB260
B/3 IPE270
C/1 HEB260
6000
C/6 HEB260
B/2 IPE270
C/9 HEB260
B/1 IPE270
C/5 HEB260
C
B
A
1502
1500
1408
1408
1500
1502

b)

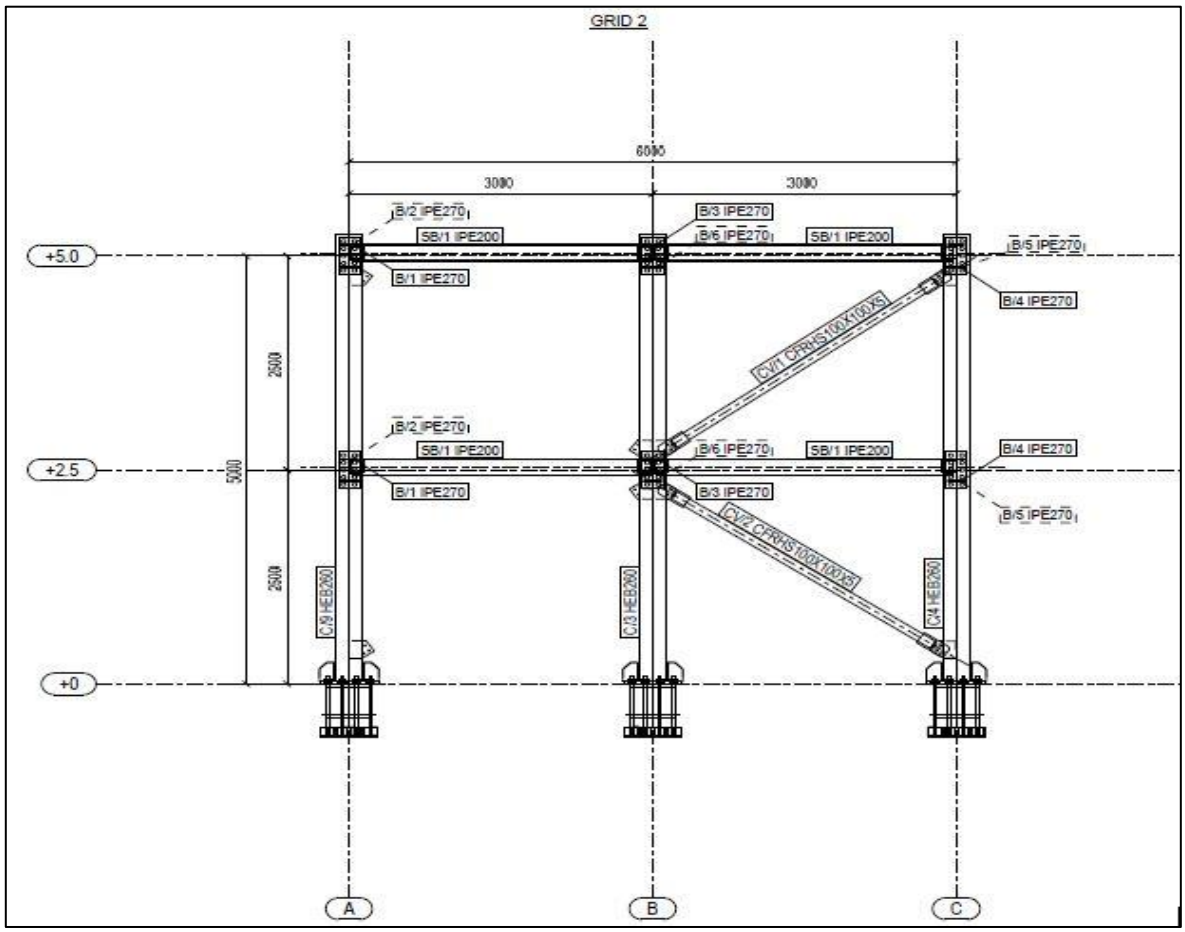
GRID 2
6000
3000
3000
+5.0
+2.5
+0
2500
5000
2500
B/2 IPE270
SB/1 IPE200
B/3 IPE270
B/6 IPE270
B/5 IPE270
B/1 IPE270
B/4 IPE270
CV/1 CFRHS100X100X5
CV/2 CFRHS100X100X5
C/3 HEB260
C/4 HEB260
C/5 HEB260
A
B
C

c)

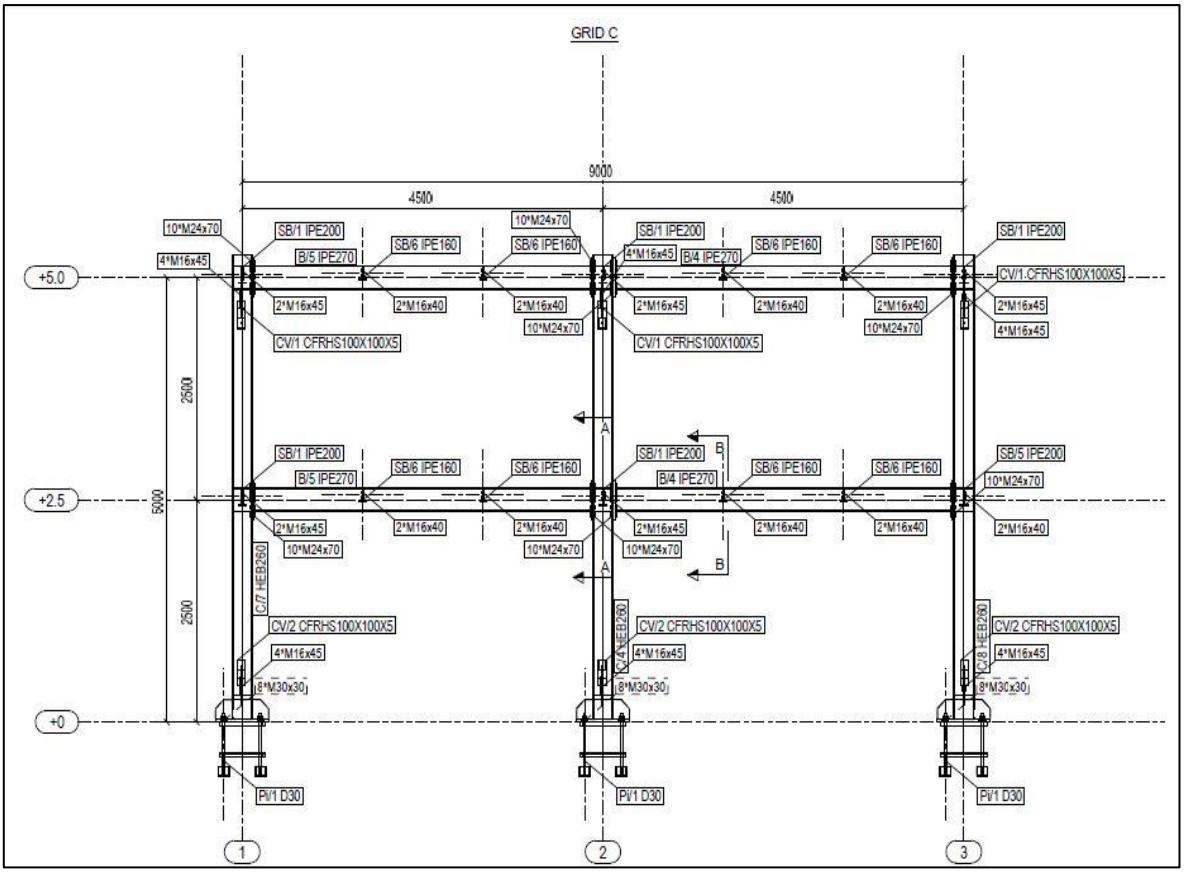
GRID C
9000
4500
4500
+5.0
+2.5
+0
5000
2500
2500
SB/1 IPE200
SB/6 IPE160
B/5 IPE270
B/4 IPE270
SB/5 IPE200
CV/1 CFRHS100X100X5
CV/2 CFRHS100X100X5
C/7 HEB260
C/4 HEB260
C/8 HEB260
10*M24x70
4*M16x45
2*M16x45
2*M16x40
8*M30x30
Pi/1 D30
A
B
1
2
3

d)

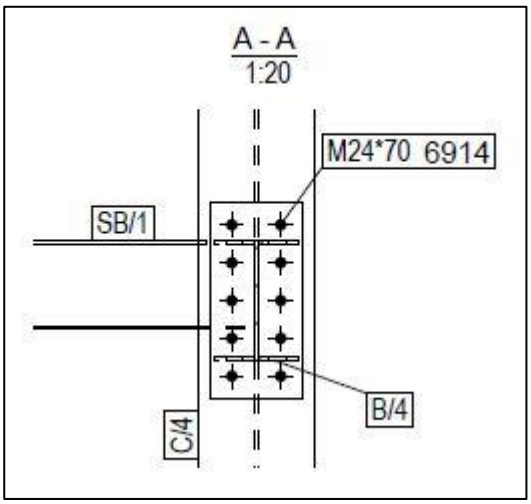
A - A
1:20
M24*70 6914
SB/1
B/4
C/4

e)

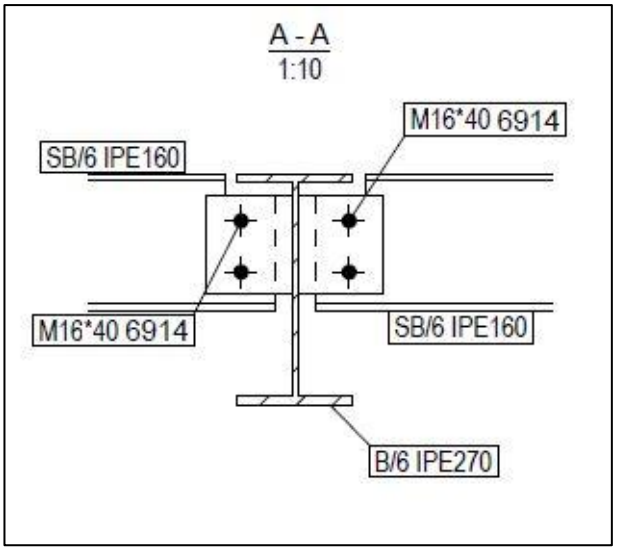
A - A
1:10
M16*40 6914
SB/6 IPE160
M16*40 6914
SB/6 IPE160
B/6 IPE270

f)

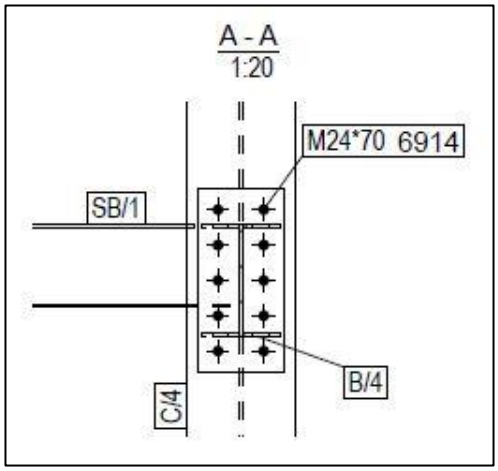
A - A
1:20
M24*70 6914
SB/1
B/4
C/4

g)

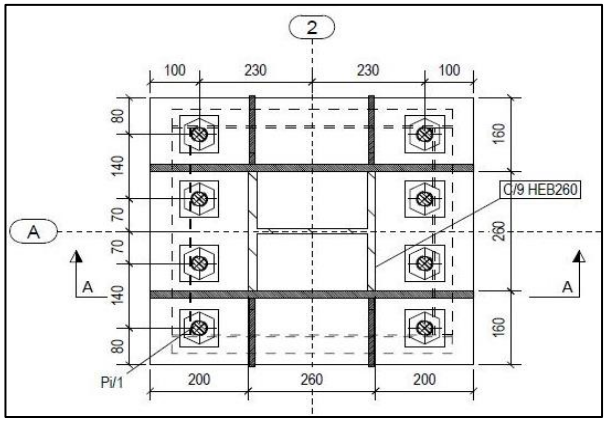
2
100
230
230
100
80
140
70
70
140
80
160
280
160
A
A
A
C/9 HEB260
Pi/1
200
260
200

h)

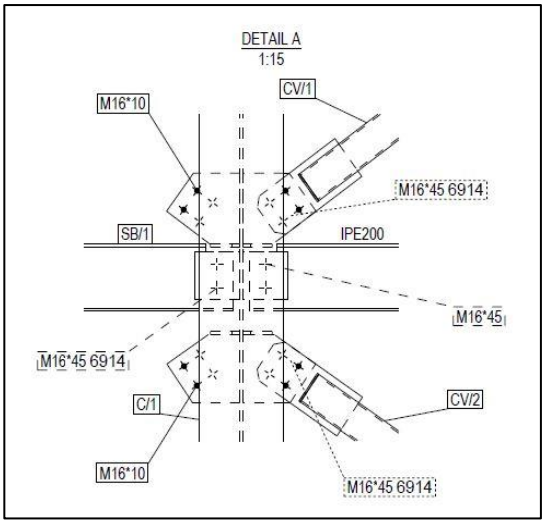

i)

Figure 59: a) Views and details of full scale building frame: 3D view; b) Floor plan view of the building; c) Transversal frame; d) Longitudinal frame; e) Beam-to-column connection; f) Secondary beam-to-primary beam connection; g) Secondary beam-to-column connection; h) Column-to-base rigid connections; i) Frame joint detailling.

4.2. Technical details and design

As planned, the steel frame building will be subjected to high explosive charges detonated in the proximity of a column, see Figure 60. Blast loading effects may produce specific local and global responses, each associated with a different failure mode. Local response is mainly characterized by direct shear or punching shear, and generally results from close detonations, while global response is typically manifested as flexural failure, and results from blasts at larger standoff distances. Therefore, for predicting the blast pressure and response of the structure in different loading scenarios, a parametric study has been developed. First, in order to assess the progressive collapse resistance, blast charge is increased until a column is lost.

Then, the level of gravity loads on the floors is incremented until the progressive collapse is initiated. The influence of the standoff distance is also assessed by comparing the effects of blast loadings with different charge weights detonated at different distances from the structure. The calibration of the numerical model is done using the results of blast tests performed on similar steel frames. In order to have a close estimation of the effects of different charges on the structure (state of damage), preliminary nonlinear simulations were done using the Extreme Loading for Structures (ELS) software. Calibration of the model was done using tests performed inside a bunker on similar 3D frames.

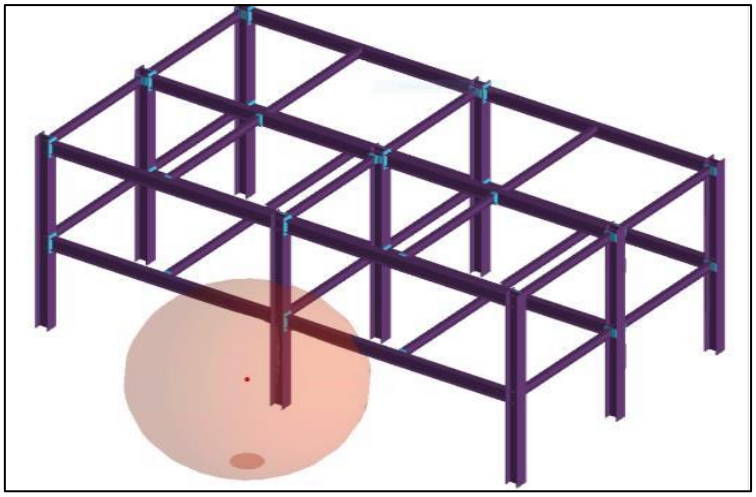

Figure 60: View of the structure with the position of the blast charge for external blast tests.

Two identical 3D specimens were designed and constructed for blast testing inside a bunker (Figure 61). Specimens were extracted from a typical moment resisting steel frame structure. Specimens include a column (with the weak axis oriented in the plane of the frame), two half-span longitudinal beams rigidly connected to the column using extended end plate bolted connections, and one half-span transversal beam, connected to the column web using a simple clip angle connection. Lateral restraints made from tubular profiles were used at the ends of longitudinal beams. An IPE 270 section was used for primary beams, IPE 200 section for main secondary beams and IPE 160 section for secondary beams between the frame, while columns were made from HEB 260, but with flanges reduced to a 160mm width. The design steel material in plates and profiles was S275 J0 and bolts were grade 10.9. The material properties measured is presented in Table 5.

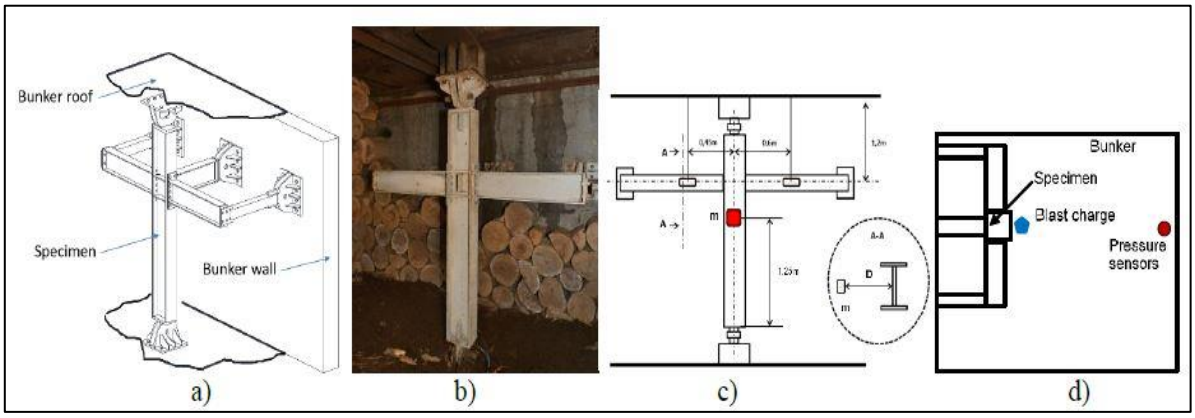

Figure 61. Test specimens inside the bunker: a) view of the specimen; b) photo inside the bunker; c) front view with the position of blast charges; d) plan view with specimen and pressure sensors inside the bunker.

Table 5: Average characteristic values for materials in steel profiles, plates and bolts.

Element	f_y (N/mm^2)	f_u (N/mm^2)	A_{gt} (%)
	yield strength	ultimate strength	Total elongation at maximum stress
Beam flange IPE 270, t = 10.2 mm	345	464	28.0
Beam web IPE 270, t = 6.6 mm	353	463	30.4
Column web HEB 260, t = 10 mm	407	539	27.0
Column flange HEB 260, t = 17.5 mm	420	529	27.0
End plate, t = 20 mm	305	417	17.1
Bolt, M24 class 10.9	965*	1080	12.0
Note: *0.2% offset yield point			

4.3. Instrumentation and vibration measurements on initial (undamaged) structure

The experimental test for full scale building in Petrosani was done by two distinct phases. First step is to fix each component of the instrument. Bruel & Kjaer experiment consist of many important tools for measuring the vibrations. Accelerometer, Impact Hammer, Force transducer, laptop and connecting cables are the most important part of the total set of instruments. Transducer and laptop is connected by the connecting cable. The model of the building frame is drawn by the numerical tools SAP2000. For experimental modal analysis geometry is needed. It can be drawn directly there or can be exported from AUTO CAD file (str file; uff) file formats and SAP2000 in dxf file format. The model was exported from SAP2000 and imported to the MTC hammer measurement software. The external longitudinal frame and internal transverse frame was selected for measuring the vibration. Corner column and central column of longitudinal frame was considered for experimental testing. But for the transverse frame, both external column and central column was taken for measuring dynamic properties. The location of the best points to excite the structure so as to create almost equal levels of response in the several modes of interest. A 3.20lb black and hard hammer is attached at a distance of 0.625m, 1.25m and 1.875m height from the bottom of the column carefully in plane and out of plane. The positions where the average response level is low will be better locations to attach the accelerometers. Accelerometers are very sensitive, if it is not fixed properly to position of the structure vibration measurement data will not be accurate. Accelerometers are fixed perfectly to the position of measurement of the structure to make it

proper connection with the member. For corner column; longitudinal and transverse frame 1st accelerometer was fixed at base of the column. The next accelerometers were positioned by keeping equal clear distance of 1.25m. The last accelerometer is positioned at top (5.0m from bottom) of the column. All accelerometers are positioned in strong and weak axis for measuring vibration in plane and out plane of structural frame. Two accelerometers are placed at the mid length (2.25m from the end of beam) of the longitudinal beam for out of plane measurement but not in plane measurement [Figure 61-64]. No accelerometers were fixed in the secondary beam. After positioning of all accelerometers, very sensitive cables were fixed in one end of the accelerometers and other end of the signal processing device LAN-XI. The point number on the frame and the channel number in the LAN-XI device must be same for best estimation of response signal. Accelerometers, hammers, and channel number is reconfigured by MTC to make sure that all connections are fixed properly.

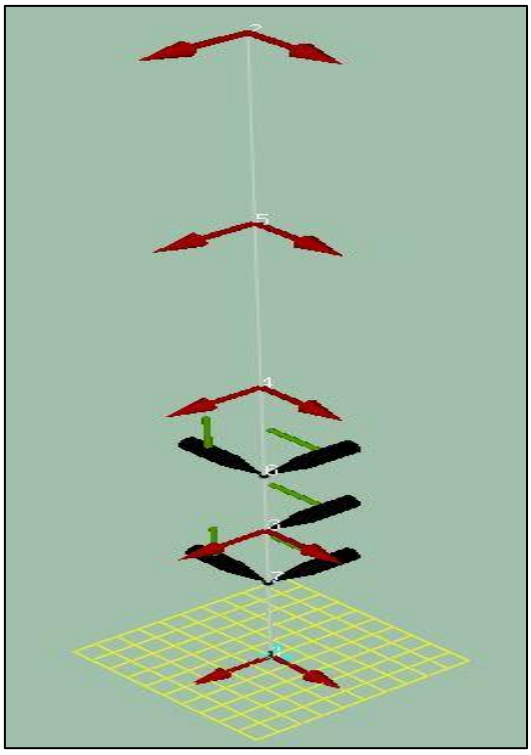

Figure 61: Positioning of accelerometers for the corner column.

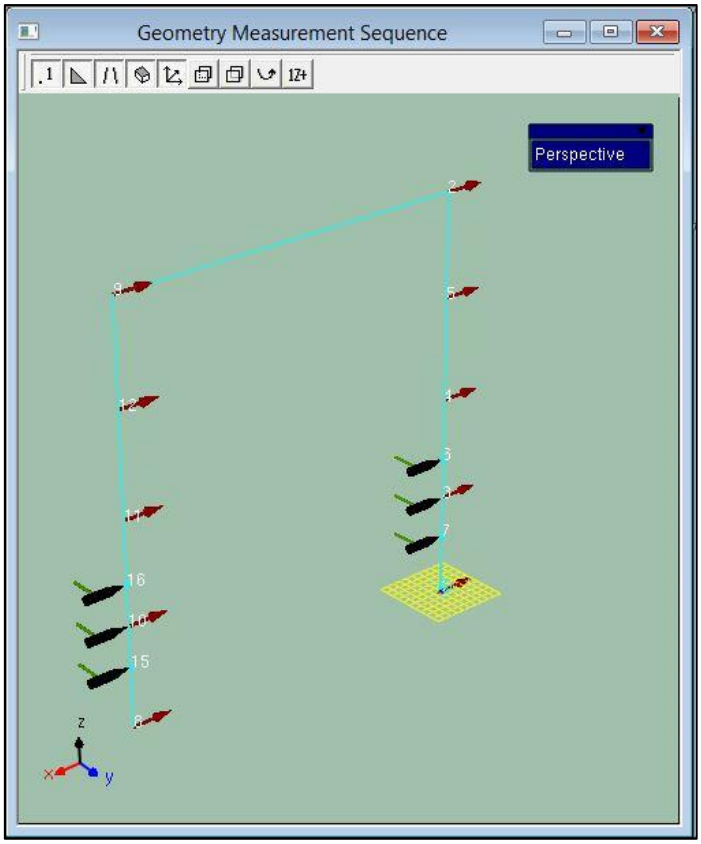

Figure 62: Positioning of accelerometers for the longitudinal frame (in plane).

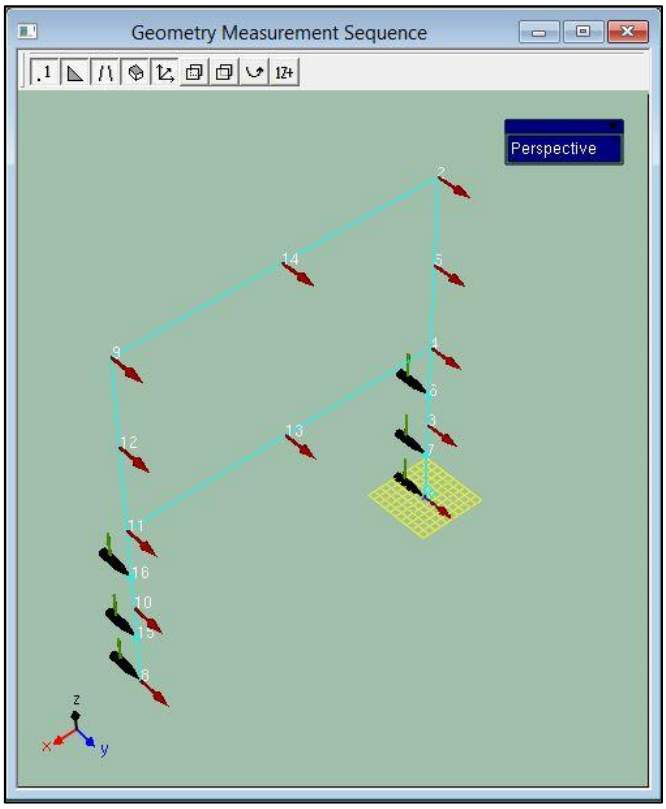

Figure 63: Positioning of accelerometers for the longitudinal frame (out of plane).

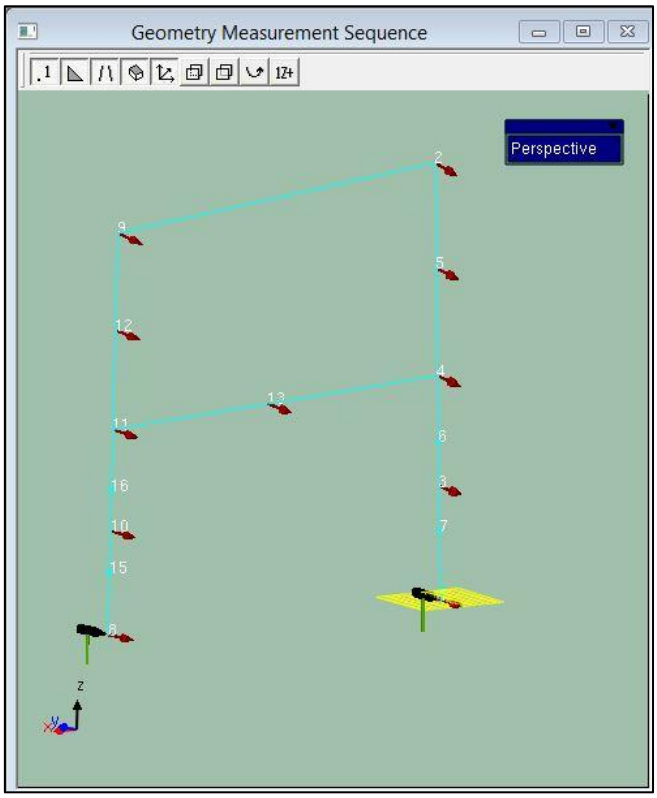

Figure 64: Positioning of accelerometers for the longitudinal frame (out of plane) after removing secondary beam.

Once set up is completed second step to perform experiment and measure the vibration of the frame for excitation by hammer. Measuring time, frequency span, average number of reading, number of hit for excitation, proper hit detection and property for checking the frequency range are very essential to set before starting measurement. The total length of measurement time is (6400/1000) 6.4 seconds and the span of frequency for FFT was fixed as 1000Hz. Five measurements were recorded for average. The more number average the more accuracy of the measurement.

Frequency domain method for measuring frequency response H1 is used for exporting spectrum for experimental modal analysis. Hammer weighting, response weighting and hammer tip is done properly during the measurement by uniform response variation. After measurement, the initial mode shape can be observed from MTC hammer test FRF validation operation. The exact modal parameters are conducted by pulse reflex experimental modal analysis for different number of iterations and interpretations.

4.4. Numerical model calibration against experimental data

4.4.1. Data pre-processing for corner column (C3-Column)

Structural identification methodologies provide rational and systematic means for data interpretation. Successful data interpretation leads to the following benefits:

- increased efficiency and effectiveness of visual inspection by providing information relating to what to look for and where.
- improved decision making for further instrumentation and testing.
- better estimations of structural reliability.
- better overall structural management for decisions such as replacement planning, retrofit strategies and maintenance budget expenditures.
- for civil infrastructure owners and designers, improved insight into what happens to structures during service.
- development of an integrated framework for structural condition assessment.
- increased generic knowledge of in-service structural behavior that can be distilled into educational materials for students and practitioners.
- quantitative contribution to extending concepts of performance-based structural engineering.

Total 10 accelerometers were used to measure the response for 5 exciting hammers. The accelerometers are positioned both in plane and out of plane. Column is exciting at three points by hammer in plane and out of plane of the column. St-Id process involves the processing and interpretation of data collected during experiment. For modal identification of the corner columns, frequency response signal from MTC, measured by 10 accelerometers that fixed in plane and out plane is processed.

The degree of freedom is five for the reference point of the column. The total number of measurement is recorded for five DOF. Frequency response function measured from the MTC hammer excitation is plotted in Figure 65-66 for two best measurement. Frequency vs acceleration curve for FRF validation is shown in Figure 67.

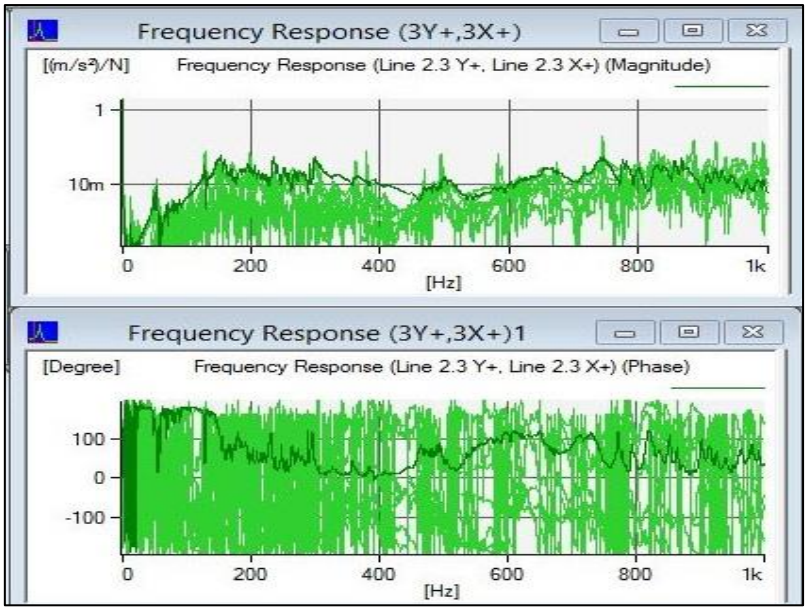

Figure 65: Frequency response function for the first DOF.

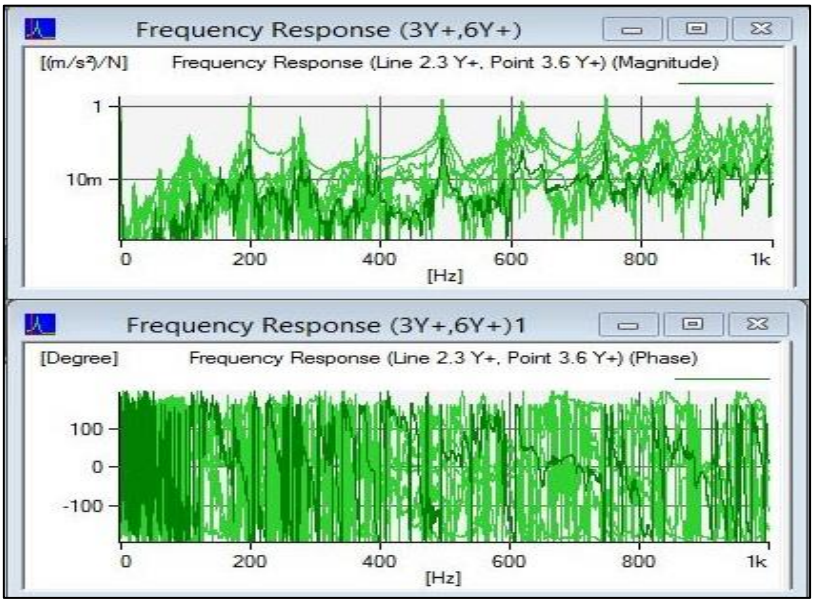

Figure 66: Frequency response function for the second DOF.

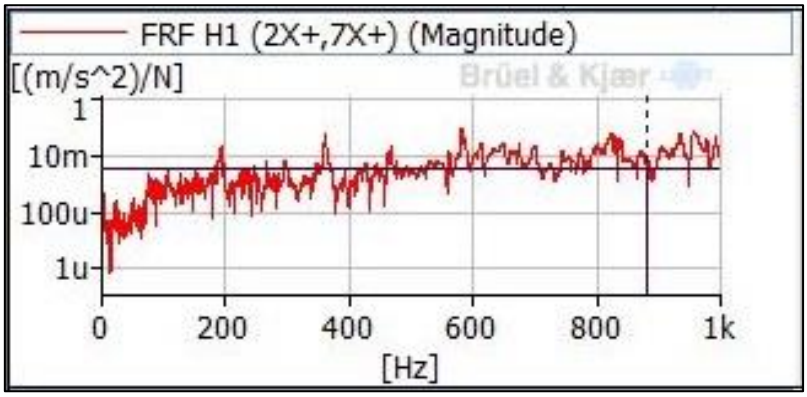

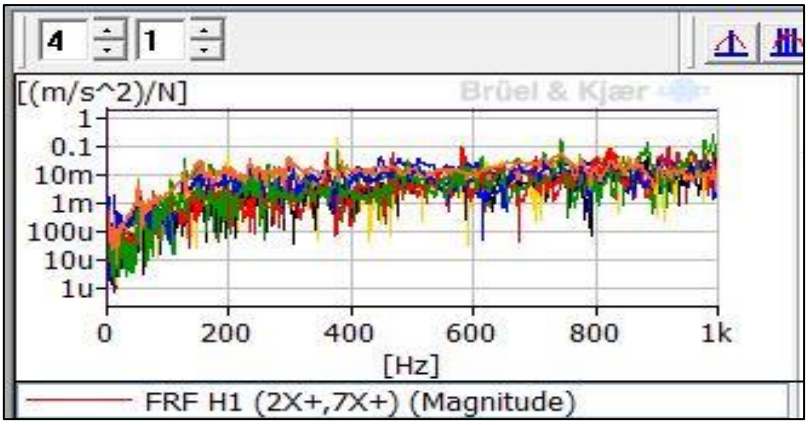

Figure 67: FRF validation by computing frequency vs acceleration curve.

4.4.2. Data post-processing for modal parameter identification

The span of the frequency where the modes are available for cumulative modal identification factor (CMIF) and frequency response function (FRF) is selected manually by the user is shown in Figure 68.a. The mode number is computed by the rational function polynomial method for 100 number of iteration. In the mode iteration process, some modes are stable and some are unstable. Red line indicates the stable mode which is selected by auto selection process.

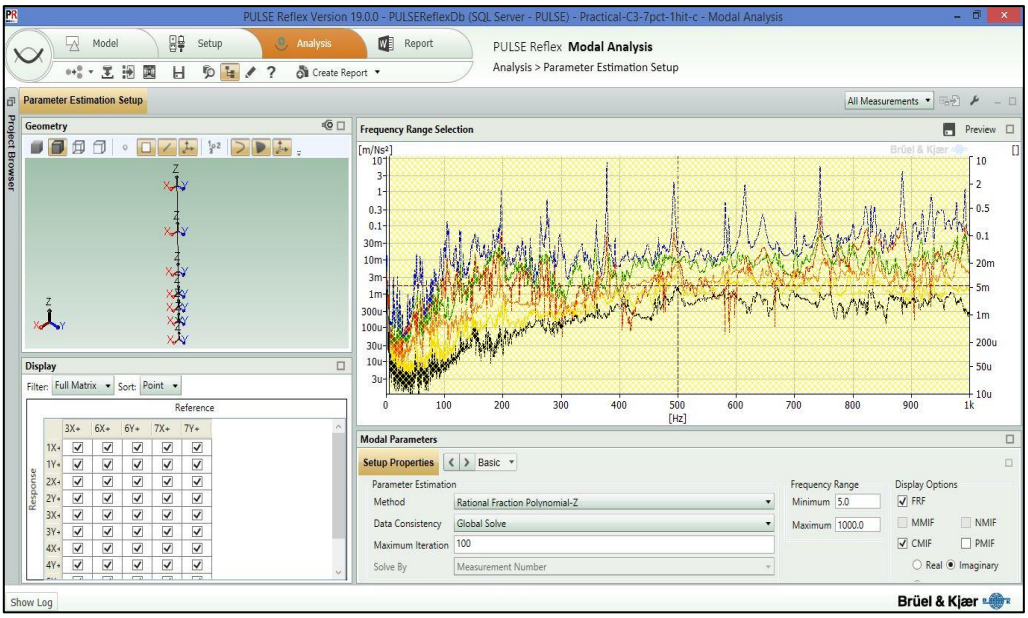

a)

The synthesis curve indicates the accuracy of iteration during the data interpretation. Actual response from MTC (red lines) and synthesis diagram (pink colour) show how accurate the interpretation and mode selection process. The error is minimized after trial and error based on

the iteration number and interpretation method. Best extraction of modal parameters highlights the minimum errors during experimental measurement. Synthesis curve is shown in the Figure 68.b.

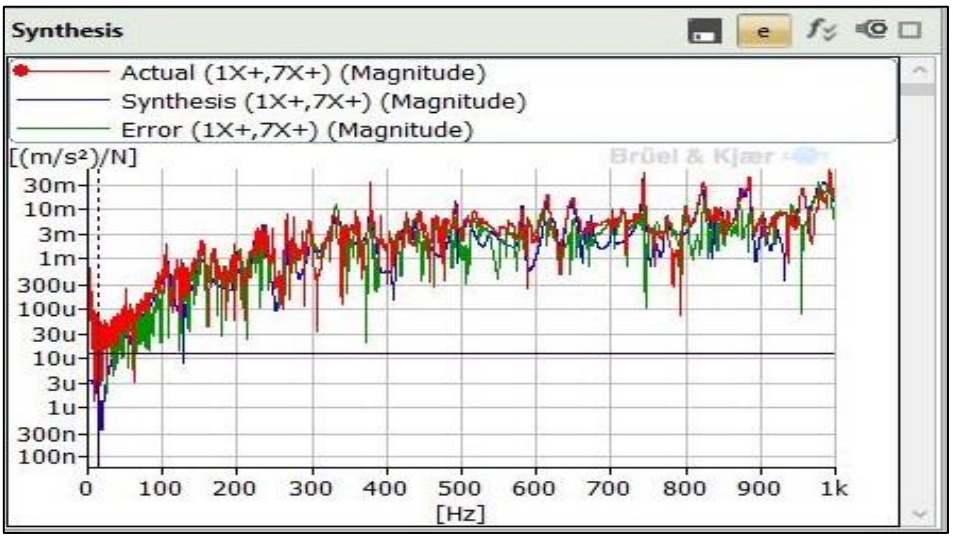

b)

Two ways for selection of modes. Either auto selection or manual selection. Auto selection always choose the stable modes. Stable modes show the minimum errors and better performance for modal parameters. Figure 68.c shows the singular value stability diagram for EMA.

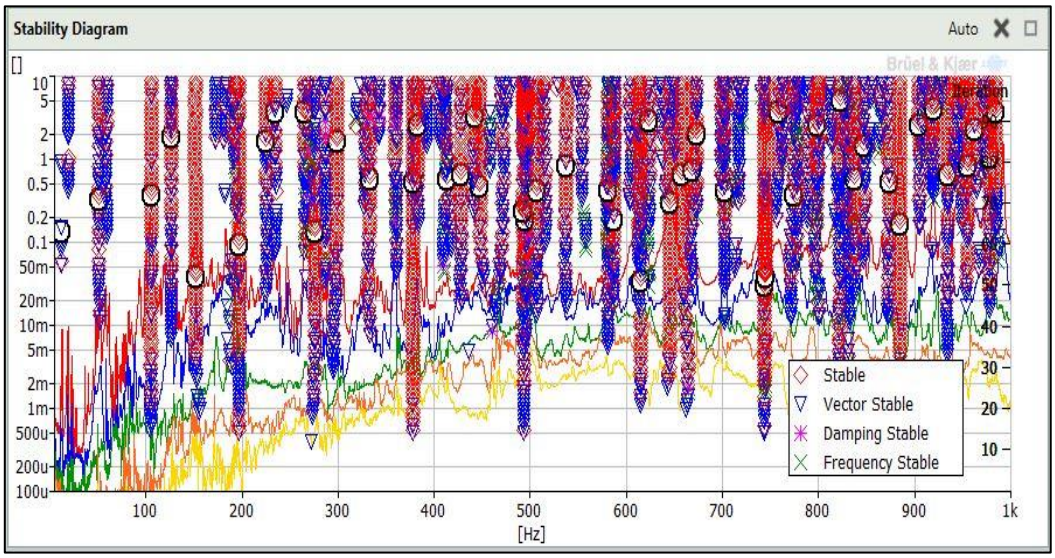

c)

The modal assurance criterion (MAC) is a scalar constant. The mode shape and modal parameters conducted from the EMA is corrected or justified by three important methods. Modal assurance criteria, phase scatter and synthesis diagram. The diagonal MAC value indicates the actual mode shapes and parameters. Along the diagonal the value should be 1.0. The diagonal line is red marked (Figure 68.d) when MAC is unity along it. MAC indicates how is the consistency of mode shapes for one modal and another reference modal vector.

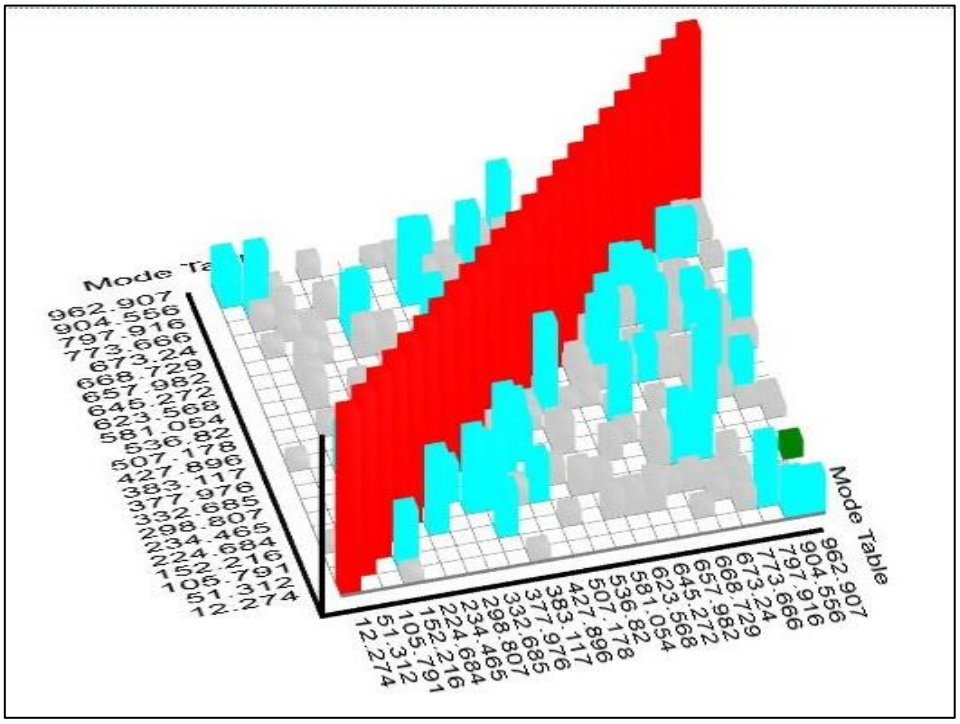

d)

Figure 68: a) Frequency span for EMA for corner column; b) Synthesis curve after iteration for EMA; c) Singular value stability diagram for EMA; d) Modal assurance criteria for modal parameters.

5. RESULTS AND DISCUSSIONS

5.1. Results for corner column (C3-Column)

The results obtained from the Bruel & Kjaer experimental modal analysis and finite element analysis is matched with good agreement if there is less number of factors present that affect the results. The factors of uncertainties are mainly responsible for error in the obtained results. In that case additional calibration/updating is needed for EMA and model is updated by the numerical software. The finite element numerical tools are the best solution to corelate, modify and updating of the modal parameters (mode shapes, natural frequency and damping). Finite element software SAP2000 was used for correlations and updating the experimental results. The natural frequencies determined from an eigenvalue analysis of the 3D FEM and these results are compared with the forced vibration data using the EMA post processing method. The first 6 mode shapes of the column obtained from the FEM analysis and the forced vibration test data are compared in Figure 70 and show very good relation with each other. The reasonable agreement observed between the experimental and analytical results indicated that the St-Id results from the FEM have not much errors in modeling and test results. The maximum difference is 4.58% for third mode and for the other modes result obtained from EMA and SAP2000 are very close to each other (Table 6).

Table 6: Modal parameters computed by EMA and FEM Software.

	EMA			SAP2000	Error (%)
Mode	Frequency (Hz)	Damping (%)	Complexity (%)	Frequency (Hz)	
1	12.27	0.76	0.00	12.72	-3.67
2	51.31	1.73	0.01	51.55	-0.47
3	105.79	2.30	0.15	110.63	-4.58
4	152.21	3.49	0.06	151.45	0.50
5	224.68	1.11	0.12	225.26	-0.26
6	234.46	0.87	0.30	234.90	-0.19

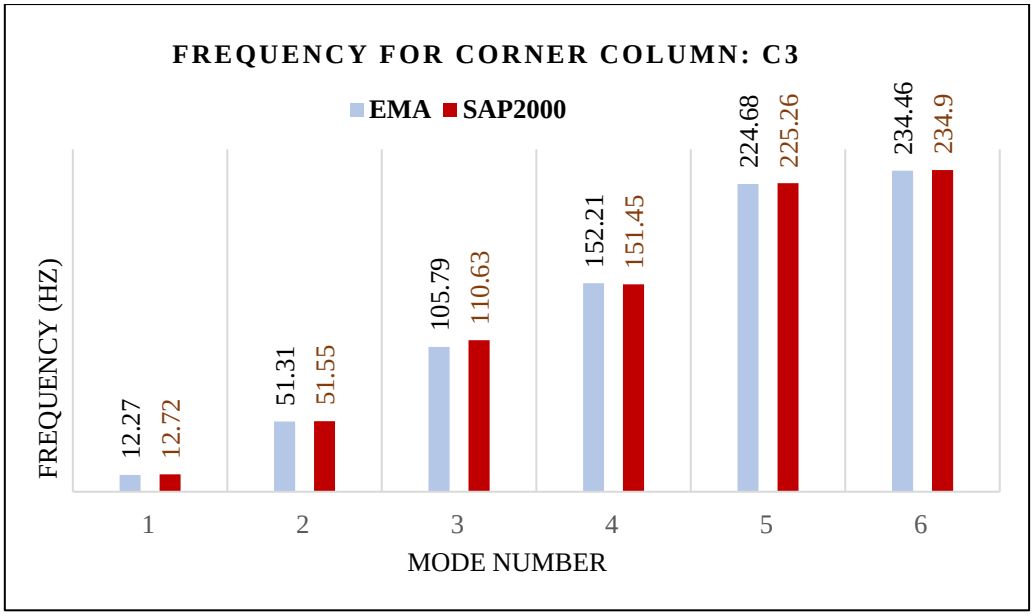

Figure 69: Frequency measured by EMA and SAP2000 for corner column.

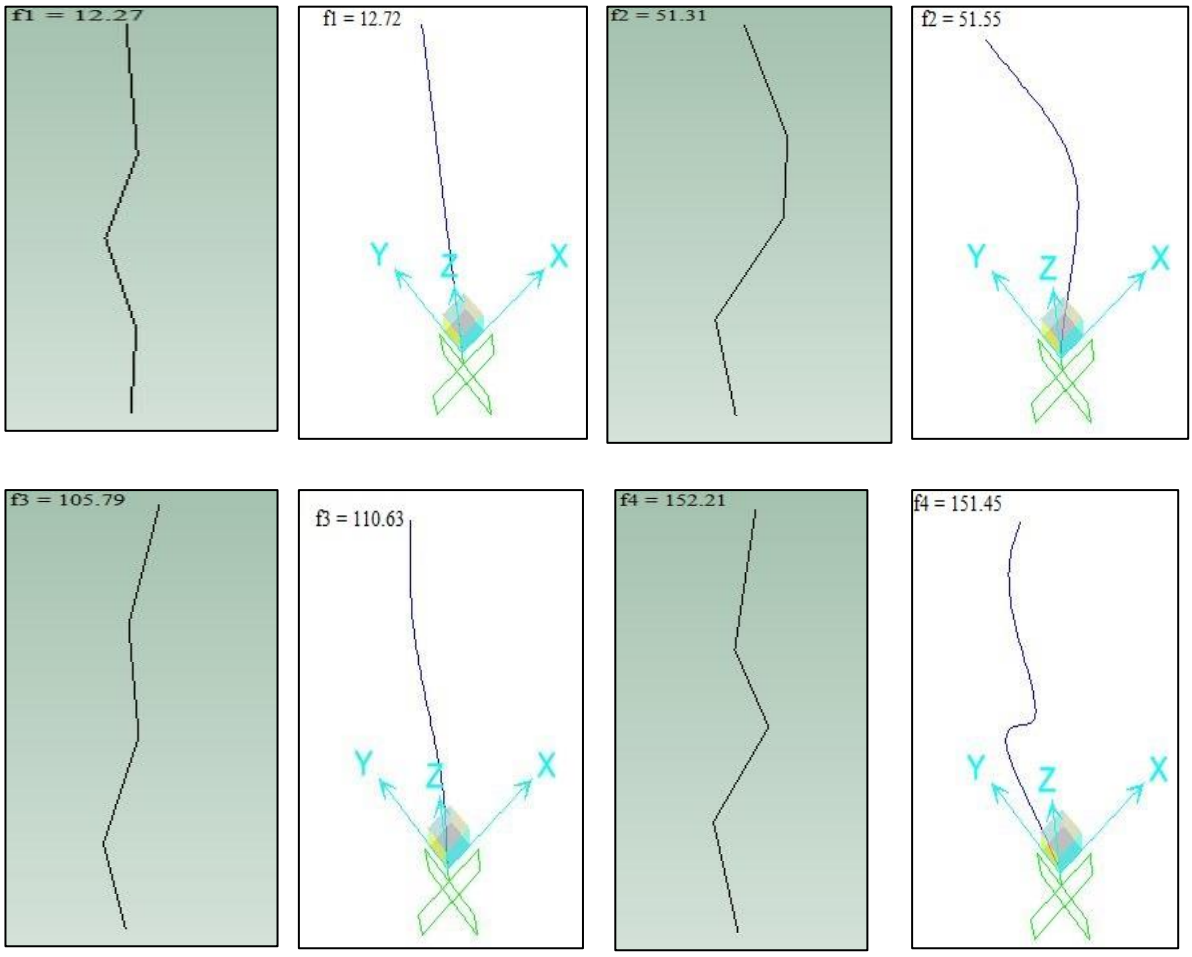

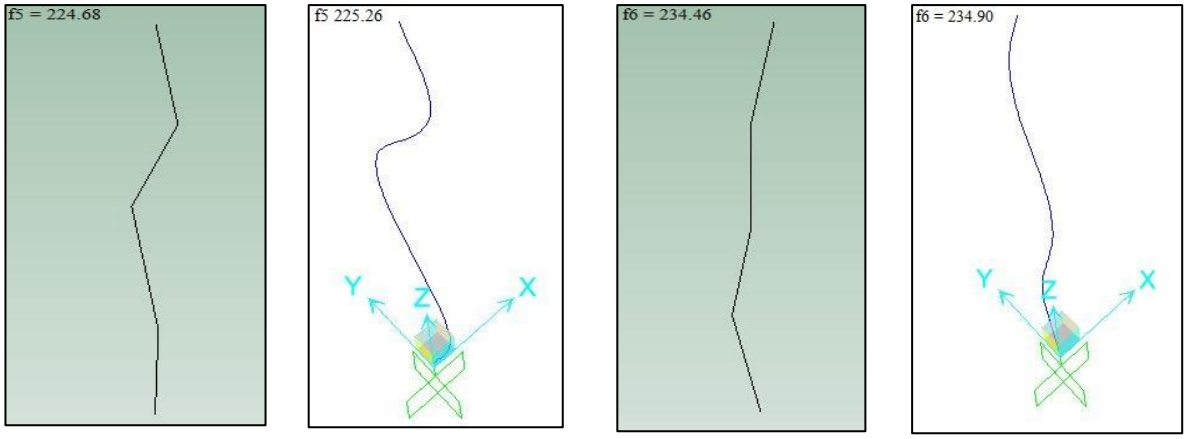

Figure 70: Mode shape comparison in EMA and SAP2000.

5.2. Modal parameter estimation for longitudinal frame column (in plane)

The vibrations of the structure were recorded by means of 10 sensitive accelerometers and the sensitivity of accelerometers is 1 V/g. A picture of the test structure including position and orientation of the accelerometers for longitudinal frame (in plane) is shown Figure 62. The comparative presentation of modal parameters for longitudinal frame (in plane) in Table 7. The detail procedure for getting best mode shapes and modal parameters from this analysis is described in Annex B.

Table 7: Parameters (initial) from EMA and SAP2000 for longitudinal frame (in-plane).

Mode	EMA			SAP2000	Error (%)	Mode type
	Frequency (Hz)	Damping (%)	Complexity (%)	Frequency (Hz)		
1	12.54	1.22	0.00	14.06	10.81	Bending
2	51.42	1.36	0.00	51.55	0.25	Bending
3	126.37	0.32	0.00	120.81	-4.40	Bending
4	150.38	2.23	0.04	151.38	0.66	Bending
5	168.63	0.85	0.09	164.21	-2.62	Bending
6	192.17	2.78	0.03	194.79	-1.72	Bending

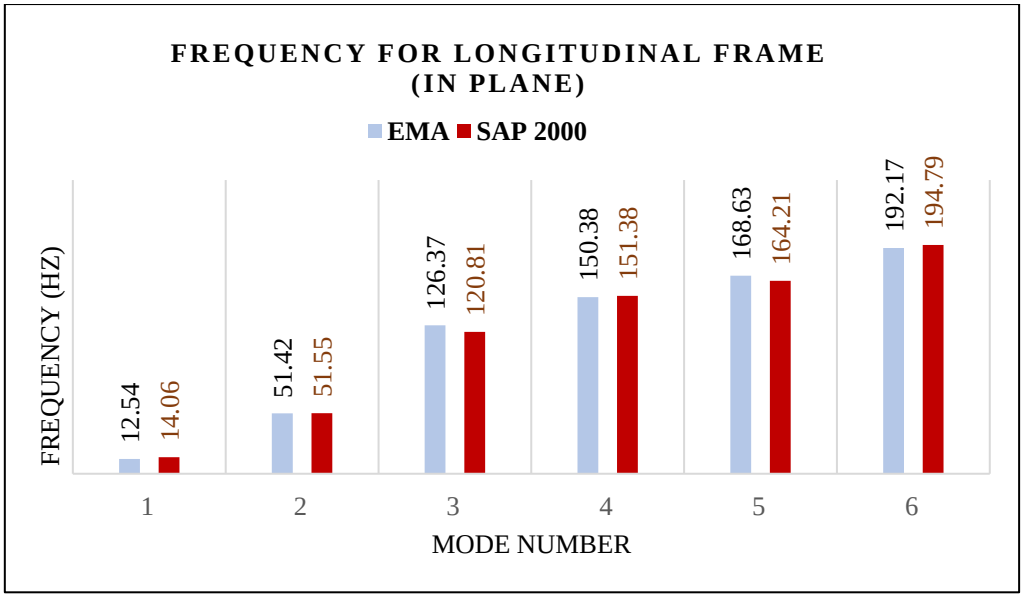

Figure 71: Frequency measured by EMA and SAP2000 for longitudinal frame (in plane).

5.2.1. Finite element model calibration and updating

The main aim of the finite element model updating procedure is to correct the initial FEM values of selected parameters to minimize the errors between experimental result and numerical result. The main steps to calibrate the model values are: i) development of an initial vibration-based FEM model and identifying the dynamic characteristics by experimental measurement of the actual structure, and ii) the next step is to calibrate and validate the vibration-based FEM model to suit the objectives of the St-Id application. Hence, the calibration step is one of the most important tasks of St-Id of a structure. In this study, the model is corrected by modifying the stiffness at the beam-to-column connections and column-base connections.

Comparison of frequencies before and after model calibration are summarized in Table 8 and it shows good improvement in frequencies. Parametric study was then introduced to find the optimum level of allowable parameter change to improve the results of the updated FE model. Here the stiffness of connections was chosen as the parameter for the parametric study. In the parametric study, the stiffness of beam-to-column and column-base connections was reduced 53% and 32% respectively. Figure 72 illustrates the relationship between error in frequency (against EMA frequency) and the corrected FEM value. The table shows the EMA frequencies and the FEM frequencies for both before and after model calibration for the first six modes. From Table 8, it can be seen that five out of six modes of the calibrated FEM are in excellent match with the corresponding EMA modes with only 0.08% or less error. The largest error of 4.77% is with the fifth mode which still shows a very good numerical-experimental correlation

for practical modelling purposes especially when considering the low frequency characteristic of this particular mode as well as the scale of this building structure. Mode shapes are found after experimental data interpretation and numerical model updating by calibration for longitudinal frame in plane is shown in Figure 73.

Table 8: Corrected modal parameters with respect to EMA and initial SAP2000 model value for longitudinal frame (in-plane).

Mode Number	Experimental Frequency (Hz)	Numerical FEM (initial) Frequency (Hz)	Numerical FEM (corrected) Frequency (Hz)
1	12.54	14.06	12.53
2	51.42	51.55	50.35
3	126.37	120.81	125.59
4	150.38	151.38	150.04
5	168.63	164.21	160.58
6	192.17	194.79	188.39

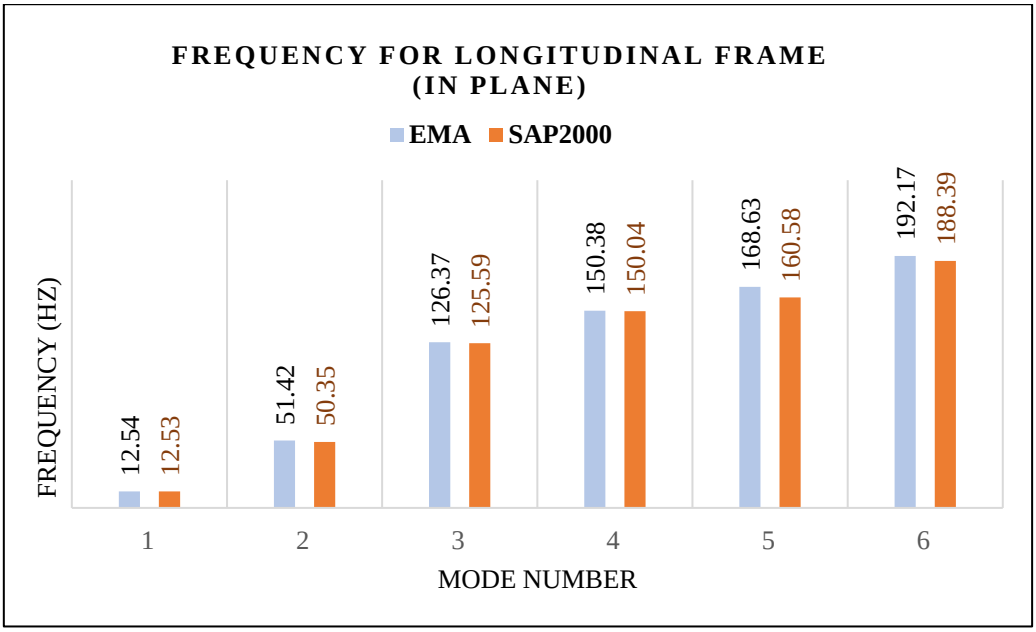

Figure 72: Experimental measurement and numerical FEM corrected model value for longitudinal frame (in plane).

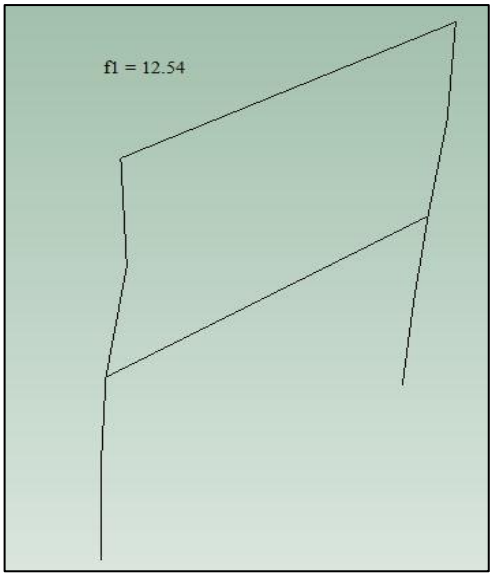
f1 = 12.54

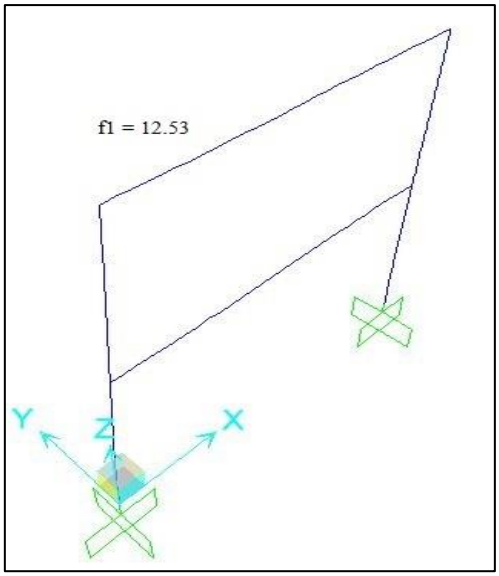
f1 = 12.53
Y
Z
X

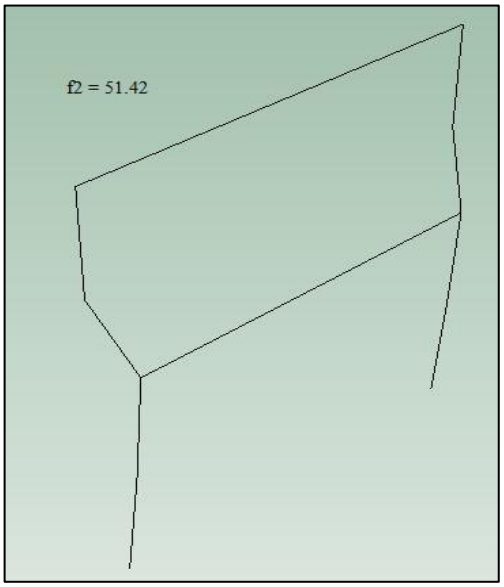
f2 = 51.42

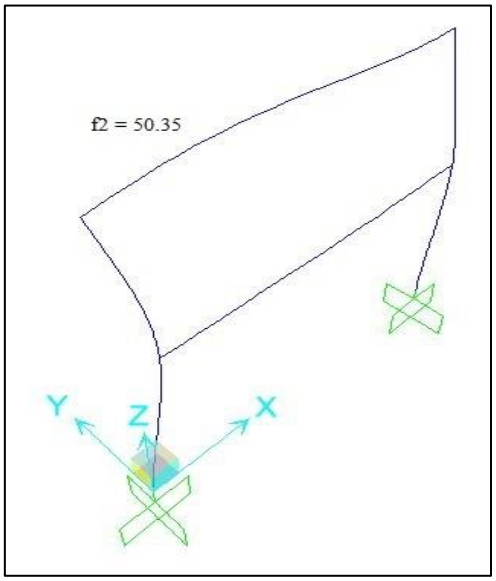
f2 = 50.35
Y
Z
X

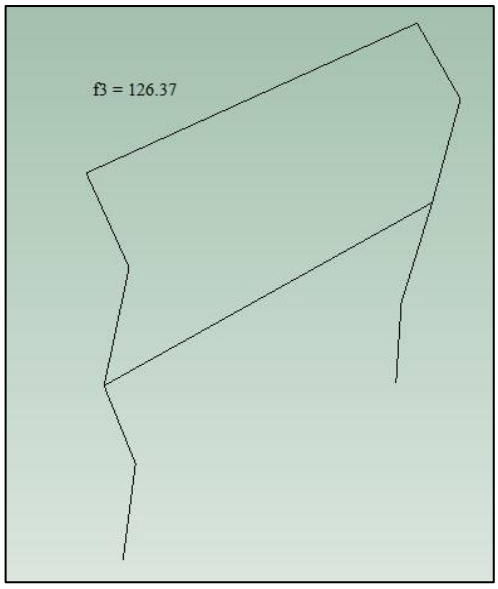
f3 = 126.37

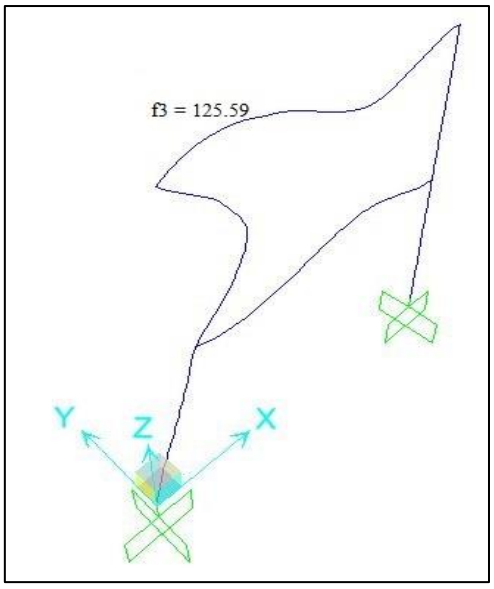
f3 = 125.59
Y
Z
X

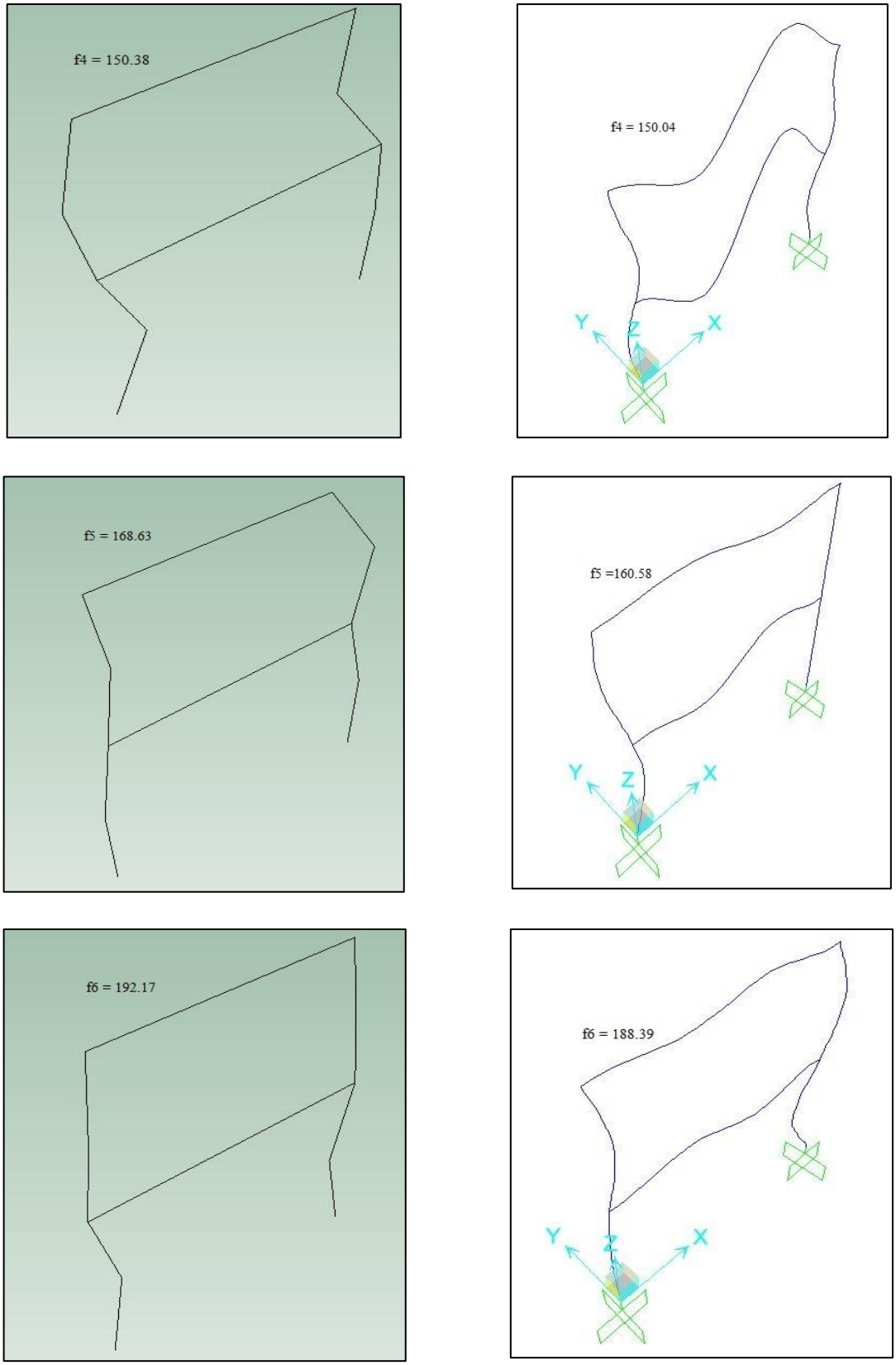

Figure 73: Comparison of experimental and numerically estimated mode shape for longitudinal frame (in plane).

5.2.2. Experimental results and discussions

The initial measurement shows the significant variation of experimental and numerical estimated result. First mode has the maximum difference is 10.81%. After calibration the first 6 mode shapes from EMA and FEM tool SAP2000 for the longitudinal frame (in plane) are almost similar. Fifth mode shape only shows the maximum difference 4.77% and it is less than 5%. After modal updating the modal parameters show the minimum errors.

5.3. Modal parameter estimation for longitudinal frame column (out of plane)

Modal parameters estimation was done by same procedure for longitudinal frame (out of plane) that was done in longitudinal frame (in plane). Total 12 accelerometers and 6 reference hammer (DOF) are fixed out of plane of the frame. The positioning and orientation of the accelerometers and hammer for longitudinal frame is shown Figure 63. Modal parameters were measured by data interpretation for longitudinal frame out of plane is shown in Figure 74. Initially estimated experimental and numerical modal parameters for longitudinal frame (out of plane) is presented in Table 9. The detail procedure for finding out best mode shapes and modal parameters from this analysis is described in Annex C.

Table 9: Modal parameters from EMA and SAP2000 for longitudinal frame (out of plane).

Mode	EMA			SAP2000	Error (%)	Mode type
	Frequency (Hz)	Damping (%)	Complexity (%)	Frequency (Hz)		
1	16.91	24.25	0.17	13.10	-29.08	Bending
2	75.48	0.07	0.91	74.75	-0.98	Bending
3	106.49	1.41	0.19	96.14	-9.72	Bending
4	226.66	0.30	0.10	225.26	-0.62	Bending
5	277.29	0.27	0.14	276.68	-0.22	Bending
6	334.18	1.50	0.89	333.34	-0.25	Bending

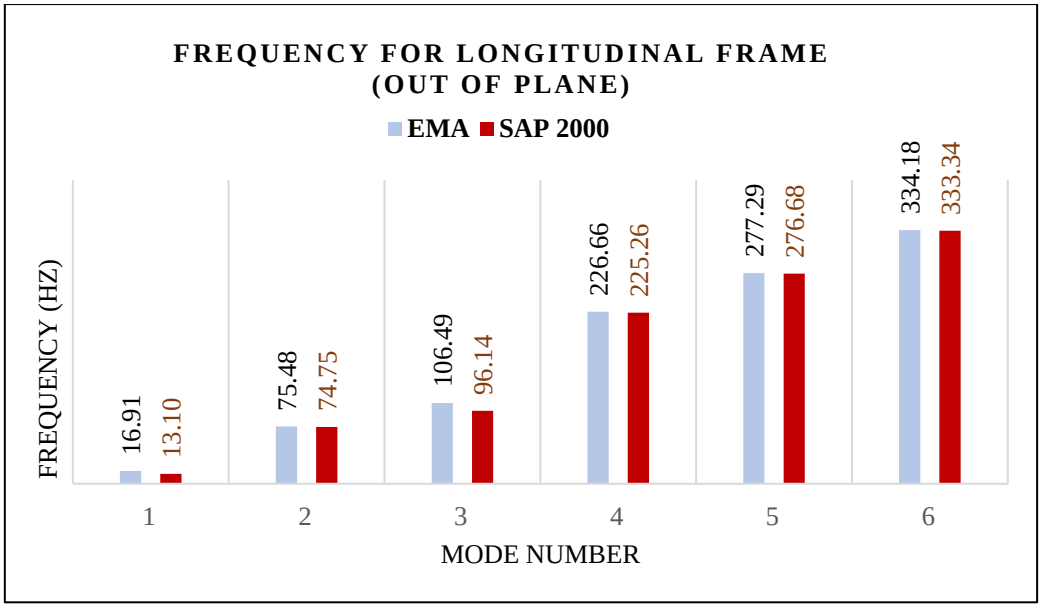

Figure 74: Frequency measured by EMA and SAP2000 for longitudinal frame (out of plane).

The corrected modal parameters after calibration is presented in Table 10. The table shows the EMA frequencies and the FEM frequencies for both before and after model calibration for the first six modes. From Table 10, it can be seen that five out of six modes of the calibrated FEM are in excellent match with the corresponding EMA modes with only 0.02% or less error. The largest error of 9.10% is with the first mode is shown in Figure 75. Mode shapes are found after experimental data interpretation and numerical model updating by calibration for longitudinal frame out of plane is illustrated in Figure 76.

Table 10: Corrected modal parameters with respect to EMA and initial SAP2000 model value for longitudinal frame (out of plane).

Mode Number	Experimental Frequency (Hz)	Numerical FEM (initial) Frequency (Hz)	Numerical FEM (corrected) Frequency (Hz)
1	16.91	13.10	15.37
2	75.48	74.75	74.77
3	106.49	96.14	110.63
4	226.66	225.26	222.96
5	277.29	276.68	275.12
6	334.18	333.34	334.09

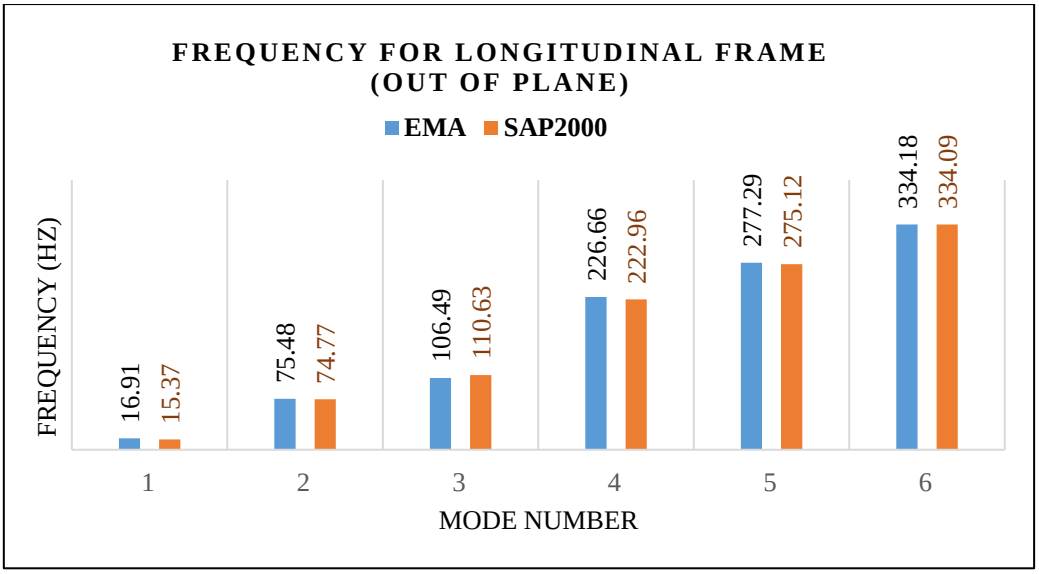

Figure 75: Experimental measurement and numerical FEM corrected model value for longitudinal frame (out of plane).

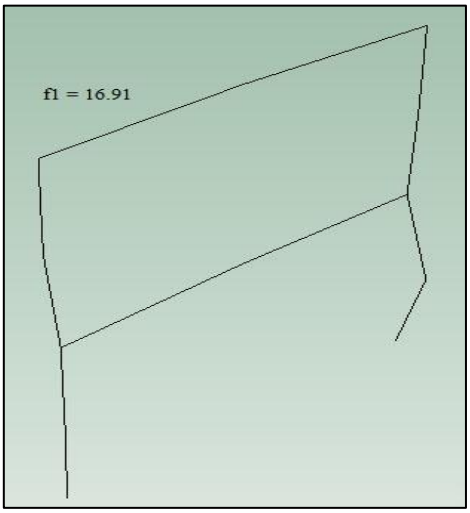

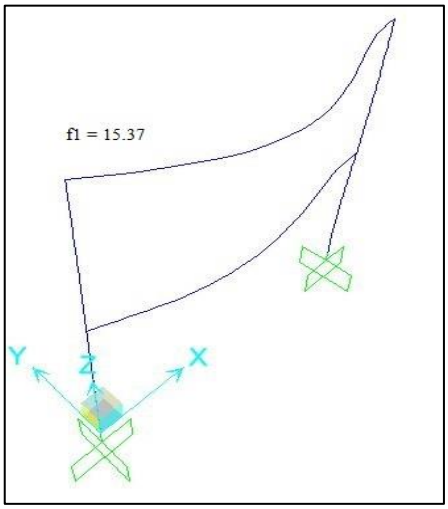

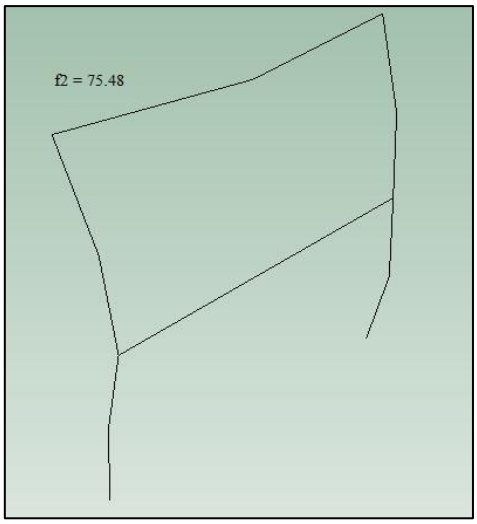

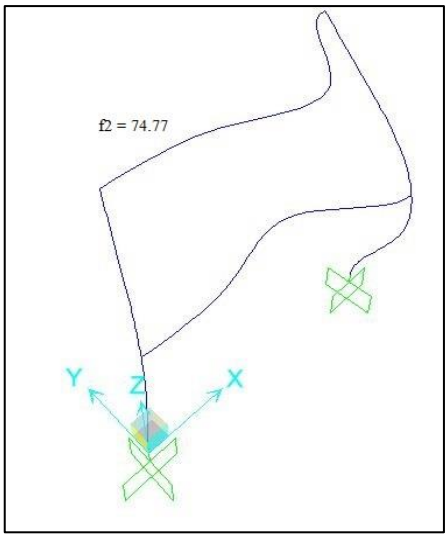

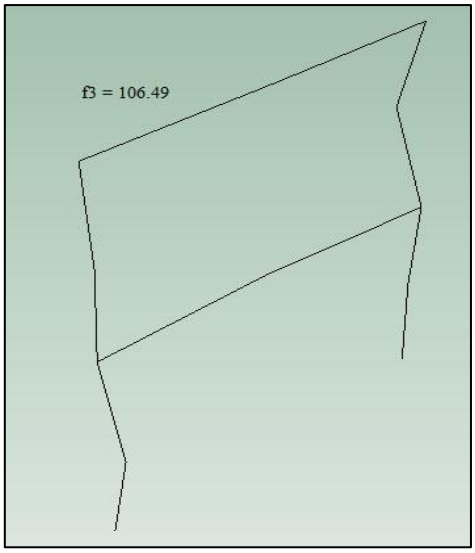
f3 = 106.49

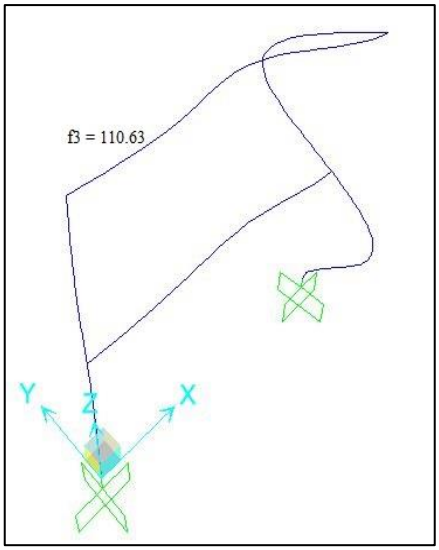
f3 = 110.63
Y
Z
X

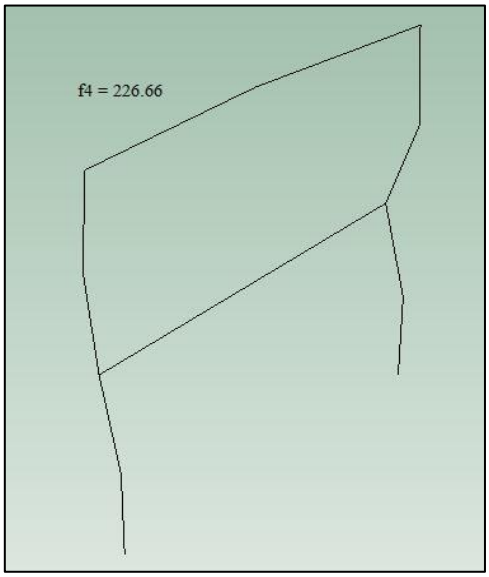
f4 = 226.66

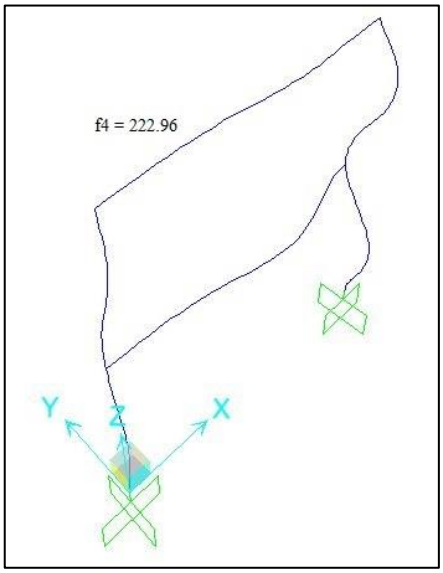
f4 = 222.96
Y
Z
X

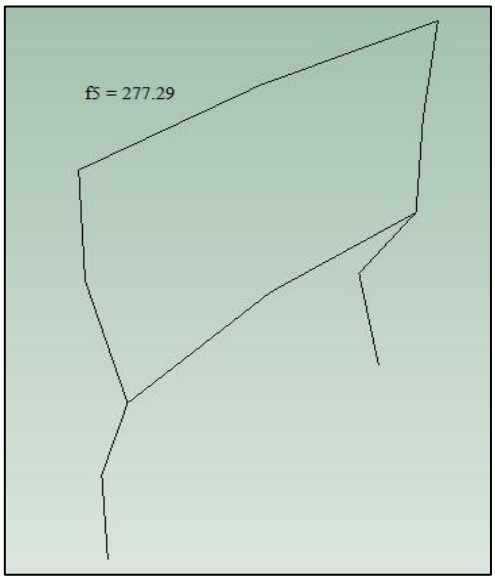
f5 = 277.29

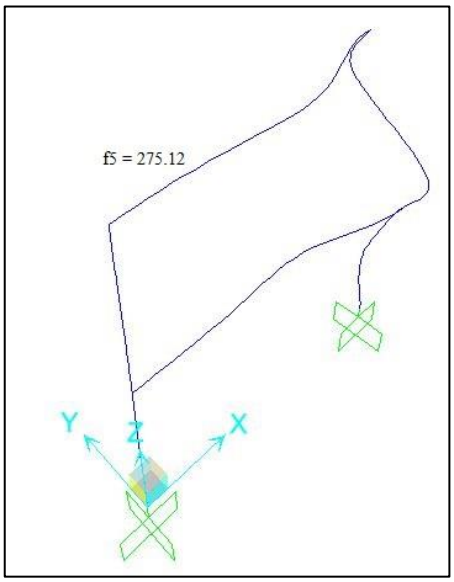
f5 = 275.12
Y
Z
X

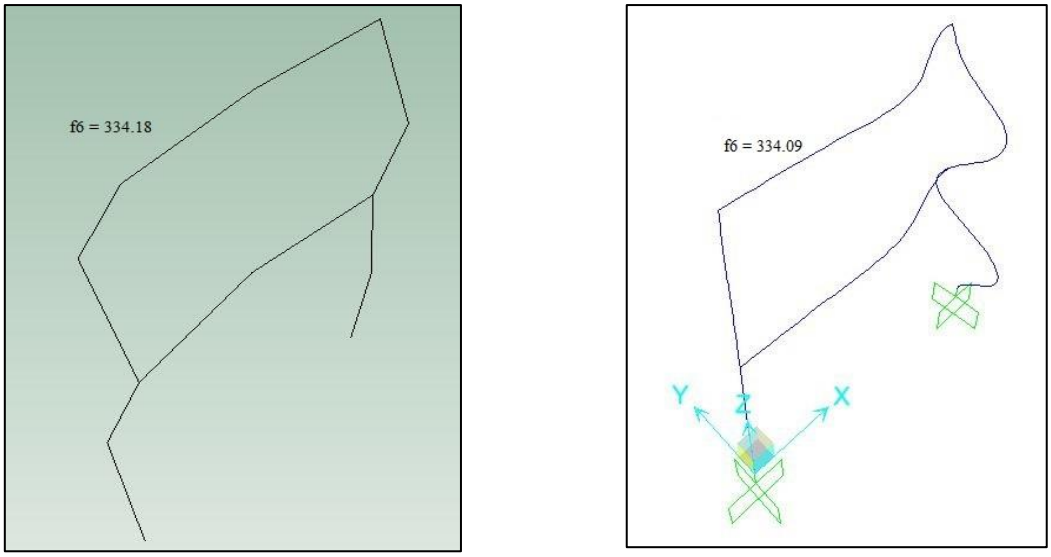

Figure 76: Comparison of experimental and numerically estimated mode shape for longitudinal frame (out of plane).

5.3.1. Experimental results and discussions

Dynamic properties measured from EMA and SAP2000 are very close to each other for the longitudinal frame (out of plane). The numerical modal values are different for first mode. For first mode of the longitudinal frame (out of plane), the initial value extracted from numerical analysis shows the maximum errors and it was 29.08%. And for the 3rd mode the deviation was 9.72%. Due to the deficient of proper calibration the bending modes were not extracted in the right way. Proper calibration for modal updating of full-scale building is essential. The deviations were minimized by proper calibration. After calibration the errors is reduced to 9.10% from 29.08%. All other modes were improved correctly and bending mode is calibrated very well.

5.4. Modal parameter estimation for longitudinal frame (out of plane) after secondary beam removed

The physical property (stability, stiffness, modal mass etc.) of the frame changed for dismantled one or more secondary beam. The red marking secondary beam was removed for observing the changes of modal parameters shown in Figure 77. Experimental modal parameters were computed by the same procedure that described for longitudinal frame (out of plane). Total 11 accelerometers and 6 reference hammer (DOF) were fixed out of plane of the frame. The positioning and orientation of the accelerometers and hammer for longitudinal

frame (out of plane) is shown Figure 64. Initial modal parameters were measured by data interpretation for longitudinal frame (out of plane) after dismantling secondary beam is shown in Figure 78. The comparative presentation of modal parameters for longitudinal frame (out of plane) in Table 11. The detail procedure for getting best mode shapes and modal parameters from this analysis is described in Annex D.

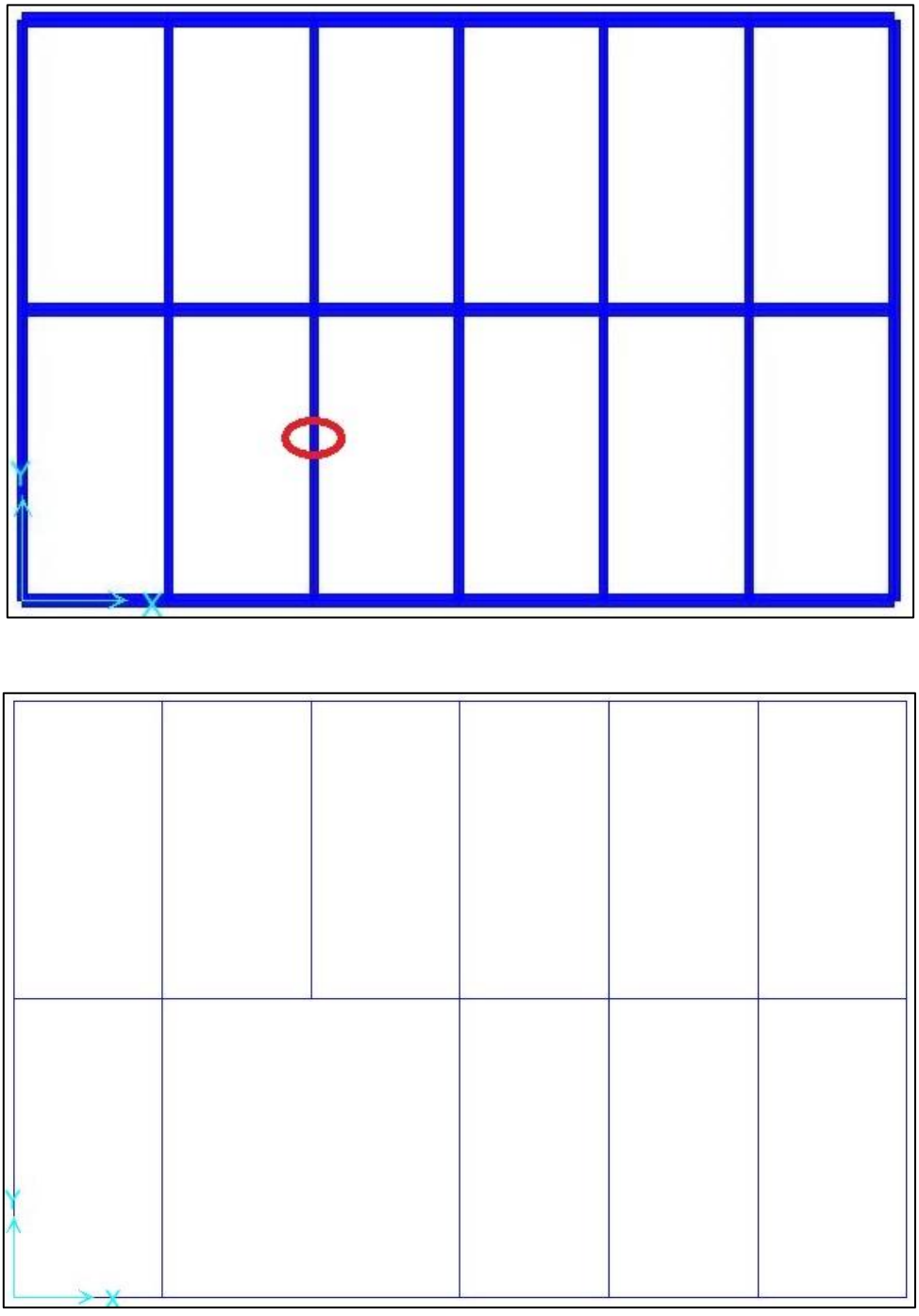

Figure 77: Dismantled of secondary beam (red marking beam).

Table 11: Comparison of frequency for longitudinal frame (out of plane) after secondary beam removed.

Mode	EMA			SAP2000	Error (%)	Mode type
	Frequency (Hz)	Damping (%)	Complexity (%)	Frequency (Hz)		
1	19.49	14.10	0.39	24.99	-28.22	Bending
2	75.75	0.11	0.82	74.82	1.23	Bending
3	105.50	0.97	0.08	96.14	8.87	Bending
4	177.56	1.35	0.19	186.54	-5.06	Bending
5	268.05	0.49	0.12	275.07	-2.62	Bending
6	277.30	0.31	0.08	285.77	-3.05	Bending

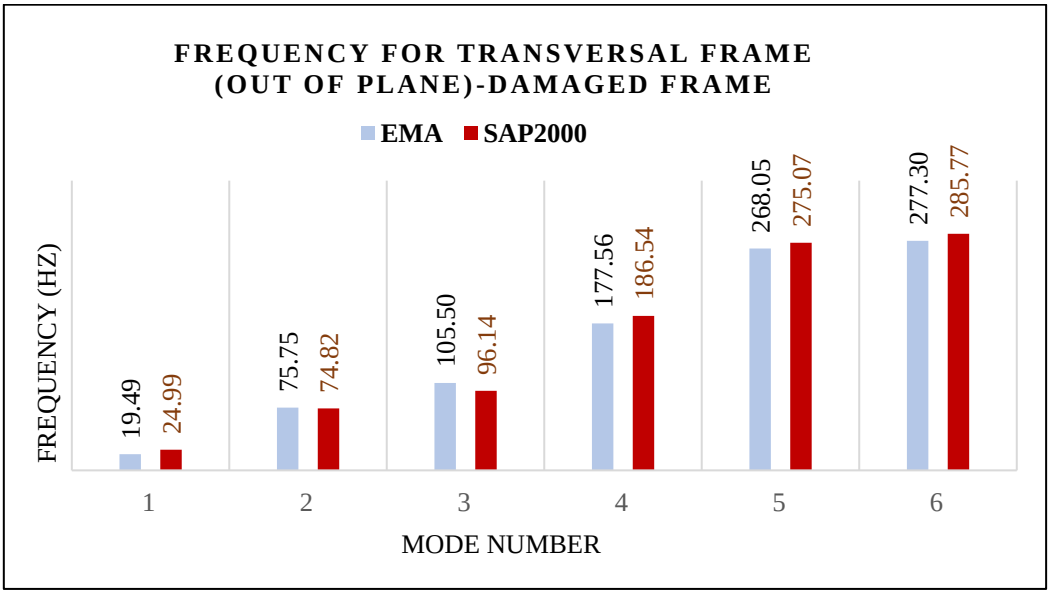

Figure 78: Frequency measured by EMA and SAP for longitudinal frame (out of plane).

The modal parameters were corrected by reducing the stiffness of base connections along both axis after calibration that is presented in table 12. The table shows the EMA frequencies and the FEM frequencies for both before and after model calibration for the first six modes. From table 12, it can be seen that five out of six modes of the calibrated FEM are in excellent match with the corresponding EMA modes with only 0.04% or less error. The largest error of 8.97% is with the 4th mode is shown in figure 79. Mode shapes are found after experimental data interpretation and numerical model updating by calibration for longitudinal frame out of plane is illustrated in figure 80.

Table 12: Corrected modal parameters with respect to EMA and initial SAP2000 model value for longitudinal frame (out of plane).

Mode Number	Experimental Frequency (Hz)	Numerical FEM (initial) Frequency (Hz)	Numerical FEM (corrected) Frequency (Hz)
1	19.49	24.99	18.79
2	75.75	74.82	75.78
3	105.50	96.14	110.25
4	177.56	186.54	193.49
5	268.05	275.07	275.04
6	277.30	285.77	284.88

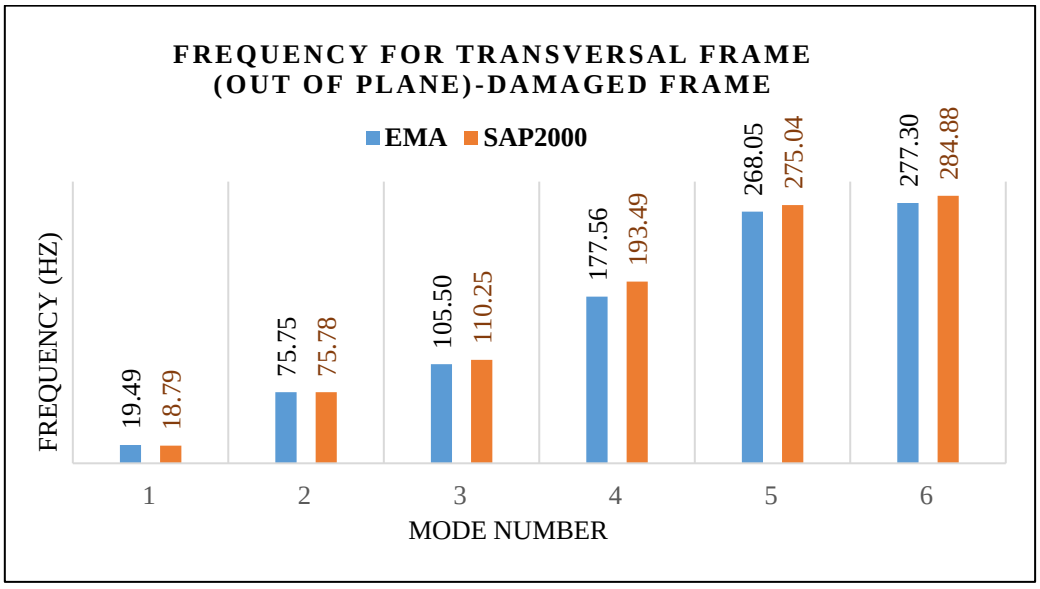

Figure 79: Experimental measurement and numerical FEM corrected model value for longitudinal frame (out of plane).

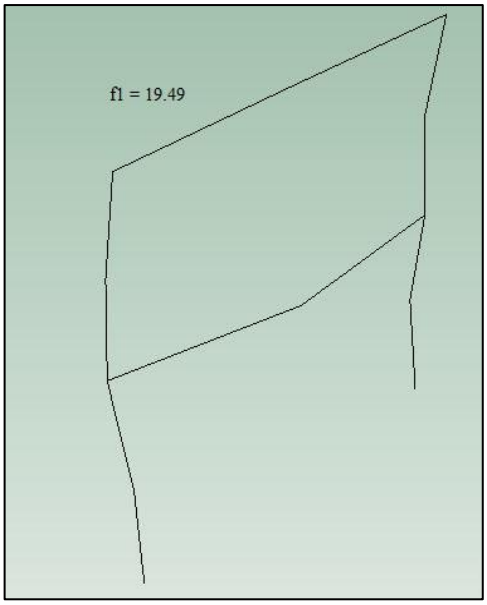
f1 = 19.49

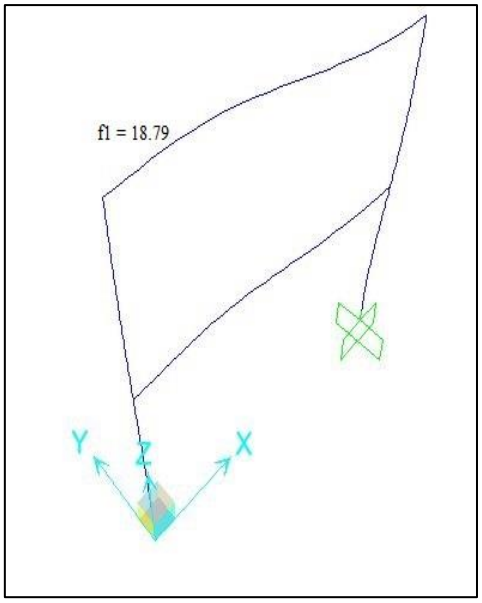
f1 = 18.79
Y
Z
X

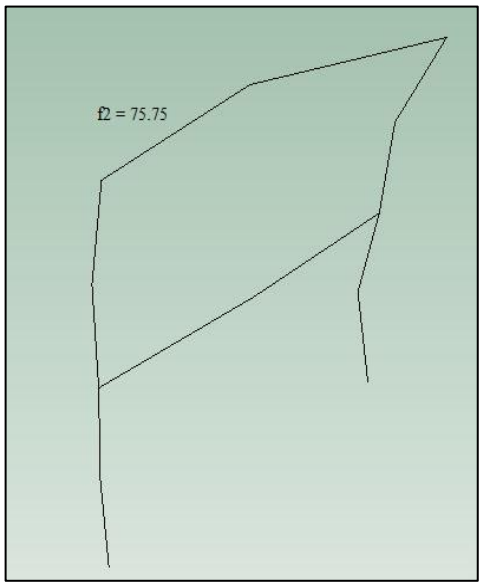
f2 = 75.75

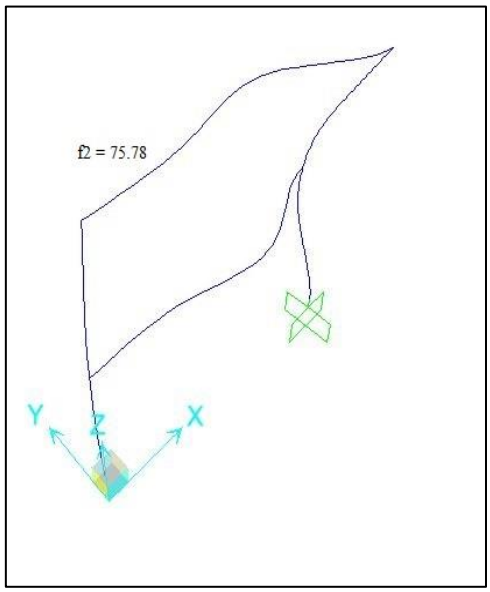
f2 = 75.78
Y
Z
X

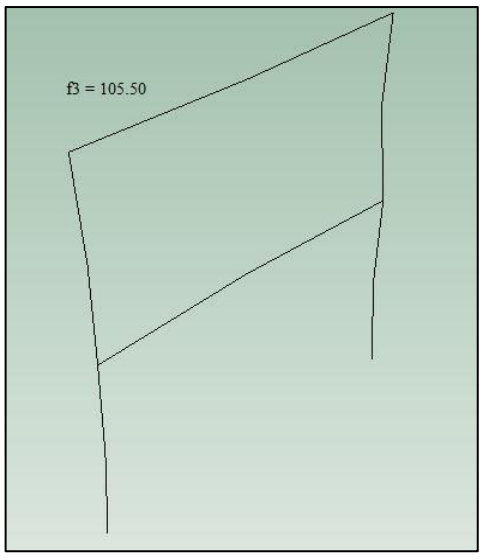
f3 = 105.50

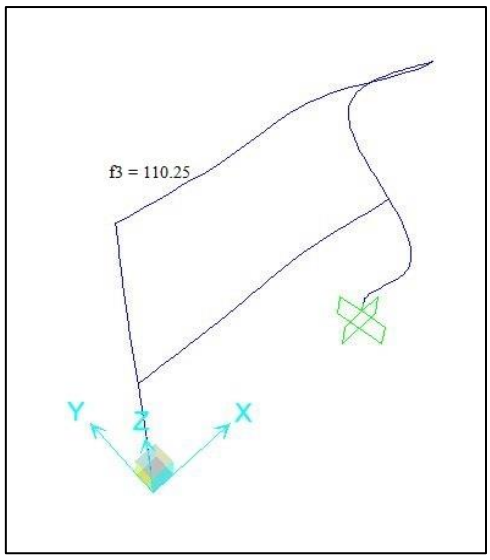
f3 = 110.25
Y
Z
X

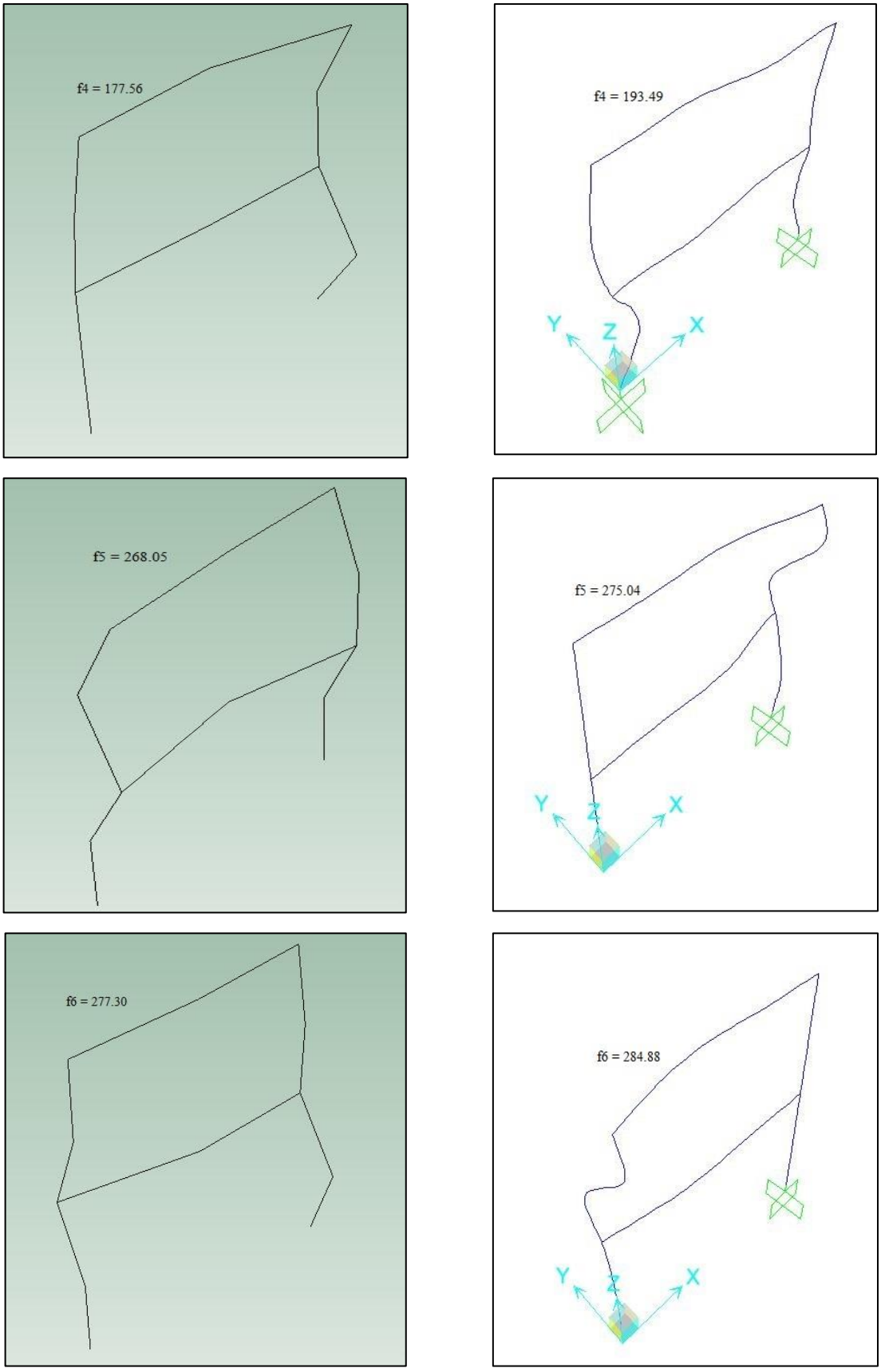

Figure 80: Comparison of experimental and numerically estimated mode shape for longitudinal frame (out of plane) after secondary beam removed.

Table 13: Correlation of frequency for longitudinal frame (out of plane) for undamaged and damaged frame.

Mode	Measured undamaged f_n (Hz)	Calibrated model undamaged f_n (Hz)	Measured damaged f_n (Hz)	After simulation f_n (Hz)	Mode type
1	16.91	15.37	19.49	18.79	Bending
2	75.48	74.77	75.75	75.78	Bending
3	106.49	110.63	105.50	110.25	Bending
4	226.66	222.96	177.56	193.49	Bending
5	277.29	275.12	268.05	275.04	Bending
6	334.18	334.09	277.30	284.88	Bending

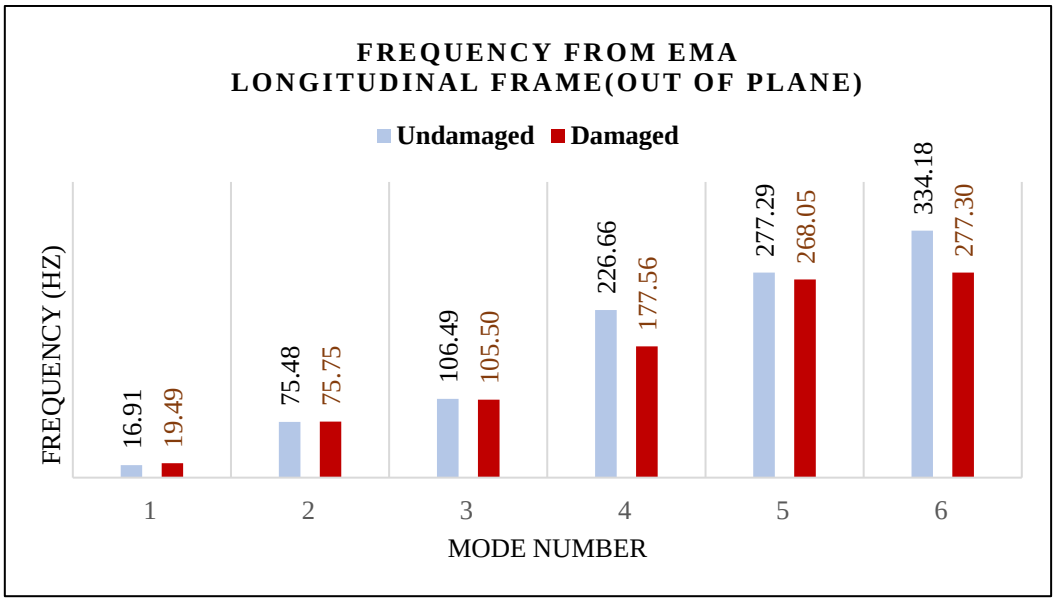

Figure 81: Frequency measured by EMA for longitudinal frame (out of plane) after secondary beam removed.

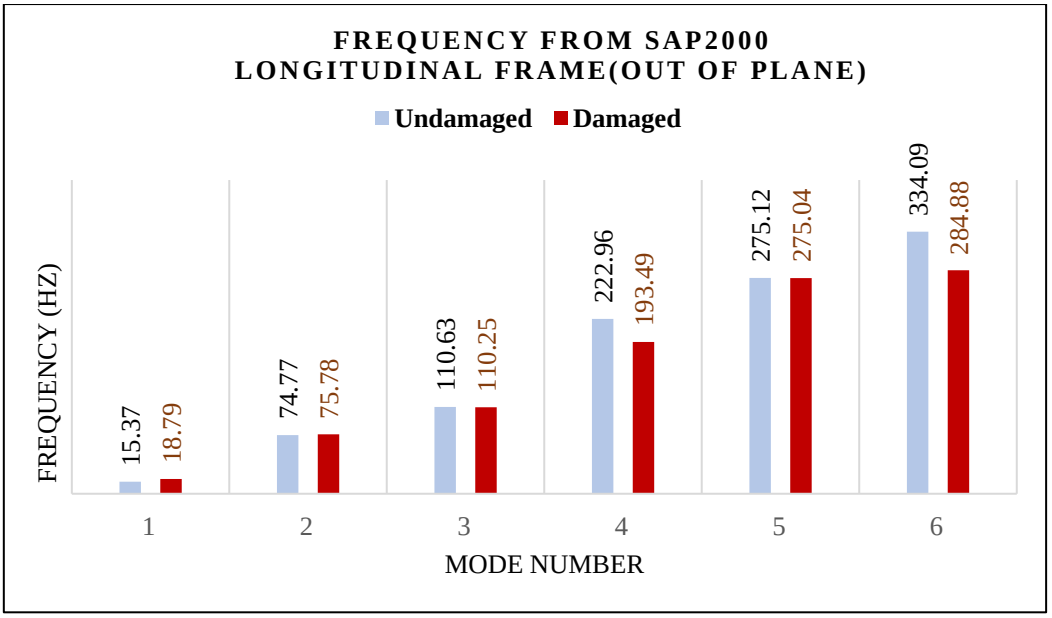

Figure 82: Frequency measured by SAP2000 for longitudinal frame (out of plane) after secondary beam removed.

5.4.1. Experimental results and discussions

The frequency measured for undamaged and damaged frame has significant change for three specific modes for longitudinal frame (out of plane). For 2nd mode, the frequency is 75.48 Hz for undamaged condition and 75.75 Hz for damaged condition from EMA. On the other hands, numerically this value is 74.77Hz and 75.78 Hz for both conditions respectively. The calibration of mode is good enough for EMA and SAP2000 in mode 4 in damaged condition. The frequency is 226.66Hz and 222.96 Hz for EMA and SAP2000 respectively for longitudinal frame (out of plane). But for removing of secondary beam there is significant difference in frequency for undamaged and damaged conditions. In undamaged condition frequency is 226.66Hz but 177.56Hz for damaged condition in EMA. Numerically also has big changes of frequency in the same mode. Frequency is 222.96 Hz and 193.49 Hz for undamaged and damaged condition respectively. Experimentally and numerically, the structural properties changed significantly for 6th mode. The frame is more flexible because of low frequency (334.18Hz and 277.30Hz respectively for both conditions). Except 4th and 6th mode all other modes have no big difference of frequency for both conditions in EMA and SAP2000. The 4th and 6th modes are affected more due to physical property changes after dismantling of secondary beam.

5.4.2. Blast testing and damage prediction

The stiffness at beam-to-column connection and column-base connection of the intact frame is 32000 kNm/mrad and 1100000 kNm/mrad respectively. The building will be subjected to blasts (TNT or equivalent) with different charge sizes and locations, resulting in different scaled distances. As the scaled distance reduces, the peak overpressure increases, thus causing the shear failure of the elements located in the proximity. The potential for progressive collapse following local damage will be also investigated in the column and beam.

The column web will be affected by the external charge (Figure 83.a) and the column flange and the bottom flange of the primary beam is affected by the internal blast (Figure 83.b). The effects of gravity load on the columns and beams are not considered for blast action during the test. Four different scenarios depend on the stiffness reduction at the column-base connection for damage prediction are considered subjected to external blast action. Damage scenario: DC1-1; DC1-2; DC1-3; DC1-4 indicates the reduction of stiffness at the base connection along the strong axis (oriented out of plane of the frame) 10%; 30%; 50% and 95% respectively. The numerical eigenvalues for these damage scenarios in both plane is presented in Table 14 -15.

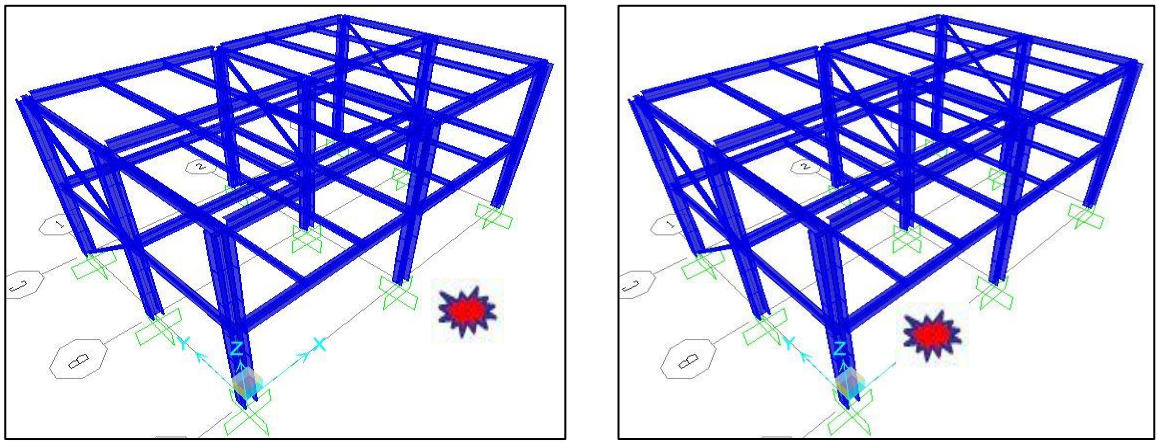

a) b)

Figure 83: View of the structure with the position of the blast charge for external and internal blast tests.

Table 14: Eigenvalues estimated by SAP2000 for different damage scenarios (in plane).

Intact frame (in plane) f_n (Hz)	Damage scenario			
	DC1-1 f_n (Hz)	DC1-2 f_n (Hz)	DC1-3 f_n (Hz)	DC1-4 f_n (Hz)
12.53	12.53	12.53	12.52	12.43
50.35	50.35	50.34	50.34	50.33
125.59	125.59	125.59	125.59	125.59
150.04	150.04	150.04	149.81	149.46
160.58	160.58	160.58	160.58	160.58
188.39	188.39	188.39	188.39	188.39

Table 15: Eigenvalues estimated by SAP2000 for different damage scenarios (out of plane).

Intact frame (out of plane) f_n (Hz)	Damage scenario			
	DC1-1 f_n (Hz)	DC1-2 f_n (Hz)	DC1-3 f_n (Hz)	DC1-4 f_n (Hz)
15.37	15.37	15.37	15.37	15.37
74.77	74.77	74.77	74.77	74.77
110.63	110.63	110.63	110.63	110.63
222.96	222.96	222.96	222.92	222.92
275.12	275.12	275.12	275.12	275.12
334.09	334.09	334.09	334.09	334.09

The flange of column and lower flange of primary beam will be affected for internal blast. Stiffness was reduced along weak axis (oriented in the plane of the frame) and four different damage scenarios are considered. Damage scenario DC2-1 means stiffness is reduced 10% along weak axis. Damage scenarios DC2-2; DC2-3; DC2-4 means the stiffness was reduced at the base connection along the weak axis 30%; 50% and 95% respectively. The numerical eigenvalues for these damage scenarios in both plane is presented in Table 16-17. Reduction of stiffness was introduced simultaneously along both major and minor axis of the base connection is presented in Table 18-19.

Table 16: Eigenvalues estimated by SAP2000 for different damage scenarios (in plane).

Intact frame (in plane) f_n (Hz)	Damage scenario			
	DC2-1 f_n (Hz)	DC2-2 f_n (Hz)	DC2-3 f_n (Hz)	DC2-4 f_n (Hz)
12.53	12.53	12.54	12.54	12.43
50.35	50.44	50.44	50.44	50.44
125.59	127.55	127.45	127.29	125.59
150.04	150.06	150.06	150.06	150.04
160.58	160.58	160.58	160.58	160.58
188.39	188.39	188.39	188.39	188.39

Table 17: Eigenvalues estimated by SAP2000 for different damage scenarios (out of plane).

Intact frame (out of plane) f_n (Hz)	Damage scenario			
	DC2-1 f_n (Hz)	DC2-2 f_n (Hz)	DC2-3 f_n (Hz)	DC2-4 f_n (Hz)
15.37	15.37	15.37	15.37	15.34
74.77	74.74	74.73	74.72	74.25
110.63	110.51	110.48	110.42	108.41
222.96	222.93	222.92	222.91	222.64
275.12	275.11	275.11	275.11	275.03
334.09	333.86	333.78	333.64	330.34

Table 18: Eigenvalues estimated by SAP2000 for different damage scenarios (in plane).

Intact frame (in plane) f_n (Hz)	Damage scenario			
	DC3-1 f_n (Hz)	DC3-2 f_n (Hz)	DC3-3 f_n (Hz)	DC3-4 f_n (Hz)
12.53	12.53	12.53	12.52	12.43
50.35	50.35	50.34	50.34	50.34
125.59	125.60	125.60	125.60	123.37
150.04	150.04	150.04	150.04	149.95
160.58	160.59	160.59	160.59	160.59
188.39	188.39	188.39	188.39	188.39

Table 19: Eigenvalues estimated by SAP2000 for different damage scenarios (out of plane).

Intact frame (out of plane) f_n (Hz)	Damage scenario			
	DC3-1 f_n (Hz)	DC3-2 f_n (Hz)	DC3-3 f_n (Hz)	DC3-4 f_n (Hz)
15.37	15.37	15.37	15.37	15.35
74.77	74.74	74.73	74.72	74.25
110.63	110.52	110.49	110.42	108.41
222.96	222.92	222.92	222.92	222.42
275.12	275.10	275.10	275.10	275.03
334.09	333.89	333.78	333.67	330.36

The effects of blast loads can result in the loss of the bearing capacity of a column, or other primary structural members. The larger effects can be attributed to additional damages in members other than the column, but also to the dynamic increase factor. Thus, the upward lift of primary beams due to direct blast pressure makes the dynamic increase factor go up, with regards to column removal. External beam-column connection and internal beam-column connection may lose the stiffness due to the internal blast and progressive damage of column. For damage prediction of the entire structure four different damage scenarios are considered for both external and internal connection. 1st , 2nd, 3rd and 4th damage scenarios are considered the reduction of stiffness 10%, 30%, 50% and 95%. Table 20-25 illustrate the changes of frequencies after losing of stiffness at column-beam connection and column base connection.

Table 20: Eigenvalues estimated by SAP2000 for different damage scenarios (in plane).

Intact frame (in plane) f_n (Hz)	Damage scenario (external column-beam connection)			
	DB1-1 f_n (Hz)	DB1-2 f_n (Hz)	DB1-3 f_n (Hz)	DB1-4 f_n (Hz)
12.53	12.53	12.52	12.51	12.43
50.35	50.35	50.35	50.35	50.34
125.59	125.60	125.60	125.60	125.60
150.04	150.04	150.04	150.04	150.04
160.58	160.41	160.03	159.52	158.33
188.39	188.39	188.39	188.39	188.39

Table 21: Eigenvalues estimated by SAP2000 for different damage scenarios (out of plane).

Intact frame (out of plane) f_n (Hz)	Damage scenario (external column-beam connection)			
	DB1-1 f_n (Hz)	DB1-2 f_n (Hz)	DB1-3 f_n (Hz)	DB1-4 f_n (Hz)
15.37	15.37	15.37	15.37	15.37
74.77	74.77	74.77	74.77	74.77
110.63	110.63	110.63	110.63	110.63
222.96	222.97	222.92	222.87	222.67
275.12	275.10	275.10	275.10	275.10
334.09	334.11	334.11	334.11	334.11

Table 22: Eigenvalues estimated by SAP2000 for different damage scenarios (in plane).

Intact frame (in plane) f_n (Hz)	Damage scenario (internal column-beam connection)			
	DB2-1 f_n (Hz)	DB2-2 f_n (Hz)	DB2-3 f_n (Hz)	DB2-4 f_n (Hz)
12.53	12.53	12.52	12.51	12.44
50.35	50.35	50.35	50.35	50.35
125.59	125.60	125.60	125.60	125.60
150.04	149.99	149.97	149.95	149.95
160.58	160.51	160.36	160.15	159.59
188.39	188.39	188.39	188.39	188.39

Table 23: Eigenvalues estimated by SAP2000 for different damage scenarios (out of plane).

Intact frame (out of plane) f_n (Hz)	Damage scenario (internal column-beam connection)			
	DB2-1 f_n (Hz)	DB2-2 f_n (Hz)	DB2-3 f_n (Hz)	DB2-4 f_n (Hz)
15.37	15.37	15.37	15.37	15.37
74.77	74.77	74.77	74.77	74.77
110.63	110.63	110.63	110.63	110.63
222.96	222.97	222.97	222.97	222.97
275.12	275.10	275.10	275.10	275.10
334.09	334.11	334.11	334.11	334.11

Table 24: Eigenvalues estimated by SAP2000 for different damage scenarios (in plane).

Intact frame (in plane) f_n (Hz)	Damage scenario (both external and internal column-beam connection)			
	DB3-1 f_n (Hz)	DB3-2 f_n (Hz)	DB3-3 f_n (Hz)	DB3-4 f_n (Hz)
12.53	12.52	12.51	12.49	12.35
50.35	50.35	50.35	50.35	50.31
125.59	125.60	125.60	125.60	125.60
150.04	149.99	149.95	149.95	149.95
160.58	160.33	159.77	159.03	157.21
188.39	188.39	188.39	188.39	188.39

Table 25: Eigenvalues estimated by SAP2000 for different damage scenarios (out of plane).

Intact frame (out of plane) f_n (Hz)	Damage scenario (both external and internal column-beam connection)			
	DB3-1 f_n (Hz)	DB3-2 f_n (Hz)	DB3-3 f_n (Hz)	DB3-4 f_n (Hz)
15.37	15.37	15.37	15.37	15.37
74.77	74.77	74.77	74.77	74.77
110.63	110.63	110.63	110.63	110.63
222.96	222.97	222.92	222.87	222.67
275.12	275.10	275.10	275.10	275.10
334.09	334.11	334.11	334.11	334.11

The flange of the column and lower beam flange can be affected simultaneously by internal blast. In that case, stiffness of the base connection and external beam-column connection and internal beam-column connection will be lost at the same time. For this substances, unforeseen damage and progressive displacement at the connections and elements can be occurred. Damage prediction will be more effective along weak axis of the column and primary beam. 10%, 30%, 50% and 95% stiffness loss are considered simultaneously for four different damage scenarios: DBC3-1; DBC3-2; DBC3-3; DBC3-4. Table 26-27 illustrate the changes of frequencies after losing of stiffness at column-beam connection and column base connection.

Table 26: Eigenvalues estimated by SAP2000 for different damage scenarios (in plane).

Intact frame (in plane) f_n (Hz)	Damage scenario (both external and internal column-beam connection and base connection)			
	DBC3-1 f_n (Hz)	DBC3-2 f_n (Hz)	DBC3-3 f_n (Hz)	DBC3-4 f_n (Hz)
12.53	12.52	12.51	12.48	12.13
50.35	50.35	50.34	50.34	50.25
125.59	125.60	125.60	125.60	125.60
150.04	149.99	149.95	149.95	149.95
160.58	160.33	159.77	159.03	156.81
188.39	188.39	188.39	188.39	188.39

Table 27: Eigenvalues estimated by SAP2000 for different damage scenarios (out of plane).

Intact frame (out of plane) f_n (Hz)	Damage scenario (both external and internal column-beam connection and base connection)			
	DBC3-1 f_n (Hz)	DBC3-2 f_n (Hz)	DBC3-3 f_n (Hz)	DBC3-4 f_n (Hz)
15.37	15.37	15.37	15.37	15.37
74.77	74.77	74.77	74.77	74.77
110.63	110.63	110.63	110.63	110.63
222.96	222.97	222.92	222.82	222.17
275.12	275.10	275.10	275.10	275.10
334.09	334.11	334.11	334.11	334.11

5.4.3. Numerical result for damage prediction and discussions

In this study, it is showed that the constructive implementation of practical structural identification for full-scale building steel structure. The modal parameters have to update in a convenient way by considering the finite element model, geometry and material properties of structural elements. The actual situations of the practical structure can be analysed by combining numerical analysis and experimental investigation. It is the real strength of FE model updating of a structure. FE model is the best tool to explain the essential physics of the

system of interest and that is capable of capturing and simulating its critical physical behaviours.

Different damage prediction was considered for calibrated numerical models and were applied to preliminary investigations on a full-scale building structure, using different blast loading conditions. This prediction is important because it will help to get good idea about the non-visible crack/damage due to loss of stiffness at connections and building elements. Different damage scenarios were considered for external and internal blast action.

Comparisons were made in terms of structural modal parameters for each damage scenario. Due to blast effects at the connections and other elements of the structure, the dynamic properties depend on the percentage reduction of stiffness at connections. From the presented numerical result above it can be concluded that very few number of lower modes are affected. But for the higher modes, significant changes in the frequency for all damage scenarios. Damage prediction at base connection when stiffness is reduced simultaneously along the strong and weak axis is more operative for some higher modes, see Figure 84-87. Most of the higher modes are highly affected for internal blast when reduced stiffness are applied simultaneously at the external and internal column-beam connections and base connections, see Figure 88-91.

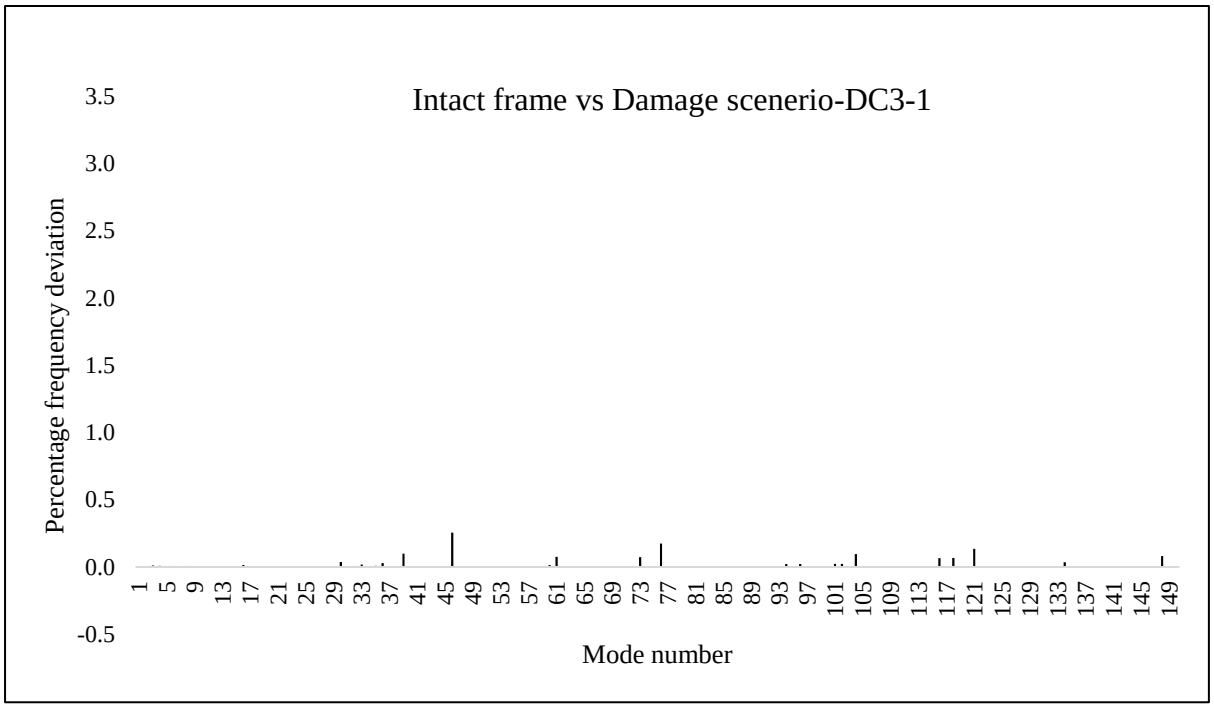

Figure 84: Relative frequency deviation between intact frame and damaged frame.

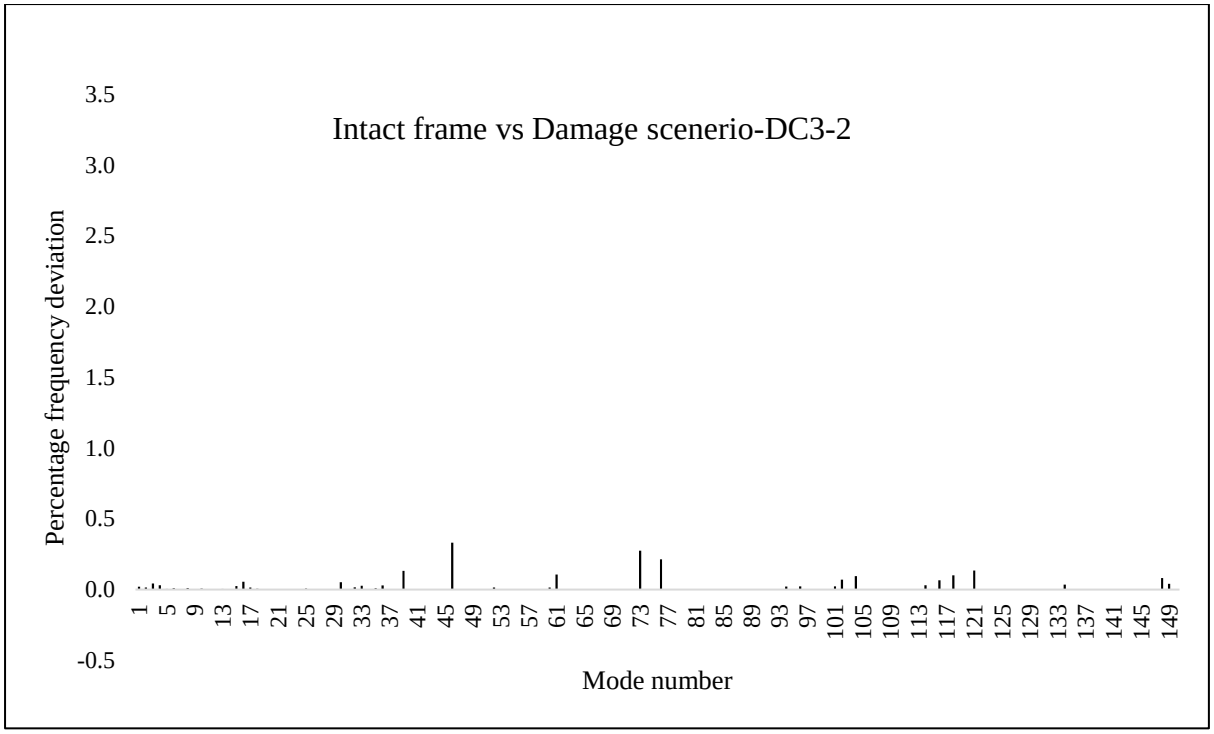

Figure 85: Relative frequency deviation between intact frame and damaged frame.

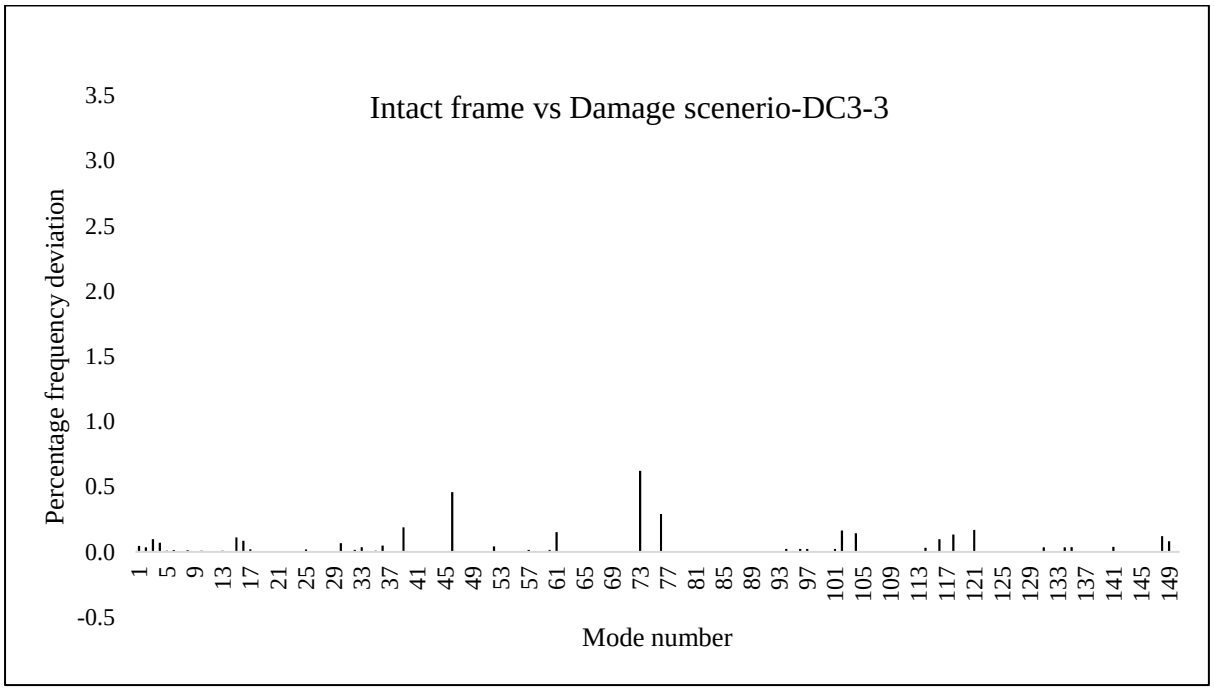

Figure 86: Relative frequency deviation between intact frame and damaged frame.

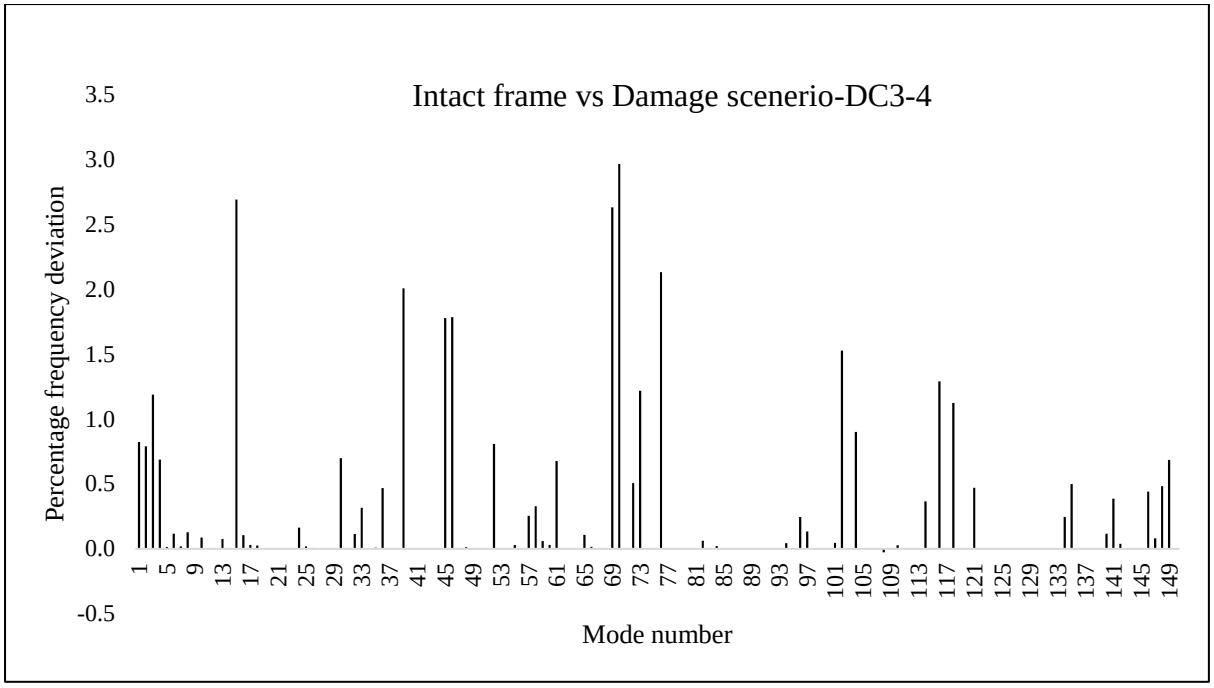

Figure 87: Relative frequency deviation between intact frame and damaged frame.

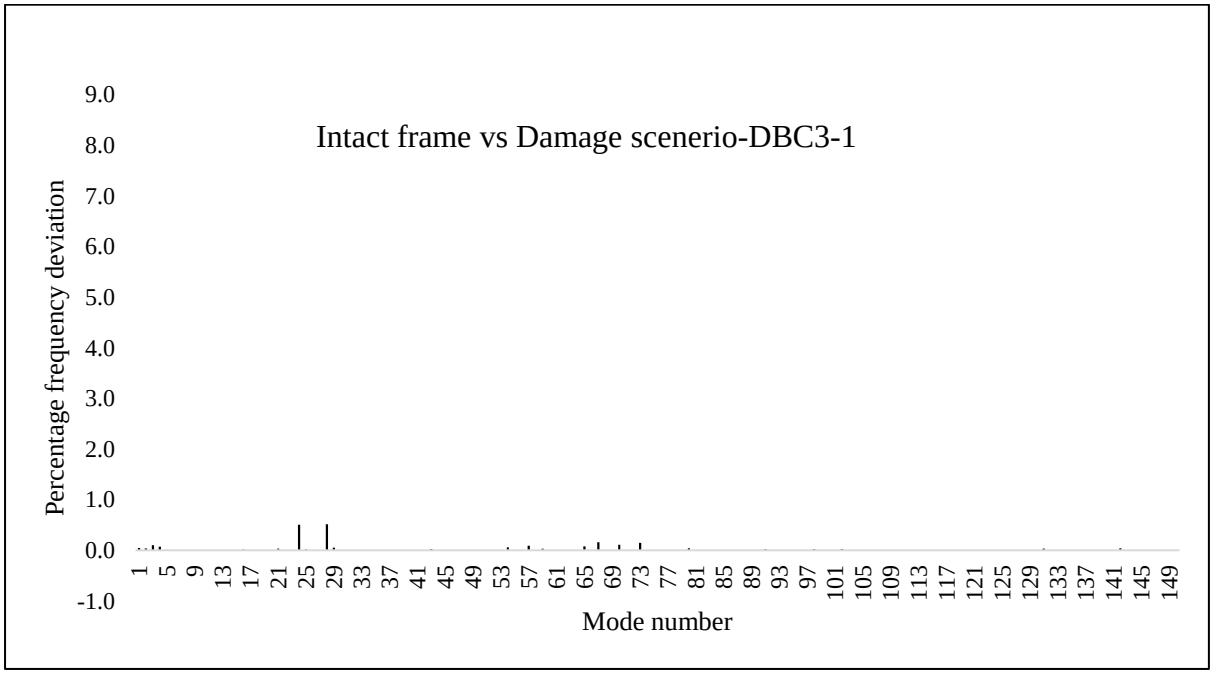

Figure 88: Relative frequency deviation between intact frame and damaged frame.

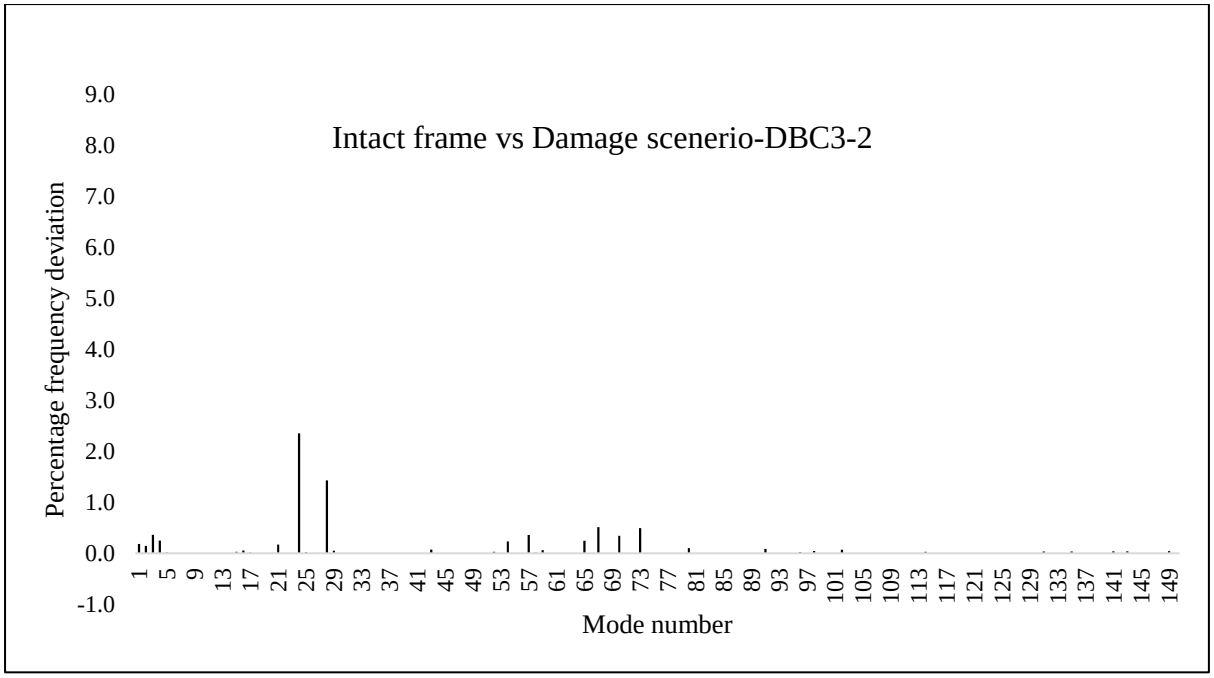

Figure 89: Relative frequency deviation between intact frame and damaged frame.

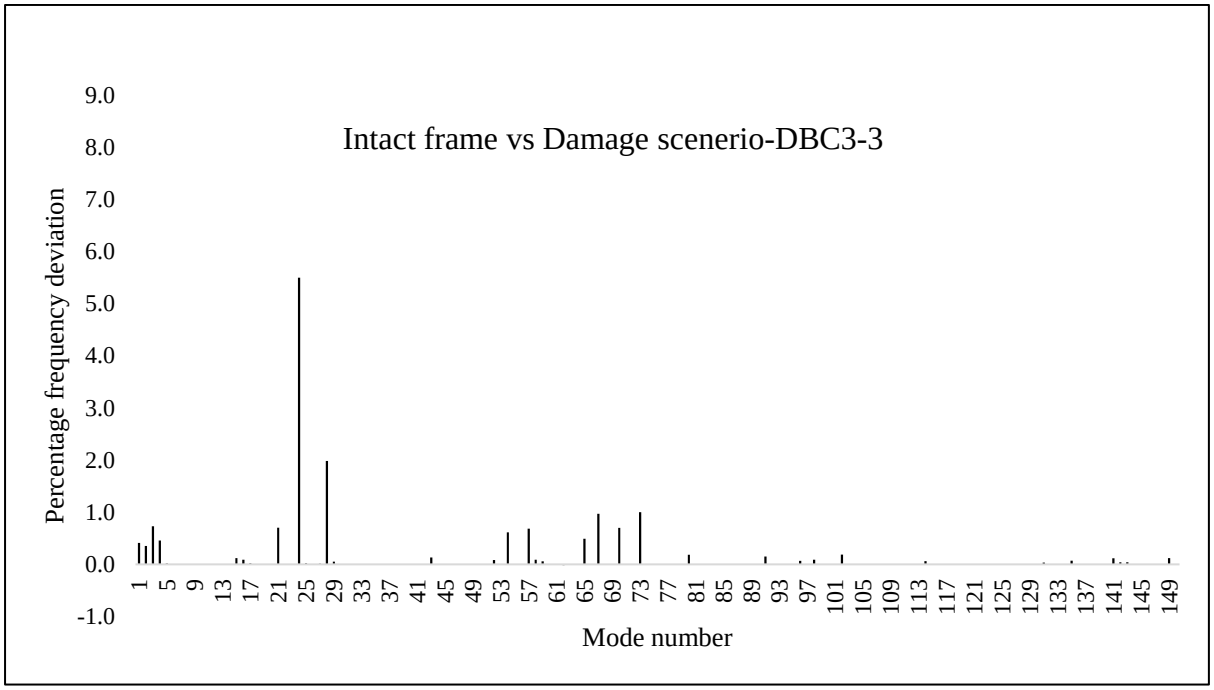

Figure 90: Relative frequency deviation between intact frame and damaged frame.

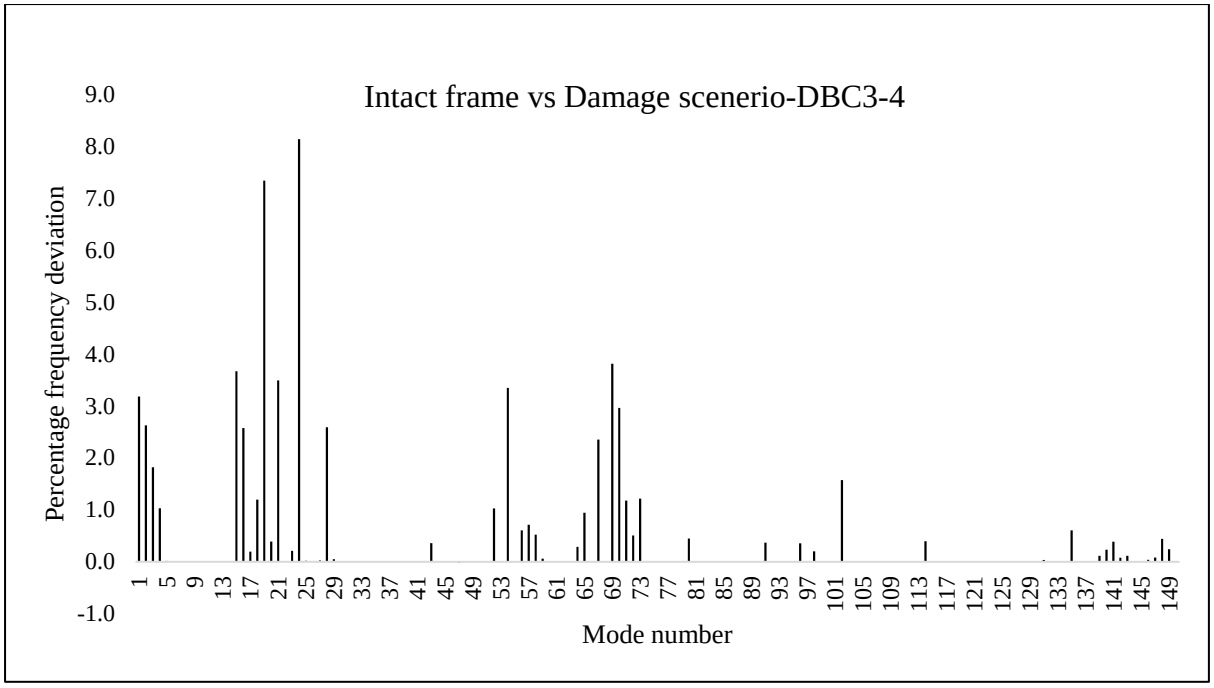

Figure 91: Relative frequency deviation between intact frame and damaged frame.

5.5. Pulse reflex correlation analysis

The correlation between experimental and numerical eigenvalues and mode shape is done by the pulse reflex correlation analysis. It has extensive application in pulse reflex modal analysis to evaluate different test and FEM strategies and to find out the shortcomings in modal test and quality of FEM. The modes shape, modal assurance criteria, auto orthogonality and paired modal data can be extracted after correlation. It clearly can indicate which mode of FEM is corelated with the measured mode. Experimental modal analysis is conducted for the steel frame in the laboratory to find the modal parameters and to demonstrate the flexibility of the frame after damage initiation. In this section, Pulse reflex correlation analysis is carried out to see the similarity of the modal results for damaged and undamaged frame. The damage location can be clearly mentioned from the mode shapes and eigenvalues. The lower beam of the frame was removed to identify the differences of mode shapes. We found one extra mode in damaged frame, see Table 2. The missing mode shape for undamaged frame is clearly mentioned in Figure 92. Fourth mode was created only in damaged frame. From Figure 92, it be seen that damaged is clearly identify for fourth mode at lower portion of the frame.

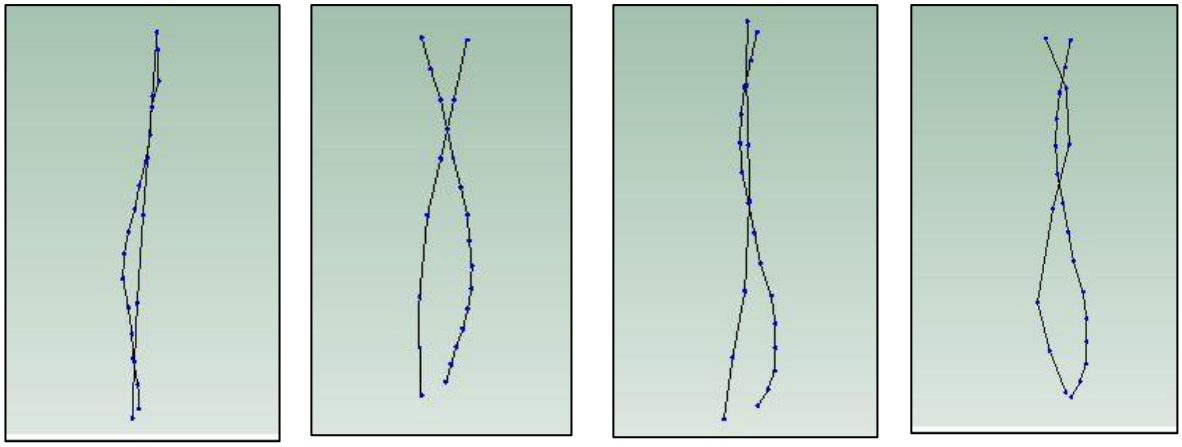

a) b) c) d)

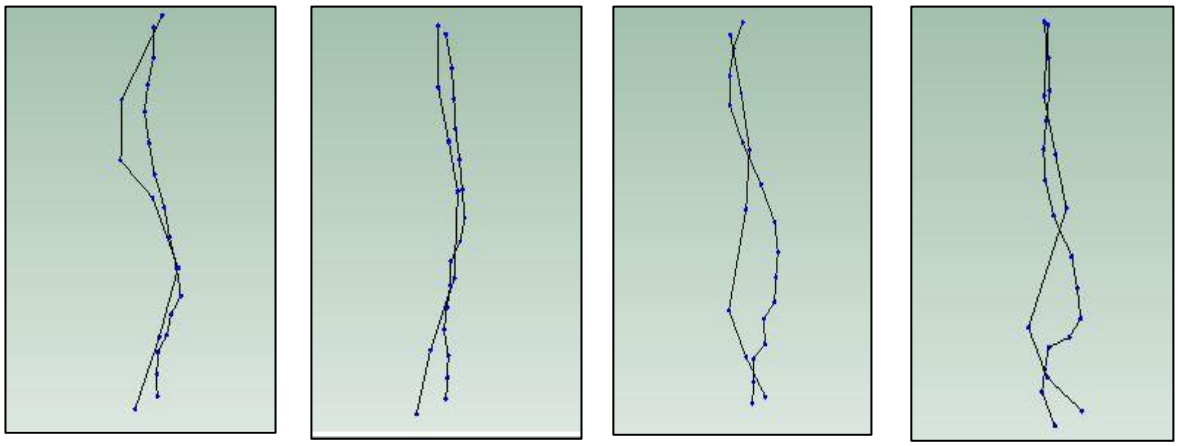

e) f) g) h)

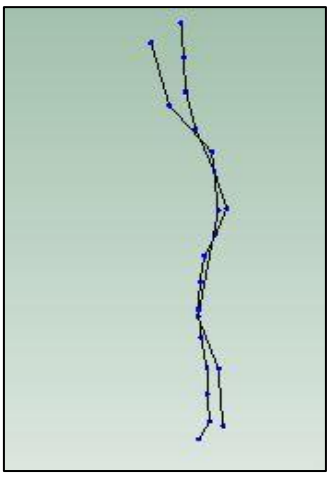

i)

Figure 92: Mode shape comparison automatically: a) first mode; b) second mode: c) third mode; d) fourth mode; e) fifth mode; f) sixth mode; g) seventh mode; h) eighth and; i) ninth mode

6. CONCLUSIONS AND FURTHER DEVELOPMENTS

6.1. Conclusions

Within the research framework of FRAMEBLAST project (experimental and numerical validation of blast load models and structural response of a typical frame building system under blast loading), the objective of the thesis was to investigate the structural identification and damage characterization of a full-scale building structure with structural deterioration and development of coherent scenarios. For this purpose, extensive experimental testing by the Bruel & Kjaer experimental modal analysis and advanced numerical finite element investigations were carried out.

- Experimental program to study the physical behavior of frame structure in the laboratory for calibration.
- Calibration, modelling, updating and correcting the model for extracting measured modal parameters.
- Experimental program for intake and damaged steel frame for measuring the change of physical behavior of steel frame in the laboratory.
- Experimental program of the full-scale building for undamaged and damaged condition.
- Modeling the longitudinal frame for best calibration of modal parameters.
- Parametric experimental study for the estimation of several parameters (natural frequency, damping ratios and mode shapes, displacement and acceleration) to study the influence on physical behavior of structures (strength, stiffness and modal mass).
- Damage characterization in full-scale building affected by blast are of high interest.
- The structural identification is a modern technique that links the changes in the dynamic properties of a system (e.g. building structural system) with a certain state of damage.
- When combined with properly calibrated numerical models, can be used for fast screening after a strong event and provide a deeper view of the damage.
- Minimizing the sources of uncertainty indicates better integrate analytical model simulation results in modal parameter identification process.
- Modal parameters estimation by the three-dimensional finite element software SAP2000 for both damaged and undamaged steel structural building.

The experimental program gives an active area of research related to the direct applications of modal parameters estimation to identify the health monitoring of structures in damaged conditions. Extensive vibration analyses were performed on the undamaged structure and

damaged structure. The experimental program presents the modal parameter identification and vibration-based damage detection of a full-scale building structure. The results obtained from the experimental method in experimental modal analysis study are focused on: (a) the effects of degree of uncertainties (noise, vibration, temperature, humidity etc.) during estimation of the identified modal parameters. A more effective means for mitigating these sources of uncertainty may be to better integrate analytical model simulation results and heuristics with the modal parameter identification process; (b) the process of selecting the DOFs used to derive the model of the testing; (c) the use of the method for the prediction of the response caused by excitation forces applied at different DOFs. The followings are the main conclusions from the study:

- To reduce the data errors, various data pre-processing techniques like inspection of the signals, time window selection, digital filtering, cross-correlation construction, exponential windowing, and data averaging in time or frequency domain had been developed.
- The measured values from experimental modal analysis has good correlation with the calculated values according to MAC factors derived from mode shapes and measurements. This means the modal characteristics of the frame considered can also be obtained successfully by experimentally with forced vibration tests.
- According to the frequency response synthesis diagram, the modal parameters from experimental test and calculated values has big influences on the structural identification/dynamic properties characterization.
- It is necessary to use the model updating process to find the closer values to the measurements.

The number of degree of freedom and the structural modeling is very important issue for modal parameters estimation. For the full-scale building, three different models were selected during experiment. The corner column of the building, the longitudinal frame in plane and out of plane were examined by experimental modal analysis. The results obtained by modal analysis are correlated, validated and updated by the three-dimensional finite element software SAP2000. The main outcomes from the parametric study are as following:

- The natural frequencies determined from experimental modal analysis and FEM are compared with each other. The parameters estimated from first 6 modes for the corner column in undamaged conditions have good agreements. The maximum difference of

the parameters is 4.88% for third mode and for the other modes result obtained from EMA and SAP is very close to each other. It means the physical properties are identified by EMA and SAP for intake structures are similar.

- Experimental modal parameters for the longitudinal frame (in plane) have the good relation with the finite element analysis results. The fifth bending mode has the maximum deviation is 4.27% and it is below 5%.
- Three-dimensional FEM analysis and experimental modal analysis were performed for the longitudinal frame out of plane also. Careful modeling of structural components in mitigating uncertainty from the analytical point of view, and produced good correlation between the results obtained from St-Id and experiment. FEM analysis results are helpful in judging the reliability of a field experiment, and integrating analysis and experiment together for understanding how is the actual behavior of structural systems. For the longitudinal frame (in plane), the errors between EMA and SAP is 4.77% for the fifth bending mode. It indicates the calibration for the frame was done properly. The other modes for external frame are also properly calibrated and the gap is below 5%.
- Significant change in the frequency for damaged initiations in longitudinal frame (out of plane). From the experimental results frequency has the maximum difference for 1st mode, the frequency is 16.91Hz and 19.49Hz in undamaged condition and damaged condition respectively. On the other hands, numerically this value is 15.37 Hz and 18.79 Hz for both conditions respectively. But after removing of secondary beam there is significant difference in frequency for undamaged and damaged conditions. In undamaged condition frequency is 226.66Hz but 177.56Hz for damaged condition in EMA for 4th mode. Numerically, also has big changes of frequency in the same mode. 222.96Hz and 193.49 Hz for undamaged and damaged condition respectively. Experimentally and numerically, the structural properties changed significantly for 6th mode. The frame is more flexible because of low frequency (334.18Hz and 277.30Hz respectively for both conditions). Except 1st, 4th and 6th mode all other modes have no big difference of frequency for both conditions in EMA and SAP2000. The 1st, 4th and 6th modes are affected more due to stability, stiffness and modal mass changes.

6.2. Recommendations for the further study

Some limitations were identified during the experimental modal parameters for structural identification because of the lack of module. The followings are the main issue can be done for the future study:

- The structural identification parameters need to be updated or corrected by automatic updating tools.
- The damage characterization can be done by the auto damage detecting module. During the service period of the structures, time to time health monitoring of the structure is very important for damage identification. The residual capacity of the damaged structures can be measured by the automatic damage identification module.
- There are some difficulties during the forced vibration testing. The number of DOFs and excitation locations, number of excitations, proper excitation of the structures, proper weight of the hammers and the environmental effects is a great deal for EMA. In that case, the operational modal analysis can be performed for assurance of actual excitation of the structure for estimating modal parameters in ambient conditions.
- There are other different methods except Bruel & Kjaer technique. The structural identification parameters can be estimated by other methods (e.g. ARTeMIS, 2D and 3D shear reference methods, Poly reference methods, Peak Picking, PolyMAX, and CMIF methods) and compare for better estimation.
- The influence of the change of mass and stiffness could not be distinguished when model calibration was conducted using modal data of the structure. The modal mass of the entire structure was considered constant and known in this study. However, modal data could be transformed into the modal flexibility and thus used as reference data for the updating. In this situation, the stiffness of the structure could be exclusively calibrated for better result. Another alternative will be to make use of static data such as static displacement and strain measurement. Besides, analytical model calibrated by static data will likely able to yield predictions of strain and stress at the critical areas of interest with more accuracy, which may be more desirable for applications such as fatigue monitoring and control.
- Non-visible damage can be identified after a certain service period of structure or blast actions. Local and global damage can be identified by measuring the stiffness at connections and structural elements for undamaged and damaged structure due to blast actions. Damage index can be the main parameters to detect the damage by comparing the limiting values.

REFERENCES

Abdurrahman Sahin and Alemdar Bayraktar, MATLAB for All Steps of Dynamic Vibration Test of Structures. Applications from Engineering with MATLAB Concepts; http://dx.doi.org/10.5772/63232; 2016.

A. Rytter, Vibration based inspection of civil structures, Ph.D. thesis, Dept. of Building Technology and structural engineering, Aalborg University, Aalborg, Denmark, 1993.

Ahmet Can Altunışık∗, Fatih Yesevi Okur, Volkan Kahya; Modal parameter identification and vibration-based damage detection of a multiple cracked cantilever beam; Engineering Failure Analysis 79 (2017) 154–170.

Aktan A, Brownjohn J. Structural identification: opportunities and challenges. Journal of Structural Engineering 2013;139: 1639–47.

Aktan, A. E., Farhey, D. N., Helmicki, A. J., Brown, D. L., Hunt, V. J., Lee, K. L., and Levi, A. (1997). "Structural identification for condition assessment: Experimental arts." Journal of Structural Engineering, 123(12), 1674-1684.

Alberto Barontini[a*], Maria-Giovanna Masciotto[a], Luis F. Ramos[a], Paulo Amando-Mendes[b], Paulo B. Lourenco[a]; An overview on nature-inspired optimization algorithms for Structural Health Monitoring of historical buildings; X International Conferences on Structural Dynamics, EURODYN 2017, 199(2017) 3320-3325.

Andres R. Perez, BAE/MAE, Penn State, Murrah Federal Office Building (April 19, 1995) 2009.

ASCE. (2011). 59-11 blast protection of buildings, Reston, Vibration Analysis.

Bakir PG, Reynders E, De Roeck G. An improved finite element model updating method by the global optimization technique coupled local minimizers. Computer Structure 2008;86: 1339–52.

Baker, W.E., Cox, P.A., Westine, P.S., Kulesz, J.J., and Strehlow, R.A. 1983. Explosion Hazards and Evaluation, Elsevier, New York.

Baroth J, Malecot Y. Probabilistic analysis of the inverse analysis of an excavation problem. Comp Geotech 2010;37(3):391–8.

Brewer, T. R., Crawford, J.E., Morrill, K.B., and Vonk, P.J., "Physics-based modelling, Testing, and Retrofit Development for Reinforced Concrete and Steel Columns Subject to

Contact and Near-contact Explosive Threats", for the 4th International Conference on Protective Structures (ICPS4), Beijing, China, October 18-21, 2016.

Brian J. Schwarz N. LARBI AND J. LARDIES; Experimental Modal Analysis of a Structure Excited by A Random Force; Mechanical Systems and Signal Processing (2000) 14(2), 181-192.

Bruel & Kjaer manual for experimental modal analysis. [Online] Available: https://www.bksv.com/en/Applications/product-vibration/structural-dynamics

Bruel & Kjaer manual for operational modal analysis. [Online] Available: https://www.bksv.com/-/media/literature/Product-Data/bp2567.ashx.

C. Kr. AAmer, C. A. M. de Smet and G. de Roeck 1999 Proceedings of IMAC 17, the International Modal Analysis Conference, Kissimmee, FL, U.S.A., 1023–1029. Z24 Bridge damage detection tests.

Çatbaş, F., Kijewski-Correa, T., and Aktan, A. (2013). Structural identification of constructed systems: Approaches, methods, and technologies for effective practice of St-Id, ASCE, Reston, Vibration Analysis.

Clarence W. de Silva. " Vibration and Shock Handbook, ISBN 0-8493-1580-8; Vibration and Shock Problems of Civil Engineering Structures, pp. 13-43.

Conte, J. P., He, X., Moaveni, B., Masri, S. F., Caffrey, J. P., Wahbeh, M., Tasbihgoo, F., Whang, D. H., and Elgamal, A. (2008). "Dynamic testing of Alfred Zampa memorial bridge." Journal of Structural Engineering, 134(6), 1006-1015.

Cunha, A., Caetano, E. & Delgado, R. “Dynamic Tests on a Large Cable-Stayed Bridge. An Efficient Approach”, Journal Bridge Engineering, ASCE, Vol.6, No.1, p.54-62, 2001.

D. Ewins, Modal Testing: Theory and Practice, Research Studies Press LTD., John Wiley & Sons Inc., Exester, 1984.

Deng L, Cai C. Bridge model updating using response surface method and genetic algorithm. Journal of Bridge Engineering 2009; 15:553–64.

Doebling, S.W.; Farrar, C.R.; Prime, M.B. A summary review of vibration-based damage identification methods. Shock Vibration Dig. 1998, 30, 91–105.

E. Peter Carden*, James M.W. Brownjohn; ARMA modelled time-series classification for structural health monitoring of civil infrastructure; Mechanical Systems and Signal Processing 22 (2008) 295–314.

Emilio Di Lorenzo[a, b, c*,] Simone Manzato[a], Bart Peeters[a], Francesco Marulo[b], Wim Desmel[c]; Structural Health Monitoring strategies based on the estimation of modal parameters; X International Conference on Structural Dynamics, EURODYN, Procedia Engineering 199 (2017) 3182-3187.

F. Dinu, "Experimental validation of the response of a building in frames subjected to explosion action - FRAMEBLAST", 2017-2018. [Online], Available:

https://www.ct.upt.ro/centre/cemsig/frameblast.htm.

F. Dinu, D. Dubina, I. Marginean and A. Kovacs, E. Ghicioi; Testing of a full-scale building under external blast; Department of Steel Structures and Structural Mechanics, Politehnica University Timisoara, Romania Laboratory of Steel Structures, Romanian Academy, Timisoara Branch, Romania.

Fontan M, Breysse D, Bos F. A hierarchy of sources of errors influencing the quality of identification of unknown parameters using a meta-heuristic algorithm. Computer Structure 2014; 139:1–17.

Fulvio Parisi; Claudio Balestrier and Domenico Asprone; Out-of-plane blast capacity of load-bearing masonry walls; 16th International Brick & Block Masonry Conference, at Padova, Italy; June 2016.

G. Acunzo a, N. Fiorini a, F. Mori a, D. Spina b, *; Modal mass estimation from ambient vibrations measurement: A method for civil buildings; Mechanical Systems and Signal Processing 98 (2018) 580–593.

Gaetan Kerschen - Jean-Claude Golinval; Experimental Modal Analysis, 2010.

Ibsen, Lars Bo; Liingaard, Morten; Experimental modal analysis; Aalborg: Department of Civil Engineering, Aalborg University. (DCE Technical Reports; No. 10).

Islam M. Ezz El-Arab; Strengthening of existing security buildings against vehicle bomb using fluid viscous dampers, in Egypt; Journal of Civil Engineering and Construction Technology; Vol. 7(5), pp. 37-47, October 2016: DOI: 10.5897/JCECT2016.0413.

J. Zhang, Ph. D[1]; J. Prader[2]; K. A. Grimmelsman, A.M. ASCE[3]; F. Moon[4]; A. E. Aktan, M. ASCE[5]; and A. Shama, Ph.D., P.E., M. ASCE[6], Experimental Vibration Analysis for Structural Identification of a Long-Span Suspension Bridge; American Society of Civil Engineers. DOI: 10.1061/(ASCE)EM.1943-7889.0000416(2013).

J. B. Hansen [a*], R. Brincker[b], M. López-Aenlle[c], C.F. Overgaard[a], K. Kloborg[a]; A new scenario-based approach to damage detection using operational modal parameter estimates; Mechanical Systems and Signal Processing 94 (2017) 359–373.

J. M. W. Brownjohn[a], Filipe Magalhaes[b], Elsa Caetano[b], Alvaro Cunha[b]; Ambient vibration re-testing and operational modal analysis of the Humber Bridge, Engineering Structures 32 (2010) 2003-2018.

Jia. He [a, b, n], You-Lin Xu [a], Sheng Zhan [a], Qin Huang [c]; Structural control and health monitoring of building structures with unknown ground excitations: Experimental investigation; Journal of Sound and Vibration 390(2017) 23–38.

Kijewski-Correa, T., and Kareem, A. (2007). "Monitoring serviceability limit states in civil infrastructure: Lessons learned from the Chicago full-scale monitoring experience." Proceedings of 6th International Workshop on Structural Health Monitoring, Palo Alto, CA.

Loendersloot R, Ooijevaar T. H, Warnet L. L, de Boer A. Vibration based structural health monitoring in fiber reinforced composites employing the modal strain energy method, Third international conference on integrity reliability and failure Porto, CD paper S1122; 2009, p. 16.

M. Hassan Haeri, Alireza Lotfi, Kiarash M. Dolatshahi∗, Ali Akbar Golafshani; Inverse vibration technique for structural health monitoring of offshore jacket platforms, Applied Ocean Research 62 (2017) 181–198.

M. Molinari[1*], A. T. Savadkoohi[1], O. S. Bursi[1], M. I. Friswell[2] and D. Zonta[1]; Damage identification of a 3D full scale steel–concrete composite structure with partial-strength joints at different pseudo-dynamic load levels; Earthquake Engineering and Structural Dynamics; Earthquake Engineering Structure Dynamics. 2009; 38:1219–1236.

Marwala T. Finite-element-model updating using computational intelligence techniques. Springer; 2010.

Mustapha Dahak[a*], Noureddine Touat[a], Noureddine Benseddiq[b]; On the classification of normalized natural frequencies for damage detection in cantilever beam; Journal of Sound and Vibration 402(2017) 70–84.

N. Larbi and J. Lardies; Experimental Modal Analysis of a Structure Excited by a Random Force; Mechanical Systems and Signal Processing (2000) 14(2), 181-192.

Peter; Experimental modal analysis (A simple non-mathematical presentation); Modal analysis and control laboratory, Mechanical engineering department, University of Massachusetts Lowell, USA.

Peeters B, De Roeck G. Reference-based stochastic subspace identification for output-only modal analysis. Mechanical System Signal Process 1999;13(6):855–78.

R. Cantieni; Experimental Methods Used in System Identification of Civil Engineering Structures, 2nd Workshop: Problem of vibrational structure civil engineering construction Mechanic Perugia, 10-11 Giugno 2004.

Romain Pasquier*, Ian F.C. Smith; Iterative structural identification framework for evaluation of existing structures; Engineering Structures 106 (2016) 179–194.

Ruqiang Yan [a], Robert X. Gao[b], Li Zhang[c]; In-process modal parameter identification for spindle health monitoring; Mechatronics 31 (2015) 42–49.

S. J. Dyke, D. Bernal, J.L. Beck, C. Ventura, Experimental phase of the structural health monitoring benchmark problem; Proceedings of the 16th Engineering Mechanics Conference, ASCE, Reston, VA, 2003.

S. Nagarajaiah[1] and B. Basu[2], Output only modal identification and structural damage detection using time frequency & wavelet techniques. Earthquake Engineering & Engineering Vibration (2009) 8: 583-605.

Schlune H, Plos M, Gylltoft K. Improved bridge evaluation through finite element model updating using static and dynamic measurements. Engineering Structures 2009;31(7):1477–85.

SUSCOS_M European Erasmus Mundus Master [Online]. http://steel.fsv.cvut.cz/suscos/index.htm

T. H. Ooijevaar*, R. Loendersloot, L.L. Warnet, A. de Boer, R. Akkerman; Vibration based Structural Health Monitoring of a composite T-beam; Composite Structures 92 (2010) 2007–2015.

Timothy Kernicky[a], Matthew Whelan[a*], Usman Rauf[b], Ehab Al-Shaer[b]; Structural identification using a nonlinear constraint satisfaction processor with interval arithmetic and contractor programming; Computers and Structures 188 (2017) 1–16.

Timothy M. Whalen. The behavior of higher order mode shape derivatives in damaged, beam-like structures. Journal of Sound and Vibration 309 (2008) 426–464.

Török, Zoltán; Ozunu, Alexandru; Hazardous Properties of Ammonium Nitrate and Modeling of Explosions using TNT Equivalency; Environmental Engineering & Management Journal (EEMJ). Nov 2015, Vol. 14 Issue 11, p 2671-2678. 8p.

W. M. West, Illustration of the use of modal assurance criterion to detect structural changes in an orbiter test specimen, in: Proceeding Air Force Conference on Air Craft Structural Integrity,1984, pp.1–6.

Wei-Xin Ren and Zhou-Hong Zong; Output-only modal parameter identification of civil engineering structures; Structural Engineering and Mechanics, Vol. 17, No. 3-4 (2004).

Wei-Xin Ren[a, b, *], Xue-Lin Peng[a], You-Qin Lin[a]; Experimental and analytical studies on dynamic characteristics of a large span cable-stayed bridge, Engineering Structures 27 (2005) 535–548.

Wikipedia, “Progressive collapse”, 2005. [Online]. Available: https://en.wikipedia.org/wiki/Windsor_Tower_(Madrid).

Wikipedia, “Russian apartment bombings”, 1999. [Online]. Available: https://en.wikipedia.org/wiki/Russian_apartment_bombings#Overview.

Wikipedia, “Russian apartment bombings”, 1999. [Online]. Available: Wikipedia, “World trade centre bombings”, 2001. [Online]. Available: https://en.wikipedia.org/wiki/September_11_attacks

Wikipedia, “Progressive collapse of a steel-framed building”, 1966. [Online]. Available: https://en.wikipedia.org/wiki/Progressive_collapse#cite_note-3.

Wikipedia, “Steel frame collapse”, 1996. [Online]. Available: https://en.wikipedia.org/wiki/Steel_frame.

Wikipedia, “Sudden collapse due to vibration of machinery”, 2013. [Online]. Available: http://www.bbc.co.uk/news/world-asia-22394094.

Wikipedia, “U.S embassy bombings”, 1998. [Online]. Available: https://en.wikipedia.org/wiki/1998_United_States_embassy_bombings.

Woodson, S.C. 1993. Response of slabs: in plane forces and shear effects. In Structural Concrete Slabs under Impulsive Loads, T. Krauthammer, Ed., pp. 51 – 68. Research Library, U.S. Army Engineer Waterways Experiment Station, Vicksburg, MS.

Xuan Kong, Chun-Sheng Cai * and Jiexuan Hu; The State-of-the-Art on Framework of Vibration-Based Structural Damage Identification for Decision Making; Applied science. 2017, 7, 497; doi:10.3390/app7050497.

Yarnold M, Moon F, Aktan A. Temperature-based structural identification of long-span bridges. Journal Structural Engineering 2015;141(11):04015027.

ANNEXES

ANNEX-A

A. Bruel & Kjaer Experimental Modal Analysis

A.1. Introduction

The natural frequency of structure is directly related to the excitation of the structure. The response of the component measures by the excitation. Modal analysis is a process of identifying the modal parameters (frequency, damping and mode shape). Modal parameters describe the dynamic characteristics of the structures. Vibration and noise is vital factor for the dynamic design of the structural components. This vibration and noise also depends on the natural frequency and mode shapes of the structures. Basically, the structures are very prone to vibration such as tall buildings, long span bridge, wind turbine, offshore structures, automotive structures, aircraft structures, spacecrafts and computers etc. are designed and validated for modal analysis.

The response is practically measured by the frequency response function (FRF). The frequency response function is measured by the applied force and response of the structural component after applying force. The component how behaves after applied force or excitation at the same time of application. Basically, the dynamic properties indicate the measurement of displacement, velocity or acceleration. Fast Fourier Transform Algorithm analyzer is strong tool that consists of measurement of time data and frequency data shown in Figure A.1.

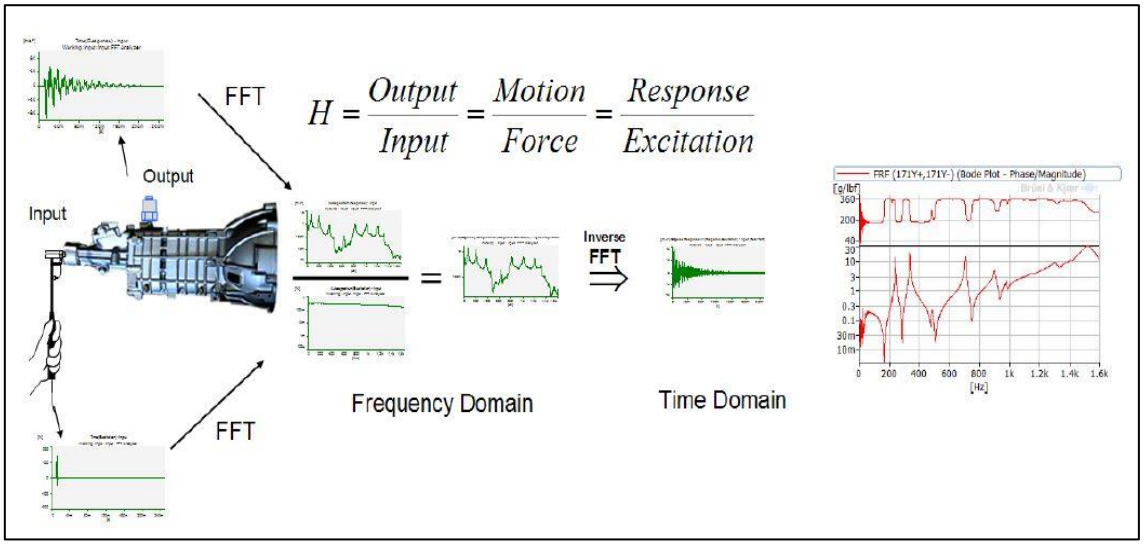

Figure A.1: Frequency response function for frequency domain and time domain

[Bruel & Kjaer manual: Access code: 636 832 431; 2017].

The response of the structure is measured by exciting either by hammer or shaker. Theoretically, shaker excitation and hammer excitation is similar but practically there are important distinction in case of forming matrix. An impact test generally results in measuring one of the rows of the frequency response function matrix whereas the shaker test generally results in measuring one of the columns of the frequency response function matrix.

The basic difference of hammer excitation and shaker excitation is to use accelerometers and hammer tip. In the shaker excitation, the weight of accelerometers is very less compare to the weight of whole structure. In that case, many numbers of accelerometers used and moving of this accelerometers around the structure to get the actual response. In hammer excitation, the most important factor is to tip the hammer exactly. The output response is totally depending on the input excitation frequency. The input excitation frequency depends on the hardness of hammer tip. The wider frequency range indicates the excitation of all modes of the component. If the tip is harder, it means all modes are excited and coherence function is clear enough shown in Figure A.2. On the other hands, soft or insufficient tip of hammer never shows the better coherence function shown in Figure A.3.

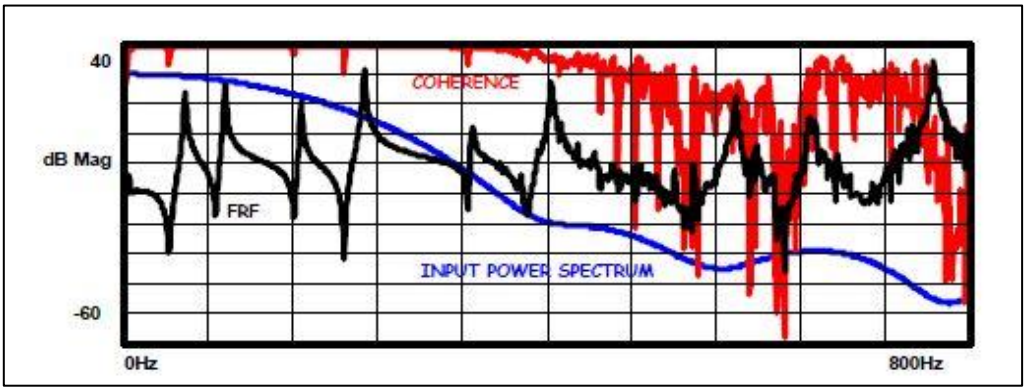

Figure A.2: Hammer tip is not sufficient to excite all modes [Peter. 2017].

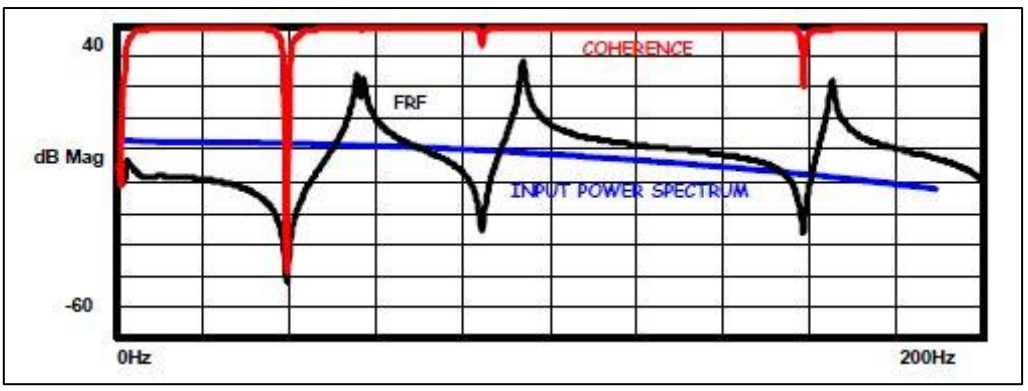

Figure A.3: Hammer tip is sufficient to excite all modes [Peter. 2017].

Impact window for the transducer depends on the damping of the structures. Lightly damped structures, the response of the structure due to the impact excitation will not die down to zero by the end of the sample interval. Signal processing by the hammer excitation is also affected by the signal leakage. The leakage can be reduced by the response weighting function measurement properly. The response weighting is obviously measured by the FFT analyzer and exponentially decaying window shown in Figure A.4.

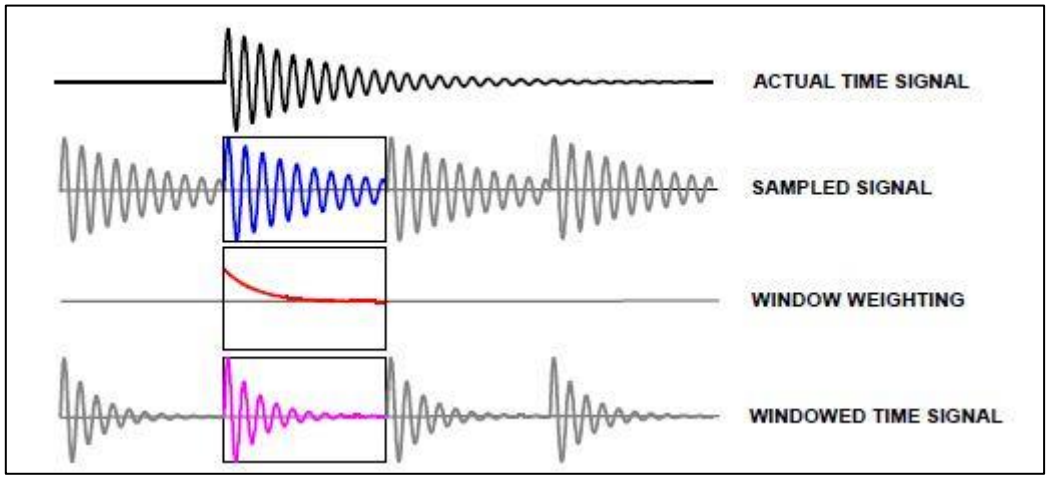

Figure A.4: Exponential window to minimize leakage effects [Peter. 2017].

Dynamic parameters (frequency, damping and mode shape) is used to design almost all types of civil and mechanical structures. Only understanding and visualization of mode shapes are not effective for the design process. But it helps to find the lacking of design and the area where improvement is really essential. The design and simulation of the design by the advance modal model and also by structural dynamic modification. The physical properties of the structure depend on modal data (frequency, damping and mode shape). To measure the physical changes, modal parameters modification to achieve a suitable set of design changes. The use of modal model by correlation and correcting the modal parameters by the finite element model. The behavior of the structure depends on the operating data. Operating data is the actual information to describe the structural behavior. Modal parameters measurement by the finite element model for finding the eigenvalues, damping and eigenvectors. In experimentally, modal parameters are the identification of natural frequency, damping ratio and mode shape.

A.2. Importance of modal testing and analysis

- Troubleshooting to reduce the excessive vibration levels.
- FE model validation and updating
    - Validation by testing on prototype
    - Refinement through inclusion of damping
    - To ensure resonances are away from excitation frequency
    - Prerequisite in aircraft industry
    - To use in automotive industry
- Structural assembly analysis to predict dynamic behavior of assembled sub-components.
- Determination of forces and response to complex excitation.

The dynamic properties change to minimise the resonance problems. The changes can be done by changing mass, stiffness, introduce tuned absorber and make sensitivity analysis.

A.3. Detailed procedure for modal testing and analysis

The complete set of measurement of modal parameters by Bruel & Kjaer analysis shown in Figure A.5. Basically, four steps to measure modal parameters: first step is to set the instrumentation for measuring the signal. Second step is to measure the signal by hammer, shaker and ambient excitation. Third step is to analyze the response function by the experimental modal analysis to identify the basic modal parameters. In this step, analysis, modification and interpretation by different curve fitting. Final step is to validate the modal parameters for best performance by modal assurance criteria (MAC), phase scatter and synthesis diagram.

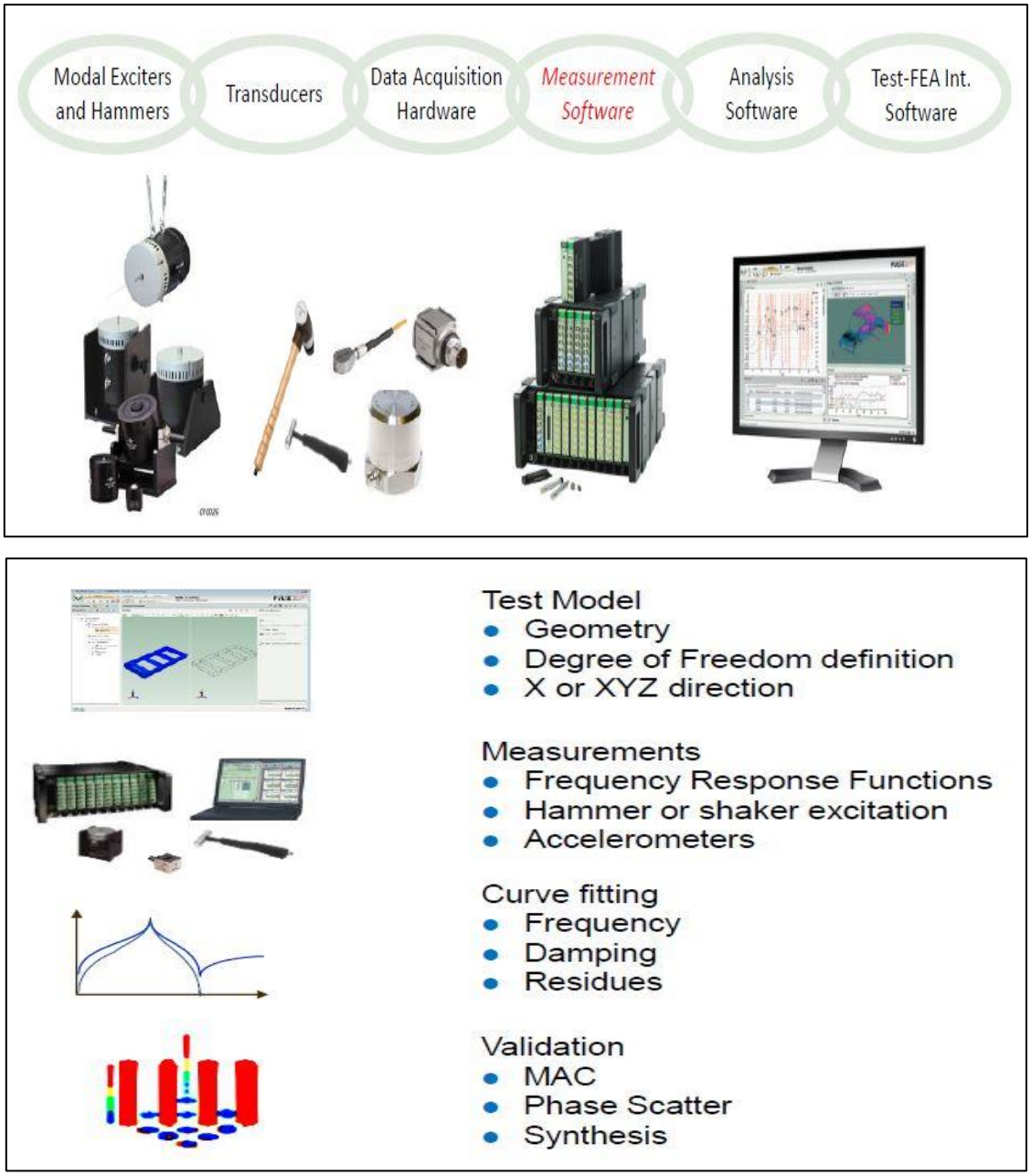

Figure A.5: The complete measurement and analysis chain [Bruel & Kjaer manual: Access code: 636 832 431; 2017].

A.4. Data recording by MTC hammer testing

Modal Test Consultant (MTC) is PULSE™ applications is the tool to measure the dynamic response. The time requirements for the measurement is reduced dramatically and to perform the dynamic measurement. MTC is to use the modal analysis by excitation of the structures either by hammer excitation or shaker excitation. Operational modal analysis for ambient excitation of structure, hammer excitation and shaker excitation based on the output only

measurement. Frequency Response Functions directly depend on in MTC. For both Structural Dynamic Test Consultants, the data generated (time, spectra, geometry and DOF information) can be used directly by leading post-processing packages. Main steps need to complete the measurement of response signal are described in below.

A.4.1. Step 1- project information

Two main options are to measure the response. Hammer can be fixed in one position or accelerometers can be fixed in one position. Most practical option is to rove the hammer in different locations and accelerometers are positioned at some fixed locations. But for the complex structure hammer is fixed in one point and accelerometers are roved location to location. It is difficult to excite the structure for the complex shape of the structure.

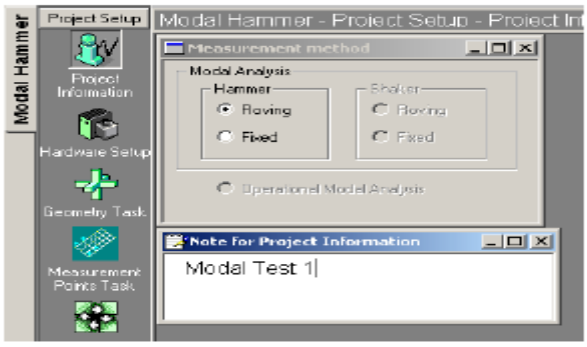

Figure A.6: Modal hammer project set up.

A.4.2. Step 2-hardware setup

Accelerometers and hammer or shaker are positioned at the specific point selected by the users. It is very important to detect the PULSE according the exact serial number of channel in the LAN-XI signal processing device. Pulse normally detects automatically detects whether or not the connected data acquisition equipment matches the saved configuration. Before each measurement set up PULSE is detected by configuring the device.

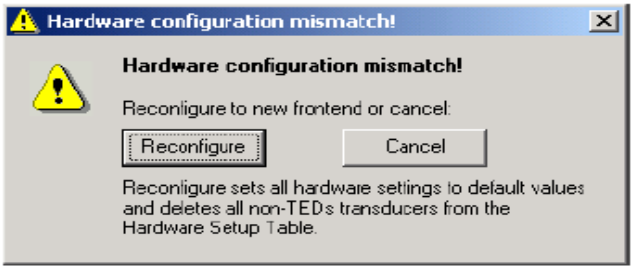

Figure A.7: Hardware set up.

Accelerometers and cable need to calibrate before recording. To minimize the recording duration and error in measurement Transducer Electronic Datasheets (TEDS) used in Bruel & Kjaer transducers. Clear and Detect HW clears all transducer data (TEDS and non-TEDS), detects new data-acquisition hardware, and automatically configures TEDS transducers.

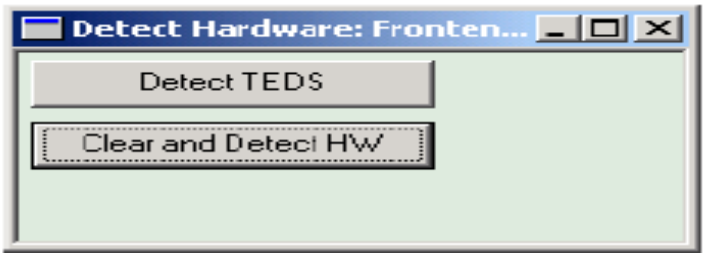

Figure A.8: TEDS selection.

According to the serial number of the position of accelerometers on the structures it is need to manually configure a channel in the MTC software. Transducer type, transducer name, transducer number, transducer family either force or accelerometers is configured in the hardware set up section.

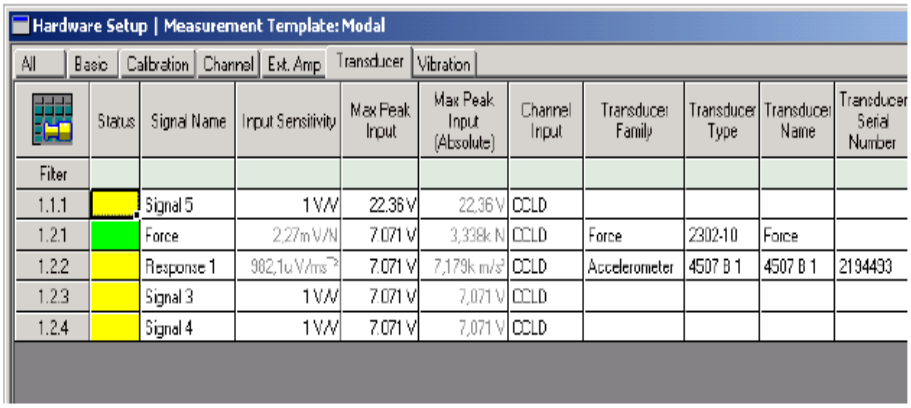

Figure A.9: Transducer selection (accelerometers and hammers).

A.4.3. Step 3-geometry

Geometry is needed to measure the signal and positioning of accelerometers and hammer on the geometry according to the practical structures/frame. Two main ways to create geometry in MTC. Geometry can be drawn directly in MTC or can be exported from Auto Cad or FEM software SAP2000.

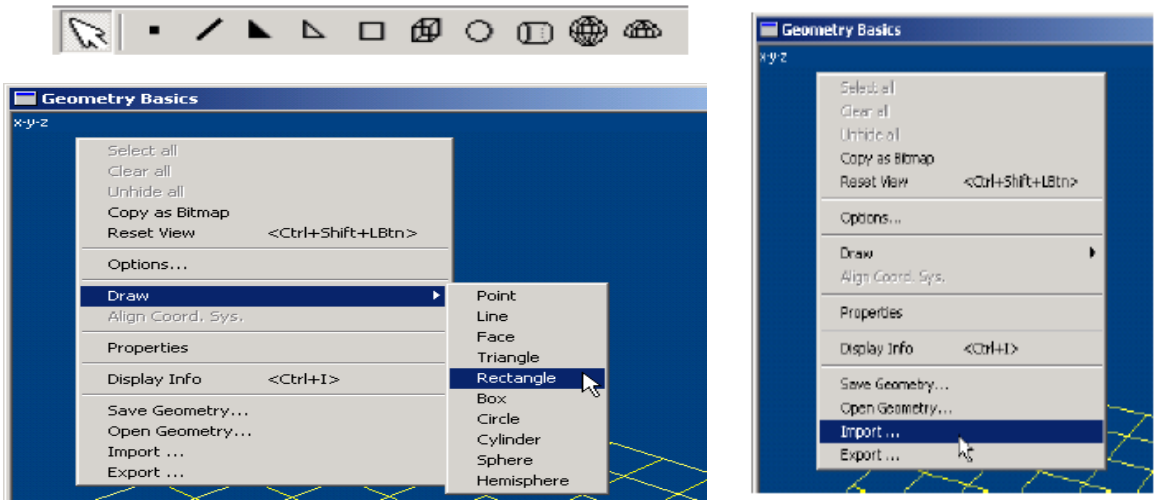

Figure A.10: Geometry import.

A.4.4. Step 4-measuring point task

The transducer list window contains the force and accelerometers defined in the hardware setup task. To assign the accelerometers and hammer on the exact point of the structure from the transducer list measuring task is important. The sequence of the points can be modified in the next task. The direction of a uniaxial transducer is selected from DOF list and then change the measurement axis either in positive or negative X, Y and Z direction. The positioned of transducers is shown in the figure below.

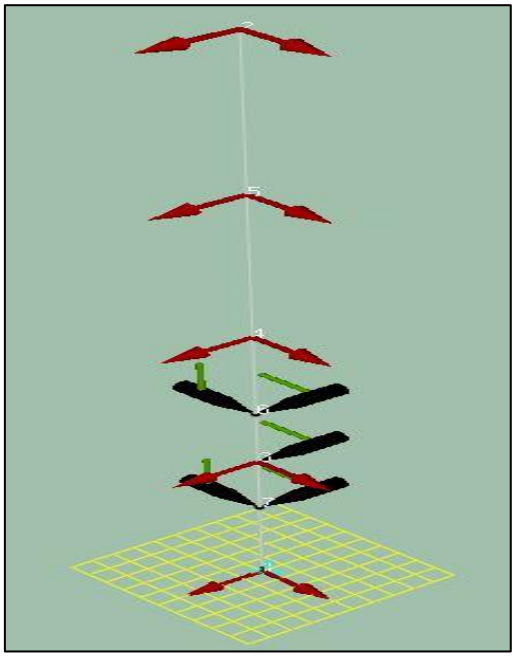

Figure A.11: Positioning of accelerometers and hammers.

A.4.5. Step 5-measurement sequence task

In the measurement sequence, a complete measurement plan is found. For each measurement, both excitation and response point and direction are indicated. The sequence is editable by the changing point numbers for a measurement.

A.4.6. Step 6-analysis setup

The measuring time is fixed from this section by selecting line numbers and span of frequency. The average number of measurement can be fixed by user.

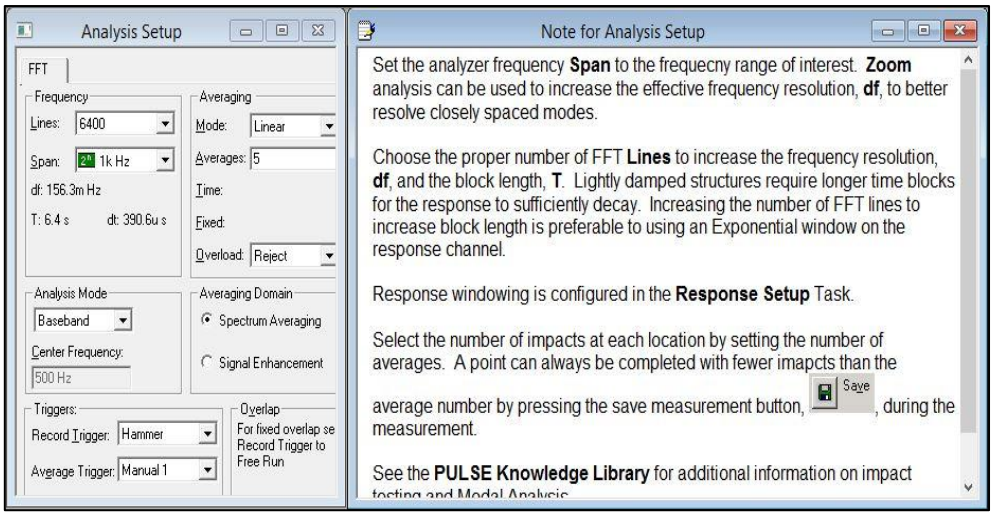

Figure A.12: Analysis set up.

A.4.7. Step 7-double hit detector

When the structures are excited by hammer, detection of double or proper hit is very much essential. If it is not proper hit then measurement will not be exact. It also indicates the presence of noise that hampers the accurate measurement. Acceptable limit of noise can be adjusted for getting exact measurement. Proper hit selection and proper hit properties can be checked by adjusting the sufficient frequency.

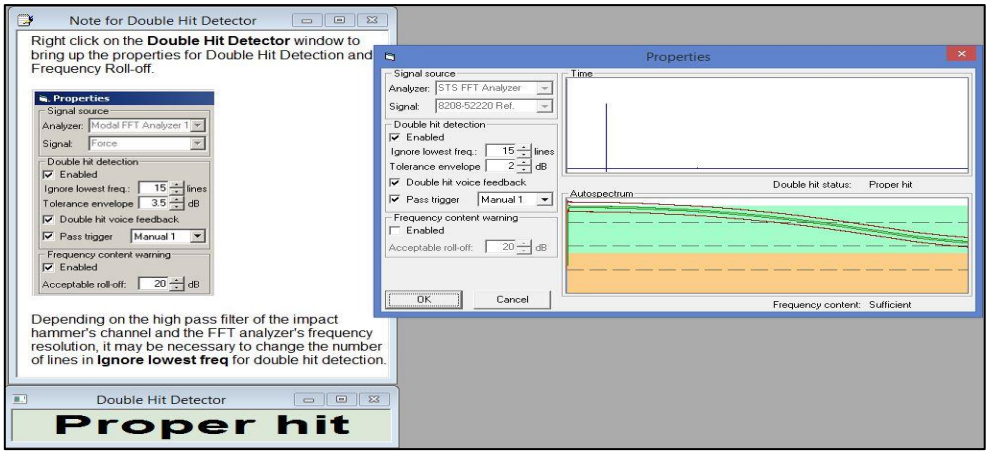

Figure A.13: Double hit detection.

A.4.8. Step 8-hammer trigger

First step to measure the response signal hammer trigger is fixed. Before starting the measurement, it is initialized. After initialized the measurement start by clicking start for hammer trigger if it is proper hit then okey. If the hit or measurement is not proper, need to repeat the procedure.

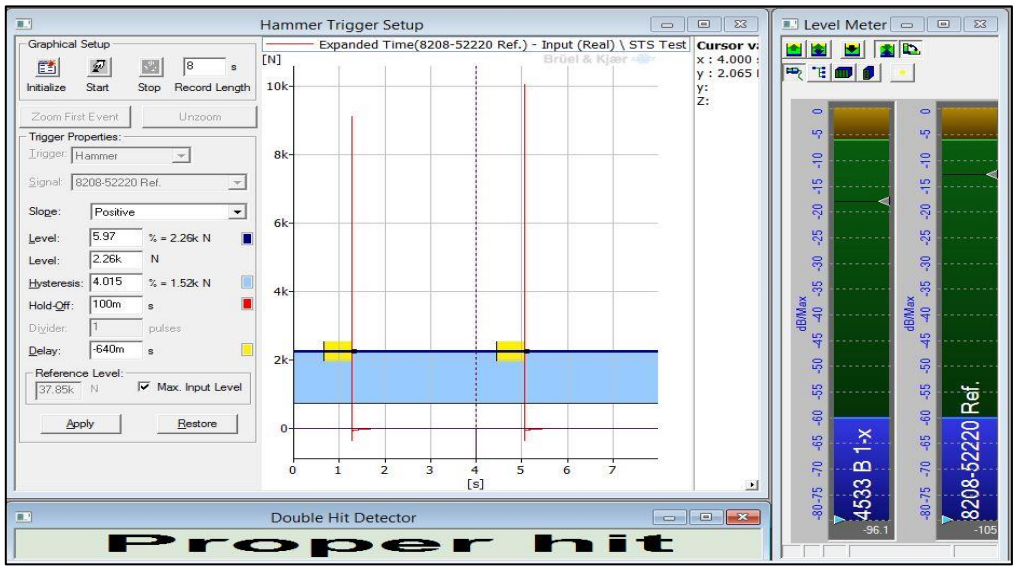

Figure A.14: Hammer trigger.

A.4.9. Step 9-hammer weighting

Hammer weighting is very important to excite all modes. Hammer excitation need to proper by uniform/exponential or transient. After initialized the measurement start by clicking start

for hammer trigger if it is proper hit then okey. If the hit or measurement is not proper, need to repeat the procedure.

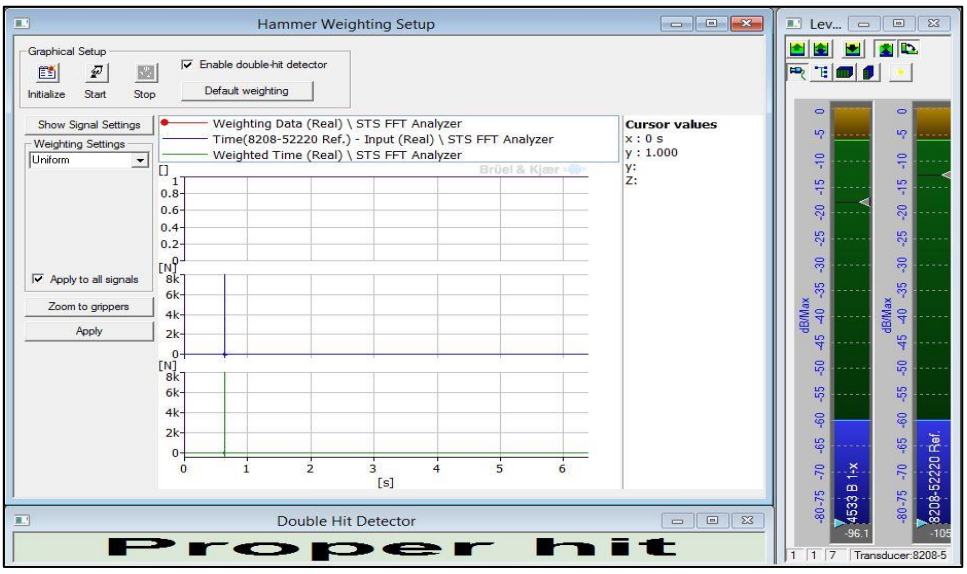

Figure A.15: Hammer weighting.

A.4.10. Step 10-response weighting

Response weighting is the variation of acceleration with respect to time. The acceleration response depends on the hammer tip. The harder the tip of hammer the wider the response of weighting. The softer the tip of hammer the less wide the response of weighting. If the response weighting is wider then it is able to excite the all modes. After initialized the measurement start by clicking start for hammer trigger if it is proper hit then okey. If the hit or measurement is not proper, need to repeat the procedure.

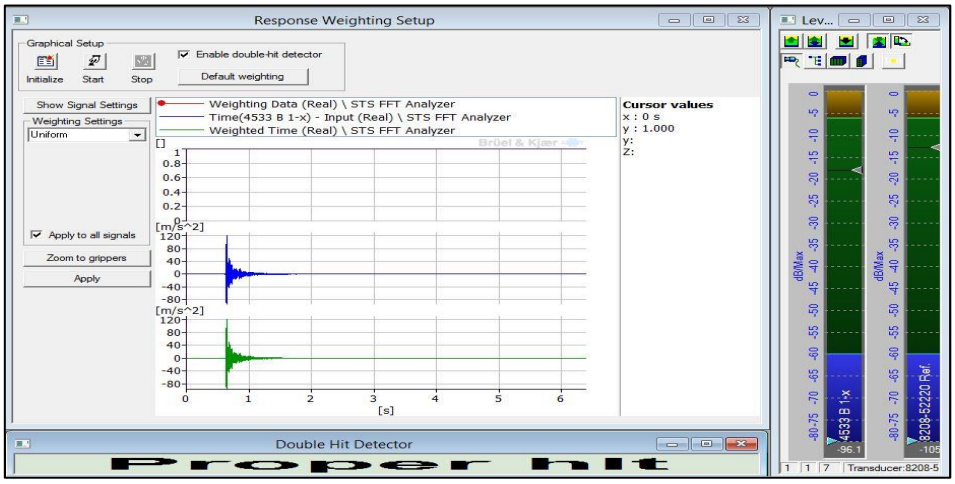

Figure A.16: Response weighting.

A.4.11. Step 11-measurement

Most important step to measure the frequency response. The number of DOF depends on the number of reference transducer. The measurement of each DOF is performed one by one. Before starting all measurements are initialized and the and start the measurement for proper hit. If the hit is not proper then measurement can be undo for start again from the beginning.

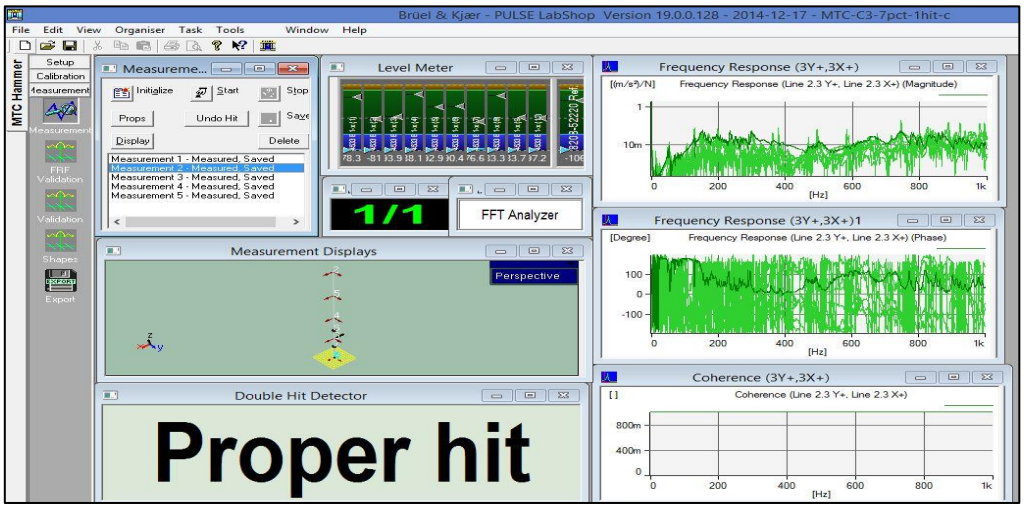

Figure A.17: Frequency response function.

A.4.12. Step 12-FRF Validation

Frequency response function is validated for initial mode shapes. The animation of initial mode shapes also can be seen for visualization.

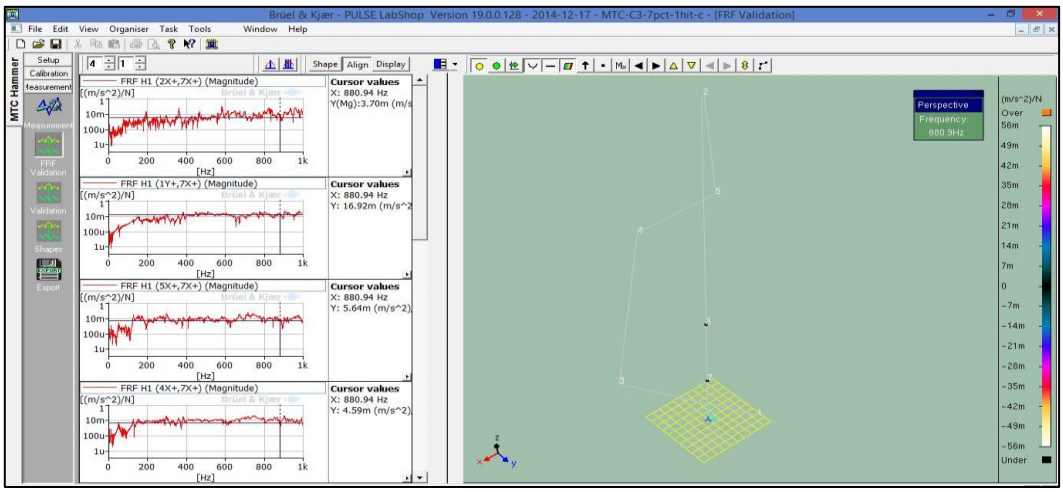

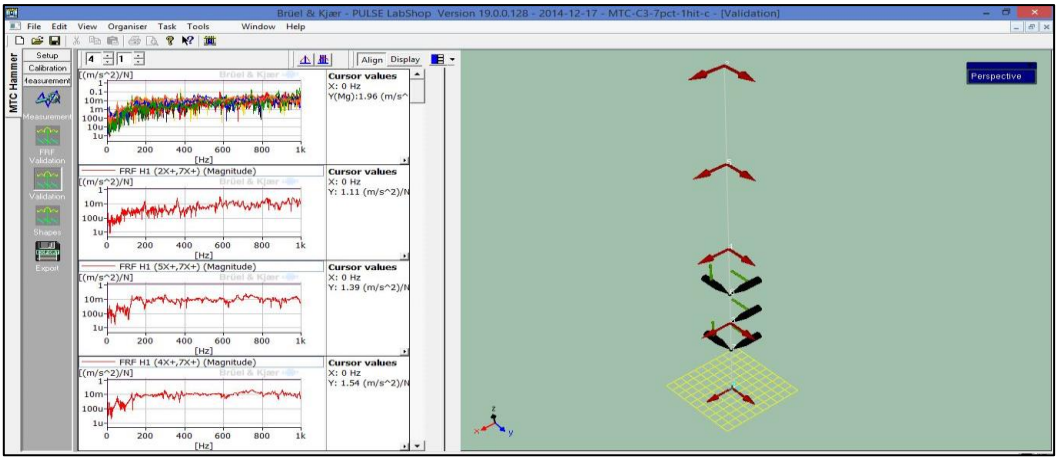

Figure A.18: Frequency response function validation.

A.4.13. Step 13-Geometry and response spectrum exporting

The geometry and response spectrum from MTC is used for identifying the exact mode shapes and modal parameters by Bruel & Kjaer experimental modal analysis. In experimental modal analysis generally, ASCII exported files is supported for next step. Frequency response function H1 is exported from MTC measurement.

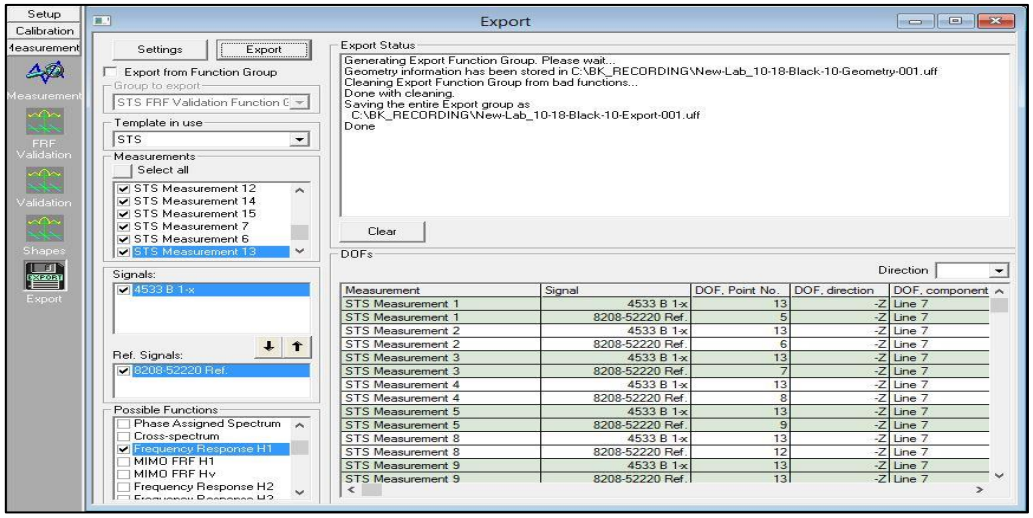

Figure A.19: Frequency response function exporting.

A.5. Pulse Reflex Modal Analysis: Bruel & Kjaer Experimental Modal Analysis

A.5.1. Step 1-analysis (measurement validation)

Experimental modal analysis is a post processing step to get the exact mode shapes and modal parameters. This method starts after getting the response functions spectrum and geometry

from MTC. Basically, this method consists of main four steps to identify modal parameters. Modern and intuitive user interface and workflow modal analysis in just four main steps: Measurement validation; Parameter estimation setup; Mode selection and Analysis validation.

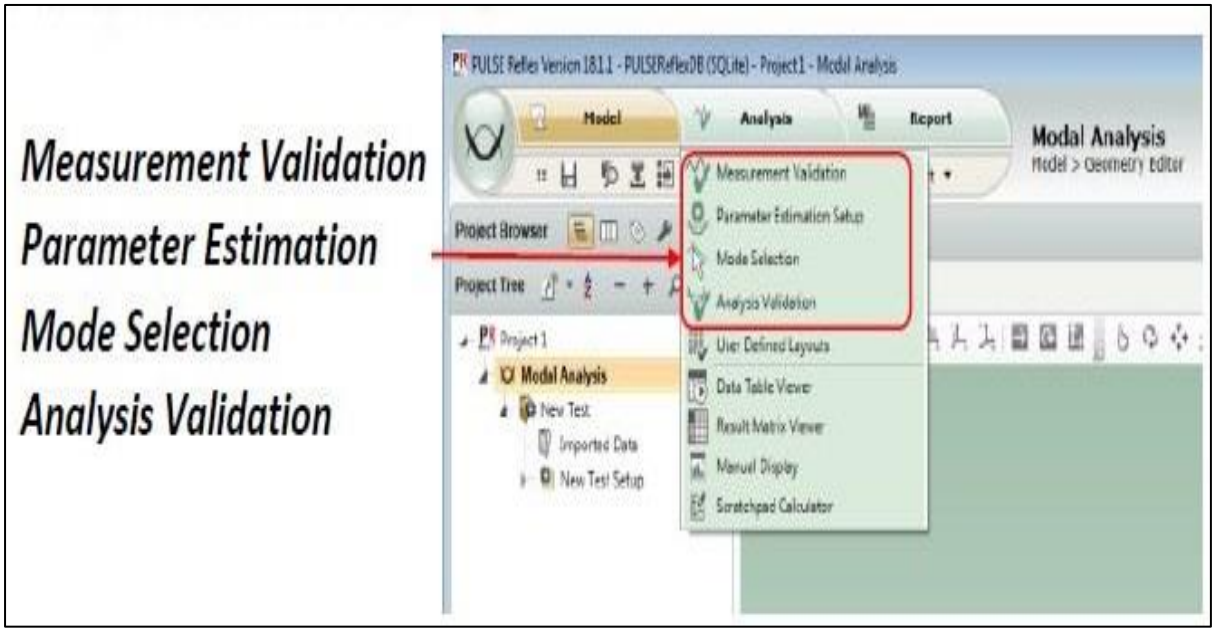

Figure A.20: Bruel & Kjaer: Pulse reflex modal analysis steps [Bruel & Kjaer manual: Access code: 636 832 431; 2017].

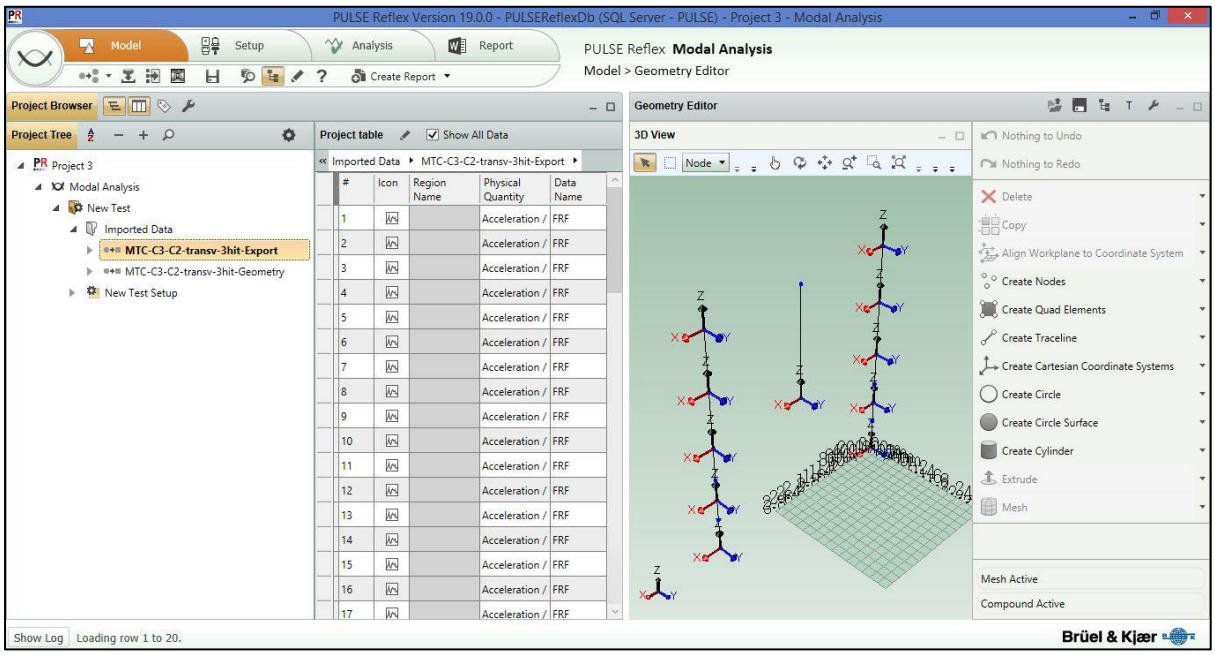

Figure A.21: Frequency response function imported for EMA.

In this step, the response spectrum and geometry are imported from MTC measurement. After importing the data, the mode shape, and function animation can be seen. The different deflected shape can be seen for different FRF.

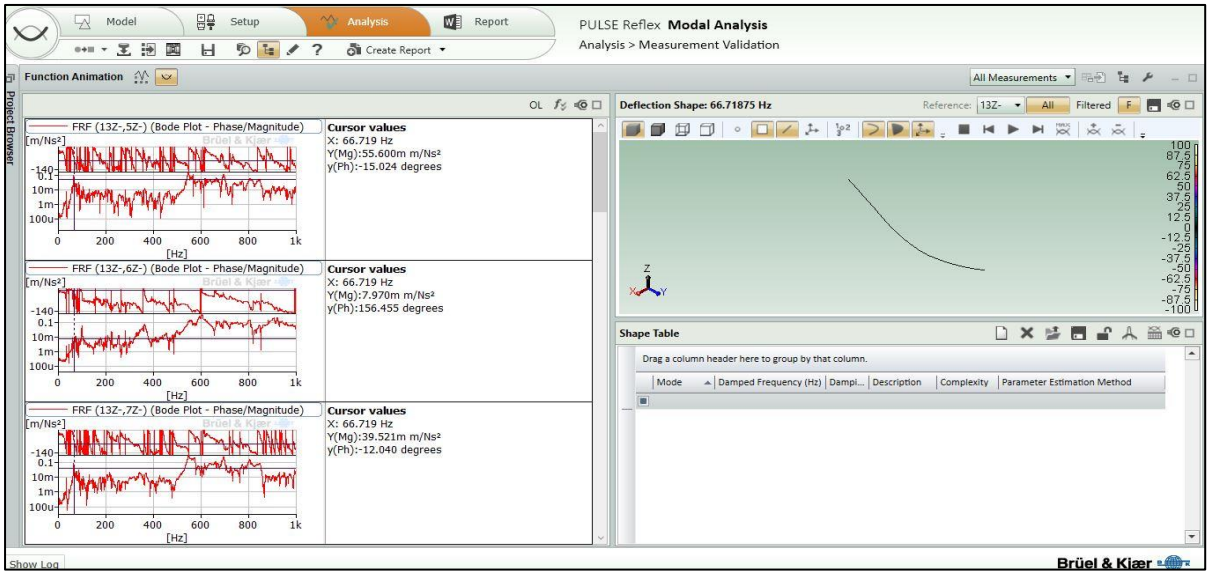

Figure A.22: Frequency response function measurement validation by EMA.

A.5.2. Step 2-analysis (parameter estimation setup)

The modal parameters depend on the range of frequency and multi- modal identification factor (MMIF) and frequency response function (FRF) are responsible for selecting modes manually by the user is shown in figure below. The mode number is computed by the rational function polynomial method for 100 number of iterations. In the mode iteration process, some modes are stable and some are unstable. Red line indicates the stable mode which is selected by auto selection process.

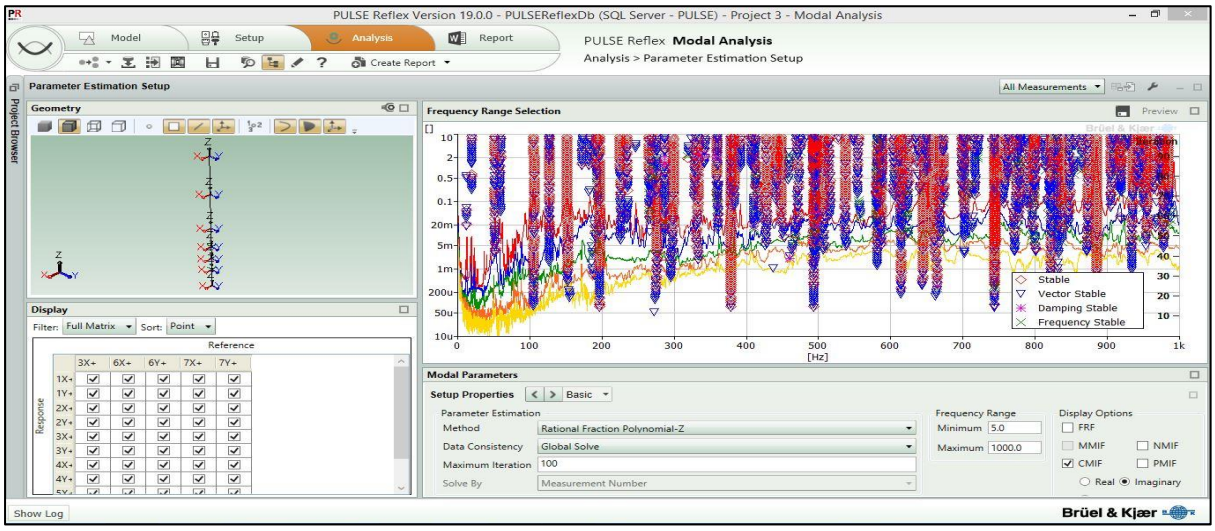

Figure A.23: Frequency span for EMA for full scale building frame.

A.5.3. Step 3-analysis (mode selection)

There are lot of numbers of mode present in this section depending on the span of frequency and number of iterations. All modes are not stable and only stable modes can indicate the reliable modal parameters. Auto selection of modes instead of manual selection show better performance of the modal parameters estimation.

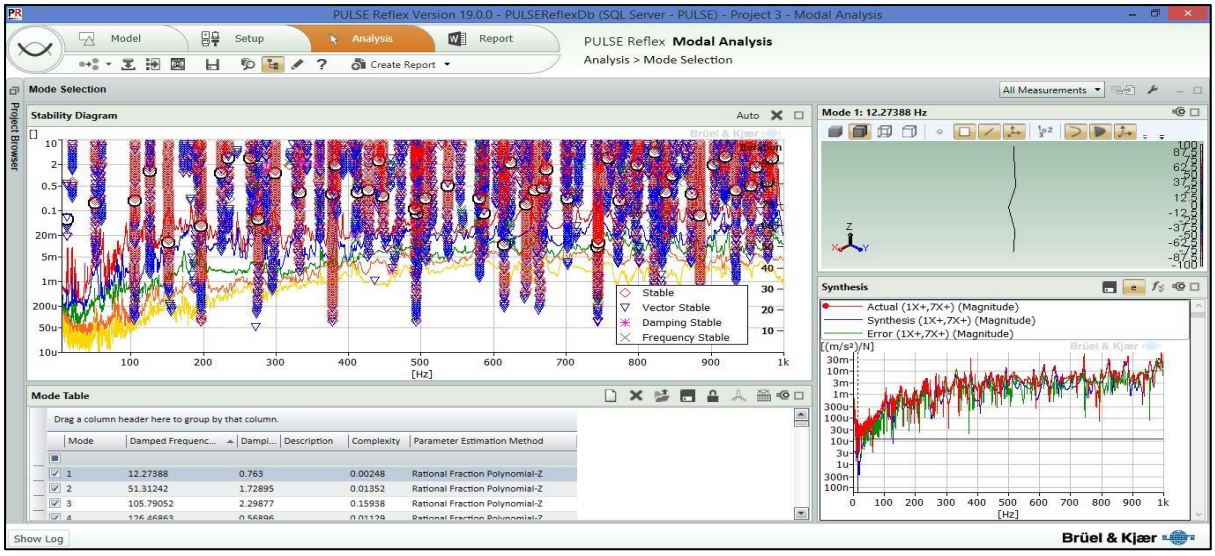

Figure A.24: Singular value stability diagram for EMA.

A.5.4. Step 4-analysis (analysis validation)

In this step analysis validation is consisted of 5 tools to validate the analysis result.

A.5.4.1. Step 4.1-analysis (analysis validation-animation)

Mode shape can be animated and visualized by selecting any mode from mode table. One or two modes can be compared by selecting them.

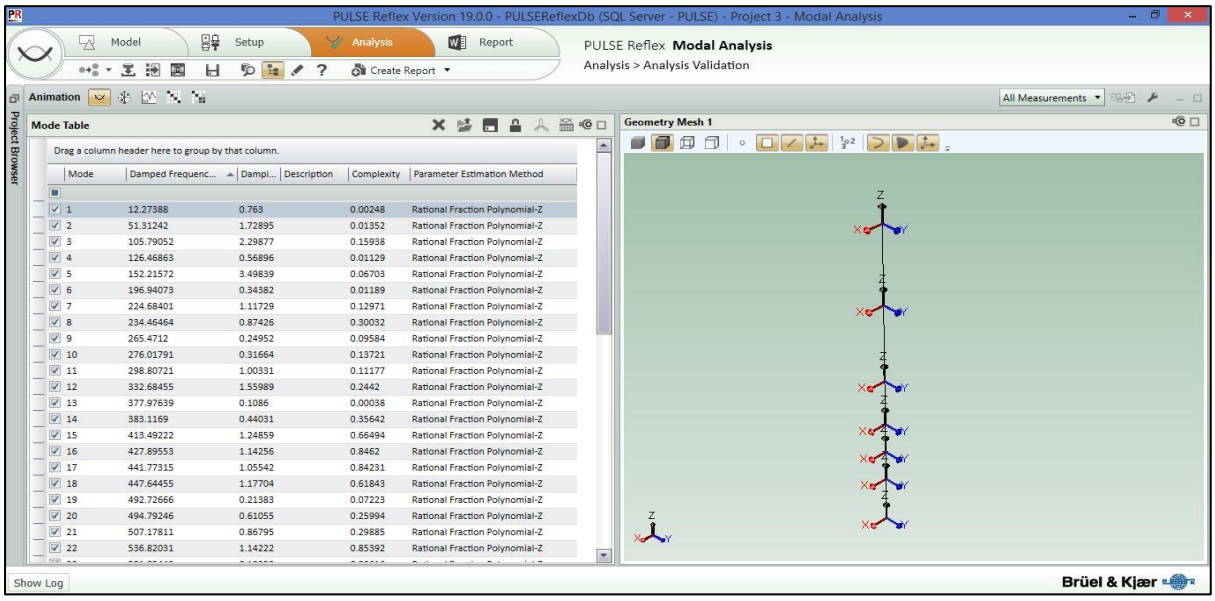

Figure A.25: Mode animation for EMA.

A.5.4.2. Step 4.2: analysis (analysis validation-mode normalization-complexity)

The complexity diagram shows each DOF the amplitude and phase in a polar plot. For a pure normal mode, all the DOF are either in phase or out of phase (-180 deg). Noise mode or poor FRF data would results in a random spread of phase and amplitude.

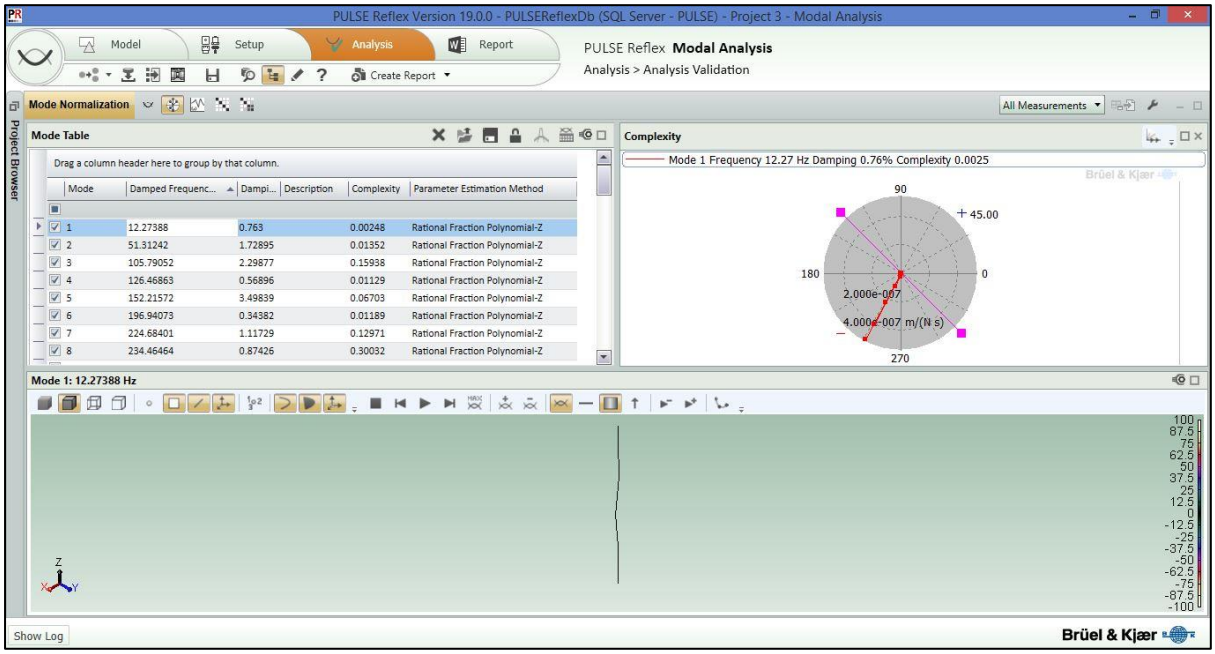

Figure A.26: Mode normalization for EMA.

A.5.4.3. Step 4.3: analysis (analysis validation-FRF synthesis)

The synthesis curve is one of most powerful tool to extract the exact modes from data interpretation. The synthesis curve and actual curve should match with each other if the iteration and data interpretation is performed properly. The more errors the more indication of inaccurate mode selection. The mode table and synthesis diagram are show in this section. Any mode is needed to select or deselect for better interpretation.

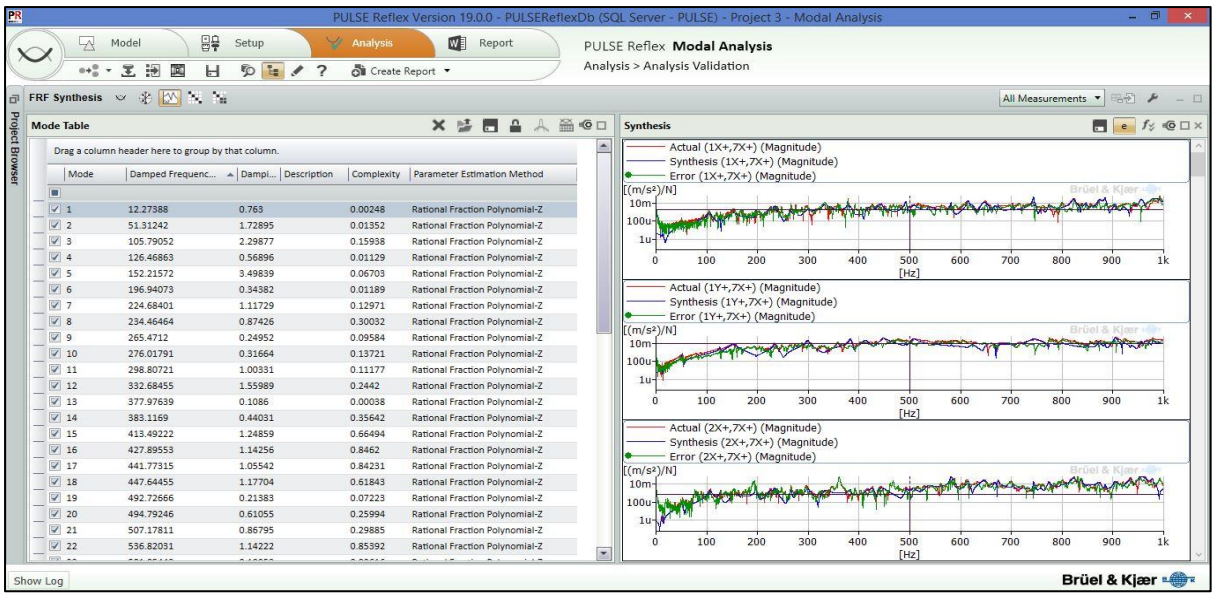

Figure A.27: Synthesis curve after iteration for EMA.

A.5.4.4. Step 4.4: analysis (analysis validation-Auto MAC)

Matrix formation by modal assurance criteria for better understanding about the modal parameters. The selected modes for EMA are accurate or not it is justified by the MAC value. Diagonal matrix formation is the main condition to validate the modes from EMA. MAC indicates how is the consistency of mode shapes for one modal and another reference modal vector. The limiting value of MAC is 0.0 to 1.0. The maximum value 1.0 shows along the diagonal (red line), it means the best curve fitting is performed in EMA. MAC value indices that indicate how well the FEM mode shapes match the experimental values.

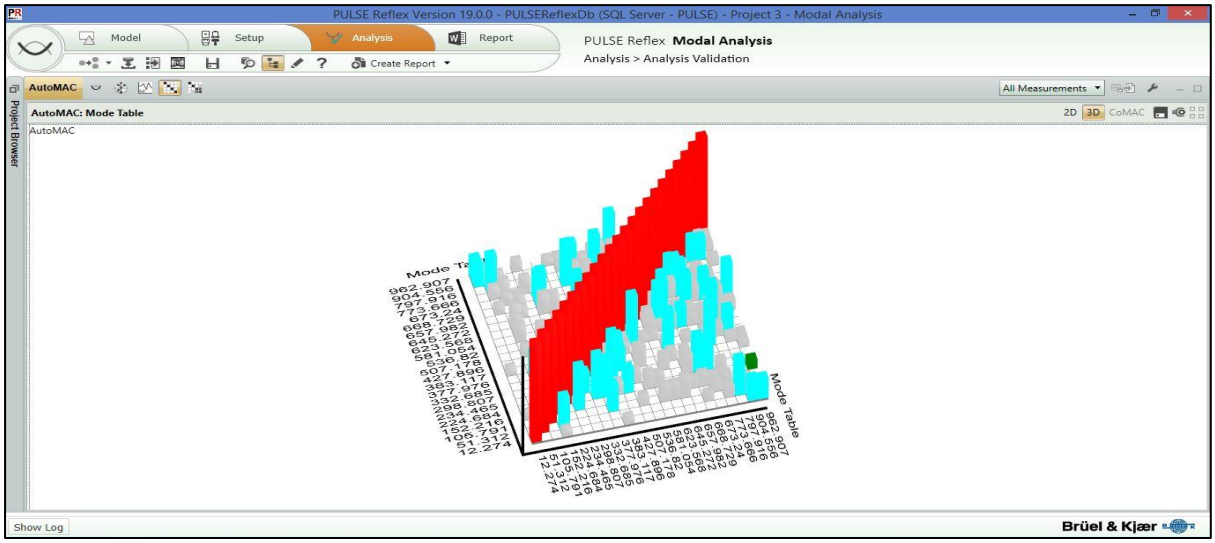

Figure A.28: Modal assurance criteria for modal parameters.

A.5.4.5. Step 4.5: analysis (analysis validation-Cross MAC)

Cross MAC ensure the modes of two different shapes. A good diagonal Cross MAC also shows the best validation of curve fitting and off diagonal values should be low.

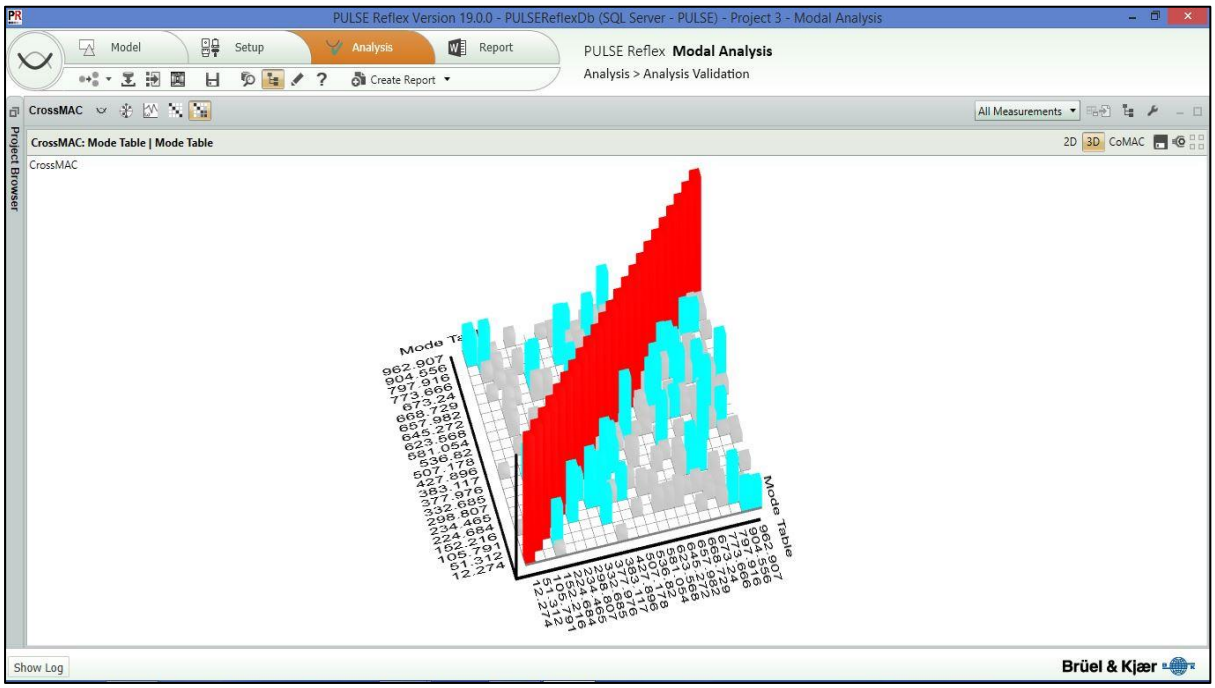

Figure A.29: Modal cross assurance criteria for modal parameters.

ANNEX-B

B. Pulse Reflex Modal Analysis: Bruel & Kjaer Method for longitudinal frame (in plane)

B.1. Data post-processing for longitudinal frame (in plane)

Frequency response function and coherence measured by the 12 accelerometers positioned in the in plane of the longitudinal frame from the MTC hammer excitation is plotted in figure B.1 and figure B.2 for two best measurement. The measurement is validated by the FRF validation by computing frequency vs acceleration curve is shown in figure B.3.

Figure B.1: Frequency response function for the first DOF.

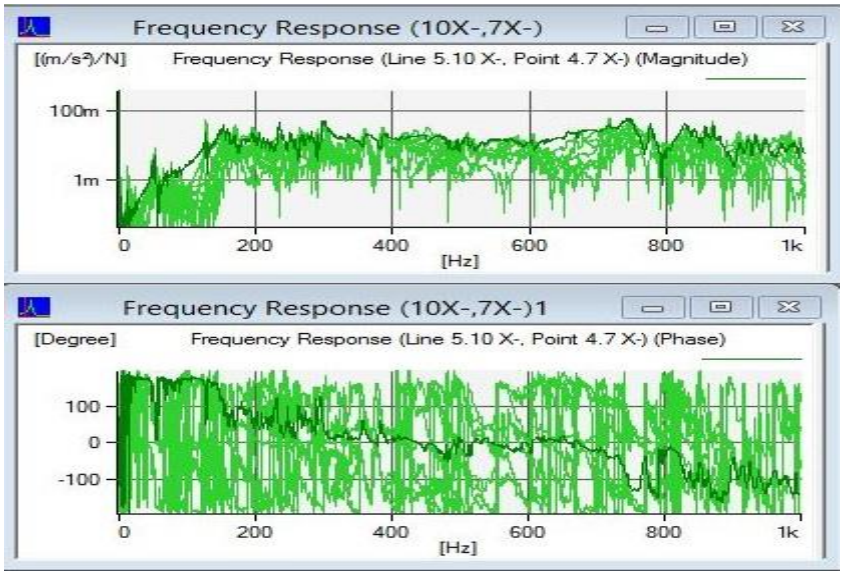

Figure B.2: Frequency response function for the second DOF.

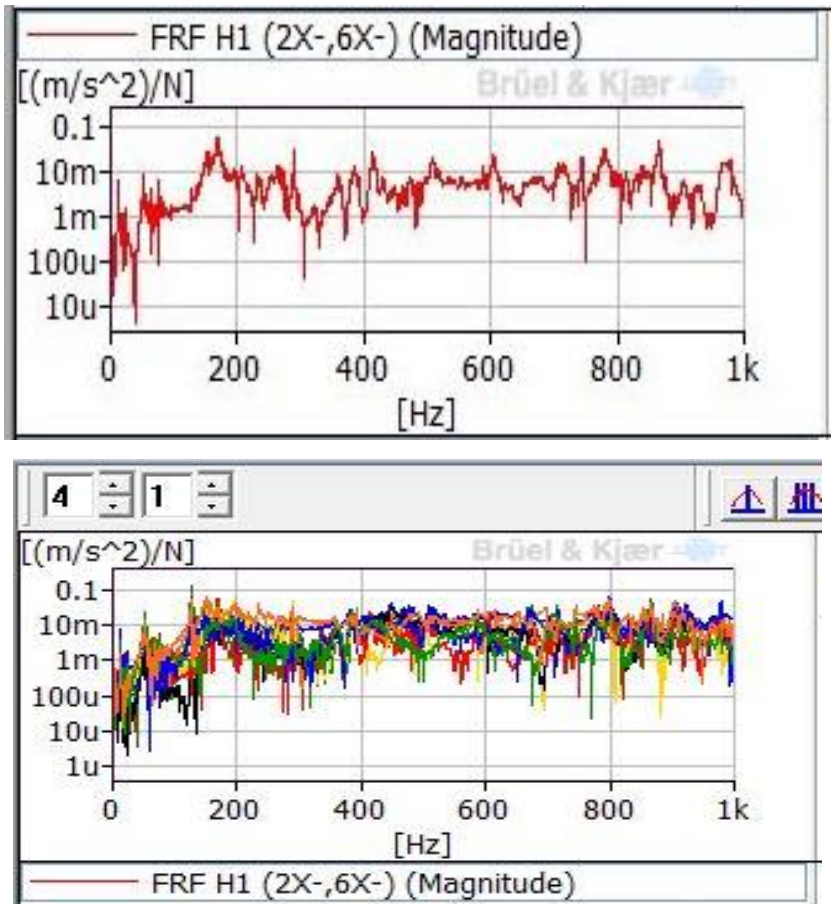

Figure B.3: FRF validation by computing frequency vs acceleration curve.

B.2. Data post processing for modal parameter identification

Rational function polynomial method shows the better performance for mode selection. There are other methods also but these methods have some drawbacks compare to rational function polynomial method. Cumulative modal identification factor (CMIF) and frequency response function (FRF) is allowed to find out the available modes for defined frequency range shown in figure B.4. The mode number and shapes totally dependent on the number of iteration. Total number of iteration is selected 100 for longitudinal frame (in plane).

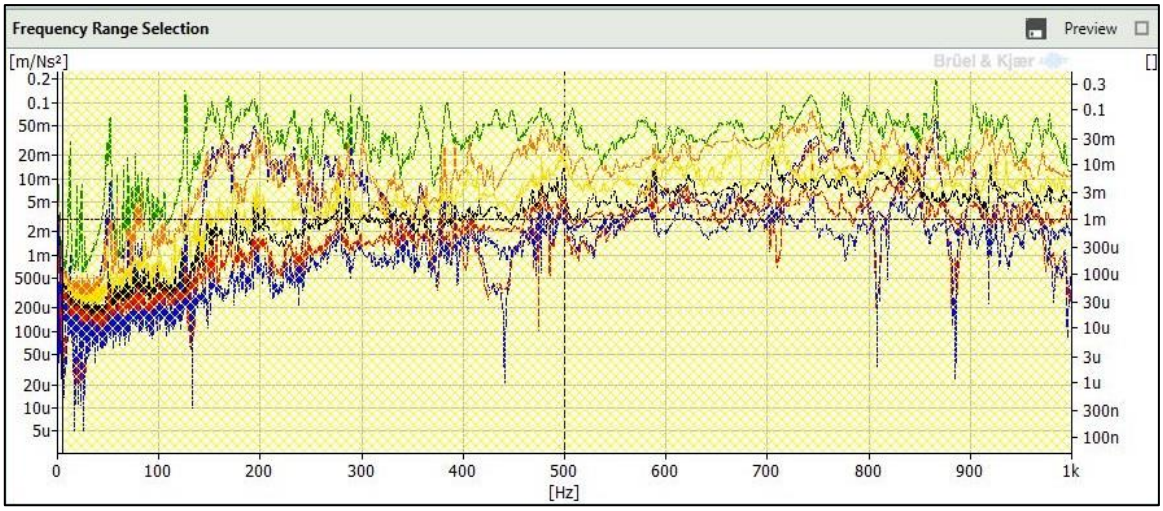

Figure B.4: Frequency span for EMA.

Synthesis diagram is basically the indication of performance of extraction of mode shape and mode numbers. The closer the actual response and synthesis diagram means the minimum errors of measurement. The errors can be more or less for selecting or deselecting any modes during EMA. The minimum error shows the better result for modal parameters and accuracy of the measurement during experimental testing. Synthesis curve is shown in the figure B.5.

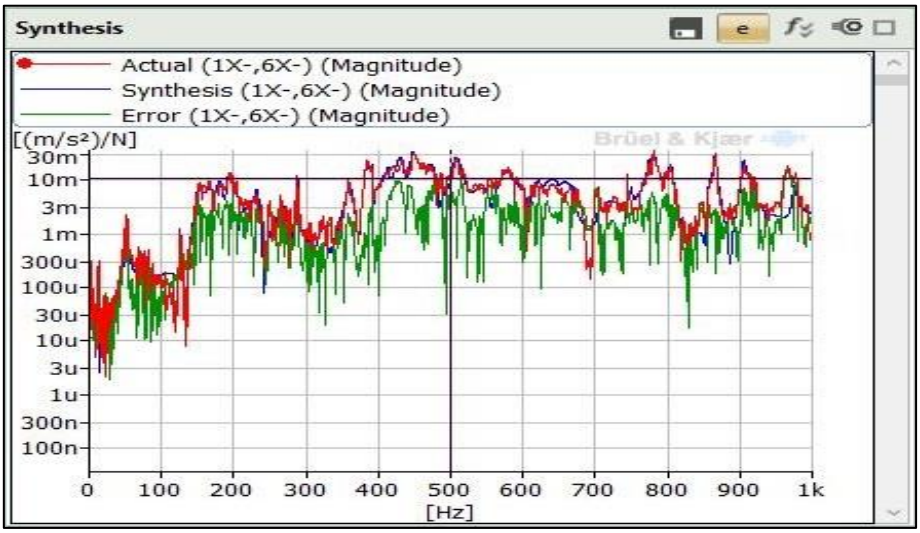

Figure B.5: Synthesis curve after iteration for EMA.

Singular value stability diagram for EMA shown in figure B.6 for mode selection by auto mode selection procedure. Sometimes manual selection can be done for extracting modal parameters but auto selection is always better than the manual selection.

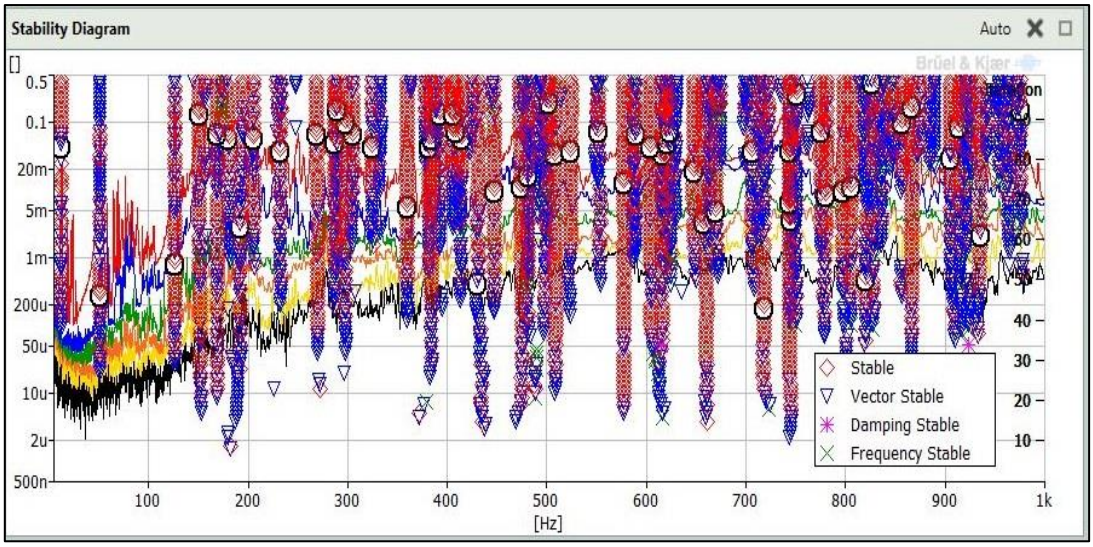

Figure B.6: Singular value stability diagram for EMA.

The mode shape and modal parameters conducted from the EMA is need to validate for better performance. This is done by the modal assurance criteria (MAC). The modal assurance criterion (MAC) is a scalar constant. MAC indicates how is the consistency of mode shapes for one modal and another reference modal vector. The limiting value of MAC is 0.0 to 1.0. The maximum value 1.0 shows along the diagonal (red line), it means the best curve fitting is performed in EMA (Figure B.7)

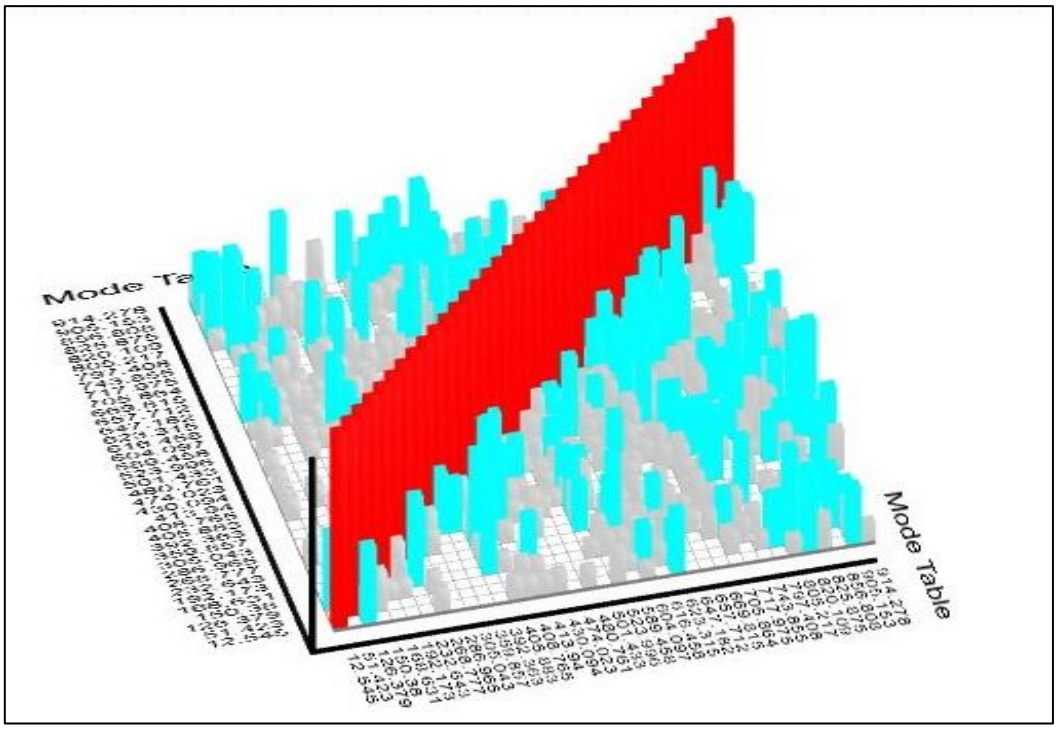

Figure B.7: Modal assurance criteria for modal parameters.

ANNEX-C

C. Pulse Reflex Modal Analysis: Bruel & Kjaer Method for longitudinal frame (out of plane)

C.1. Data post-processing for longitudinal frame (out of plane)

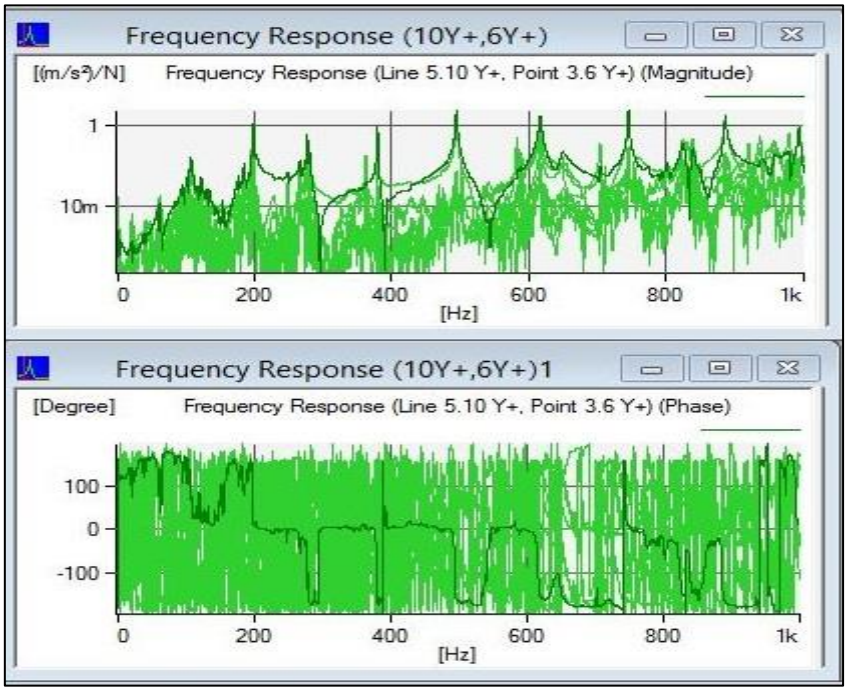

Figure C.1: Frequency response function for the first DOF.

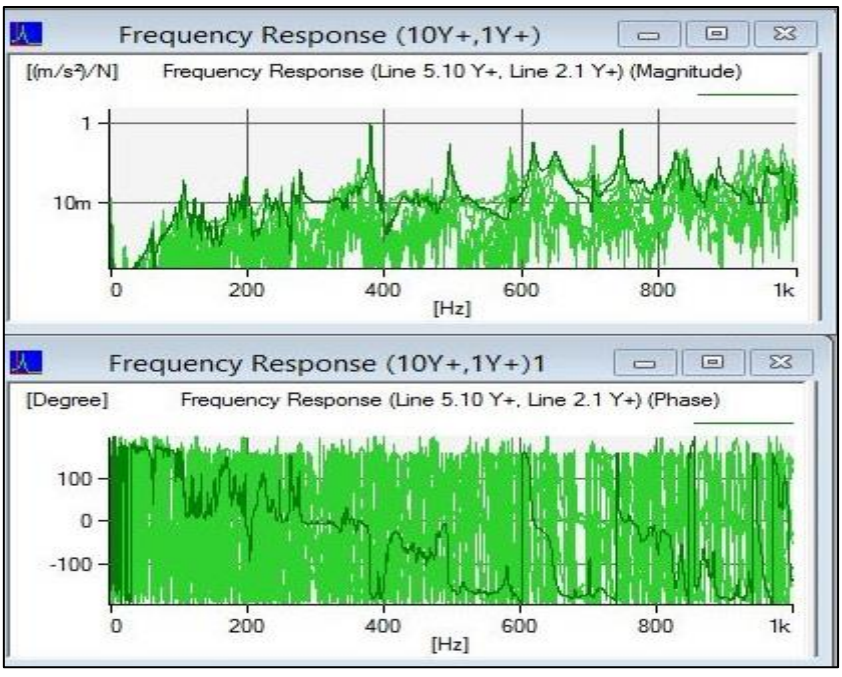

Figure C.2: Frequency response function for the second DOF.

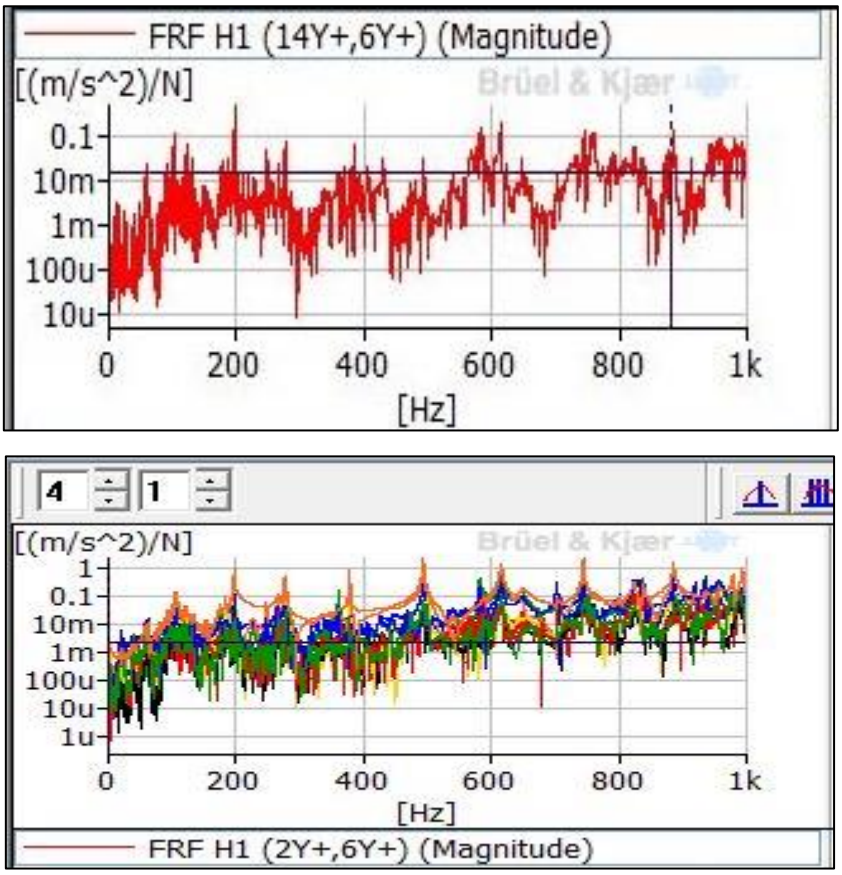

Figure C.3: FRF validation by computing frequency vs acceleration curve.

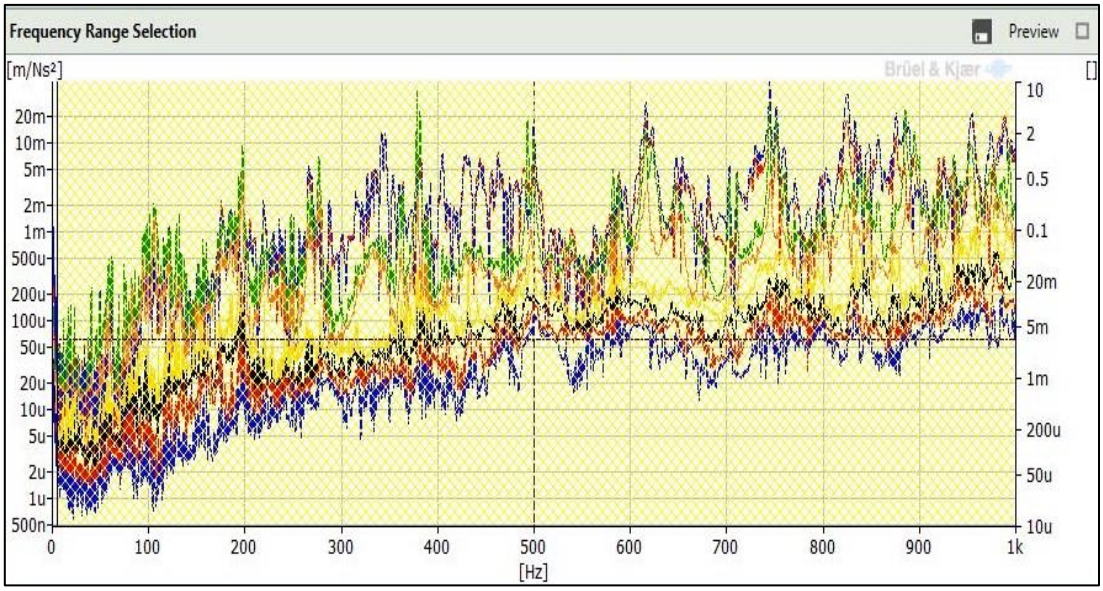

Figure C.4: Frequency span for EMA.

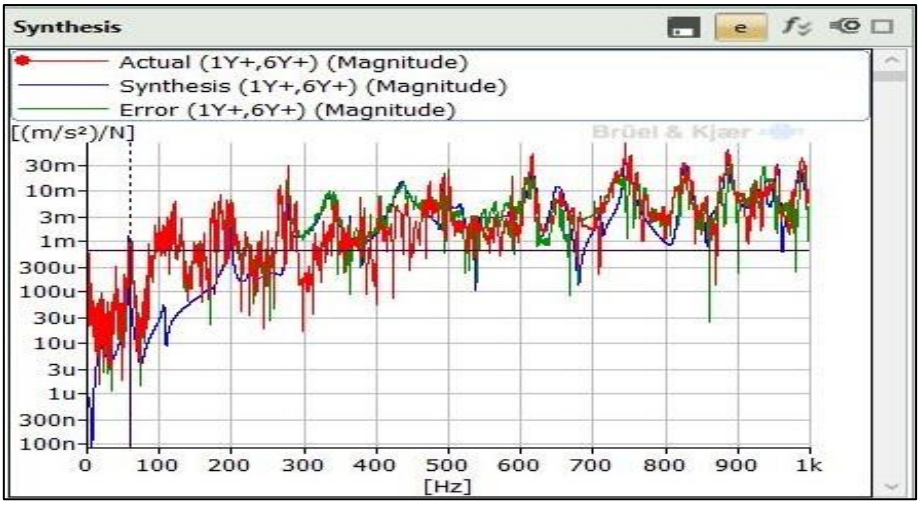

Figure C.5: Synthesis curve after iteration for EMA.

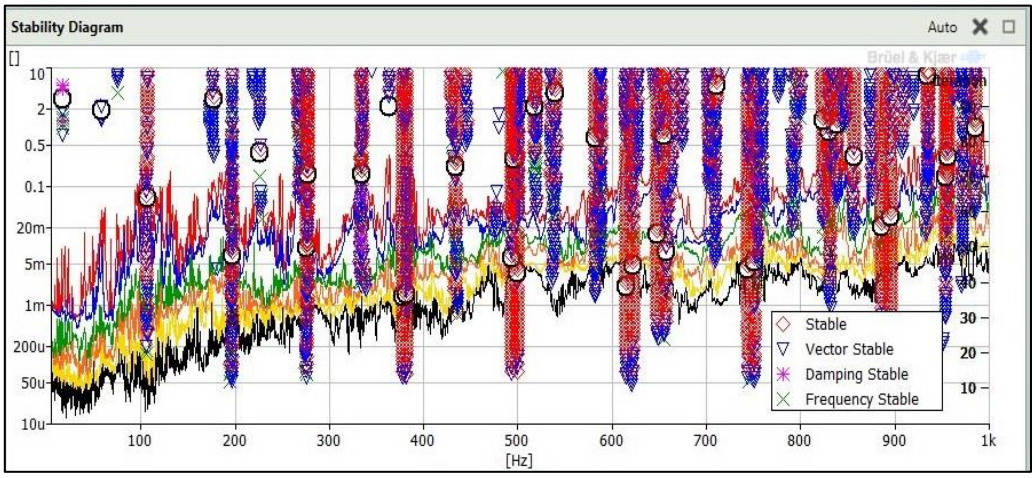

Figure C.6: Singular value stability diagram for EMA.

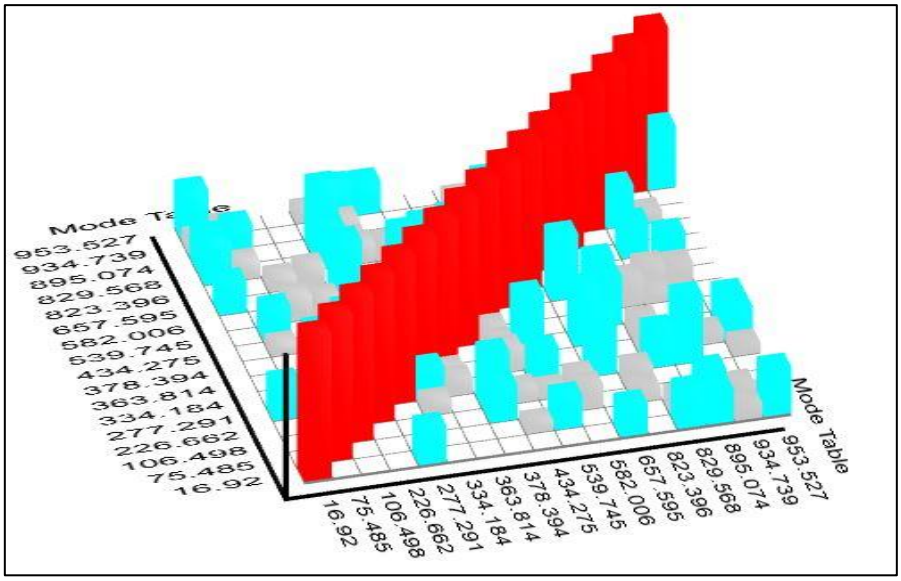

Figure C.7: Modal assurance criteria for modal parameters.

ANNEX-D

D. Pulse Reflex Modal Analysis: Bruel & Kjaer Method for longitudinal frame (out of plane) after removing of secondary beam

D.1. Data post-processing for longitudinal frame (out of plane) after removing of secondary beam

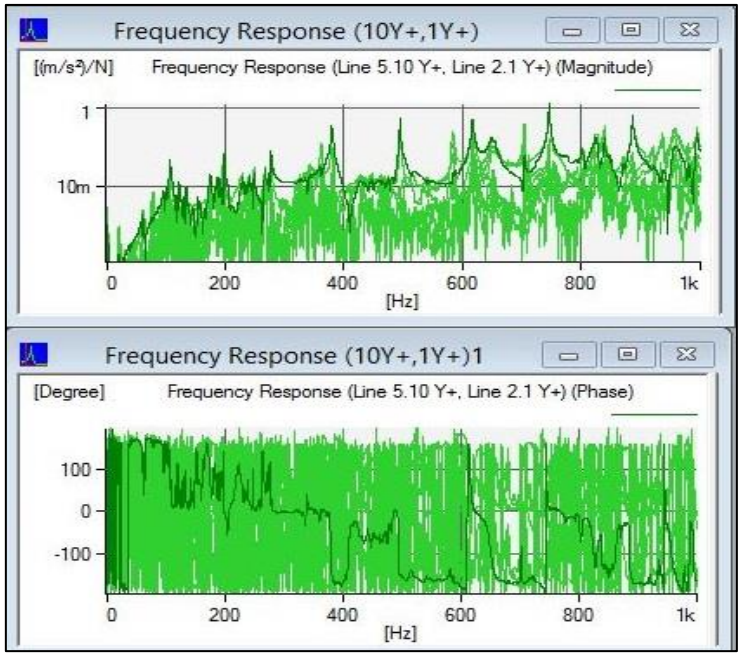

Figure D.1: Frequency response function for the first DOF.

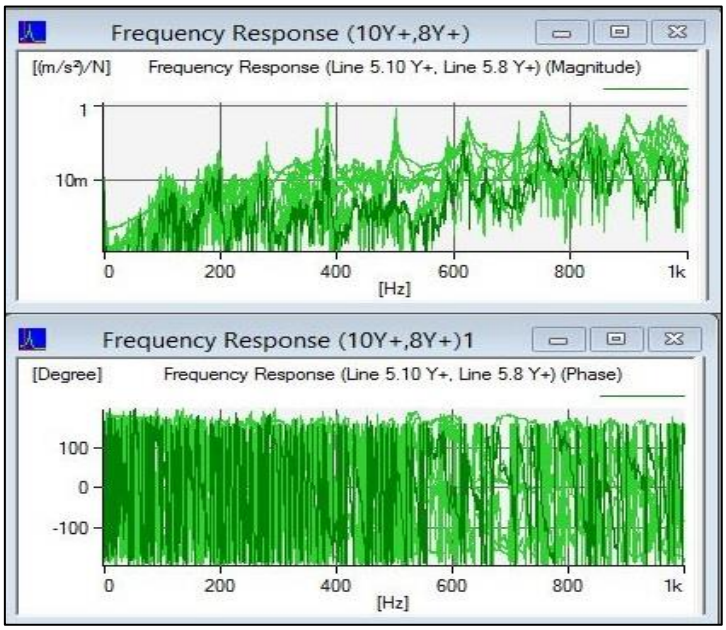

Figure D.2: Frequency response function for the second DOF.

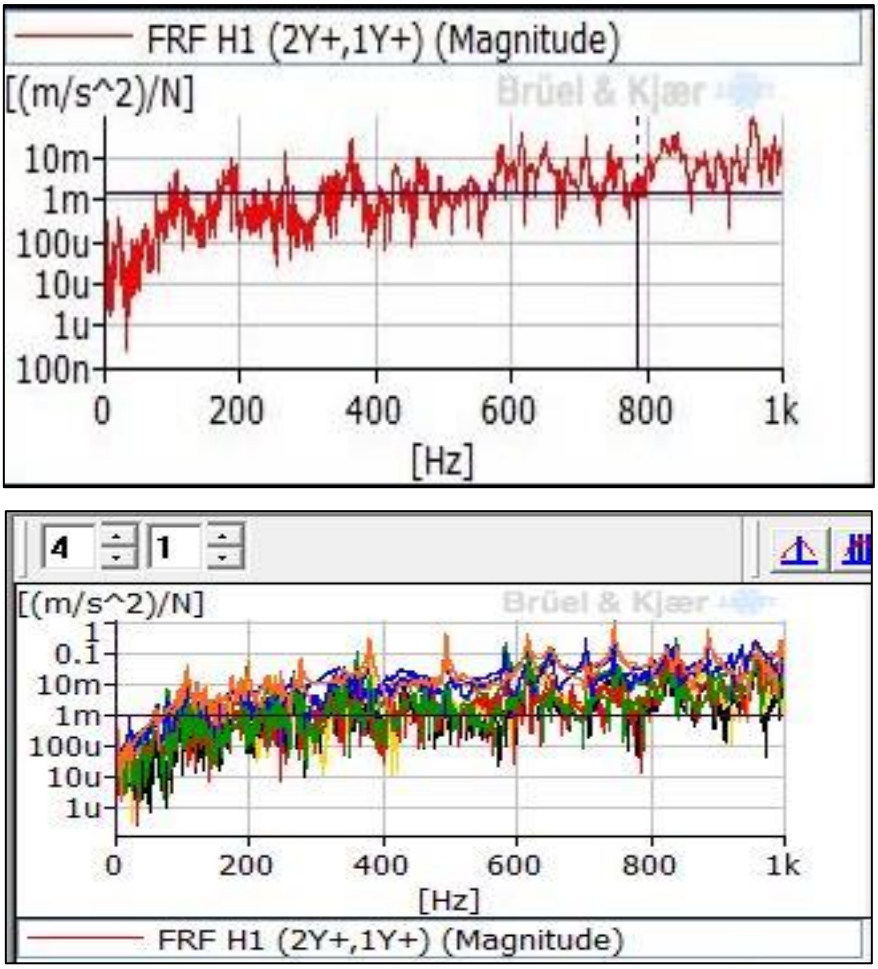

Figure D.3: FRF validation by computing frequency vs acceleration curve.

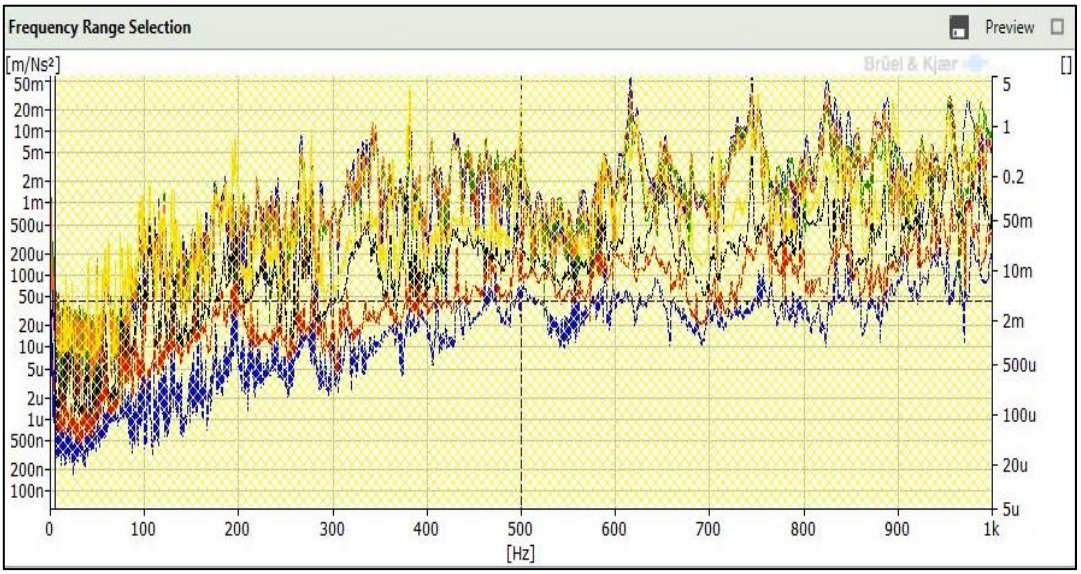

Figure D.4: Frequency span for EMA.

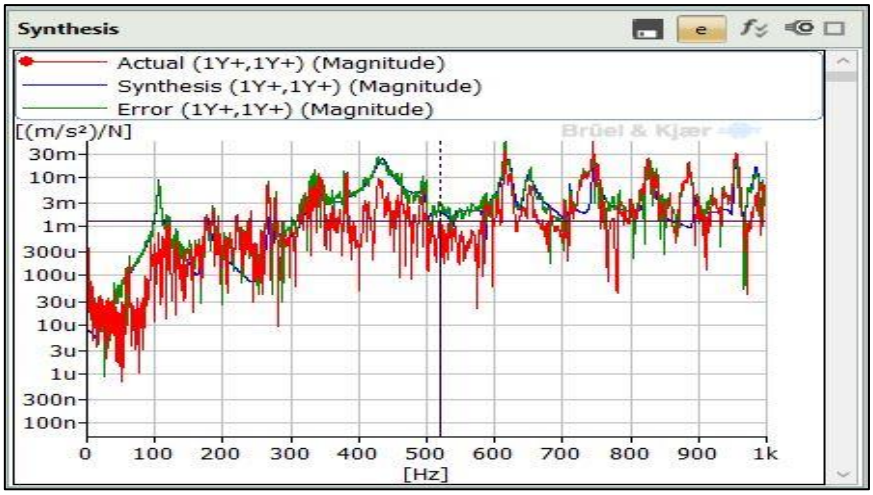

Figure D.5: Synthesis curve after iteration for EMA.

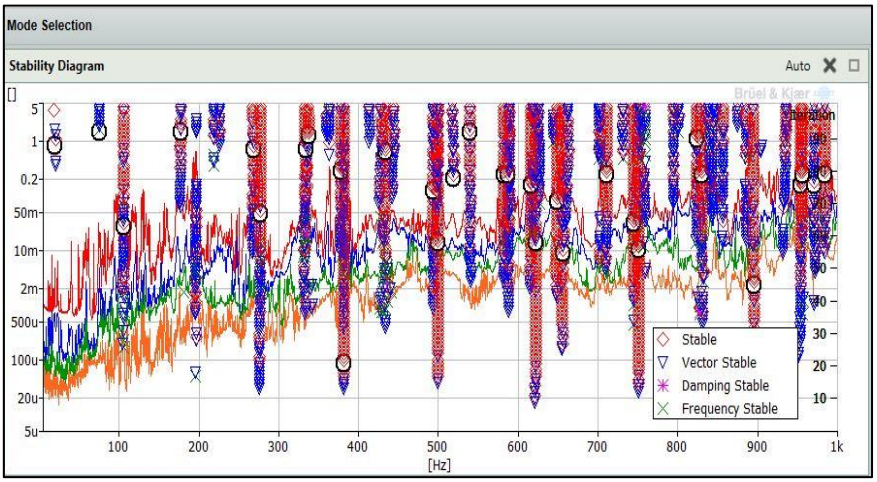

Figure D.6: Singular value stability diagram for EMA.

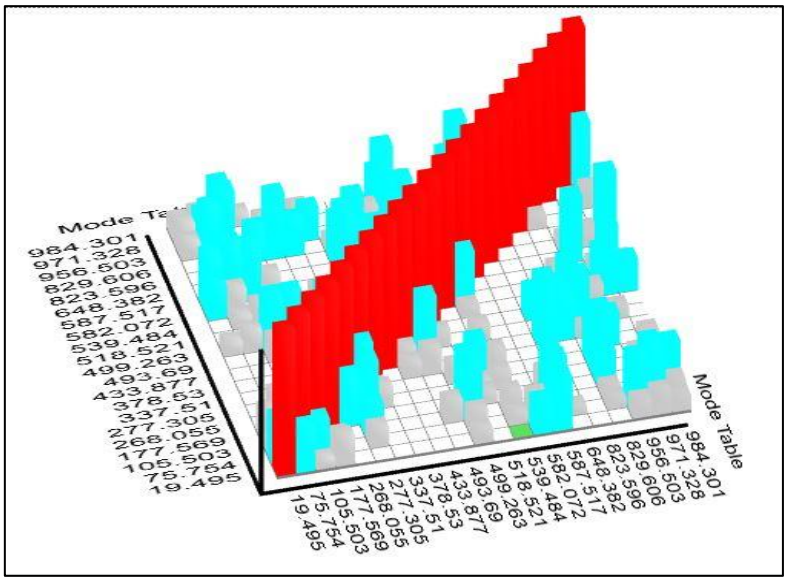

Figure D.7: Modal assurance criteria for modal parameters.